9-15-2011 12:00 AM

Trace metal limitation and its role in oxidative stress of coral algal symbionts; implications for thermally induced coral bleaching events.

Katrina Lynn Iglic, *University of Western Ontario*

Supervisor: Dr. Charles Trick, *The University of Western Ontario*

A thesis submitted in partial fulfillment of the requirements for the Doctor of Philosophy degree in Biology

TRACE METAL LIMITATION AND ITS ROLE IN OXIDATIVE STRESS OF CORAL ALGAL SYMBIONTS; IMPLICATIONS FOR THERMALLY INDUCED CORAL BLEACHING EVENTS.

(Spine title: Trace metal limitation and oxidative stress in coral algal symbionts)

(Thesis format: Integrated-Article)

by

Katrina Lynn Iglic

Graduate Program in Biology

A thesis submitted in partial fulfillment
of the requirements for the degree of
Doctor of Philosophy

The School of Graduate and Postdoctoral Studies
The University of Western Ontario
London, Ontario, Canada

THE UNIVERSITY OF WESTERN ONTARIO
School of Graduate and Postdoctoral Studies

CERTIFICATE OF EXAMINATION

Supervisor	Examiners
_____	_____
Dr. Charles Trick	Dr. Susan Koval
Supervisory Committee	_____
	Dr. Marc-Andre Lachance
_____	_____
Dr. Norm Huner	Dr. Graeme Taylor
_____	_____
Dr. Marc-Andre Lachance	Dr. Marc Warner

The thesis by

Katrina Lynn Iglic

entitled:

TRACE METAL LIMITATION AND ITS ROLE IN OXIDATIVE STRESS OF CORAL ALGAL SYMBIONTS; IMPLICATIONS FOR THERMALLY INDUCED CORAL BLEACHING EVENTS.

is accepted in partial fulfillment of the
requirements for the degree of
Doctor of Philosophy

_____	_____
Date	Chair of the Thesis Examination Board

Abstract

Coral bleaching, the process in which corals expel their photosynthetic symbionts (Genus *Symbiodinium*), is caused by high temperature and irradiance stress. The synergistic effect of each stressor is the generation of damaging reactive oxygen and nitrogen species (ROS and RNS), which are normally mitigated physiologically by antioxidant enzyme activity. Antioxidant enzymes require iron, copper, manganese and zinc in their structure and the limited nature of these trace metals in reef environments may enhance ROS production under elevated temperature and irradiance. The hypothesis tested within this thesis was that a limited availability of the trace metals Fe, Mn, Cu and Zn would cause increases in intracellular ROS and RNS load of the symbiotic dinoflagellates of corals isolated from the Great Barrier Reef (GBR), Australia, under conditions of temperature and irradiance stress. Pulse amplitude fluorometry, flow cytometery and fluorescent ROS and RNS probes were utilized to measure photochemical efficiency (charge separation at PSII) and intracellular ROS and RNS levels. Trace metal limitation experiments on *Stylophora pistillata* collected from various GBR locations showed that Fe limitation under elevated temperature directly reduced PSII photochemical efficiency and increased protective pigments of symbiotic dinoflagellates *in hospite*. Increases in intracellular ROS were not detected, however, and decreases or an absence of change in intracellular ROS occurred under Fe limited conditions. Culture experiments on *Symbiodinium* Strains were then employed to understand this phenomenon and cells were grown under Fe-replete and deplete conditions in continuous culture and subjected to heat and irradiance stress. Enhanced intracellular ROS and RNS were detected within *Symbiodinium* Strains 831 and 2432 in culture under Fe-deplete conditions at high temperature and irradiance. This thesis illustrates the intricate role of Fe in *Symbiodinium* photochemistry and oxidative stress in culture and *in hospite*, providing insight to the physiology behind coral bleaching.

Key words; Oxidative stress, coral bleaching, trace metal limitation, *Symbiodinium*, *Stylophora pistillata*, PSII photochemical efficiency

Co-Authorship statement

Within Chapter 2 of this thesis, Katrina Iglic contributed to this co-authored paper by being involved in conducting the experiment, collecting and processing all PAM data and playing a role in the breakdown of the experiment and harvesting of zooxanthellae. Furthermore, Miss Iglic was involved in the preparation of pigment analysis prior to running on the HPLC and during the writing process of the co-authored paper, Miss Iglic was involved in supplying methodology information and editing.

Co-authored paper:

Shick, M.J., K. Iglic, M.L. Wells, C.G. Trick, J. Doyle and W.C. Dunlap. 2011. Responses to iron limitation in two colonies of *Stylophora pistillata* exposed to high temperature: Implications for coral bleaching. *Limnol. Oceanogr.* 56: 813-828.

Acknowledgements

Words cannot begin to describe the gratitude that I feel towards so many wonderful people that have helped shape this thesis and given me the inspiration, knowledge and unending support required to complete it.

First and foremost, I would like to sincerely thank my supervisor, Dr. Charles Trick, who has been such an inspiration and mentor to me. I will feel forever indebted to him for the opportunity that he gave me to be a part of such and amazing project and wonderful lab. His confidence in my skills and capacity as a scientist has been critical to my development and I will be forever grateful for it, knowing that I wouldn't be where I am today if it weren't for him. The chance he took on me even after I had killed off the two cyanobacteria strains that I was to study for my fourth year thesis was incredible. I feel truly honoured and blessed to have worked with Dr. Trick and I wish that I could truly express my gratitude in an adequate way.

Secondly, I would like to thank my family and friends. They have stood strong by my side and supported my passion for science, believing in me every step of the way. Their support has been invaluable and I will be forever thankful to them for this. From the long talks and tears over experimental woes and wins, they have always been there to support me and listen, something for which I will always be grateful. I would like to thank my mom and dad, they have supported me every step of the way and I would have never been able to achieve what I have achieved today with out their love and support.

A dear spot in my heart exists for my lab mates and I feel so appreciative to have been able to work and know such wonderful people. From my early days in the lab, I was welcomed and made to feel so comfortable. I am and will always be grateful for the patience and kindness I received when working in the lab, from my questions to my mistakes, someone was always there to lend a helping hand. I would like to thank Liza for teaching me how to sterilely culture algae and set up experiments. I would also like to thank Ben, for his all of his help with my statistical endeavors and questions. I would also like to thank Tory, who was such an amazing field assistant and has become such a

close and dear friend. A special thank you also goes to Bea, who has been such an incredible lab mate, friend and a person to share a good laugh with. I would like to thank all Trick lab members, past and present, for their support and help in all that I have done and for all of the great experiences we have shared. The Creed lab members and Dr. Creed have also been so helpful and supportive of my work and I would extend my deepest appreciation to them for all of their advice and the wonderful times that we have had.

I would also like to extend my deepest gratitude to the Dr. Mark Wells, Dr. Malcolm Shick and Dr. Walt Dunlap. They have been so supportive in my work and I am grateful for their kindness, for welcoming me in to their homes and for making my research in Australia both exciting and informative. I would also like to thank Dr. Anke Kleuter, she has been a scientific and personal inspiration to me since the moment we met and I feel so fortunate to have worked, laughed and cried with such a wonderful woman. I would also like to extend my thanks to Florita Flores, she was my first friend in Australia and her help and support has been invaluable. My deepest thanks also go to the employees at the Australian Institute of Marine Science. They have been so accommodating and helpful to me during my field seasons and I am deeply grateful to them.

I would like to thank my wonderful advisory committee members Dr. Huner and Dr. Lachance for all of their insight and guidance over the course of my graduate education. I would like to thank both NSERC and NSF for the funding that they have provided for the projects that I have been fortunate enough to be involved in.

Finally, I would like to thank Michael, my husband, my friend and my life partner. From the moment we met, his support for my research has been unwavering and he has always believed in me so much, pushed me to be the best I could be, and encouraged me to follow my dreams. From enduring cold winters alone while I was doing fieldwork in Australia to dealing with my crazy stressed out antics, he has been a pillar of support to me, and for that I will be forever grateful.

Table of Contents

List of Tables

List of Figures

List of abbreviations

ATP: Adenosine tri-phosphate

ANOVA: Analysis of variance

°C: Degrees Celsius

CCMP: Provasoli-Guillard national center for culture of marine phytoplankton

CAT: Catalase

Cu: Copper

CO_2: Carbon dioxide

$CO_3^{\bullet-}$: Carbonate radical

DAF-FM: 4-amino-5-methylamino-2',7'-difluorofluorescein diacetate

DD: Diadinoxanthin

DFB: Desferrioxamine B

DHE: Dihydroethidium

DHR 123: Dihydrorhodamine 123

D: Dilution

DMSO: Dimethyl sulphoxide

DNA: Deoxyribonucleic acid

DT: Diatoxanthin

FAD: Flavin adenine dinucleotide

Fe: Iron

Fe^{3+}: Ferric cation

Fe^{2+}: Ferrous cation

$FeCl_3 \cdot 6H_2O$: Iron chloride hexahydrate

F_m: Maximal fluorescence

F_o: Minimal fluorescence

FSC: Forward scatter

F_v: Variable fluorescence

EDTA: Ethylenediaminetetraacetic acid

ENSO: El Nino-Southern Oscillation

ETC: Electron transport chain

F_v/F_m: Maximal PSII photochemical efficiency

GBR: Great Barrier Reef

GHS: Glutathione

H_2O_2: Hydrogen peroxide

HCL: Hydrochloric acid

HEPA: High-efficiency particle

HPLC: High performance liquid chromatography

HSD: Tukey's Honestly Significant Difference

In hospite: In host

ITS: Internal transcribed spacer

CMH_2DCF-DA: 5-(and 6) chloromethyl-2',7'-dichlorodihydrofluorescein diacetate, acetyl ester

km: Kilometer

L: Liter

LH: Light-harvesting

M: Molar

MDA: Malondialdehyde

Mn: Manganese

NaCl: Sodium chloride

NADPH: Nicotinamide adenine dinucleotide phosphate

NaOH: Sodium hydroxide

nM: Nanamolar

NO: Nitric oxide

$NO_2^{\bullet}$: Nitrogen dioxide

NOAA: National Oceanic and Atmospheric Administration

NPQ: Non-photochemical quenching

$^1O_2$: Singlet oxygen

O_2: Dioxygen

$O_2^{\bullet-}$: Superoxide

$OH^{\bullet}$: Hydroxyl radical

$ONOO^-$: Peroxynitrite

PAM: Pulse amplitude fluorometry

PAR: Photosynthetically available radiation

PASW: Predictive Analytics SoftWare

PCR: Polymerase chain reaction

PDA: Photo-diode array

ppm: Parts per million

PSI and PSII: Photosystem one or photosystem two, respectively

psu: Practical salinity units

PVC: Polyvinyl chloride

Qa: Quinone A

$QH^{\bullet}$: Ubisemiquinone radical

REML: Restricted Maximum Likelihood

RNS: Reactive nitrogen species

ROS: Reactive oxygen species

SAS: Statistical Analysis System

SD: Standard deviation

SDS: Sodium dodecyl sulfate

SE: Standard error

SNK: Student Newman Keuls post-hoc test

SOD: Superoxide dismutase

SOW: Synthetic ocean water

SSC: Side scatter

SW: Seawater

TBBA: tetrabutyl ammonium acetate

μm: Micometer

μM: Micromolar

μ_N: Specific growth rate

UV: Ultraviolet

v/v: Volume to volume

XP: Xanthophyll

Zn: Zinc

Chapter 1

Introduction

1.1 Coral reef ecosystems

Coral reef ecosystems are some of the most diverse and important ecosystems on Earth. The productivity and biodiversity of these ecosystems is high and humans rely strongly on them for resources and income in the forms of tourism, medical products, shoreline protection, fishing and building materials (Hoegh-Guldberg 1999). It has been estimated that 0.5 billion people depend upon coral reef resources, and this number is projected to double over the next 50 years (Smith *et al.* 2005). The reliance upon global coral reefs makes humans dependent upon the foundation of these ecosystems, the reef building activity of hermatypic (reef building) corals (Smith *et al.* 2005) that are intricately linked to global patterns influencing their distribution.

Physical parameters, including light, temperature and salinity regulate the biogeography of global coral reefs. Primarily confined to euphotic zones (light penetrating zones) of warm (minimum mean annual temperature of 18 °C) shallow tropical seas between 30° N and 30° S Latitude, coral reefs span 6 x 10^5 km^2 of the earth's surface (Muscatine and Weiss 1992). The productivity of coral reef ecosystems is unique to tropical waters, where low nutrient (oligotrophic) supplies shape the nature of the community. These ecosystems show uniquely high levels of productivity in comparison to their surrounding seas. Coral reef productivity can exist at 40 g $C \cdot m^{-2} \cdot day^{-1}$ while their neighbouring open seas have productivity rates of 0.01 g $C \cdot m^{-2} \cdot day^{-1}$ (Hoegh-Guldberg 1999). Within the coral reef ecosystem, a symbiotic relationship has been selected to promote the proliferation and persistence of these biodiverse ecosystems in their oligotrophic environments.

At the basis of a coral reef ecosystem is a symbiotic relationship between photosynthetic dinoflagellates (zooxanthellae) and a Cnidarian animal host (Muscatine and Weis 1992). Whilst residing within the tissue of the host, the symbiotic dinoflagellates

photosynthesize and selectively transfer amino acids, sugars, complex carbohydrates and small peptides across the host-symbiont barrier. In exchange, the host provides the algal symbiont with nutrient rich waste consisting of the essential nutrients of photosynthesis including ammonia, phosphate (Hoegh-Guldberg 1999), CO_2, and a protective substratum deployed in the sun (Rupert *et al.* 2004). The location of the symbiotic dinoflagellates is within one of the two host dermal layers, the gastrodermal tissue. The density of the algal symbionts within this tissue may range from 10^6 cells•cm^{-2} or greater (Muscatine and Weiss 1992) and they have the potential to supplement the Cnidarian with 90-95% of their nutritional requirements (Falkowski *et al.* 1984, Muscatine *et al.* 1984, Berkelmans and van Oppen 2006). The stony reef building corals (Order Scleractinia) are especially sensitive to this relationship, with their ability to build reefs dependent upon the presence of the zooxanthellae of the genus *Symbiodinium* (Muscatine and Weis 1992, Berkelmans and van Oppen 2006). The calcification rate of reef building corals is enhanced 15 fold with symbiotic dinoflagellate photosynthetic activity (Muscatine and Weiss 1992) compared to corals without zooxanthellae. The importance of this symbiotic relationship to the overall reef community is great because it is within the reef crevices and the various habitats created by Scleractinian corals that the many phyla of reef organisms persist, making reef environments rich in biodiversity (Nybakken 1997, Lesser 2011).

1.2 Coral bleaching: how and why?

Although the Cnidarian and dinoflagellate symbiosis has been present for over 200 million years (Barber *et al.* 2001, Berkelmans and van Oppen 2006, Stabler 2011), its current stability is threatened by a phenomenon called coral bleaching. Coral bleaching involves the loss of photosynthetic symbiotic dinoflagellates or the breakdown of the algal symbiont's individual pigments in a coral (Glynn 1993, Lesser 1997, Douglas 2003) resulting in the white colouration of an affected coral colony. Reported incidents of bleaching events have been on the rise since the 1980's and are increasing in global distribution, ranging from regions in the Atlantic Ocean, from the Caribbean to the Bahamas, and the equatorial eastern Pacific Ocean (Glynn 1996). This raises concern for the fate of the global coral reefs because severe and frequent bleaching events cause decreases in coral disease resistance, survivorship, reproduction capacity and growth in

bleached corals over large distances (Donner *et al.* 2005). Furthermore, the fate of any coral bleaching event is death if the algal symbionts are not restored in the host after a short period of time (Glynn 1996, Douglas 2003), indicating the severity of a global increase in coral bleaching events.

Coral bleaching can result from many different perturbations to the reef environment including sharp increases or decreases in sea surface temperature, high solar irradiance, decreases in salinity, pollution, pathogenic microorganisms, heavy metals, and prolonged darkness (Brown *et al.* 1999, Douglas 2003). Although the causes of coral bleaching are multifaceted, increased sea surface temperature in conjunction with the high photosynthetically available radiation (PAR) found in shallow reef environments (Brown *et al.* 2000, Fitt *et al.* 2001, Lesser and Farrell 2004) have been established as the main driving factors behind bleaching, with increases of only 1-2 ºC above the mean summer maxima resulting in bleaching events (Jones *et al.* 1998, Donner *et al.* 2005). Widespread bleaching and coral mortality was detected in the coral reefs of Costa Rica, Panama, Columbia, and the Galapagos Islands after a prolonged period of warming following the El Nino-Southern Oscillation (ENSO) of 1982-1983 (Glynn 1989). Furthermore, a global mass-bleaching event occurred in 1998, where corals within 60 countries and states in the Pacific Ocean, Indian Ocean, Red Sea, Arabian Gulf and the Caribbean experienced bleaching. Notably 1998 was marked as the warmest year of the century, with abnormally high combined land-air and sea surface temperatures (Reaser *et al.* 2000). The trend of bleaching following warming events has been a common occurrence globally, and in the North Atlantic and Caribbean all large-scale bleaching events significantly correlate with increases in sea surface temperature, measured by the National Oceanic and Atmospheric Administration (NOAA) satellite-derived sea surface temperature records (Reaser *et al.* 2000). The negative impact of minimal temperature increases on coral bleaching is enhanced under conditions of high irradiance, especially in the ultraviolet wavelengths (Harriot 1985, Glynn 1996, Reaser *et al.* 2000). The synergistic effect of increased temperature and irradiance on coral bleaching has been a topic of extensive research and both have been established as the main drivers of coral bleaching (Lesser and Farrell 2004). In light of the increases in sea surface temperature under the proposed climate

change regimes, coral reefs are at heightened risk, making the understanding of the physiology behind bleaching events critical.

1.3 Oxidative stress and coral bleaching

High temperature and irradiance disrupt the physiological balance between the Cnidarian animal host and its symbiotic dinoflagellates due to their positive effects on reactive oxygen species (ROS) production (Lesser *et. al*. 1990, Downs *et al.* 2002). Increased oxidative stress has been implicated as one of the main causes of bleaching under temperature (Smith *et al.* 2005) and irradiance stress (Lesser and Farrell 2004, Lesser 2006). Indirect and direct measurements have shown that oxidative damage and oxidative load within corals and their symbiotic dinoflagellates play a significant role in thermal and solar radiation bleaching. In the Scleractinian coral *Acropora microphthalma,* the propagation of ROS under conditions of high irradiance was inferred by the distribution of antioxidant enzymes in the coral and their symbiotic dinoflagellates across a range of depths. Within this species, higher levels of antioxidant enzymes, protective against ROS damage, were detected in shallow water colonies (2 m) relative to deeper water colonies (30 m) that experience 4-fold reduced PAR and 100-fold reduced UV radiation (Shick *et al.* 1995). In the Caribbean coral, *Montastraea faveolata*, a similar antioxidant response was detected under elevated temperatures and solar radiation, with increased superoxide dismutase expression under the stressful conditions (Lesser and Farrell 2004). The elevated antioxidant gene expression and enzyme activity under increased temperature and irradiance may be directly linked to increases in intracellular ROS. Spin trap analysis indicated a direct relationship between photodynamic ROS production under conditions of bright light, especially in the UV region, in the host and zooxanthellae of *Anthopleura elegantissima* (Dykens *et al.*1992), indicating the role of this stress in the generation of ROS. Furthermore, direct increases in ROS in *Symbiodinium* sp. isolated from the coral *Stylophora pistillata*, detected using the fluorescent probe H_2DCFDA and microscopy, showed that increases in ROS were detectable in corals exposed to elevated light and temperature (Franklin *et al.* 2004). Experiments on alga symbionts in culture have enhanced the understanding of the role that ROS play in bleaching under conditions of high temperature and irradiance. Lesser (1996) detected increases in ROS in the

symbiotic dinoflagellates of the sea anemone, *Aiptasia pallida*, in culture under conditions of increased temperature (25 vs. 31 °C) in the presence and absence of UV light. The involvement of ROS within both the algal symbiont and the coral host in thermal and irradiance bleaching events highlights the importance of understanding the nature and characteristics of these molecules in an attempts to understand their role in bleaching.

1.4 Reactive oxygen species and reactive nitrogen species

ROS include both oxygen radicals, oxygen species able to exist independently containing one or more unpaired electrons, and oxygen non-radicals that are oxidizing agents or easily converted into radicals (Halliwell 2006). The inherent danger surrounding ROS pertains to their over-production. When ROS levels within an organism exceed the organism's ability to quench or transform ROS into less harmful molecules via antioxidants, direct damage of proteins, lipids and DNA can occur, and an organism enters a state of oxidative stress (Halliwell 2006). Multiple ROS exist naturally and range in their reactivity and membrane permeability. Such examples include: singlet oxygen ($^1O_2$), which is highly reactive and one of the main ROS produced by illuminated photosynthetic organisms as a result of electron transfer from excited chlorophyll molecules to molecular oxygen (Scandalios 1993), hydrogen peroxide (H_2O_2), which is highly permeable across biological membranes, and superoxide ($O_2^{\bullet-}$), which is less permeable and transfers across membranes at a rate of 2.1×10^{-6} cm•s^{-1} (Lesser 2006). Although differing in permeability, both H_2O_2 and $O_2^{\bullet-}$ have selective reactivity with biological molecules (Halliwell 2006), reacting with specific enzymes and not others. One example of this is the main reactivity of hydrogen peroxide with chloroplast Fru and sedoheptulose bisphosphatases (Halliwell 2006) and the inactivation of enzymes through the oxidation of their iron-sulphur centers by $O_2^{\bullet-}$ (Lesser 2006). Although of intermediate toxicity themselves, the potential danger of H_2O_2 and $O_2^{\bullet-}$ over-production *in vivo* is in their conversion to the highly reactive hydroxyl radical ($OH^{\bullet}$) (Halliwell and Gutteridge 1992). $OH^{\bullet}$ is the most reactive of all ROS, reacting with anything surrounding it at its site of formation (Halliwell and Gutteridge 1992, Halliwell 2006) in a diffusion-

controlled fashion with a lifetime of 10^{-7} s and mean diffusion distance of 4.5 nm (Lesser 2006). $OH^{\bullet}$ can modify all four of the DNA bases, causing damage to an organism's genetic composition, while other ROS are either non-reactive with DNA bases ($O_2^{\bullet-}$ and H_2O_2) or selectively modify guanine ($^1O_2$ and peroxyl radicals) (Halliwell and Gutteridge 1992). Furthermore, $OH^{\bullet}$ can initiate free radical chain reactions, oxidize membrane lipids, cause protein and nucleic acid denaturation (Lesser 2006) and cause irreparable metabolic dysfunction, which often leads to cell death (Scandalios 1993). The generation of $OH^{\bullet}$ is intricately linked to the H_2O_2 and $O_2^{\bullet-}$ for multiple reasons, it is produced by the Harber Weiss reaction involving $O_2^{\bullet-}$ and H_2O_2 and is generated in Fenton chemistry involving H_2O_2 and iron (Halliwell and Gutteridge 1992) in the reaction of $H_2O_2 + Fe^{2+} \rightarrow OH^- + \cdot OH + Fe^{3+}$ (Gutteridge and Halliwell 2000).

Uncontrolled production of reactive nitrogen species (RNS) poses a physiological threat to organisms in a similar fashion to ROS in their ability to cause damage to DNA, lipids and proteins and their ability to generate noxious ROS and RNS. The RNS nitric oxide (NO), produced by the enzyme nitric oxide synthase, catalyzes the formation of many other ROS and poses a great risk to organisms due to its high diffusibility across membranes (Lesser 2006). In the reaction of NO and $O_2^{\bullet-}$, peroxynitrite ($ONOO^-$) can be generated (Murrant and Reid 2001) which can diffuse across membranes at rates 400 times faster than $O_2^{\bullet-}$ (Lesser 2006). In itself, $ONOO^-$ is known to directly damage proteins, lipids and DNA. Furthermore, when it reacts with carbon dioxide (CO_2) or undergoes hemolytic fission it can generate the toxic products nitrogen dioxide ($NO_2^{\bullet}$), $OH^{\bullet}$, and the carbonate radical ($CO_3^{\bullet-}$), all of which are all capable of causing biological damage (Halliwell 2006). The multifaceted damage caused by ROS and RNS and their involvement in the generation of each other highlight the importance for controls to exist *in vivo* to limit the over-production of NO, $O_2^{\bullet-}$, H_2O_2, $OH^{\bullet}$ and other noxious species.

Reactive oxygen species can be generated in various ways in the algal symbiont of reef environments. Predominant areas of ROS production in these photosynthetic organisms include mitochondria, chloroplasts, peroxisomes (Apel and Hirt 2004) and glyoxysomes (Lesser 2006). The hypoxic conditions generated by photosynthesis within the chloroplast make this organelle a prime producer of ROS within photosynthetic organisms (Furla *et*

al. 2005, Lesser 2006). Photoreduction of O_2 to $O_2^{\bullet-}$ occurs in the electron transport chain (ETC) by reduced electron transport components associated with PSI (Apel and Hirt 2004) through Mehler reaction chemistry, making this photosystem the main source of $O_2^{\bullet-}$ in the chloroplast (Asada 2006). $^1O_2$ is continuously produced in PSII by energy transfers between triplet state P680 and O_2 (Apel and Hirt 2004, Asada 2006, Halliwell 2006) and $O_2^{\bullet-}$ and $HO^{\bullet}$ are also generated within this photosystem (Lesser 2006). Furthermore, H_2O_2 can be generated by Rubisco activity in the chloroplast, which generates P-Glycolate, and glycolate-oxidase and CAT-peroxidase activity in the peroxisome, which then use P-Glycolate as a substrate to form H_2O_2 (Apel and Hirt 2004).

ROS production can occur in other areas within the cell in addition to the choroplast, including the mitochondrion. The early ETC components of a mitochondrion can leak electrons directly to O_2 and form $O_2^{\bullet-}$ (Halliwell 2006) which then form H_2O_2 by dismutation (Turrens 1997). The main sources of electrons that cause mitochondrial $O_2^{\bullet-}$ formation are the ubisemiquinone radical ($QH^{\bullet}$) of complex III and at complex I, the FMN cofactor, various Fe-S clusters or the Q binding site (Brooks 2005) and NADH dehydrogenase (Turrens 1997). In addition to the mitochondrion, enzymes can be involved in ROS generation. The main categories of enzymes that have been attributed to ROS production are peroxidases and oxidases, including NADPH-oxidases, xanthine oxidases, and amine oxidase (Apel and Hirt 2004). Furthermore, within the endoplasmic reticulum, a collective group of cytochromes called cytochrome P-450 have the potential to generate $O_2^{\bullet-}$ through their involvement in electron transport between O_2 and organic substrates through the use of NADPH as an electron donor (Lesser 2006).

1.5 The role of antioxidants and antioxidant enzymes

A paradox in ROS generation and control *in vivo* exists in the important physiological roles that they play, as secondary messengers in gene expression, components of cell apoptosis (Lesser 2006), protection against pathogens (Apel and Hirt 2004), and their ability to cause excess damage when overproduced. Organisms have developed mechanisms to balance intracellular ROS through the synthesis and employment of

antioxidant molecules and enzymes. Antioxidant molecules that quench ROS include glutathione GSH, cysteine, hydroquinones, mannitol, vitamins C and E, flavonoids, some alkaloids, and β-carotene (Scandalios 1993). These antioxidants are utilized by a variety of antioxidant enzymes in their quenching processes and these enzymes include: (1) ascorbate peroxidase and GHS reductase, which are believed to quench chloroplast and mitochondrial generated H_2O_2 respectively, (2) catalase and peroxidase enzymes that quench H_2O_2 and (3) the superoxide dismutase (SOD) enzymes that quench $O_2^{\bullet-}$ (Scandalios 1993) in the reaction of $2O_2^{\bullet-}+2H^+ \rightarrow H_2O_2+O_2$ (Halliwell 2006).

The distribution and structure of antioxidant enzymes within photosynthetic organisms are not uniform. Various forms of SODs contain different active site trace metals and are distributed selectively within a cell. The first of these variants is the manganese (MnSOD) form, which is found in the mitochondrial matrix. In addition, a copper and zinc (Cu/ZnSOD) form can be found in the mitochondrial intermembrane space, the chloroplast, the cytosol (Halliwell 2006), peroxisomes and in extracellular regions (Lesser 2006). The final SOD form contains iron as its active group (FeSOD), and is found in the chloroplast (Halliwell 2006, Lesser 2006). Within the host (animal) and symbiont (alga) cells of corals, various isoforms of SODs have been detected. MnSODI can be found in the mitochondria of the host and symbiont and three non-mitochondrial SODs (MNSODII, III and IV) can be detected in the host endomeral tissue layer. Furthermore, two FeSOD isoforms are present in the symbiont and host endoderm (FESODI and II) while only a CuZnSOD isoform has been detected in the host ecto and endoderm tissues (Furla *et al.* 2005).

In addition to the wide variety of functional SODs, other antioxidant enzymes function in the control and sequestration of ROS and RNS. Enzymatic catalase, a tetrameric heme-containing enzyme (Lesser 2006), is located within the peroxisome while very little of the enzyme is detected in mitochondria and chloroplast (Halliwell 2006). In comparison, ascorbate peroxidase, a momeric heme-containing enzyme (Lesser 2006), is found throughout plants cells, occurring within chloroplasts and the cytosol (Halliwell 2006). Glutathione peroxidase is an additional antioxidant enzyme that may play a role in ROS quenching within the coral symbiosis but not from the algal standpoint. This antioxidant

is not found within plant cells and located in the mitochondria and cytosol of animal tissues (Lesser 2006), indicating it's potential role in the Cnidarian host.

In light of the extensive antioxidant defenses within cells, ROS production may overcome these quenching mechanisms under stressful conditions and result in oxidative damage. Photosynthetic organisms are susceptible to oxidative damage under stressful environmental conditions for multiple reasons. Localized hypoxia (2-3 fold greater than normal atmosphere conditions) occurs in the algal symbiont, and therefore the host, due to the generation of O_2 during photosynthesis (Furla *et al.* 2005), enhancing the potential for photodynamic ROS generation. In addition to these hypoxic conditions, any factor that decreases the rate of photosynthesis (photon utilization capacity) under levels of high solar radiation (photon intensity) can increase ROS production due to the presence of excess excitation energy and reducing equivalents within the chloroplast (Asada 1996) of the symbiotic alga. Conditions of excess incoming solar radiation at levels exceeding photosynthetic electron utilization can lead to reductions in photosynthetic rate, originally measured as sustained decreases in oxygen flux at high irradiance, and result in photoinhibition (Hoegh-Guldberg and Jones 1999). Photoinhibition can be either dynamic or chronic, with both types of photoinhibition characterized by a down regulation of photosynthetic systems (photoprotective processes divert excess energy from photosystem II (PSII) reaction center) or by irreversible damage to PSII that requires *de novo* synthesis of primary reaction center proteins before photochemistry can resume, respectively (Brown *et al.* 1999, Hoegh-Guldber and Jones 1999). Such declines in photosynthetic energy utilization have been detected in the algal symbionts of corals through the employment of pulse amplitude fluorometry (PAM), which allows an efficient determination of photochemical parameters that are indicative of stress in zooxanthellae whilst residing in the host (*in hospite)* (Jones *et al.* 1999). This rapid and non-invasive (Jones *et al.* 1999) technique has provided much insight into the declines of maximal PSII photochemical efficiency (F_v/F_m) of zooxanthellae under conditions of temperature stress (Brown *et al.* 1999). Studies of corals exposed to increased temperature have detected photoinhibition and decreases in the F_v/F_m of zooxanthellae; making declines in F_v/F_m an accepted indicator of stress and an established precursor to bleaching events (Jones *et al.* 1999). The impairment of photosynthesis and decreases in

F_v/F_m under conditions of temperature stress have been attributed to damage or specific components of the photosynthetic process including: excessive damage to the reaction center of the PSII complex, specifically at the D1 protein (Warner *et al.* 1999) and impaired CO_2 fixation and limitations in assimilatory electron flow (Jones *et al.*1998). Although each theory invokes different mechanisms that result in decreased maximal photosynthetic efficiency, each have the potential to generate similar effects. If incoming energy is not dissipated from the excited components of the photosynthetic electron transport chain, increased ROS production will occur and coincide with an increase in ROS transfer to the host, resulting in coral bleaching.

1.6 Variable bleaching and trace metals in offshore coral reefs

The synergistic effect of high temperature and irradiance stress on the oxidative load of the coral-algal symbiosis has been established as a main cause of bleaching. When examining bleaching occurrences over an entire reef flat it becomes obvious that bleaching responses are not uniform between or within coral species when exposed to uniform temperature and irradiance stress. Intraspecific variation exists in the thermal tolerance of species of corals exhibiting the same genotypes. Bleaching can occur on the coral head of one colony on a reef flat while adjacent colonies of the same species do not show signs of bleaching, suggesting a genotypic component associated with bleaching response (Jokiel and Coles 1990). In addition to the genetic component involved in various bleaching responses, the physical environment, in particular the availability of inorganic nutrients, of the reef has the potential to influence the coral algal symbionts response to increased temperature and irradiance.

Coral reef environments are oligotrophic, characterized by waters containing low concentrations of macronutrients (nitrogen and phosphorus) and micronutrients. The trace metal iron (Fe) often controls phytoplankton photophysiology and is present at low concentrations within open oceans due to the insolubility of its most prevalent form, the ferric cation (Fe^{3+}), in oxygenated seawater (Shi *et al*. 2007). This limitation is further enhanced in coral reef environments far removed from continental shore lines, for example the Great Barrier Reef (GBR) in Australia, due to little enrichment of iron from

terrestrial origin, i.e. river inflow (Entsch *et al.* 1983), or dust deposition (Shi *et al.* 2007). Focusing on the GBR in Australia, the neighbouring Coral Sea has been found to contain 0.2-0.3 nM of total Fe (Obata *et al.* 2008). Furthermore, Entsch *et al.* (1983) detected low concentrations of iron in the waters (2×10^{-8} M Fe), the surface sediments (66 ± 26 (1SD) ppm total Fe) and the interstitial water near the surface (5×10^{-7} M Fe) of a mid-shelf reef of the GBR, Davies Reef. Signatures of iron limitation are detectable within reef organisms and were found in zooxanthellae isolated from a soft coral, *Sinularia sp.* and in zooxanthellae isolated from the giant clam, *Tridacna maxima*. The zooxanthellae of *Sinularia* contained a three-fold lower concentration of total iron and ferredoxin, indicating iron limitation of the zooxanthellae *in hospite* and that certain species on a reef may be exposed to different levels of iron stress which can affect their biomass and species distribution (Entsch *et al.* 1983). In addition to iron, other trace metals may be limited within the GBR due to low input from the continental shoreline and have serious impacts on the physiology of the existent coral-symbiont populations.

A trace metal limited environment can have profound impacts on coral-algal symbiont physiology due to the role of trace metals in important biological molecules. Iron is an important trace metal for photosynthetic organisms due to its structural and functional role in antioxidants (see above), photosynthetic and respiratory electron transport, nitrate and nitrite reduction, N_2 fixation, and chlorophyll synthesis (Geider and La Roche 1994). The photosynthetic electron transport chain itself is highly reliant upon iron because the trace metal is involved in the structure of PSII, the cytochrome b_6F complex, PSI, ferredoxin and cyt c553, with estimates of 23-24 molecules of iron required per photosynthetic unit (Shi *et al.* 2007, Figure 1.1). The trace metals manganese and copper also have critical structural and functional roles in antioxidant activity (*see above*) and photosynthesis. Within the photosynthetic unit, four molecules of manganese are required for the function of the oxygen evolving complex of PSII (Yachandra *et al.* 1996, Figure 1.1) and copper is required in the structure of plastocyanin, a molecule involved in electron flow between the cytochrome b_6f complex and photosystem 1(Shcolnick and Keren 2006). The key roles of iron, manganese, and copper in photosynthetic organisms illustrates the importance of these molecules to coral-algal symbionts and the negative effects that can be generated by their absence.

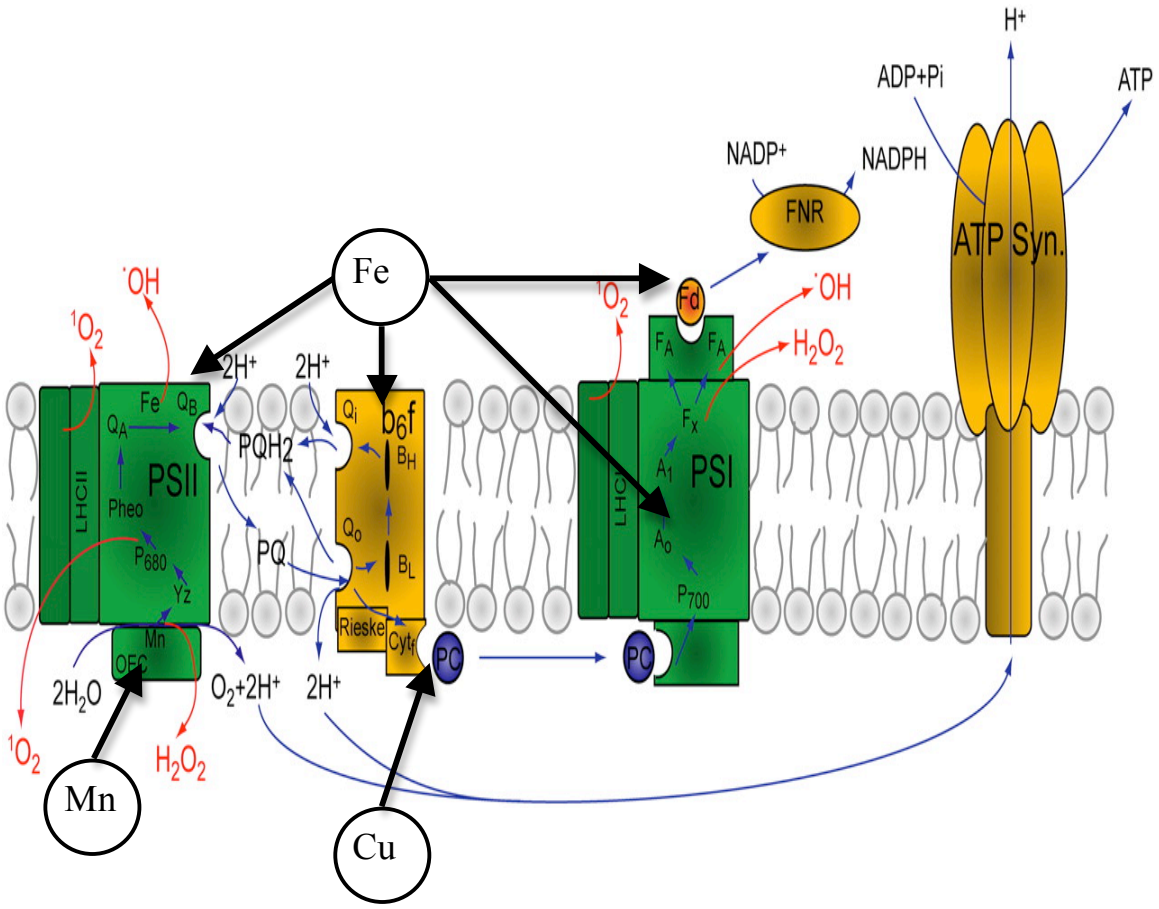
H+
ADP+Pi
ATP
NADP+
NADPH
FNR
ATP Syn.
Fe
OH
1O2
2H+
2H+
Fe
QB
QA
PSII
LHCII
Pheo
P680
Yz
Mn
OEC
PQH2
PQ
Qi
b6f
BH
Qo
BL
Rieske
Cytf
PC
Fd
FA
FA
Fx
A1
PSI
LHCI
Ao
P700
PC
OH
H2O2
1O2
2H2O
O2+2H+
2H+
1O2
H2O2
Mn
Cu

Figure 1.1 Diagram of the photosynthetic electron transport chain, ROS generation and trace metal requirements, modified from Shcolnick and Keren (2006). Highlighted within the diagram are the locations of Cu, Fe, and Mn within the photosynthetic electron transport chain. Cu is a critical component of plastocyanin (PC), a molecule responsible for electron movement between cytochrome b_6f and PSI (Shcolnick and Keren 2006). Fe plays structural roles within PSII, the cytochrome b6f complex, PSI and the protein ferredoxin (fd) and four Mn ions are responsible for the transfer of electrons from water to PSII (Shcolnick and Keren 2006).

The role of trace metals in photosynthetic organisms is known to induce changes in photophysiology and many studies have focused on such effects under iron-limited conditions. In the diatom *Phaeodactylum tricornutum,* iron limitation resulted in decreases in the relative abundance of many PSII proteins, including D1, CP43 and CP47. These results suggest that an increase occurred in the fraction of nonfunctional reaction centers under iron-limited conditions because no change was detected in the levels of light-harvesting chlorophyll proteins (Green *et al.* 1991). Influences of iron limitation on photosynthetic capacity have also been detected in the chlorophyte *Dunaliella tertiolecta* and the marine diatom *Phaeodactylum tricornutum.* Iron limitation to each of these species resulted in reduced variable/maximum fluorescence ratios and reduced fluorescence per unit absorption at all wavelengths (400-575 nm) (Green *et al.* 1992). Furthermore, Shi *et al.* (2007) determined that iron deficient *Trichodesmium erythraeum* IMS101 cells display reductions in the functional absorption cross-sections of PSII, 80% decreases in PSII quantum yield and declines in the Qa-reoxidation rate, suggesting reduced electron transfer components on the acceptor side of PSII. The multifaceted effect of iron limitation on photophysiology is prevalent in natural environments, influencing the biota living under these trace metal limited conditions.

Limitation in trace metal availability within reef environments may explain the variable bleaching responses of corals when exposed to uniform high temperature and high irradiance. Limitation in trace metals could potentially influence the occurrence and activity of antioxidant enzymes, which contain trace metals such as iron, manganese, copper, and zinc within their structure (Lesser 2006). Increases in oxidative load have been detected in phytoplankton species exposed to limiting trace metal conditions. In the diatom, *Thalassiosira weissflogii*, Peers and Price (2004) detected increases in oxidative load under iron limiting conditions using the probe H_2DCF-DA and fluorometry. Furthermore, they determined that when the cells were exposed to iron limiting conditions, *T. weissflogii* required more manganese to activate the antioxidant enzyme superoxide dismutase. Their study concluded that iron and manganese limitation might simultaneously increase oxidative stress in phytoplankton by increasing ROS production (iron limitation) and decreasing ROS consumption (manganese limitation) (Peers and

Price 2004). The effects of trace metal limitation on the ROS load of phytoplankton may be extendable to the ROS load of algal symbionts *in hospite.* As illustrated by Entsch *et al.* (1983), algal symbionts of certain host species are iron-limited and might be limited by other trace metals as well. If these trace metals are limited to the algal symbionts and they are subjected to stressful environmental conditions, increases in ROS and RNS will occur. Differential availability of these trace metals within the tropical waters of coral reefs would influence each colonies internal trace metal concentration, their alga's access to these trace metals and their ability to handle oxidative stress.

The intricate role that oxidative stress plays within coral bleaching emphasizes the importance of measuring oxidative load within algal symbionts freshly isolated from corals under conditions of temperature and irradiance stress. Direct measures of oxidative stress are difficult due to the reactive and unstable nature of ROS and RNS, their short persistent times *in vivo* (Halliwell and Whiteman 2004) and the fact that they may be produced in very small quantities (Murrant and Reid 2001). The effective scavenging systems, including the antioxidant molecules and enzymes discussed above, complicate the measurement of oxidative load further due to their high scavenging affinity for ROS. Cellular components including thiol residues, molecular oxygen, metalloproteins and even other ROS and RNS may further complicate the detection of intracellular ROS and RNS due their high reactivity with the molecules (Murrant and Reid 2001). Furthermore, if *in hospite* measurements are desired, a detection method at the point source of production would be required (Driever *et al.* 2009), necessitating a cell permeable assay. An optimal method that overcomes the challenges of ROS and RNS detection should be highly sensitive to the species of detection, should be able to gain access to the intracellular location of ROS or RNS production, be calibratible and should be of a high degree of sensitivity to the ROS or RNS of choice (Murrant and Reid 2001).

1.7 Fluorescent probes, flow cytometry and understanding oxidative stress

The employment of fluorescent probes and flow cytometry is an effective way to assay intracellular ROS and RNS generation. Fluorescent probes can penetrate cellular

membranes readily and permit the detection of intracellular ROS when combined with flow cytometry (Halliwell and Whiteman 2004) eliminating the problem of point source detection. Fluorescent probes are further attractive in their use due to their high sensitivity, simplicity and reproducibility (Chen *et al.* 2010). A wide variety of fluorescent probes exist to detect intracellular ROS species. A general indicator of intracellular ROS and RNS is the commonly used probe 5-(and 6) chloromethyl-2', 7'-dichlorodihydrofluorescein diacetate, acetyl ester (CMH_2DCFDA), which detects $NO^{\bullet}$, $OH\bullet$, $ONOO^-$ and H_2O_2. Furthermore, dihydroethidium (DHE), is an effective probe to detect $O_2^{\bullet -}$ $ONOO\bullet^-$ and $OH\bullet^-$ (Murrant and Reid 2001) while 4-amino-5-methylamino-2', 7'-difluorofluorescein diacetate (DAF-FM) can be utilized to detect intracellular $NO^{\bullet}$ (Kojima *et al.* 1998). Dihydrorhodamine 123 (DHR 123) can be utilized to determine intracellular ROS generated within the mitochondria (Lesser 1996). The wide variety of fluorescent probes, their reactivity with different ROS and RNS and the measurement of their oxidation using flow cytometry permit an overall generalization of oxidative load within the algal symbionts of corals exposed to temperature and irradiance stress under conditions of trace metal limitation.

Few studies have examined the effect of trace metal limitation on host-symbiont physiology of corals within reef environments. Ferrier-Pages *et al.* (2001) conducted the first experiment on the effects of iron enrichment on the reef building coral, *Stylophora pistillata* and the effects it had on photosynthesis and calcification rates. Under supplementation of 6 nM Fe, the aerial density of zooxanthellae and their maximal photosynthesis, when normalized to the surface area of the coral, increased. Calcification rates declined and were attributed to an imbalance of photosynthate transfer from the symbiont to the host (Ferrier-Pages *et al.* 2001), which is critical for the success of Scleractinian corals (Berkelmans and van Oppen 2006). Although Ferrier-Pages *et al.* (2001) did show an enhancement of zooxanthellae growth and photosynthesis under iron supplemented conditions, the role of iron and other trace metal limitation on symbiont photophysiology and oxidative stress levels remains to be explored.

1.8 Thesis objectives and hypothesis

The objective of this thesis is to determine the effects of trace metal limitation on the ROS and RNS load of coral-algal symbionts through the employment of flow cytometry. This area of research is unique and attractive as it will provide an understanding of the role of trace metal limitation in the process of oxidative coral bleaching. The trace metals selected for this thesis include iron, manganese, copper, and zinc due to their presence in antioxidant enzymes (as discussed above, Lesser 2006) and the role that iron, manganese and copper play within the photosynthetic electron transport chain (Raven 1990, Shcolnick and Keren 2006). The main hypothesis tested is that altering the availability of trace metals, in particular iron, manganese, copper, and zinc, will cause detectable increases in intracellular ROS and RNS of the symbiotic dinoflagellates of corals when residing in culture or *in hospite* under conditions of temperature and irradiance stress, leading to coral bleaching.

1.9 References

Apel, K., and H. Hirt. 2004. Reactive oxygen species: metabolism, oxidative stress and signal transduction. *Annu. Rev. Plant Biol*. 2004. 55:373–9.

Asada, K. 1996. Radical production and scavenging in the chloroplasts. p.123-150. *In* Baker, L.R. [eds.], Photosynthesis and the Environment. Kluwer Academic Publishers. The Netherlands.

Asada, K. 2006. Production and scavenging of reactive oxygen species in chloroplasts and their functions. *Plant Physiol.* 141:391-396.

Barber, R.T., A.K. Hilting and M.L. Hayes. 2001. The changing health of coral reefs. *Human and Ecological Risk Assessment*. 7:1255-1270.

Berkelmans, R. and M.J.H. van Oppen. 2006. The role of zooxanthellae in the thermal tolerance of corals: a 'nugget of hope' for coral reefs in an era of climate change. *Proc. R. Soc. B*. 273:2305-2312.

Brookes, P.S. 2005. Mitochondrial H^+ leak and ROS generation: An odd couple. *Free Radical Biol. Med.* 38:12-23.

Brown, B.E. 1997. Coral bleaching: causes and consequences. *Coral reefs*. 16: Suppl. S129-S138.

Brown, B.E., I. Ambarsari, M.E. Warner, W.K. Fitt, R.P. Dunne, S.W. Gibb and D.G. Cummings. 1999. Diurnal changes in photochemical efficiency and xanthophyll concentrations in shallow water reef corals: evidence for photoinhibition and photoprotection. *Coral Reefs* 18:99-105.

Brown, B.E., R.P. Dunne, M.E. Warner, I. Ambarsari, W.K. Fitt, S.W. Gibb and D.G. Cummings. 2000. Damage and recovery of photosystem II during a manipulative field experiment on solar bleaching in the coral *Goniastrea aspera*. *Mar. Ecol. Prog. Ser*. 195:117-124.

Chen, X., Z. Zhong, Z. Xu, L. Chen, and Y. Wang. 2010. 2`,7`-Dichlorodihydrofluorescein as a fluorescent probe for reactive oxygen species measurement: Forty years of application and controversy. *Free Radical Research* 44**:** 587-604.

Donner, S.D., W.J. Skirving, C.M. Little, M. Oppenheimer and O. Hoegh-Guldberg. 2005. Global assessment of coral bleaching and required rates of adaptation under climate change. *Global Change Biol.* 11: 2251-2265.

Douglas, A.E. 2003. Coral bleaching- how and why? *Mar. Pollut. Bull.* 46: 385-392.

Downs, C.A., Fauth, J.E., Halas, J.C., Dustan, P., Bemiss, J. and C.M. Woodley. 2002. Oxidative stress and seasonal coral bleaching. *Free Rad. Biol. & Med.* 33:533-543.

Driever, S.M., M.J. Fryer, P.M. Mullineaux and N.R. Baker. 2009. Imagining of reactive oxygen species *in vivo. Methods Mol. Biol*. 479:109-16.

Dykens, J.A., J.M. Shick, C. Benoit, G.R. Buettner and G.W. Winston. 1992. Oxygen radical production in the sea anemone *Anthopleura elegantissima* and its endosymbiotic algae. *J. Exp. Biol*. 168: 219-241.

Entsch, B., R.G. Sim and B.G. Hatcher. 1983. Indications from photosynthetic components that iron is a limiting nutrient in primary producers on coral reefs. *Mar. Biol.* 73: 17-30.

Falkowski, P.G., Z. Dubinsky, L. Musacatine and J.W. Porter. 1984. Light and the bioenergetics of a symbiotic coral. *Bioscience*. 34: 704-709.

Ferrier-Pages, C., V. Schoelzke, J. Jaubert, L. Muscatine and O. Hoegh-Guldberg. 2001. Response of a Scleractinian coral, *Stylophora pistillata* to iron and nitrate enrichment. *J. Exp. Mar. Biol. Ecol.* 259:249-261.

Fitt, W.K., Brown, B.E., Warner, M.E. and R.P. Dunne. 2001. Coral bleaching: interpretation of thermal tolerance limits and thermal thresholds in tropical corals. *Coral Reefs*. 20: 51-65.

Franklin, D.J., O. Hoegh-Guldberg, R.J. Jones and J.A. Berges. 2004. Cell death and degeneration in the symbiotic dinoflagellates of the coral *Stylophora pistillata* during bleaching. *Mar. Ecol. Prog. Ser.* 272: 117-130.

Furla, P., D. Allemand, J.M. Shick, C. Ferrier-Pages, S. Richier, A. Plantivaux, P. Merle, and S. Tambutte. 2005. The symbiotic anthozoan: a physiological chimera between alga and animal. *Integ. Comp. Biol*. 45: 595-604.

Geider, R.J. and J. La Roche. 1994. The role of iron in phytoplankton photosynthesis, and the potential for iron-limitation of primary productivity in the sea. *Photosynth. Res.* 39. 275-301.

Glynn, P.W. 1989. Coral mortality and disturbances to coral reefs in the tropical Eastern Pacific. p. 55-126. *In* Glynn, P.W. [eds.], Global consequences of the 1982-83 El Nino-Southern Oscillation, Elsevier Oceanography Series. Elsevier Science Publishers B.V. Amsterdam, The Netherlands.

Glynn, P.W. 1993. Coral reef bleaching: ecological perspectives. *Coral Reefs* 12: 1-17.

Glynn, P.W. 1996. Coral reef bleaching: facts, hypotheses and implications. *Global Change Biol.* 2: 495-509.

Greene, R.M., R.J. Geider and P.G Falkowski. 1991. Effect of iron limitation on photosynthesis in a marine diatom. *Limnol. Oceanogr.* 36: 1772-1782.

Green, R.M., R.J. Geider, Z. Kolber and P.G. Falkowski. 1992. Iron-induced changes in light harvesting and photochemical energy conversion processes in eukaryotic marine algae. *Plant. Physiol.* 100: 565-575.

Gutteridge, J.M.C. and Halliwell, B. 2000. Free radicals and antioxidants in the year 2000: A historical look to the future. *Annals of the New York Academy of Sciences.* 899:136-147.

Halliwell, B. 2006. Reactive species and antioxidants. redox biology is a fundamental theme of aerobic life. *Plant Physiol*. 141:312-322.

Halliwell, B. and M. Whiteman. 2004. Measuring reactive species and oxidative damage *in vivo* and in cell culture: how should you do it and what do the results mean? *British J. of Pharmacol.* 142: 231-255.

Halliwell, B. and J.M.C. Gutteridge. 1992. Biologically relevant metal ion-dependent hydroxyl radical generation, an update. *FEBS.* 307: 108-112.

Harriot, V.J. 1985. Mortality rates of Scleractinian corals before and during a mass bleaching event. *Mar. Ecol. Prog. Ser*. 21:81-88.

Hoegh-Guldberg, O. 1999. Climate change, coral bleaching and the future of the worlds coral reefs. *Mar. Freshwater Res*. 50: 839-66.

Hoegh-Guldberg, O. and R.J. Jones. 1999. Photoinhibition and photoprotection in symbiotic dinoflagellates from reef-building corals. *Mar. Ecol. Prog. Ser.* 183: 73-86.

Jones, R.J., O. Hoegh-Guldberg, A.W.D Larkum and U. Schreiber. 1998. Temperature-induced bleaching of corals begins with impairment of the CO_2 fixation mechanism in zooxanthellae. *Plant, Cell, Environ*. 21: 1219-1230.

Jones, R.J., T. Kildae and O. Hoegh-Guldberg. 1999. PAM chlorophyll fluorometry: a new *in situ* technique for stress assessment in Scleractinian corals, used to examine the effects of cyanide from cyanide fishing. *Mar. Pollut. Bull*. 38: 864-874.

Jokiel, P.L. and S.L. Coles. 1990. Response of Hawaiian and other Indo-Pacific reef corals to elevated temperatures. *Coral Reefs* 8:155-162.

Kojima, H., Nakatsubo, N., Kikuchi., Kawahara, S., Kirino, Y., Nagoshi, H., Hirata, Y. and T. Negano. 1998. Detection and imagining of nitric oxide with novel fluorescent indicators: Diaminofluoresceins. *Anal. Chem.* 70: 2446-2453

Lesser, M.P. 1996. Elevated temperatures and ultraviolet radiation cause oxidative stress and inhibit photosynthesis in symbiotic dinoflagellates. *Limnol Oceanogr*. 41: 271-283.

Lesser, M.P. 1997. Oxidative stress causes coral bleaching during exposure to elevated temperatures. *Coral Reefs* 16:187-192.

Lesser, M.P. 2006. Oxidative stress in marine environments. *Annu. Rev. Physiol*. 68:253-278.

Lesser, M.P. 2011. Coral bleaching: causes and mechanisms, pp. 405-419. *In* Z. Dubinsky and N. Stamber [eds.], Coral reefs, an ecosystem in transition. Springer science USA.

Lesser, M.P. and J.H. Farrell. 2004. Exposure to solar radiation increases damage to both host tissues and algal symbionts of corals during thermal stress. *Coral Reefs* 23:367-377.

Lesser, M., W.R. Stochaj, D.W. Tapley and J.M. Shick. 1990. Bleaching in coral reef anthozoans effects of irradiance, ultraviolet radiation, and temperature on the activities of protective enzymes against active oxygen. *Coral Reefs* 8:225-232.

Murrant, C.L. and M.B. Reid. 2001. Detection of reactive oxygen and reactive nitrogen species in skeletal muscle. *Microsc. Res. and Techniq.* 55: 236-248.

Muscatine, L. and V. Weis. 1992. Productivity of zooxanthellae and biogeochemical cycles. p. 257 -271. *In* P.G. Falkowski and A.D. Woodhead [eds.], Primary productivity and biogeochemical cycles in the sea. Plenum Press, New York, USA.

Muscatine, L., Falkowski, P.G., Porter, J.W. and Z. Dubinsky. 1984. Fate of photosynthetic fixed carbon in light and shade-adapted colonies of the symbiotic coral *Stylophora pistillata. Proc. R. Soc. Lond*. 222: 181-202.

Nybakken, J.W. 1997. Tropical communities. p. 338-394. *In*: Marine biology, An ecological approach, fourth edition. Addison-Wesley Educational Publishers Inc. MA, USA.

Obata, H., K. Shitashima, K. Issiki and E. Nakayama. 2008. Iron, manganese and aluminum in upper waters of the western South Pacific Ocean and its adjacent seas. *Oceanogr.* 64:233-245.

Peers, G. and N.M. Price. 2004. A role for manganese in superoxide dismutases and growth of iron-deficient diatoms. *Limnol. Oceanogr*. 49: 1774-1783.

Raven, J.A. 1990. Predictions of Mn and Fe use efficiencies of phototrophic growth as a function of light availability for growth and of C assimilation pathway. *New*

Phytol. 116:1-18.

Reaser, J.K., R. Pomerance, and P.O. Thomas. 2000. Coral bleaching and global climate change: Scientific findings and policy recommendations. *Conserv. Biol*. 14:1500-1511.

Ruppert, E., R. Fox and R. Barnes. 2004. Cnidaria p. 111-180. *In*: Invertebrate zoology, a functional evolutionary approach. Brooks/Cole-Thomson Learning. Belmont, CA, USA.

Turrens, J.F. 1997. Superoxide production by the mitochondrial respiratory chain. *Biosci. Report*s 17: 3-8.

Scandalios, J.G. 1993. Oxygen stress and superoxide dismutases. *Plant Physiol*. 101: 7-12.

Shcolnick, S. and N. Keren. 2006. Metal homeostasis in cyanobacteria and chloroplasts. Balancing benefits and risks to the photosynthetic apparatus. *Plant Physiol*. 141: 805-810.

Shi, T., Y. Sun and P.G. Falkowski. 2007. Effects of iron limitation on the expression of metabolic genes in the marine cyanbobacterium *Trichodesmium erythraeum* IMS101. *Environ.l Microbiol*. 9: 2945- 2956.

Shick, J.M., M.P. Lesser, W.C. Dunlap, W.R. Stochaj, B.E. Chalker and J.W. Won 1995. Depth-dependent responses to solar ultraviolet radiation and oxidative stress in zooxanthellate coral *Acropora microphthalma. Mar. Biol*. 122: 41-51.

Smith, D.J., D.J. Suggett and N.R. Baker. 2005. Is photoinhibition of zooxanthellae photosynthesis the primary cause of thermal bleaching in corals? *Global Change Biol.* 11:1-11.

Stabler, N. 2011. Zooxanthellae: the yellow symbionts inside animals. pp. 87-106. *In* Z. Dubinsky and N. Stamber [eds.], Coral reefs, an ecosystem in transition. Springer science USA.

Yachandra, V.K., K. Sauer, and M.P. Klein. 1996. Manganese cluster in photosynthesis: where plants oxidize water to dioxygen. Chem. Rev. 95: 2927-2950.

Warner, M.E., W.K. Fitt and G.W. Schmidt. 1999. Damage to photosystem II in symbiotic dinoflagellates: A determinant of coral bleaching. *Proc. Natl. Acad. Sci.* 96: 8007-8012.

Chapter 2
Responses to iron limitation in two colonies of *Stylophora pistillata* exposed to high temperature: implications for coral bleaching.

2.1 Introduction

The persistence and paradoxical productivity of modern coral reefs in oligotrophic tropical seas rests in the great diversity of reef-building scleractinians that owe their success to a mutualistic exchange of nutrients between the coral hosts and their co-evolved endosymbiotic algae, typically dinoflagellates of the genus *Symbiodinium.* Metabolic wastes of the coral are utilized by its endosymbiotic alga for the production of photosynthetically reduced carbon metabolites that are shared with the host (Muscatine 1990, Stanley 2006). Environmental conditions that reduce the productivity of coral photosynthesis tend to be destabilizing, in extreme cases leading to the loss of endosymbionts or their pigments (the condition known as coral bleaching) and ultimately to the death of the colony if the symbiosis is not re-established (Glynn 1996). Such perturbations of the partnership ultimately may have caused the collapse of reefs and mass extinctions of scleractinians throughout the Phanerozoic (Stanley and Schootbrugge 2009).

Geographically widespread mass bleaching of coral reefs has been unambiguously linked to prolonged periods (days to weeks) of summer temperatures 1 °C–2 °C above the long-term maximum for the area affected (Hoegh-Guldberg 1999, Lough 2000, Jokiel 2004). The mass bleaching of corals is an extreme response to severe conditions that is superimposed on the normal adjustments of the algal population in the host's tissues during acclimatization to local and seasonal variations in the thermal, nutrient, and photic environments of a coral reef (Fitt *et al.* 2001). Even so, elevated temperatures alone are often not sufficient to cause bleaching, and the specific biological mechanisms underlying the destabilization of coral-endsymbiont partnerships remain to be fully elucidated.

The emerging consensus on coral bleaching relates high temperatures and solar irradiances to oxidative stress created when over-reduced photosystems of the algal endosymbionts produce excessive levels of reactive oxygen species (ROS) that overwhelm the antioxidant defenses in the alga and their coral host, thereby leading to damage and loss of endosymbionts (Hoegh-Guldberg 1999, Lesser 2006, Weis 2008). Therefore, because the major enzymatic antioxidants in algae, including endosymbiotic dinoflagellates, are metalloenzymes [Cu/Zn-superoxide dismutase (Cu/Zn-SOD), Mn-SOD, Fe-SOD, and iron-containing catalase and ascorbate peroxidase] (Asada 1999, Raven *et al.* 1999, Richier *et al.* 2005), we hypothesize that the stress contributing to coral bleaching is increased by a limitation in the bioavailability of iron and other trace metals essential to antioxidant defenses and the photosynthetic apparatus, manifested in phytoplankton as the loss of primary production (Palenik *et al.* 1991, Peers and Price 2004, Allen *et al.* 2007).

The basis for the inadequacy of the normally robust antioxidant defenses of algae under exceptionally stressful conditions has not been critically addressed in the context of coral bleaching. Corals in tropical seas characteristically experience low levels of inorganic nutrients (Muscatine and Porter 1977) and low concentrations of essential trace metals (Measures and Vink 1999, Obata *et al.* 2008, M. L. Wells *et al.* unpubl.), so that like other microalgae and cyanobacteria on coral reefs and phytoplankton in the surrounding waters, the photochemical efficiency of endosymbiotic dinoflagellates may be limited during metal-deficient conditions (Entsch *et al.* 1983, Sakka *et al.* 1999). This limitation may be pronounced because the host will tightly regulate trace metal speciation and intracellular availability of free metal ions (e.g., via the iron-sequestering protein ferritin: Császár *et al.* 2009) to avoid their cytotoxic effects (Weinberg 1999, Ferrier-Pagès *et al.* 2001, Gaetke and Chow 2003). Such trace-metal limitation may become more acute during thermal stratification in summer when microbial competition for metals in surface waters would be intense.

The coincident effects of water column stratification and decreased metal availability under high insolation might help to explain the patchiness of coral bleaching under apparently uniform thermal stress. For example, spatial analyses of the 1998 and 2002

mass bleaching events on the Great Barrier Reef (GBR), Australia, showed that coral bleaching over scales of tens of km of apparently uniform temperature was not spatially consistent but displayed a patchiness that might arise from local oceanographic conditions (Berkelmans *et al.* 2004, Wooldridge and Done 2004) that could influence, among other variables, trace metal distributions. Even so, considering the metals' multifarious roles in the metabolic redox biochemistry of phototrophs (Raven *et al.* 1999), the effects of trace metal limitation on defenses against oxidative stress may be just one factor contributing to the complex symbiotic dysfunction of coral bleaching.

Although strong iron chelators experimentally added to seawater can induce iron limitation in phytoplankton (Wells *et al.* 1994; Hutchins *et al.* 1999; Wells and Trick 2004), such experiments have yet to be performed on symbiotic corals. It is therefore unknown how symbiotic algae *in hospite* may respond to iron depletion in the seawater bathing the host coral, although exogenous iron enrichment is known to cause an increase in the surface areal density of dinoflagellates in the coral *Stylophora pistillata* (Ferrier-Pagès *et al.* 2001). Herein we report the results of initial experiments on the effect of chronic iron restriction at different experimental temperatures on maximum quantum yield in PSII (F_v:F_m) in dinoflagellates in two colonies of *S. pistillata* from reefs separated by >100 km in the central GBR. We also present data on the concentrations of photosynthetic pigments and photoprotective xanthophylls in symbiotic dinoflagellates isolated from these colonies to afford biochemical evidence for non-photochemical quenching of excess photon energy, which presumably reduce the production of ROS under chronically iron-limited conditions.

2.2 Methods

2.2.1 Collection and maintenance of corals—A colony of *Stylophora pistillata* Esper, 1797 was collected in early January 2008 on Davies Reef, central GBR, Australia (18° 49.334' S: 147°37.730' E), at a depth of 10.5 m, where the water temperature was 28.4°C. Midday levels of photosynthetically available radiation (PAR, 400-700 nm) at the collection site, measured at the depth of the collected colony, ranged from ~100 to 500

μmol photons•m^{-2}•s^{-1}. The coral subsequently was maintained at the Australian Institute of Marine Science, Townsville, in an outdoor tank of flowing seawater at 27 °C–28 °C under a translucent roof and additional shade cloth that reduced maximum PAR to 80–100 μmol photons•m^{-2}•s^{-1}.

In early February 2008, multiple nubbins approximately 4 to 5 cm long were cut from the colony, suspended individually on 0.25 mm diameter nylon monofilament line, and allowed to recover in the holding tank. Heavy rains in February diluted the coastal seawater pumped into the holding tank, where salinity was approximately 30 psu for two weeks. When the salinity continued to fall, the flow rate into the tank was reduced and the natural seawater was supplemented thrice daily with a brine prepared from commercial swimming pool salts (99% NaCl, no anti-caking agent added) to maintain the salinity at 30–32 psu; at no time did the salinity drop below 27.4 psu, and the corals evinced no paling from low-salinity stress. When experiments were commenced on these nubbins in late February, they were considered fully acclimatized to a salinity of 30 psu due to their high PSII photochemical efficiency (>0.65), and the onsuing experiments were conducted at this salinity to avoid osmotic shock.

A second colony of *S. pistillata* was collected in late March 2008 at Pelorus Reef adjacent to Orpheus Island, central GBR (18°39.311' S : 146°29.679' E) at a depth of 6 m. The coral was maintained in the outdoor holding tank described above in normal salinity at 27 °C– 28 °C and 80–100 μmol photons•m^{-2}•s^{-1}. In mid-April multiple nubbins were cut from vertical branches of the colony and suspended using nylon monofilament. To prevent the proliferation of endolithic algae and bacteria seen in the earlier experiment using coral collected from Davies Reef (*see* below), the cut surfaces of the Orpheus Island nubbins were sealed immediately with waterproof epoxy (Mr. Sticky's 001327 Underwater Glue, Advanced Adhesion). The slow healing of cut surfaces in *S. pistillata* was not simply a reflection of salinity stress on the Davies Reef colony, but also occurred in colonies from several other sites under optimal conditions. Coral tissue immediately adjacent to the epoxy remained brown and apparently healthy. The nubbins from the Orpheus Island colony were then allowed to recover for three weeks in an indoor aquarium with flowing seawater filtered to 1 μm at 26.5 °C, at an irradiance of 50 μmol

photons•m^{-2}•s^{-1}. Nubbins were fed twice weekly on freshly hatched brine shrimp nauplii during the recovery period.

2.2.2 Experimental apparatus — Both experiments were conducted in low-density polyethylene chambers (700 mL, Sistema Plastics) containing 300 mL of 0.5 μm-filtered seawater. Before use, the experimental chambers were cleaned of trace metal and organic contaminants by an initial wash with a low-residue detergent (Extran MAO3; Merck Pty.), followed by soaking with 3 mol L^{-1} trace-metal analytical grade HCl (Fisher Scientific) for a minimum of 1 week. The chambers then were successively rinsed a minimum of four times with Milli-Q (Millipore Corporation) deionized water and stored in 10% trace-metal grade HCl in deionized water for > 1 week. Chambers finally were rinsed three times with deionized water and once with the specific treatment medium immediately prior to the experiments.

Each chamber was fitted with plastic hooks attached to the lid from which coral nubbins were suspended in the contained seawater via the monofilament tethers. Nubbins cut from the Davies Reef colony were suspended with their long axis horizontal, giving each experimental nubbin a top, diurnally brightly illuminated surface and a bottom, shaded surface. Nubbins from the Orpheus Island colony were suspended vertically in the light field, with the branch tips uppermost, in the normal growth position. The seawater was continuously mixed in the chambers (sealed by lids with silicone gaskets and clips) by bubbling with air delivered from an aquarium pump utilizing an in-line filter (0.45 μm) to prevent entry of any particulate contaminants; the air exited via a syringe filter (0.4 μm) press-fitted into the lid of each chamber. Treated seawater in the chambers was replaced daily.

The sealed experimental chambers were ballasted externally and placed in four tanks (four chambers per tank) of flowing seawater (1.5 L min^{-1}) where the temperature was regulated to ± 0.1 °C. Room temperature was held at 24 °C– 25 °C, and fans circulated air across the exposed, sealed tops of the experimental chambers as an additional measure to reduce heating of the chambers during illumination. Each experimental treatment (*see* below) was split among four separate chambers, each containing two nubbins, and the

chambers for each treatment were distributed between the appropriate seawater tanks that served as temperature-controlled water baths set at low and high temperature.

Illumination during a 12:12 h light: dark cycle was provided by a 400 W metal halide lamp (BLV) suspended above each tank. Neutral density filters (plastic diffusers) were interposed between the lamps and the tanks. PAR (measured inside the chambers) averaged ~100 μmol photons•m^{-2}•s^{-1} in the preliminary experiment using the Davies Reef specimen, and ~150 μmol photons•m^{-2}•s^{-1} in the experiment conducted on the Orpheus Island coral. These relatively low irradiances, although above photosynthetic saturation for shade-acclimatized colonies of this species (Jones and Hoegh-Guldberg 2001), were chosen to prevent the onset of high light-induced bleaching and allowed for long-term experimentation. No significant variation in the internal irradiance was measured among the chambers before the experiment and to insure a uniform integrated irradiance among the treatments, chambers were rotated daily among marked positions in the baths under the lamps. Each lamp was fitted with a 5 mm thick Schott ROBAX® glass ceramic filter to remove ultraviolet wavelengths. No detectable ultraviolet-B radiation (measured using an International Light IL1400A radiometer and SEL240B sensor) reached the chambers, and ultraviolet-A measured beneath the chamber lids was only 25-μW cm^{-2} (IL1400A radiometer and SEL033 sensor).

2.2.3 Experimental protocol— Experiments involved four treatments: low temperature (28 °C with the Davies Reef colony and 27 °C with the Orpheus Island colony) in normal seawater (effectively a control, non-stressful condition); low temperature in seawater to which the strong iron chelator desferrioxamine B (DFB, Sigma-Aldrich Pty.) was added at a final concentration of 300 nmol L^{-1} to restrict iron availability (Wells *et al.* 1994; Wells and Trick 2004); high temperature (30 °C with the Davies Reef colony, and 30°C, then 31 °C, with the Orpheus Island colony) in normal seawater; and high temperature in seawater with 300 nmol L^{-1} DFB added. Desferrioxamine B limits iron uptake in phytoplankton at concentrations equimolar to the total dissolved iron concentrations in surface seawater (Wells *et al.* 1994; Wells and Trick 2004) but the iron concentrations in the flowing seawater source for these incubations would be higher and variable, from both contamination in the seawater distribution system and the effects of tides and

currents on the shallow intake water. We therefore chose to use an overwhelming DFB concentration to ensure that all labile (reactive) iron in the filtered seawater would be bound in DFB-Fe complexes.

For the experiment using the Davies Reef coral, $n = 6$ nubbins were subjected to each treatment, whereas for the experiment using Orpheus Island coral, $n = 8$ nubbins were subjected to each treatment. In the former case, two of the four chambers in each experimental treatment held two nubbins each, and the other two chambers each held one nubbin. In the latter case all four chambers housed two nubbins. Corals in both experiments were allowed three days to adjust to the experimental chambers containing unmodified seawater placed in the seawater baths at 28 °C (Davies Reef colony) or 27 °C (Orpheus Island colony) at the irradiance selected for the particular experiment. Initial measurements of chlorophyll fluorescence (*see* below) were made on days -2 and -1 (i.e., for two days prior to the application of experimental conditions). On day 0 of the experiment with the Davies Reef specimen, DFB was added to the appropriate chambers to produce iron-limited conditions and the temperature was ramped up from 28 °C to 30 °C during four days (0.5 °C d^{-1}) and then maintained at 30 °C for the rest of the experiment, which was terminated on day 11. On day 0 of the experiment with the Orpheus Island colony, DFB was added and the temperature was ramped from 27 °C to 30 °C over four days (0.75 °C d^{-1}) and held at 30°C until day 10, when temperature was further increased to 31°C over four days (0.25 °C d^{-1}). Temperature was held at 31 °C from day 14 until day 19, when the experiment was terminated.

2.2.4 Measurement of chlorophyll fluorescence—'Dark-adapted' maximum quantum yield in PSII (a measure of photochemical efficiency), calculated as the ratio of variable (F_v = maximal F_m minus minimal F_o) chlorophyll fluorescence to maximal chlorophyll fluorescence (F_v:F_m), was measured daily from day 0 until the end of each experiment by pulse amplitude modulation (PAM) fluorometry using a Diving-PAM instrument (Walz). A measuring light set to an intensity of 8 took all fluorescence measurements, and the samples were saturated with a saturating pulse set at an intensity of 8 and duration of 0.8 seconds. All measurements were made during the final 3 h of the 12 h dark period.

Experimental chambers were removed from the temperature baths in the dark and transported in a dark, insulated container to a darkened trace-metal clean room.

The clean room was fabricated within a standard laboratory using wood framing, plastic sheeting, and a downward-directed 0.61 × 1.22 m high-efficiency particle (HEPA) filter and fan module ducted to draw air (19.8 m^3 min^{-1}) from outside the enclosure through the filter, thereby generating a positive-pressure workspace. The bench area directly beneath the module was curtained off with plastic sheeting to create an ultraclean work surface. The chambers were transported first to plastic-covered bench-space in the clean room, the outer chamber surfaces rinsed with deionized water and wiped dry with low-lint tissues, and finally moved to the ultraclean work surface where they were opened for measurements. The variable chlorophyll fluorescence of each coral nubbin was measured using a custom-made clip to hold the tip of the fiber optic probe from the Diving-PAM at a fixed distance and angle from selected areas of the nubbin surface (*see* fig. 3 in Warner *et al.* 2010). All daily measurements of variable chlorophyll fluorescence were made the trace metal clean lab space.

The PAM measurements were made at several discrete points on both the top (diurnally illuminated) and bottom (shaded) surfaces of the nubbins cut from the Davies Reef specimen. Equal numbers of measurements for top and bottom surfaces were combined to give the response of the entire nubbin. The PAM measurements were made at several points around the periphery along the full length of the nubbins cut from the Orpheus Island specimen, and no distinction was made between the sampling points. The appropriate seawater (equilibrated at the experimental high or low temperature, with or without added DFB) in each experimental chamber was replaced following the daily PAM measurements, and the chambers were returned to the seawater baths prior to the onset of the light phase. The position of each chamber in the bath was changed daily to insure uniformity of sample irradiation. The experiments were terminated when F_v:F_m values dropped below 0.5, or if the nubbins began to slough tissue.

2.2.5 Isolation of dinoflagellates — On day 0 and at the end of the experiment on the Orpheus Island colony of *S. pistillata*, tissue was stripped from four nubbins using a jet of

compressed air in normal, filtered (0.22 μm pore size) seawater and recovered quantitatively for subsequent counting and biochemical analysis of the algae. The slurry containing algae and disrupted host tissue was passed through a 25 μm Nitex mesh and then centrifuged at 750 × *g* for 10 minutes at 4 °C. Pellets of these freshly isolated algae were resuspended and washed twice in 0.22 μm-filtered seawater with centrifugation between washes. The algae were isolated and cleaned under dim ambient illumination (5 μmol photons•m^{-2}•s^{-1}or lower). Quantified portions of the washed algae were taken for counting, for the determination of algal pigments, and for flow cytometric analysis (K. Iglic *et al.* unpubl., *see* Chapter 3). Algal cells destined for pigment analysis were frozen at -80°C and a portion was retained for genotypic identification of the clade to which the symbiotic dinoflagellates belonged.

2.2.6 Pigment analyses—Frozen pellets each containing approximately 1–2 × 10^5 dinoflagellates (determined by counting a portion of the final suspension of clean cells in a hemacytometer) were suspended in 1 mL of ice-cold 98% (v/v) high performance liquid chromatography (HPLC)-grade methanol and 2% (v/v) of 0.5 mol L^{-1} tetrabutyl ammonium acetate (TBAA, pH 6.5). The suspension was sonicated for 1 min on ice and then allowed to sit on ice for 1 h in the dark. Following a second sonication, the suspension of lysed cells was centrifuged at 10,000 × *g* for 5 min at 2 °C. The supernatant was passed through a pre-cleaned 0.2 μm syringe filter, and 0.4 mL of this extract was combined with 1.0 mL of 0.5 mol L^{-1} TBAA. Extracts were stored at -80 °C until HPLC analysis.

All solvents were of HPLC grade and sourced from Mallinckrodt Baker. Certified phytoplankton pigment standards were from DHI. All other chemicals were from Sigma. Pigments were separated on an endcapped Agilent Eclipse eXtra Defense Bonding C8 HPLC column (4.6 x 150 mm, 3.5 μm particle size; Agilent Technologies) using a Shimadzu HPLC (Shimadzu Australia) equipped with a single pump and solvent mixer, online degasser, refrigerated autosampler, column oven and photo-diode array (PDA) detector monitoring wavelengths 400–800 nm. The binary gradient method of Van Heukelem and Thomas (2001) was used with minor modifications. Solvent A consisted of 70:30 methanol containing 28 mmol L^{-1} TBAA (pH 6.5) and solvent B was neat

methanol. The programmed gradient was as follows (minutes; % solvent A:% solvent B): (0; 95:5), (11; 45:55), (15; 45:55), (22; 5:95), (29; 5:95), (31; 95:5), (40; 95:5). Pigments were identified by comparing their retention times and PDA profiles with those of certified standards. Calibration curves prepared from certified standards allowed the quantification of individual pigments in each sample.

2.2.7 Genotypic analyses—Portions of dinoflagellate samples frozen on day 0 and at the end of the Orpheus Island experiment were analyzed as follows to determine their genotypic affinity. Samples (approximately 1–2 mm^3) were frozen and thawed three times successively and then each was placed in a microtube with 750 µL extraction buffer containing 100 mmol L^{-1} Tris (pH 9.0), 100 mmol L^{-1} ethylenediaminetetraacetic acid (EDTA), 1% (w/v) sodium dodecyl sulfate (SDS), and 100 mmol L^{-1} NaCl. The extraction tubes were vortex-mixed and incubated overnight at 60 °C. The samples were then cooled on ice before adding 187.5 µL of 5 mol L^{-1} potassium acetate, vortex-mixed again, and incubated on ice for a further 10 min. The samples were centrifuged for 10 min at room temperature at 16,100 × *g* and the supernatants were transferred to clean microtubes. Isopropanol (600 µL) was added to precipitate deoxyribonucleic acid (DNA) and the samples were mixed by several gentle inversions. After a 5-min incubation at room temperature, the samples were centrifuged again for 15 min at room temperature at 16,100 × *g*. The supernatants were carefully removed and the pellets washed by adding 150 µL of 70% (v/v) ethanol, followed by gentle mixing and centrifuging as above for 5 min. The supernatants were removed and the pellets air-dried for 5 min. Samples were resuspended in 100 µL of 10 mmol L^{-1} Tris (pH 9.0). Polymerase chain reaction (PCR) amplification of the internal transcribed spacer (ITS)1 region and genotypic determination from the amplicon was performed by single-stranded conformational polymorphic analysis following the method described in Ulstrup and van Oppen (2003). Reference ITS1 samples of *Symbiodinium* genetic types C1, C2, and C3 were run in parallel with these samples.

2.2.8 Measurement of surface areas of coral nubbins—Experimental nubbins from the Orpheus Island colony from which the tissues had been stripped were cleaned in a dilute solution of commercial bleach, rinsed in deionized water, and dried in air. Following

shipment to Orono, Maine, nubbins were dusted with talc to reduce light scattering and scanned using a high-definition, multi-laser three-dimensional (3D) Scanner and ScanStudio™ software (version 1.1.0) from NextEngine. Surface areas were calculated by the ScanStudio™ software, which was empirically calibrated using a chalk cylinder of known surface area about the same size as the coral nubbins. The surface area of the nubbins was the divisor used to normalize the algal counts as an indicator of bleaching.

2.2.9 Statistical analyses—The effects over time for temperature increases and the addition of DFB on maximum photochemical efficiency (F_v:F_m) measured in nubbins of *S. pistillata* were tested using mixed-effect model analyses of variance (ANOVAs) that incorporated the random effect of replicate nubbins (every replicate nubbin in each condition was measured every day). Random effects were handled by an iterative Restricted Maximum Likelihood (REML) approach that automatically corrected variances across interaction effects (SAS Institute 2002). For the Davies Reef experiment, the fixed effect of nubbin surface (illuminated top; shaded bottom) also was incorporated into the analysis. The statistical analysis of fixed effects in both experiments was conservative, in that it considered all data beginning on day 0 (from which temperatures were increased), not only data taken when the final higher temperature actually was achieved four days later.

Numbers of dinoflagellates per square centimeter of nubbin surface, the amount of pigment per alga, and ratios of certain pigments in the four treatments (Low-SW, Low-DFB, High-SW, High-DFB) of the Orpheus Island colony were analyzed in two-factorial ANOVAs. Differences among the treatment means were assessed using the Tukey's Honestly Significant Difference (HSD) multiple comparison Post-Hoc test.

The regression equations for the relationship between F_m and F_o on day 0, day 14, and day 19 were compared within each treatment of the Orpheus Island colony according to the method of Zar (1999), employing Student-Newman-Keuls (SNK) multiple comparison tests. All other statistical analyses were performed using SAS Statistical Institute's JMP Statistical Discovery Software (version 5.0.1a, 2002).

2.3 Results

2.3.1 Davies Reef colony — The bases of nubbins cut from the colony for this preliminary experiment did not quickly heal and become covered with new tissue. Thus, during the course of the daily manipulations of the nubbins, it became evident that endolithic algae or pigmented bacteria had invaded the exposed skeletal surfaces. Accordingly, PAM readings were restricted to more distal areas of the nubbins lacking obvious contamination by underlying endoliths. At the end of the experiment, the coral tissues were stripped from several nubbins and PAM fluorescence data were again acquired. Chlorophyll fluorescence in distal areas was determined to be minimal (typically <5% of the pre-stripping value), which indicated there was little or no contribution of fluorescence from invading endoliths to fluorescence measured distally in the living nubbins.

F_v:F_m in the endosymbionts *in hospite* remained relatively constant on the lower (shaded) sides of the horizontally-suspended nubbins at both temperatures, with and without the presence of DFB (Fig. 2.1A). Values for F_v:F_m varied between ~ 0.65–0.70, indicative of highly efficient photochemistry at photosystem II (PSII) in all treatments. Photochemical efficiencies on the upper, light-exposed surface of the nubbins in the low temperature treatments decreased only slightly (to ~0.63) with time in the low temperature treatment and was not affected by DFB addition (Fig. 2.1B). In contrast, F_v:F_m values decreased markedly on the upper nubbin surfaces after Day 6 in both high temperature treatments, especially with DFB added (Fig. 2.1B).

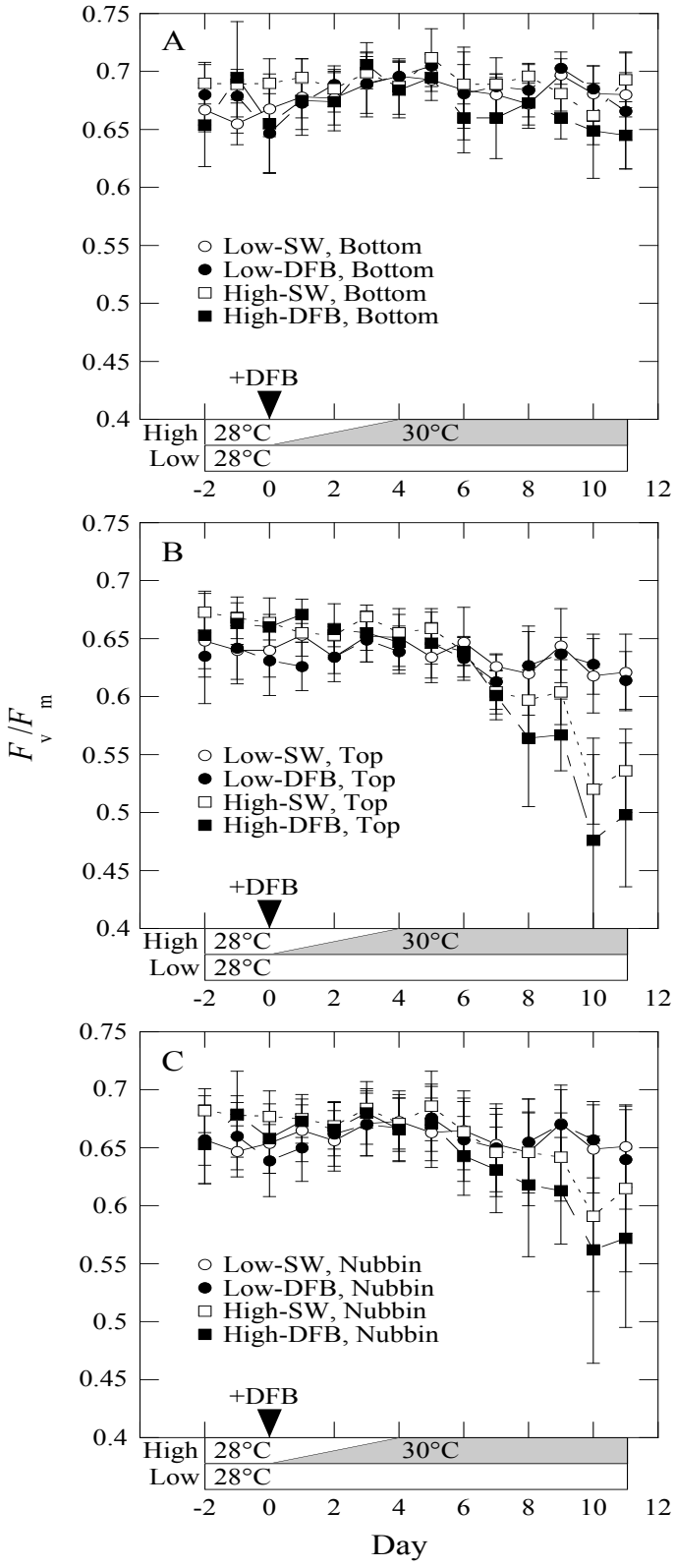
A
B
C
Low-SW, Bottom
Low-DFB, Bottom
High-SW, Bottom
High-DFB, Bottom
Low-SW, Top
Low-DFB, Top
High-SW, Top
High-DFB, Top
Low-SW, Nubbin
Low-DFB, Nubbin
High-SW, Nubbin
High-DFB, Nubbin
+DFB
High
Low
28°C
30°C
28°C
F_v/F_m
Day
0.75
0.7
0.65
0.6
0.55
0.5
0.45
0.4
-2
0
2
4
6
8
10
12

Figure 2.1 F_v:F_m in nubbins cut from the Davies Reef colony of *S. pistillata* exposed to the variable experimental treatments; values are mean ± 95% confidence limits (n=6). Treatments included; low temperature (28 °C) in normal seawater (Low-SW), low temperature (28 °C) in seawater amended with the strong iron chelator desferrioxamine B (Low-DFB); high temperature (30 °C) in normal seawater (High-SW); and high temperature (30 °C) in seawater amended with DFB (High-DFB). (A) Measured on the bottom (shaded) surface. There were no discernible differences among the treatments. (B) Measured on the top (diurnally illuminated) surface. Tukey's HSD tests were used to discern overall effects for data on top (A) and bottom (B) surfaces, where groups not connected by the same letter are significantly different ($p < 0.05$). (C) Combined measures of F_v/F_m from top and bottom surfaces of nubbins, taken as representative of the entire nubbin. Tukey's HSD tests discerned overall effects on entire nubbins, where groups not connected by the same letters are significantly different ($p < 0.05$).

Results of the least squares model incorporating the random effect of replicates (nubbin number) on F_v:F_m are given in Table 2.1. REML analysis indicated that the random effect (nubbin number) accounted for 14.6% of the total variance. Analysis showed a highly significant overall effect of the statistical model ($F_{95, 480} = 14.068$, $p < 0.0001$). Briefly, there were significant fixed effects of temperature, DFB, surface, and day of experiment, as well as relevant interactions. These interactions can be understood most clearly by comparing Table 2.1A with Fig. 2.1A and B, which presents F_v:F_m values at low and high temperature, with and without added DFB, and measurements taken on bottom and top surfaces. For example, the interaction of day × surface × temperature reflected the lack of temperature effect on the shaded bottom surface throughout the experiment, with a thermal effect emerging on the top surface only later in the experiment. Likewise, interacting day × temperature × DFB reflected the appearance of a thermal effect only late in the experiment, and the effect of DFB only at high temperature. The four-way interaction day × surface × temperature × DFB was not significant, but incorporating the random effect of individual nubbin did reveal a significant effect in this higher-level interaction, as shown in Table 2.1A.

Overall, the analysis clearly distinguished between the top and bottom surfaces of the nubbins under all conditions. Tukey's HSD tests grouped all treatments involving the shaded bottom surface as a series of overlapping means that could not be distinguished at $p = 0.05$ (Fig. 2.1A), but that were significantly different from all treatments involving the light-exposed top surface (Fig. 2.1B). Means for the top surface at low temperature with and without added DFB, and the top surface at high temperature without DFB, constituted an overlapping series, but F_v:F_m in the illuminated top surface of nubbins at high temperature with DFB added was significantly lower than all other groups. This is seen in Fig. 2.1B, where F_v:F_m measured on the top surface of nubbins at high temperature with added DFB tended to be lower than the other treatments from day 8 onward.

Table 2.1 Significant treatment effects on F_v:F_m in mixed-model REML analysis of data for separate and combined measurements of top (brightly illuminated) and bottom (shaded) surfaces of nubbins from the Davies Reef colony of *Stylophora pistillata*. REML analysis shrinks the estimate for the random effect (nubbin) toward zero, and adjusts the fixed effects accordingly. (A) When top and bottom surfaces were considered separately, the overall effect of the statistical model was highly significant ($F_{95, 480} = 14.068$, $p < 0.0001$), and the random effect of nubbin accounted for 14.6% of the total variance. (B) When surfaces were combined to give the overall response of the nubbin, the overall effect of the statistical model was highly significant ($F_{47, 280} = 7.808$, $p < 0.0001$), and the random effect of nubbin accounted for 12.1% of the total variance. na = not applicable. ns = not significant ($p > 0.05$).

	A) Separate surfaces			(B) Combined surfaces		
Source	**df**	***F***	***P***	**df**	***F***	***p***
Day	1, 480	144.462	<0.0001	1, 240	120.17	<0.0001
Nubbin and Random	5, 480	shrunk	shrunk	4, 240	shrunk	shrunk
Temperature	1, 480	24.332	<0.0001	1, 240	18.527	<0.0001
Surface	1, 480	548.794	<0.0001	na	na	na
DFB	1, 480	16.128	<0.0001	1, 240	7.761	0.0058
Surface × Temperature	1, 480	11.849	0.0006	na	na	na
Temperature × DFB	1, 480	10.207	0.0015	1, 240	4.912	0.0276
Nubbin × Temperature	5, 480	6.546	<0.0001	5, 240	3.096	0.0100
Nubbin × DFB	5, 480	7.208	<0.0001	5, 240	4.699	0.0004
Nubbin x Surface x DFB	5, 480	3.215	0.0072	na	na	na
Nubbin × Temperature × DFB	5, 480	7.568	<0.0001	5, 240	4.369	0.0008
Nubbin × Surface × Temperature × DFB	5, 480	2.729	0.0191	na	na	na
Day × Temperature	1, 480	115.422	<0.0001	1, 240	82.844	<0.0001
Day × Surface *or* Nubbin	1, 480	114.322	<0.0001	5, 240	2.546	0.0287
Day × Surface × Temperature	1, 480	49.630	<0.0001	na	na	na
Day × Temperature × DFB	1, 480	7.073	0.0081	ns	ns	ns
Day × Nubbin × Temperature × DFB	ns	ns	ns	5, 240	2.337	0.0427
Day × Nubbin x Temperature x Surface x DFB	5, 480	3.982	0.0015	na	na	na

Tukey's HSD tests on data for individual days revealed no significant differences ($p > 0.05$) among treatments on any day for the shaded bottom surfaces of nubbins. Similar tests on the top surfaces showed a fortuitous effect of designated temperature group (but not DFB) on day 0 (measured in the morning before the temperature was increased). Later in the experiment, on days 9 and 10, means of both low temperature groups tended to be higher than the nubbins at high temperature with DFB, but the high temperature group lacking DFB was intermediate and statistically bridged the means for the other groups. The overall analysis combined to show significant effects of elevated temperature and the presence of DFB, but only on the top, brightly illuminated surfaces of the nubbins (Fig. 2.1B).

Similar analysis of pooled data measured on both the top and bottom surfaces gives the integrated response for the entire nubbin. Table 2.1B presents the results of this analysis, where the overall effect is highly significant ($F_{47, 287} = 7.808$, $p < 0.0001$). In this case REML analysis indicated that the random effect (nubbin number) accounted for 12.1% of the total variance. Again, there were significant fixed effects of temperature, DFB, and day of experiment, as well as relevant interactions. The most clearly evident interactions were day × temperature (i.e., F_v:F_m remained unchanged in all nubbins at low temperature throughout the experiment, but declined at high temperature late in the experiment: Fig. 2.1C). Likewise, there was a clear interaction of temperature × DFB, where there was no effect of DFB at low temperature, only at high temperature (Fig. 2.1C). Overall, the analysis discerned that F_v:F_m in the nubbins held at high temperature in the presence of DFB was significantly different from all other treatments, which were indistinguishable from each other by Tukey's HSD tests (Low-SW = Low-DFB = High-SW > High-DFB).

Owing to the differential response on the top and bottom surfaces and the random effect of individual nubbin, there was no clear separation of the treatments on any day of the experiment for the combined surface measurements (Fig. 2.1C). Only on days 9–11 did any heterogeneity emerge in multiple comparison tests, where nubbins at low temperature were indistinguishable, nubbins at high temperature with DFB tended toward a lower F_v:F_m value than the low temperature treatments, and those treated at high temperature without DFB tended to be intermediate to these groups. Overall there was a significant effect of DFB that was manifested only at high temperature.

2.3.2 Orpheus Island colony— Failure of cut surfaces of other colonies of *S. pistillata* to heal quickly was the norm, not simply an effect of salinity stress in the Davies Reef colony. The failure of cut surfaces to heal may underlie the high frequency of colony invasion by microbes, an observation that was common in the field. Therefore, sample preparation for the experiment with the Orpheus Island colony was modified to include sealing the cut surface, following the realization that endolithic algae had invaded the skeletons of nubbins cut from the Davies Reef colony of *S. pistillata* and in other colonies subsequently tested. Nevertheless, the experimental treatments gave qualitatively and quantitatively similar results to those obtained in the preliminary experiment with the Davies Reef specimen. Briefly, F_v:F_m did not change in corals at low temperature for the duration of the experiment. The effect of high temperature on photochemical efficiency was not evident until midway through the experiment, occurring a few days after the temperature had reached 30 °C and exacerbated by the transition to 31 °C, and being enhanced by the effect of DFB at high temperature only (Fig. 2.2). Results of the least squares model incorporating the random effect of replicate (individual nubbin identification) on F_v:F_m are given in Table 2.2. There was a highly significant overall effect of the treatments detected by the statistical model ($F_{63, 576} = 33.032$, $p < 0.0001$). REML analysis indicated that the random effect (nubbin number) accounted for 10.6% of the total variance. The fixed effects of day of the experiment and temperature, but not added DFB, were significant. Significant interactions existed between the other factors and DFB: day × DFB, temperature × DFB, and day × temperature × DFB, as well as day × temperature, as shown in Fig. 2.2. Overall, mean values of F_v:F_m showed significant differences in Tukey's HSD multiple comparisons among all four treatments: Low-DFB > Low-SW > High-SW > High-DFB. The photochemical efficiency in the Low-SW nubbins tended initially to be lower than in Low-DFB nubbins for the first half of the experiment, thereby accounting for the overall significant difference between these treatments, but these means converged from day 10 onward. High-DFB treated nubbins had the lowest F_v:F_m, but a decrease in F_v:F_m in those nubbins compared with the High-SW nubbins was not evident until the second temperature ramp (from 30 °C to 31 °C) was completed on day 14.

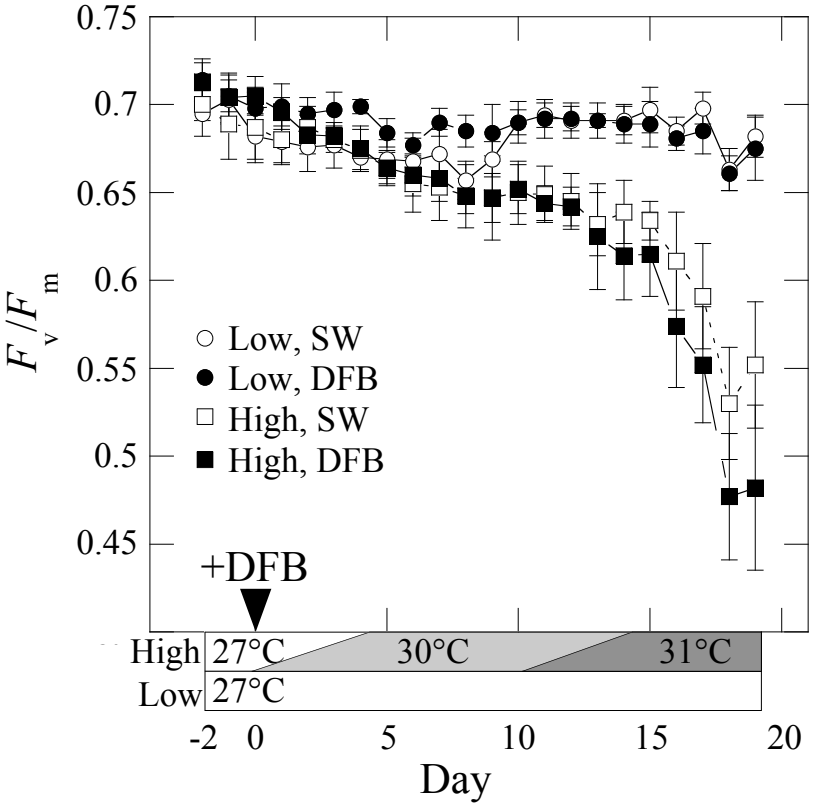
0.75
0.7
0.65
0.6
0.55
0.5
0.45
F_v/F_m
Low, SW
Low, DFB
High, SW
High, DFB
+DFB
High
27°C
30°C
31°C
Low
27°C
-2
0
5
10
15
20
Day

Figure 2.2 F_v:F_m measured around the periphery along the full length of nubbins cut from the Orpheus Island colony of *S. pistillata* during the course of the experimental treatments. Experiments involved four treatments: low temperature (27 °C) in normal seawater (Low-SW), low temperature (27 °C) in seawater amended with the strong iron chelator desferrioxamine B (Low-DFB); high temperature (30 °C then increased to 31 °C) in normal seawater (High-SW); and high temperature (30 °C then increased to 31 °C) in seawater amended with DFB (High-DFB). Values are mean ±95% confidence limits (n = 8). Tukey's HSD tests discerned overall effects, where groups not connected by the same letters are significantly different ($p < 0.05$).

Table 2.2 Significant treatment effects on F_v:F_m in mixed-model REML analysis of data for the Orpheus Island colony of *Stylophora pistillata*. REML analysis shrinks the estimate for the random effect (nubbin) toward zero, and adjusts the fixed effects accordingly. The overall effect of the statistical model was highly significant ($F_{63, 576} = 33.032$, $p < 0.0001$), and the random effect of nubbin accounted for 10.6% of the total variance.

Source	**df**	***F***	***P***
Day	1, 576	563.070	<0.0001
Nubbin and Random	7, 576	shrunk	shrunk
Temperature	1, 576	620.094	<0.0001
Temperature x DFB	1, 576	22.244	<0.0001
Nubbin x Temperature	7, 576	6.258	<0.0001
Nubbin x DFB	7, 576	9,677	<0.0001
Nubbin x Temperature x DFB	7, 576	6.675	<0.0001
Day x Temperature	1, 576	526.761	<0.0001
Day x DFB	1, 576	57.942	<0.0001
Day x Temperature x DFB	1, 576	5.071	0.0247
Day x Nubbin x Temperature x DFB	7, 576	3.783	0.0005

Analysis by day indicated that Low-DFB nubbins had F_v:F_m values that were significantly different from all other treatment groups on days 4 and 8, but that Low-SW and Low-DFB nubbins converged thereafter and remained statistically indistinguishable. F_v:F_m in High-SW and High-DFB nubbins were the same from day 10–17, and both were different than both groups of nubbins held at low temperature during that time. On days 18 and 19, after which the experiment was terminated, photochemical efficiency in High-DFB nubbins had declined significantly below all other treatments, while High-SW nubbins remained intermediate between High-DFB and both treatment groups at low temperature. Again, the random effect of replicate nubbin contributed to the large variance in F_v:F_m, especially for nubbins at high temperature.

The relationship between F_o and F_m in individual nubbins in each treatment at day 0, day 14 (i.e., after 10 d at 30 °C), and day 19 (at the end of the experiment, after a further 5 d at 31 °C) is shown in Figure 2.3. In both low temperature treatments, i.e. with natural seawater (day 0: $F_m = 382.98 + 2.69\ F_o$, $r^2 = 0.871$, $p < 0.001$; day 14: $F_m = 31.041 + 3.19\ F_o$, $r^2 = 0.958$, $p < 0.001$; day 19: $F_m = -100.43 + 3.37\ F_o$, $r^2 = 0.892$, $p < 0.001$) and with added DFB (day 0: $F_m = 127.56 + 3.14\ F_o$, $r^2 = 0.936$, $p < 0.001$; day 14: $F_m = -148.36 + 3.48\ F_o$, $r^2 = 0.922$, $p < 0.001$; day 19: $F_m = 44.516 + 3.03\ F_o$, $r^2 = 0.899$, $p < 0.001$), the slopes of the regression lines were identical on all days (Fig. 2.3A, B). The intercepts of the regressions differed significantly among days within each low-temperature treatment, although over the range of the data, the regression lines were essentially coincident (Fig. 2.3A, B). In natural seawater at high temperature (Fig. 2.3C), the regression lines were significantly translated downward over time, with no change in slope (day 0: $F_m = 470.90 + 2.60\ F_o$, $r^2 = 0.810$, $p < 0.001$; day 14: $F_m = 445.35 + 2.29\ F_o$, $r^2 = 0.827$, $p < 0.001$; day 19: $F_m = 93.24 + 2.17\ F_o$, $r^2 = 0.762$, $p < 0.001$.) In seawater at high temperature with added DFB (Fig. 2.3D), a significant downward (clockwise) rotation of the curves was evident over time (day 0: $F_m = 16.89 + 3.40\ F_o$, $r^2 = 0.863$, $p < 0.001$; day 14: $F_m = 314.16 + 2.17\ F_o$, $r^2 = 0.821$, $p < 0.001$; day 19: $F_m = 256.56 + 1.56\ F_o$, $r^2 = 0.724$, $p < 0.001$), indicating a progressive reduction in F_m, particularly at higher values of F_o,

whereas the mean values of F_o did not vary significantly among treatments on day 0, 14, or 19 (Tukey's HSD tests, $p > 0.05$).

The NextEngine 3D scanner proved effective in creating a realistic 3D model and calculating the surface area of the cleaned skeletons of coral nubbins (Fig. 2.4), with triplicate measurements of the surface area of individual skeletons being reproducible to within 1% of the mean (0.99%; range 0.21–3.10%, $n = 16$). This system is more generally accessible than X-ray computed tomography (CT) scans using hospital-based equipment (Veal *et al.* 2010), although CT equipment importantly also allows the scanning of living colonies (Laforsch et al. 2008). The 3D laser scanner provides an accurate alternative to methods involving wax dipping or the manual photogrammetric approach to building a three-dimensional model (Jones *et al.* 2008), and the less accurate foil-wrapping method (Veal *et al.* 2010).

There were no significant effects of temperature or DFB on the number of dinoflagellates per cm^2 of coral surface area at the termination of the experiment conducted with nubbins from the Orpheus Island coral ($F_{3, 12} = 3.391$, $p = 0.054$), where Tukey's HSD tests indicated a series of overlapping means in the four treatments (Fig. 2.5A). The density of algal cells in all groups appeared to be lower (by about one-half) than for a reference group of nubbins sampled at the start of the experiment (day 0, not included in the statistical test). This probably was the result both of starving the nubbins (Ferrier-Pagès *et al.* 2003) during their 22 days of confinement in the experimental chambers, and of the higher irradiance used in the experiment than during the pre-experimental period.

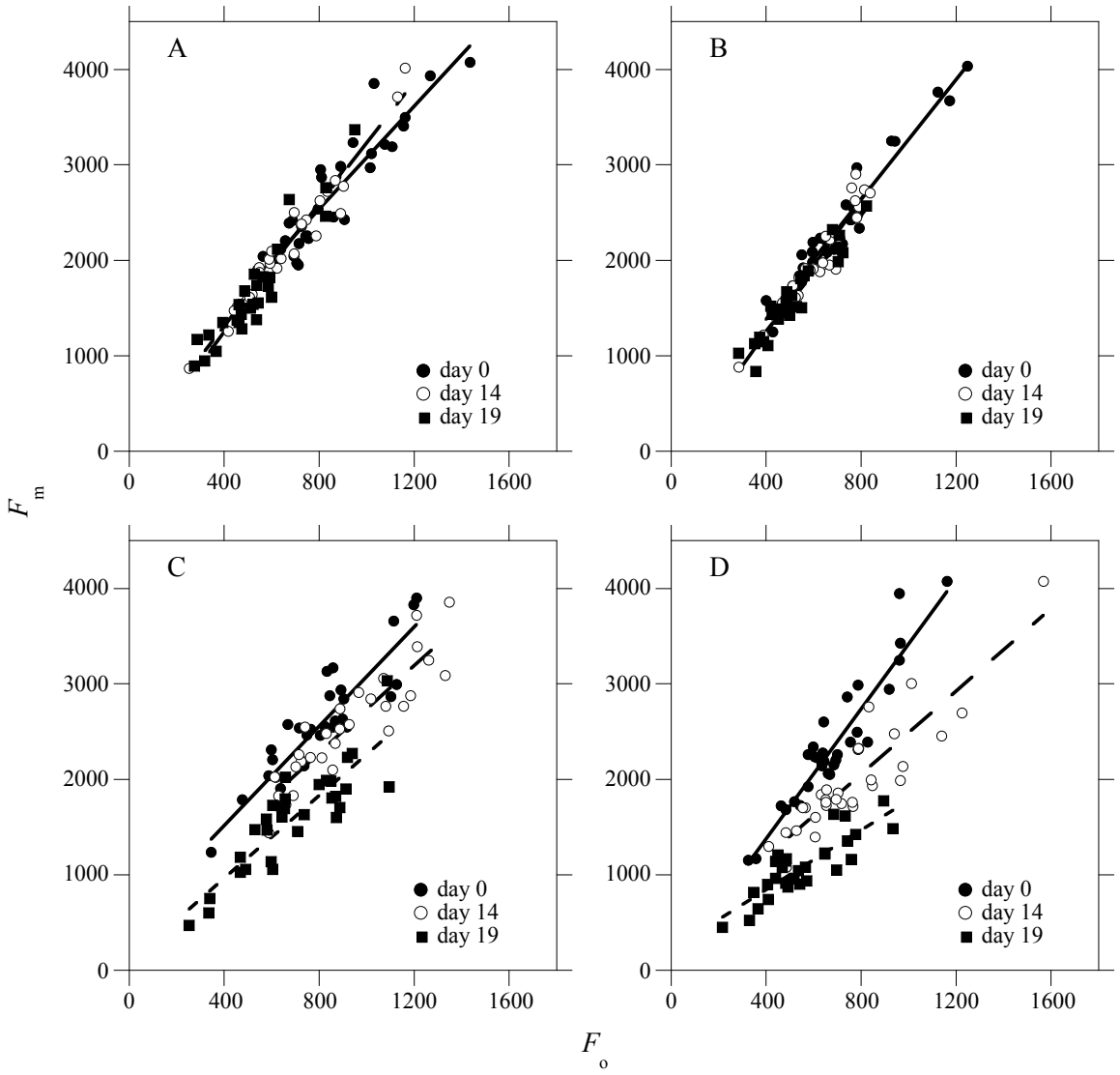
A
B
C
D
day 0
day 14
day 19
0
1000
2000
3000
4000
400
800
1200
1600
F_m
F_o

Figure 2.3 Relationship between F_m and F_o in nubbins cut from the Orpheus island colony on days 0, 14, and 19 in the four experimental treatments. Data points are for all individual measurements on all nubbins on each day. Each graph represents one of the experimental treatments; A: low temperature (27 °C) in normal seawater, B: low temperature (27 °C) in seawater amended with DFB, C: high temperature (30 °C then increased to 31°C) in normal seawater and D: high temperature (30 °C then increased to 31°C) in seawater amended with DFB. There were no significant differences among the slopes of the regressions (SNK test, $p > 0.05$) in panels A, B, and C. In panel A, the elevations (intercepts) of all regressions differed significantly from each other (SNK, $p < 0.001$) in the sequence day 0 > day 14 > day 19. In panel B, the elevations (intercepts) of all regressions differed significantly from each other ($p < 0.001$) in the sequence day 0 > day 19 > day 14. In panel C, the elevations (intercepts) of all regressions differed significantly from each other ($p < 0.001$) in the sequence day 0 > day 14 > day 19. In panel D, the slopes of the regressions all differed significantly from each other in the sequence day 0 > day 14 > day 19, where all comparisons involving day 0 were significant at $p = 0.001$ and day 14 vs. day 19 was different at $p = 0.05$.

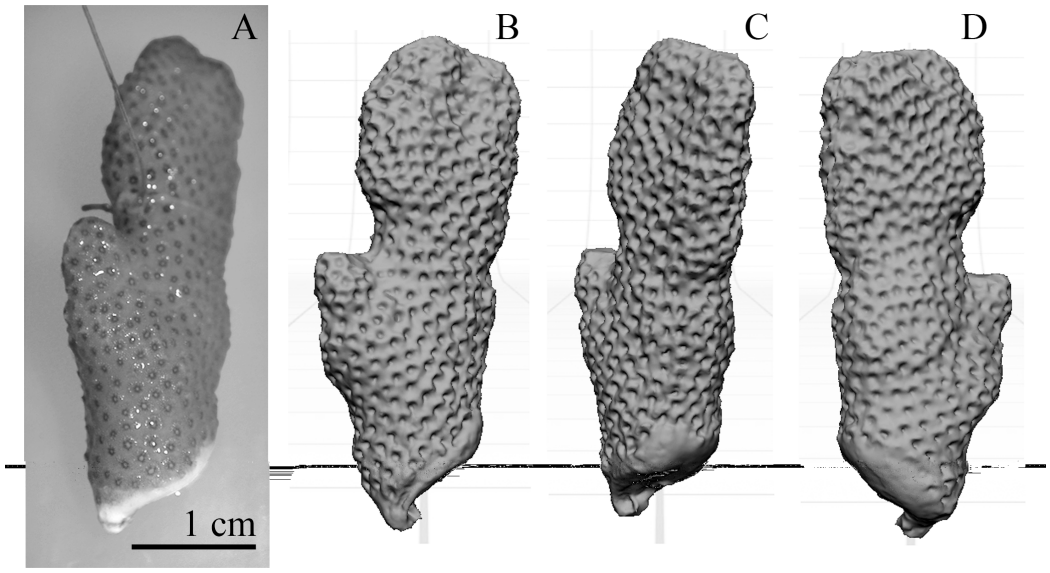
A
B
C
D
1 cm

Figure 2.4 (A) Live nubbin of *S. pistillata* cut from the Orpheus Island colony, suspended (in air) by a nylon monofilament. (B–D) Successive views (120° rotation between each) of the 3D model of the cleaned skeleton of the same nubbin prepared from 12 successive scans (30° between each) using the NextEngine 3D multiple laser scanner and ScanStudio^{TM} software. The patch of waterproof epoxy is visible at the base of this nubbin; this was digitally removed from the model using the application software prior to calculating the living surface area (14.492 cm^2 in this example) used to normalize the surface tissue density of dinoflagellates in each nubbin.

A.

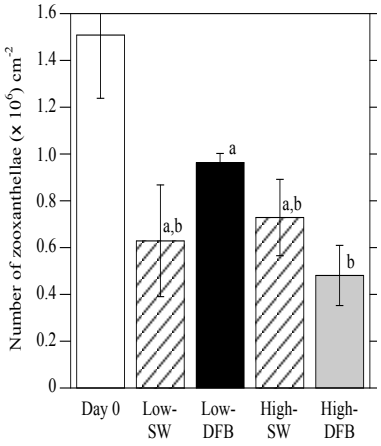
Number of zooxanthellae (× 10^6) cm^-2
1.6
1.4
1.2
1.0
0.8
0.6
0.4
0.2
0
a
a,b
a,b
b
Day 0
Low-SW
Low-DFB
High-SW
High-DFB

B.

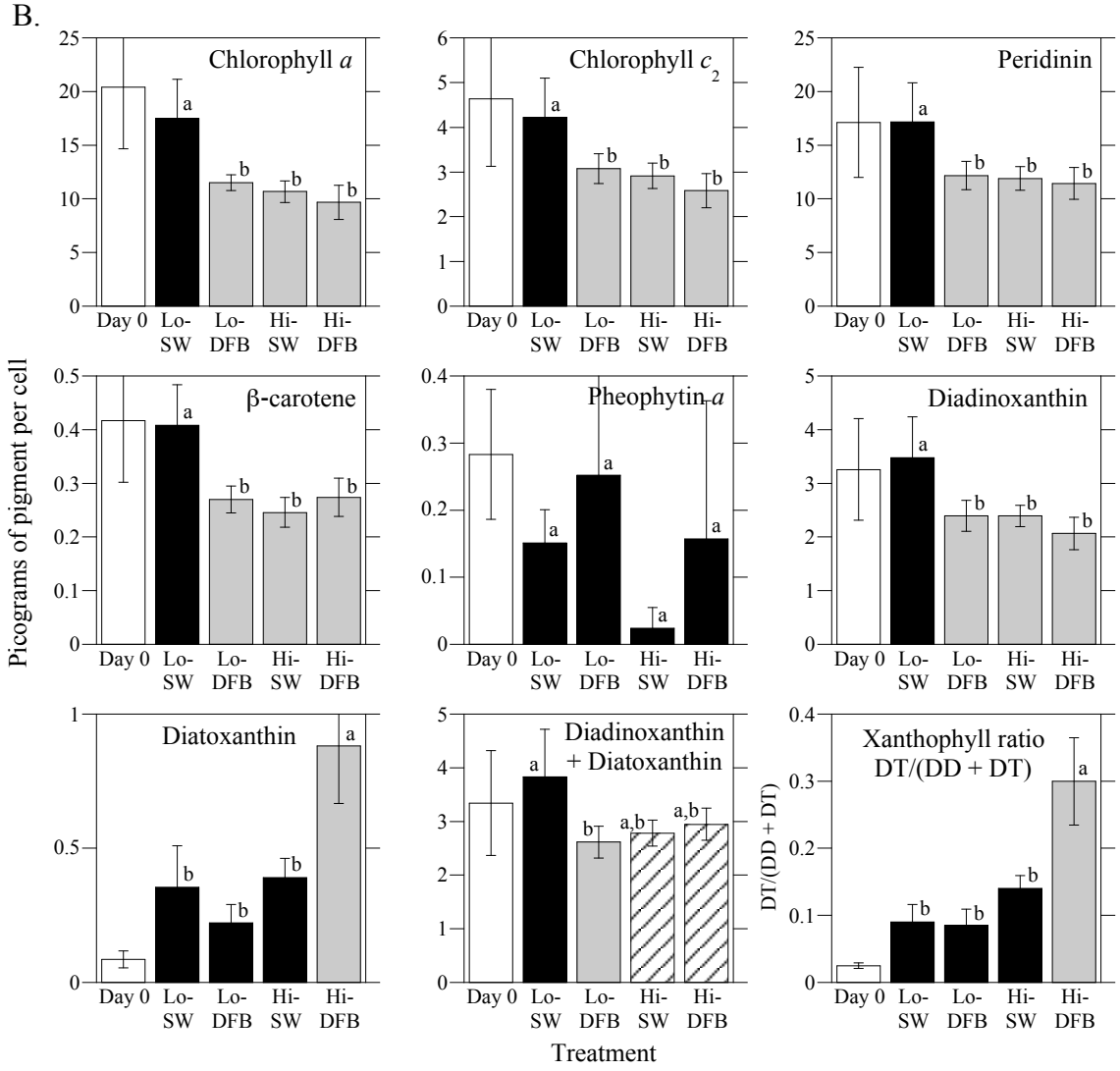
Picograms of pigment per cell
Chlorophyll a
Chlorophyll c2
Peridinin
β-carotene
Pheophytin a
Diadinoxanthin
Diatoxanthin
Diadinoxanthin + Diatoxanthin
Xanthophyll ratio DT/(DD + DT)
DT/(DD + DT)
Day 0
Lo-SW
Lo-DFB
Hi-SW
Hi-DFB
Treatment

Figure 2.5 Algal measurements taken in experimental nubbins (n = 4 per treatment) at the start (day 0, for reference only) and end (day 19) of the experiment on the Orpheus Island colony. Vertical bars represent ±1 SD. Experimental treatments included: low temperature (27 °C) in normal seawater (Low-SW), low temperature (27 °C) in seawater amended with the strong iron chelator desferrioxamine B (Low-DFB); high temperature (30 °C then increased to 31°C) in normal seawater (High-SW); and high temperature (30 °C then increased to 31°C) in seawater amended with DFB (High-DFB).Treatment means were compared using Tukey's HSD test, where means not connected by the same letters are significantly different ($p < 0.05$). Day 0 was not included in the statistical analysis. (A) Surface density of dinoflagellates (10^6 cells cm^{-2}). No significant differences among treatments were found, and all means were connected by overlapping letters ($p > 0.05$). (B) Cellular concentrations of pigments (pg pigment $cell^{-1}$) in dinoflagellates isolated from experimental nubbins. The last panel shows the ratio of diatoxanthin (DT) to total xanthophylls (diadinoxanthin, DD, plus DT).

Experimental treatment had a significant effect on the amount of pigment per algal cell at the end of the experiment for all components except for phaeophytin *a* (Fig. 2.5B). In most cases, individual pigment content per cell was greatest in Low-SW nubbins, with lesser amounts in the Low-DFB treatment, which did not differ discernibly from either of the high temperature treatments (Fig. 2.5B). The exception was the xanthophyll diatoxanthin being most concentrated in the dinoflagellates in High-DFB nubbins, with the remaining groups being lower and statistically indistinguishable. No difference was detected among the treatments in the total amount of xanthophyll (diadinoxanthin, DD + diatoxanthin, DT) per cell. The proportion of xanthophyll pigments present as diatoxanthin, DT/(DD + DT), was significantly greater in High-DFB nubbins than in all other groups.

On the last day of the experiment, dark-adapted F_v:F_m of the pooled samples was inversely related both to DT/(DD + DT) and to the ratio of the xanthophylls (XP) DD + DT to total xanthophyll (XP) plus light-harvesting (LH) pigments (chlorophyll *a* and c_2, and peridinin), i.e., F_v:F_m was also inversely related to XP/(XP + LH). Both relationships (shown in Fig. 2.6A and B, respectively) are highly significant: F_v:F_m = 0.71826 – 0.88099 DT/(DD + DT); r^2 = 0.610, $p < 0.001$; F_v:F_m = 1.4379 – 9.7871 XP/(XP + LH); r^2 = 0.642, $p < 0.001$. Both relationships indicate an increase in non-photochemical quenching of PS II with increasing proportions of xanthophylls.

Analysis of the ITS1 region showed that the symbiotic dinoflagellates isolated from nubbins of the Orpheus Island colony on day 0 and at the end of the experiment belonged to the highly diverse clade C prevalent among populations of *S. pistillata* and related corals (Sampayo *et al.* 2007), but did not correspond to any of the sub-cladal standards (C1, C2, C3) available to us. Only a single cladal type was present, and this population did not change during the experimental treatments.

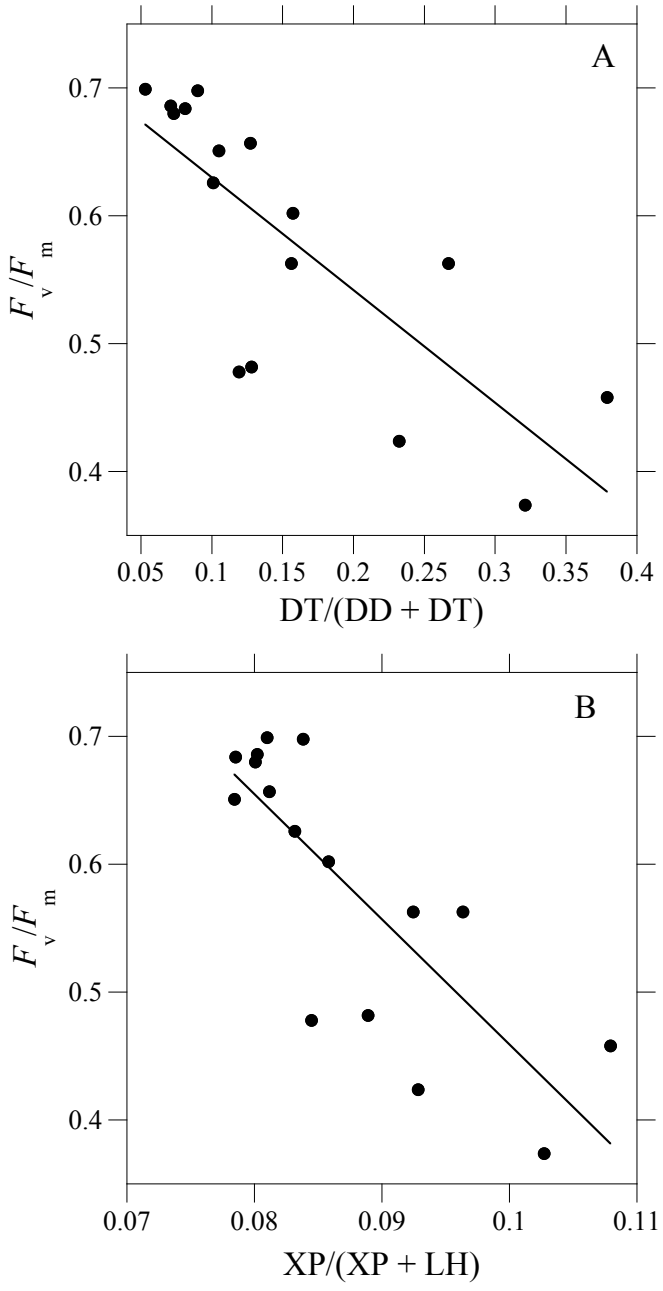
A
0.7
0.6
0.5
0.4
F_v/F_m
0.05
0.1
0.15
0.2
0.25
0.3
0.35
0.4
DT/(DD + DT)
B
0.7
0.6
0.5
0.4
F_v/F_m
0.07
0.08
0.09
0.1
0.11
XP/(XP + LH)

Figure 2.6 The relationship between F_v:F_m and pigment ratios measured on the final day of the experiment in dinoflagellates isolated from nubbins cut from the Orpheus Island colony of *S. pistillata*. Data were pooled across the four treatments for linear regression analysis. (A) F_v:F_m vs. the ratio DT/(DD + DT); $r^2 = 0.610$, $p < 0.001$. (B) F_v:F_m vs. the ratio of xanthophyll pigments (XP = DD + DT) to total xanthophyll + light-harvesting (LH) pigments, XP/(XP + LH); $r^2 = 0.642$, $p < 0.001$.

2.4 Discussion

The phenomenon of coral bleaching is thought to stem from overwhelming oxidative stress induced by over-reduction of PSII in symbiotic dinoflagellates, resulting in elevated ROS damage to the photosymbionts and their coral host. However, non-uniform spatial patterns of reef bleaching under similar light and temperature conditions indicate that the threshold for catastrophic oxidative stress varies among corals. Although these differences may be attributed in part to the presence of dinoflagellate clades having dissimilar bleaching tolerances (Lajeunesse *et al.* 2008), including their ability to avoid or mitigate oxidative stress, it also is possible that spatial differences in oceanographic conditions influence the trace metal nutrition of corals and thus the ability of the endosymbionts to produce critical antioxidant enzymes. Iron is required for a vast array of metabolic processes that include photosynthesis and antioxidant enzymic defenses, and evidence that iron may become limiting in coral reef environments (Sakka *et al.* 1999) makes it a promising candidate to begin assessing the involvement of trace metal nutrition in the onset of coral bleaching.

The fluorescence ratio (F_v:F_m) in dark-adapted cells is a measure of the maximum quantum efficiency of PSII photochemistry (Kitajima and Butler 1975), which depends on the efficient transfer of excitation energy to the reaction centers and on functional and open reaction centers (Greene *et al.* 1992). Despite concerns that much of the theoretical groundwork for interpreting the dark-adapted quantum yield of PSII derives from studies of higher plants and may not reflect the physiological variability one is likely to encounter in symbiotic dinoflagellates (Warner 2005), measurement of F_v:F_m remains one of the primary tools for assessing algal stress responses. There also is evidence that dark-reduction of the plastoquinone pool, which increases the minimum fluorescence yield (F_o), is active in corals and can cause artificially low estimates of the true maximum quantum yield of PSII (K. Asada, pers. comm. 2001, Hill and Ralph 2008). However, these considerations are secondary here because all of our fluorescence measurements were preceded by uniform (overnight) dark-exposure periods, and we employed F_v:F_m as a relative measure of stress effects among the treatments.

The dark-adapted quantum yield of photochemistry remained high (~0.65-0.70) in our experiments at low temperature (with and without DFB) on both the Davies Reef and Orpheus Island colonies of *S. pistillata* (Figs. 2.1, 2.2). These levels of quantum yield are very near the theoretical maximum efficiency for PSII in dinoflagellates inhabiting corals (Jones and Hoegh-Guldberg 2001), indicating that the symbiotic dinoflagellates remained in good health at the lower temperature over the duration of both experiments. In contrast, the sharp decrease in photochemical efficiency at elevated temperature (Figs. 2.1, 2.2) with and without DFB illustrates a significant impairment of charge separation between P680 and $P680^+$ of PSII relative to the F_v/F_m of coral algal symbionts at lower temperature. These results are consistent with the impairment of energy transfer to carbon fixation that result from high temperature generated photoinhibition in plants (Hurry and Huner 1992) and phytoplankton, in the latter particularly in conjunction with trace metal limitation in stratified surface waters (Falkowski and Raven 2007).

At face value, the loss of maximal photochemical efficiency may signify increases in some component of non-photochemical quenching (Hill *et al.* 2005) of light energy dissipated as heat to decrease energy flow into photosynthesis (i.e., photoprotection), or represent oxidative damage to PSII associated with increased ROS production (i.e., photoinhibition), or some combination of both.

The progressive decrease in photochemical efficiency over the duration of experimental thermal stress is similar to the chronic photoinhibition observed in other long-term studies of experimental bleaching of corals (Warner *et al.* 1996, 1999; Berkelmans and Van Oppen 2006). The absence of a recovery in photochemical efficiency at high temperature after a dark incubation of 12 hours confirms the occurrence of chronic photoinhibition and contests the occurrence of dynamic photoinhibition, which would have resulted in a recovery in F_v/F_m after the dark period (Hoegh-Guldberg and Jones 1999). The progressive decrease in photochemical efficiency is also fully consistent with short-to-intermediate term experiments conducted with *S. pistillata* (Jones *et al.* 1998; Bhagooli and Hidaka 2003; Fitt *et al.* 2009). Such a decrease is seen likewise in field populations of corals during the summer, indicating the natural seasonal peak of thermal and photic stresses (Warner *et al.* 2002; Franklin *et al.* 2006), a trend that under severe stress can

culminate in catastrophic bleaching. Moreover, the thermal stress on F_v:F_m was evident only on the upper, brightly illuminated surface of nubbins taken from the Davies Reef colony and not on the lower, shaded surface of these nubbins (Fig. 2.1A, B), similar to results reported by Jones *et al.* (1998), Brown *et al.* (2000), and Warner and Berry-Lowe (2006), each of which were obtained under bright as opposed to dim incident illumination. All of these results demonstrate the importance of light to the thermal stress response of corals.

An important extension to previous experimental studies of coral bleaching is our finding that limiting iron availability to *S. pistillata* by treatment with DFB clearly exacerbates the effect of high-temperature stress on the maximum potential quantum yield of PSII (Figs. 2.1, 2.2). The implication is that the degree of coral stress in natural environments under high light and temperature may be modulated by trace metal nutrition. The effect of iron limitation is well known from studies of eukaryotic phytoplankton and cyanobacteria, and our work extends such findings to coral symbionts *in hospite*.

Of particular note is that although iron limitation in phytoplankton impairs the electron transport capacity of photosystem II (Kolber *et al.* 1994) and photosystem I (Moseley *et al.* 2002) this effect is exacerbated by low-light conditions that necessitate photoacclimation and increase iron requirements for added synthesis of chlorophyll and PSII constituents (Sunda and Huntsman 1995). The opposite response was observed in *S. pistillata*, indicating that the effects of iron stress in its endosymbionts stemmed less from insufficient electron transport capacity than from secondary processes associated with PSII, such as increased oxidative stress.

Unlike the case in phytoplankton, there was no effect of DFB on F_v:F_m in symbiotic dinoflagellates at physiologically benign temperatures (Figs. 2.1, 2.2). It may be that the iron reserves of the endosymbionts are sufficient to enable normal photosynthesis and control of oxidative stress at low temperatures, but that the increase in ROS production with temperature, related among other things to the destabilization of membranes where PSII is located (Tchernov *et al.* 2004), exceed the capacity for acclimatization. The key factor here may be the extremely low growth rates of zooxanthellae *in hospite*, which are on the order of 0.1 d^{-1}, so that there simply is not a high iron requirement for growth,

unlike pelagic phytoplankton, which do require high iron for growth. One can imagine that this will reduce the need for iron uptake to minimal values. Also, these corals were maintained at low irradiance before the experiment, resulting in high concentrations of most pigments (Fig. 2.5B), so that redistributions of iron from degraded photosystems under high light conditions would provide an additional iron resource, enabling the cells to maintain high photochemical efficiency as long as ROS production did not exceed some threshold. As would be expected, even at low temperature the addition of DFB to the seawater in which the corals were incubated led to lower cellular concentrations of these pigments (Fig. 2.5B).

The decreases in F_v:F_m during iron starvation of marine phytoplankton at high irradiances are accompanied by decreases in chlorophyll *a*, increases in xanthophylls, and alteration of the ratio of diatoxanthin (DT) to the total of diatoxanthin (DT) + diadinoxanthin (DD) (Greene *et al.* 1992; Geider *et al.* 1993; Van de Poll *et al.* 2009). Adding DFB to the warm seawater bathing *S. pistillata* induced similar changes in its dinoflagellates *in hospite*, including a lower cellular content of light-harvesting pigments (chlorophylls *a* and c_2, and peridinin) and of β-carotene (Fig. 2.5B). Although the depletion of pigmentation also occurred at elevated temperature in the absence of DFB, as reported in other experimental studies of coral bleaching, iron limitation exacerbated the effect and caused substantial increases in DT/(DD + DT) at high temperature. In corals this increase in the conversion of diadinoxanthin to the photoprotective de-epoxidated form, diatoxanthin (Ambarsari *et al.* 1997; Brown *et al.* 1999; Warner and Berry-Lowe 2006), results in higher quenching of singlet chlorophyll by non-photochemical quenching (NPQ) in the algae, typically to avert photooxidative damage (Casper-Lindley and Björkman 1998).

However, NPQ in corals, including *S. pistillata*, typically causes decreases in F_o (Krause 1988; Jones and Hoegh-Guldberg 2001), and while there was a wide range of variability in F_o in all treatments on all days in our experiment, it did not differ among experimental treatments (Fig. 2.3). Nevertheless, changing the chemical speciation of iron in the seawater to less available forms clearly caused changes in pigmentation consistent with a

photoprotective response in the symbionts to reduce photosynthetic performance (i.e., decrease F_v:F_m) under iron-limiting conditions.

Although increases in DT/(DD + DT) are consistent with NPQ decreasing quantum yield of fluorescence at high temperatures, the observed changes in the relationship between F_m and F_o (Fig. 2.3) indicate that photodamage may also have contributed to the changes in PSII photochemistry. At low temperature in the presence or absence of DFB, F_m increased linearly with increasing F_o on Days 0, 14, and 19 of the incubation, with no substantial change in slope and with essentially coincident regression lines (Fig. 2.3A, B), and thus no observable change in photochemical efficiency [$(F_m - F_o)/ F_m$)]. In contrast, after 19 days at elevated temperature, values for F_m decreased with only minor changes in F_o, a pattern that was markedly exacerbated by the presence of DFB at elevated temperature (cf. Fig. 2.3C, D). Greene *et al.* (1992) found that iron limitation in a marine diatom and a unicellular chlorophyte inhibited the synthesis or assembly of the cytochrome b_6f complex responsible for coupling electron transport between PSII and PSI to proton translocation across the thylakoid membrane. The result was over-reduction of the plastoquinone pool that not only impeded the efficient transfer of electrons from PSII to PSI but also likely increased the production of ROS, which can degrade the D1 protein in PSII (Richter *et al.* 1990; Setlik *et al.* 1990).

Characteristically, the foregoing photoinhibition process results in a marked decline in maximal fluorescence (F_m) with a smaller decrease in F_o, similar to what we observed in the symbiotic dinoflagellates of *S. pistillata* in the high-temperature DFB treatment (Fig. 2.3D). The implication, then, is that the observed decreases in photochemical efficiency under high temperature and lowered iron availability resulted from both the energy dissipation associated with higher xanthophyll-derived non-photochemical quenching and an increased damage to PSII reaction centers. Direct measurements of photosynthesis, components of non-photochemical quenching (which may involve down-regulation of the photosynthetic apparatus without the involvement of xanthophylls: Hill *et al.* 2005), and photodamage would be required to confirm and quantify the changes in these parameters in the symbiotic dinoflagellates of *S. pistillata* under the combined stress of high temperature and reduced iron availability.

The marked shift in xanthophyll concentrations toward photoprotection under the added stress of iron limitation (Fig. 2.5B) may indicate an additional, compensatory defensive role of diatoxanthin—perhaps as a carotenoid stabilizer of thylakoid membranes as suggested by Dove *et al.* (2006) or, in view of the lowered concentrations of β-carotene, as a supplementary antioxidant to detoxify ROS directly under conditions of chronic photooxidative stress, rather than just a quencher of excess energy in excited chlorophyll (Havaux and Niyogi 1999; Dove *et al.* 2006; Warner and Berry-Lowe 2006). The last-named authors likewise note "relatively static and high levels of diatoxanthin" in *Acropora cervicornis* throughout the day and suggest an additional role for diatoxanthin as an antioxidant other than just quenching singlet chlorophyll. In our data, the increase in xanthophyll ratio after 19 days in all experimental groups regardless of temperature or DFB treatment compared with the reference group on day 0 (Fig. 2.5B) may include the response to a greater photooxidative challenge at the higher irradiance (150 μmol photons•m^{-2}•s^{-1}) during the experiment than during shade acclimation in pre-experimental maintenance (50 μmol photons•m^{-2}•s^{-1}).

Accordingly, the relative responses of F_o and F_m and the apparent shift in xanthophyll balance together are indicative of photoacclimation but the absence of recovery indicate an increase in potential or actual oxidative stress associated with over-reduction of PSII. As noted above, our findings suggest that the larger decrease in F_v:F_m under iron starvation at elevated temperature (Figs. 2.1, 2.2) results from both increased NPQ and damage to PSII. This result is consistent with, but does not confirm, the view that antioxidant metalloenzymes in coral symbioses may also be compromised, as in iron-deficient phytoplankton (Peers and Price 2004; Allen *et al.* 2007).

It is important to note that we designed our two experiments in each case using multiple replicate nubbins from a single coral colony to minimize experimental variability among different genotypes (Shick and Dowse 1985). The nubbins were chosen to provide an adequate representation of any regional physiological differences within each colony (Csásár *et al.* 2009). This study design is appropriate to assess the physiological responses of individual colonies to iron limitation but cannot fully represent the broader metabolic response in the coral population (Crawford and Oleksiak 2007), which may involve

genotypic variation in the defensive responses in *S. pistillata*. The latter goal would require the testing of multiple coral and endosymbiont genotypes simultaneously, with multiple replicates of each, which was logistically prohibited by the requirements for many closed chambers and extensive space in water baths to contain them for such an experiment. Therefore, we opted to maximize replicates from a single colony in each experiment to maximize analytical robustness for these two hologenotypes from different reefs. Still, our within-colony results were unexpectedly variable, and similar to the intra-clonal variation in the oxidative stress response observed by Császár *et al.* (2009). Nevertheless, our results for F_v:F_m were qualitatively and quantitatively identical in both experiments using different individual colonies from the mid-shelf Davies Reef and the inshore Orpheus Island. These consistent findings indicate that the increased environmental stress induced by iron limitation at elevated temperature may be a general phenomenon affecting colonies of *S. pistillata* in the central region of the GBR. Further experiments with diverse corals are required to validate this assertion, particularly in view of the salinity stress experienced by the Davies Reef colony prior to the experiment.

While there is a growing consensus that oxidative stress is a unifying cause of coral bleaching (Lesser 2006), the fundamental processes whereby ROS production overwhelms the capacity of the antioxidants in the algal symbionts have not been elucidated (Smith *et al.* 2005). Our results show that decreasing iron availability in seawater surrounding *S. pistillata* affects the corals by decreasing photochemical efficiency in their endosymbionts, owing likely both to NPQ protection and chronic photoinhibition—effects that presage coral bleaching. This effect of iron limitation also occurs in free-living phytoplankton (Geider *et al.* 1993; Kolber *et al.* 1994), suggesting that low dissolved iron concentrations in reef waters may affect corals there and contribute to natural coral bleaching. Moreover, given both that phytoplankton exhibit the capacity for 'luxury' iron uptake under replete conditions (Sunda and Huntsman 1995), and there is little reason to speculate that *Symbiodinium* spp. lack this capability within the coral holobiome, spatial distributions of coral bleaching may be linked in part to the recent local history of oceanographic conditions affecting metal transport to reef environments.

2.5 References

Allen, M. D., J. Kropat, S. Tottey, J. A. Del Campo, and S. S. Merchant. 2007. Manganese deficiency in *Chlamydomonas* results in loss of Photosystem II and MnSOD function, sensitivity to peroxides, and secondary phosphorus and iron deficiency. *Plant Physiol*. 143: 263-277.

Ambarsari, I., B. E. Brown, R. G. Barlow, G. Britton, and D. Cummings. 1997. Fluctuations in algal chlorophyll and carotenoid pigments during solar bleaching in the coral *Goniastrea aspera* at Phuket, Thailand. *Mar. Ecol. Prog. Ser*. 159: 303-307.

Asada, K. 1999. The water-water cycle in chloroplasts: scavenging of active oxygens and dissipation of excess photons. *Annu. Rev. Plant Physiol. Plant Mol. Biol.* 50: 601-639.

Berkelmans, R., G. De'ath, S. Kininmonth, and W. J. Skirving. 2004. A comparison of the 1998 and 2002 coral bleaching events on the Great Barrier Reef: spatial correlation, patterns, and predictions. *Coral Reefs* 23: 74–83.

Berkelmans, R., and M. J. H. van Oppen. 2006. The role of zooxanthellae in the thermal tolerance of corals: a 'nugget of hope' for coral reefs in an era of climate change. *Proc. R. Soc. Lond. B* 273: 2305–2312.

Bhagooli, R., and M. Hidaka. 2003. Comparison of stress susceptibility of *in hospite* and isolated zooxanthellae among five coral species. *J. Exp. Mar. Biol. Ecol*. 291: 181–197.

Brown, B. E., I. Ambarsari, M. E. Warner, W. K. Fitt, R. P. Dunne, and S. W. Gibb. 1999. Diurnal changes in photochemical efficiency and xanthophyll concentrations in shallow water reef corals: evidence for photoinhibition and photoprotection. *Coral Reefs* 18: 99–105.

Brown, B. E., R. P. Dunne, M. E. Warner, I. Ambarsari, W. K. Fitt, S. W. Gibb, and D. G. Cummings. 2000. Damage and recovery of Photosystem II during a manipulative field experiment on solar bleaching in the coral *Goniastrea aspera*. *Mar. Ecol. Prog. Ser*. 195: 117-124.

Casper-Lindley, C., and O. Björkman. 1998. Fluorescence quenching in four unicellular algae with different light-harvesting and xanthophyll-cycle pigments. *Photosyn. Res*. 56: 277-289.

Crawford, D. L., and M. F. Oleksiak. 2007. The biological importance of measuring individual variation. *J. Exp. Biol.* 210: 1613-1621.

Császár, N. B. M., F. O. Seneca, and M. J. H. van Oppen. 2009. Variation in antioxidant gene expression in the scleractinian coral *Acropora millepora* under laboratory thermal stress. *Mar. Ecol. Prog. Ser.* 392: 93–102.

Dove, S., J. C. Ortiz, S. Enríquez, M. Fine, P. Fisher, R. Iglesias-Prieto, D. J. Thornhill, and O. Hoegh-Guldberg. 2006. Response of holosymbiont pigments from the scleractinian coral *Montipora monasteriata* to short-term heat stress. *Limnol. Oceanogr*. 51: 1149-1158.

Entsch, B., R. G. Sim, and B. G. Hatcher. 1983. Indications from photosynthetic components that iron is a limiting nutrient in primary producers on coral reefs. *Mar. Biol.* 73: 17–30.

Falkowski, P. G., and J. A. Raven. 2007. Photosynthesis and primary production in nature, p. 319–363. *In* P. G. Falkowski and J. A. Raven, Aquatic Photosynthesis, 2nd ed. Princeton.

Ferrier-Pagès, C., V. Schoelzke, J. Jaubert, L. Muscatine, and O. Hoegh-Guldberg. 2001. Response of a scleractinian coral, *Stylophora pistillata*, to iron and nitrate enrichment. *J. Exp. Mar. Biol. Ecol*. 259: 249–261.

Ferrier-Pagès, C., J. Witting, E. Tambutté, and K. P. Sebens. 2003. Effect of natural zooplankton feeding on the tissue and skeletal growth of the Scleractinian coral *Stylophora pistillata*. *Coral Reefs* 22: 229-240.

Fitt, W. K., R. D. Gates, O. Hoegh-Guldberg, J. C. Bythell, A. Jatkar, A. G. Grottoli, M. Gomez, P. Fisher, T. C. LaJeunesse, O. Pantos, R. Iglesias-Prieto, D. J. Franklin, L. J. Rodrigues, J. M. Torregiani, R. van Woesik, and M. P. Lesser. 2009. Response of two species of Indo-Pacific corals, *Porites cylindrica* and *Stylophora pistillata*, to short-term thermal stress: The host does matter in determining the tolerance of corals to bleaching. *J. Exp. Mar. Biol. Ecol.* 373: 102-110.

Franklin, D. J., C. M. Molina Cedrés, and O. Hoegh-Guldberg. 2006. Increased mortality and photoinhibition in the symbiotic dinoflagellates of the Indo–Pacific coral *Stylophora pistillata* (Esper) after summer bleaching. *Mar. Biol*. 149: 633–642.

Gaetke, L. M., and C. K. Chow. 2003. Copper toxicity, oxidative stress, and antioxidant nutrients. *Toxicology* 189: 147–163.

Geider, R. J., J. La Roche, R. M. Greene, and M. Olaizola. 1993. Response of the photosynthetic apparatus of *Phaeodactylum tricornutum* (Bacillariophyceae) to nitrate, phosphate, or iron starvation. *J. Phycol*. 29: 755-766.

Glynn, P. W. 1996. Coral reef bleaching: facts, hypotheses and implications. *Global Change Biol.* 2: 495–509.

Greene, R. M., R. J. Geider, Z. Kolber, and P. G. Falkowski. 1992. Iron-induced changes in light harvesting and photochemical energy conversion processes in eukaryotic marine algae. *Plant Physiol*. 100: 565-575.

Havaux, M., and K. K. Niyogi. 1999. The violaxanthin cycle protects plants from photooxidative damage by more than one mechanism. *Proc. Nat. Acad. Sci.* USA 96: 8762-8767.

Hill, R., C. Frankart, and P. J. Ralph. 2005. Impact of bleaching conditions on the components of non-photochemical quenching in the zooxanthellae of a coral. *J. Exp. Mar. Biol. Ecol.* 322: 83-92.

Hill, R., and P. J. Ralph. 2008. Dark-induced reduction of the plastoqunone pool in zooxanthellae of Scleractinian corals and implications for measurements of chlorophyll *a* fluorescence. *Symbiosis* 46: 45-56.

Hoegh-Guldberg, O. 1999. Climate change, coral bleaching and the future of the world's coral reefs. *Mar. Freshwater. Res*. 50: 839–866.

Hoegh-Guldberg, O., and Jones, R.J. 1999. Photoinhibition and photoprotection in symbiotic dinoflagellates from reef-building corals. *Mar. Ecol. Prog. Ser.* 183: 73-86.

Hurry V. M., and N. P. A. Huner. 1992. Effect of cold hardening on sensitivity of winter and spring wheat leaves to short-term photoinhibition and recovery of photosynthesis. *Plant Physiol.* 100: 1283–1290.

Hutchins, D. A., V. M. Franck, M. A. Brzezinski, and K. W. Bruland. 1999. Inducing phytoplankton iron limitation in iron-replete coastal waters with a strong chelating ligand. *Limnol. Oceanogr*. 44: 1009–1018.

Jokiel, P. L. 2004. Temperature stress and coral bleaching, p. 401–425. *In* E. Rosenberg and Y. Loya [eds.], Coral health and disease. Springer-Verlag, Heidelberg

Jones, A. M., N. E. Cantin, R. Berkelmans, B. Sinclair, and A. P. Negri. 2008. A 3D modeling method to calculate the surface areas of coral branches. *Coral Reefs* 27: 521-526.

Jones, R. J., and O. Hoegh-Guldberg. 2001. Diurnal changes in the photochemical efficiency of the symbiotic dinoflagellates (Dinophyceae) of corals: photoprotection, photoinactivation and the relationship to coral bleaching. *Plant Cell Envir.* 24: 89–99.

Jones, R. J., O. Hoegh-Guldberg, A. W. D. Larkum, and U. Schreiber. 1998. Temperature-induced bleaching of corals begins with impairment of the CO_2 fixation mechanism in zooxanthellae. *Plant Cell Envir*. 21: 1219–1230.

Kitajima, M., and W. L. Butler. 1975. Quenching of chlorophyll fluorescence and primary photochemistry in chlorophlasts by dibromothymoquinone. *Biochim. Biophys. Acta.* 376: 105–115.

Kolber, Z. S., R. T. Barber, K. H. Coale, S. E. Fitzwateri, R. M. Greene, K. S. Johnson, S. Lindley, and P. G. Falkowski. 1994. Iron limitation of phytoplankton photosynthesis in the equatorial Pacific Ocean. *Nature* 371: 145-149.

Krause, G. H. 1988. Photoinhibition of photosynthesis. An evaluation of damaging and protective mechanisms. *Physiol. Plant*. 74: 566–574.

Laforsch, C., E. Christoph, C. Glaser, M. Naumann, C. Wild, and W. Niggl. 2008. A precise and non-destructive method to calculate the surface area in living Scleractinian corals using X-ray computed tomography and 3D modeling. *Coral Reefs* 27: 811-820.

LaJeunesse, T. C., H. R. Bonilla, M. E. Warner, M. Wills, G. W. Schmidt, and W. K. Fitt. 2008. Specificity and stability in high latitude eastern Pacific coral-algal symbioses. *Limnol. Oceanogr.* 53: 719-727.

Lesser, M. P. 2006. Oxidative stress in marine environments: biochemistry and physiological ecology. *Annu. Rev. Physiol.* 68: 253–278.

Lough, J. M. 2000. 1997–1998: Unprecedented thermal stress to coral reefs? *Geophys. Res. Lett.* 27: 3901–3904.

Measures, C. I., and S. Vink. 1999. Seasonal variations in the distribution of Fe and Al in the surface waters of the Arabian Sea. *Deep-Sea Res. II* 46: 1597-1622.

Moseley, J.L., Allinger, R., Herzog, S., Hoerth, P., Wehinger, E., Merchant, S. and Hippler, M. 2002. Adaptation to Fe-deficiency requires remodeling of the photosynthetic apparatus. *The EMBO journal*. 21: 6709-6720.

Muscatine, L. 1990. The role of symbiotic algae in carbon and energy flux in reef corals, p. 75–84. *In* Z. Dubinsky [ed.], Coral reefs. Ecosystems of the world, No. 25. Elsevier, Amsterdam.

Muscatine, L., and J. W. Porter. 1977. Reef corals: mutualistic symbioses adapted to nutrient-poor environments. *BioScience* 27: 454–460.

Obata, H., K. Shitashima, K. Isshiki, and E. Nakayama. 2008. Iron, manganese and aluminum in upper waters of the western South Pacific Ocean and its adjacent seas. *J. Oceanogr.* 64: 233–245.

Palenik, B., N. M. Price, and F. M. M. Morel. 1991. Potential effects of UV-B on the chemical environment of marine organisms. *Envir. Poll*. 70: 117–130.

Peers, G., and N. M. Price. 2004. A role for manganese in superoxide dismutases and growth of iron-deficient diatoms. *Limnol. Oceanogr*. 49: 1774–1783.

Raven, J. A., M. C. W. Evans, and R. E. Korb. 1999. The role of trace metals in photosynthetic electron transport in O_2-evolving organisms. *Photosyn. Res*. 60: 111–149.

Richier, S., P. Furla, A. Plantivaux, P.-L. Merle, and D. Allemand. 2005. Symbiosis-induced adaptation to oxidative stress. *J. Exp. Biol*. 208: 277–285.

Richter, M., W. Rühle, and A. Wild. 1990. Studies on the mechanism of photosystem II photoinhibition II: The involvement of toxic oxygen species. *Photosyn. Res.* 24: 237-243.

Sakka, A., L. Legendre, M. Gosselin, B. Leblanc, B. Delasalle, and N. M. Price. 1999. Nitrate, phosphate, and iron limitation of the phytoplankton assemblage in the lagoon of Takapoto Atoll (Tuamotu Archipelago, French Polynesia). *Aquat. Microb. Ecol*. 19: 149–161.

Sampayo, E. M., L. Franceschinis, and O. Hoegh-Guldberg. 2007. Niche partitioning of closely related symbiotic dinoflagellates. *Mol. Ecol.* 16: 3721-3733.

SAS Institute. 2002. Standard least squares: Random effects, p. 251–265. JMP, version 5. Statistics and Graphics Guide. SAS Institute.

Setlik, I., S. I. Allakhverdiev, L. Nedbal, E. Setlikova, and V. V. Klimov. 1990. Three types of Photosystem II photoinactivation. *Photosyn. Res.* 23: 39-48.

Shick, J. M., and H. B. Dowse. 1985. Genetic basis of physiological variation in natural populations of sea anemones: intra- and interclonal analyses of variance, p. 465-479. *In* P. E. Gibbs [ed.], Proceedings of the Nineteenth European Marine Biology Symposium. Cambridge University Press, Cambridge.

Smith, D. J., D. J. Suggett, and N. R. Baker. 2005. Is photoinhibition of zooxanthellae photosynthesis the primary cause of thermal bleaching in corals? *Global Change Biol.* 11: 1–11.

Stanley, Jr., G. D. 2006. Photosymbiosis and the evolution of modern coral reefs. *Science* 312: 857–858.

Stanley, Jr., G. D., and B. Van De Schootbrugge. 2009. The evolution of the coral–algal symbiosis, p. 7–19. *In* M. J. H. van Oppen and J. M. Lough [eds.], Coral bleaching: Patterns, processes, causes and consequences. Ecological Studies. Springer-Verlag, Berlin.

Sunda, W.G. and S.A Huntsman. 1995. Iron uptake and growth limitation in oceanic and coastal phytoplankton. *Mar. Chem.* 50: 189-206.

Tchernov, D., M. Y. Gorbunov, C. de Vargas, S. N. Yadav, A. J. Milligan, M. Häggblom and P. G. Falkowski. 2004. Membrane lipids of symbiotic algae are diagnostic of sensitivity to thermal bleaching in corals. *Proc. Nat. Acad. Sci.* USA 101: 13531-13535.

Ulstrup, K. E., and M. J. H. van Oppen. 2003. Geographic and habitat partitioning of genetically distinct zooxanthellae (*Symbiodinium*) in *Acropora* corals on the Great Barrier Reef. *Mol. Ecol.* 12: 3477–3484.

Van de Poll, W. H., P. J. Janknegt, M. A. van Leeuwe, R. J. W. Visser, and A. G. J. Buma. 2009. Excessive irradiance and antioxidant response of an Antarctic marine diatom exposed to iron limitation and to dynamic irradiance. *J. Photochem. Photobiol. B, Biology* 94: 32-37.

Van Heukelem, L., and C. S. Thomas. 2001. Computer-assisted high-performance liquid chromatography method development with applications to the isolation and analysis of phytoplankton pigments. *J. Chromatogr.* 910: 31–49.

Veal, C. J., G. Holmes, M. Nunez, O. Hoegh-Guldberg, and J. Osborn. 2010. A comparative study of methods for surface area and three-dimensional shape measurement of coral skeletons. *Limnol. Oceanogr. Methods* 8: 241-253.

Warner, M. E. 2005. An overview of the intepretation and current use of chlorophyll fluorescence to understand coral bleaching, p. 18-20. *In* O. Hoegh-Guldberg [ed.], Understanding the stress response of corals and *Symbiodinium* in a rapidly changing environment. Unidad Académica Puerto Morelos, Instituto de Ciencias del Mar y Limnología, UNAM, Mexico.

Warner, M. E., and S. Berry-Lowe. 2006. Differential xanthophyll cycling and photochemical activity in symbiotic dinoflagellates in multiple locations of three species of Caribbean coral. *J. Exp. Mar. Biol. Ecol.* 339: 86-95.

Warner, M. E., G. C. Chilcoat, F. K. McFarland, and W. K. Fitt. 2002. Seasonal fluctuations in the photosynthetic capacity of photosystem II in symbiotic dinoflagellates in the Caribbean reef-building coral *Montastraea*. *Mar. Biol.* 141: 31–38.

Warner, M. E., W. K. Fitt, and G. W. Schmidt. 1996. The effects of elevated temperature on the photosynthetic efficiency of zooxanthellae *in hospite* from four different species of reef coral: a novel approach. *Plant Cell Envir.* 19: 291–299.

Warner, M. E., W. K. Fitt, and G. W. Schmidt. 1999. Damage to photosystem II in symbiotic dinoflagellates: A determinant of coral bleaching. *Proc. Nat. Acad. Sci.* USA 96: 8007–8012.

Warner, M. E., M. P. Lesser, and P. J. Ralph. 2010. Chlorophyll fluorescence in reef building corals. *In* D. J. Suggett, O. Prasil and M. A. Borowitzka [eds.], Chlorophyll *a* fluorescence in aquatic sciences: Methods and applications. Springer-Verlag, Berlin.

Weinberg, E. D. 1999. Iron loading and disease surveillance. *Emerging Infectious Diseases* 5: 346–352.

Weis, V. M. 2008. Cellular mechanisms of Cnidarian bleaching: stress causes the collapse of symbiosis. *J. Exp. Biol.* 211: 3059–3066.

Wells, M. L., N. M. Price, and K. W. Bruland. 1994. Iron limitation and the cyanobacterium *Synechococcus* in equatorial Pacific waters. *Limnol. Oceanogr*. 39: 1481–1486.

Wells, M. L., and C. G. Trick. 2004. Controlling iron availability to phytoplankton in iron-replete coastal waters. *Mar. Chem.* 86: 1–13.

Wooldridge, S., and T. Done. 2004. Learning to predict large-scale coral bleaching from past events: A Bayesian approach using remotely sensed data, in-situ data, and environmental proxies. *Coral Reefs* 23: 96–108.

Zar, J. H. 1999. Comparing simple linear regression equations, p. 360–376. *In* J. H. Zar, Biostatistical analysis 4th ed. Prentice Hall, Englewood Cliffs, NJ.

Chapter 3

Flow cytometric measurements of oxidative stress in freshly isolated algal symbionts as a function of temperature and iron availability to coral colonies.

3.1 Introduction

Coral reef ecosystems are some of the most diverse and productive ecosystems on earth. The productivity of these rich ecosystems relies on a symbiotic relationship between stony, reef building corals (Scleractinian) and photosynthetic dinoflagellates (*Symbiodinium*), more commonly termed zooxanthellae (Weis 2008). Presently, the success of Scleractinian corals is threatened by a collapse in this symbiotic relationship, manifested as the phenomenon coral bleaching. Coral bleaching involves the loss of coral pigmentation due to the expulsion of their zooxanthellae or the breakdown of the zooxanthellae's photosynthetic pigments. Once bleached, corals may recover if their zooxanthellae are reacquired, but death is the final result if the absence persists (Glynn 1993, Douglas 2003).

Many factors contribute to coral bleaching events, including changes in sea surface temperature, ultraviolet (UV) exposure, sedimentation, salinity and pollution (Lesser 1997) and the influence they have on zooxanthellae photophysiology plays a critical role in the process. Under conditions of high temperature and irradiance, zooxanthella photosystems become saturated with unmanageable excitation energy, which can result in the photoinhibition of photosynthesis or photodamage to photosystem II (PSII) (Smith *et al.* 2005). In heat stressed corals, it has been established that this 'photoinhibition model' of coral bleaching occurs due to either decreases in carbon assimilation (sink limitation, Jones *et al.* 1998) or due to direct damage to PSII (Warner *et al.* 1999). Photoinhibition and photodamage are detrimental to zooxanthellae and their coral hosts because both phenomena occur in oxygen (O_2) rich environments, generated by photosynthetic activity. The high concentration of O_2 in the chloroplast, in combination with excess excitation energy, enhances the production of detrimental reactive oxygen species (ROS) such as

singlet oxygen ($^1O_2$), the superoxide radical ($O_2^{\bullet-}$), hydrogen peroxide (H_2O_2) and the hydroxyl radical ($OH\bullet^-$) (Lesser 1997). Previous studies have shown that ROS play a critical role in coral bleaching with ultraviolet (UV) light exposure and thermal stress in various coral species and their zooxanthellae (Lesser *et al*. 1990, Lesser 1996, 1997, Smith *et al*. 2005). The involvement of ROS in coral bleaching indicates the requirement of both the coral host and zooxanthellae to control the proliferation of these toxic molecules.

Zooxanthellae mitigate the damaging effects of increased energy absorption and ROS generation through a variety of protective cellular processes. Such processes include the Mehler-peroxidase reaction, xanthophyll cycling, photosystem state transitions (Smith *et al.* 2005) and the activity of antioxidant enzymes such as superoxide dismutases, catalase and ascorbate peroxidase (Weiss 2008). Many of the antioxidant enzymes contain the trace metals iron, manganese, copper or zinc as constitutive and specific cofactors. Specifically, ascorbate peroxidase, a heme-containing monomeric enzyme, catalase, a tetrameric heme-containing enzyme, and iron-superoxide dismutase (Fe-SOD) require iron for proper structure and function (Geider and La Roche 1994, Lesser 2006). The activity of these iron-containing antioxidant enzymes may be intricately linked to changes in the ratio and concentration of intracellular iron and the availability of the trace metal in the environment. As a result, the residence time and concentrations of ROS in both zooxanthellae and their coral hosts may be affected by variations in ambient free iron concentrations. Free total iron concentrations in the Coral Sea can range from 0.2-0.3 nM (Obata *et al.* 2008), indicating that Coral Sea corals, and by association their zooxanthellae, may encounter iron limitation. Negative signatures of iron limitation have been detected in phytoplankton species, manifested as decreases in PSII photochemical efficiency (F_v/F_m) (Kobler *et al.* 1994) and antioxidant concentrations, potentially subjecting iron-deficient cells to photochemical damage under saturating conditions. The iron rich nature of the photosynthetic electron transport chain (ETC) and antioxidant enzymes in photosynthetic organisms further increases their susceptibility to iron limitation (Geider and La Roche 1994) and there is little reason to believe that zooxanthellae may not encounter a similar effect. In particular, if zooxanthellae *in hospite* are exposed to stressful conditions, such as elevated temperature and light, iron

limitation may prevent the necessary increase in photosynthetic activity and antioxidant enzyme activity necessary to alleviate the stress, leading to increased ROS production and coral bleaching. This study examines the relationship between iron availability and coral bleaching in the Indo Pacific coral, *Stylophora pistillata* under temperature stress.

3.2 Methods

3.2.1 Coral collection and maintenance- A colony of *Stylophora pistillata,* Esper 1797*,* was collected at Orpheus Island on the Great Barrier Reef (GBR) 18º36.768S/146º28.986E and maintained in a flowing seawater tank at the Australian Institute of Marine Science, Townsville Australia, until experimentation. Coral explants 10 cm in length were excised from upright positioned coral branches and suspended vertically with monofilament fishing line (6lb, 0.25mm, Neptune Tackle, Port Adelaide, Australia). To prevent the proliferation of endolithic algae, the cut surfaces of the explants were sealed with a waterproof epoxy (Mr. Sticky 001327, AAI, Fair Oaks, CA, USA). To allow recovery and acclimation (determined by a sustained PSII photochemical efficiency >0.65-0.7 in zooxanthellae), corals were maintained for three weeks in filtered (1 μm) seawater at an irradiance of 50 μmol photons·m^{-2}·s^{-1}, and a seawater temperature of 25 °C.

3.2.2 Experimental design- S. pistillata explants were placed in trace metal-clean plastic chambers (700 ml, Sistema Plastics, New Zealand) containing 300 mL of 0.5 μm filtered seawater (8 explants per treatment). All treatments were acclimated to low temperature conditions (27 ºC) for 3 days in iron-replete seawater. On day 0, the strong iron chelator, desferrioxamine B (DFB) (Wells and Trick, 2004) was added to iron deplete treatments at a concentration of 300 nM and the temperature was ramped up from 27 °C to 30 °C over four days (0.75 °C d^{-1}) and maintained at 30°C until day 10. On day 10, the temperature was then further increased to 31°C over four days (0.25 °C d^{-1}) and this elevated temperature was maintained until the experiment was terminated. Over the course of the experiment, the temperature was maintained within a narrow range of ± 0.1 °C and monitored using an electronic heater response system. All treatments were exposed to an irradiance of 150 μmol photons·m^{-2}·s^{-1}.

3.2.3 Analysis of PSII photochemical efficiency in zooxanthellae- Dark-adapted PSII photochemical efficiency (F_v/F_m) was measured daily under trace metal clean conditions (see Chapter 2) using Pulse Amplitude Modulation (PAM) fluorometry (Diving-PAM, S/N: UWFA0257A, Walz Mess-und Regeltechnik, Germany). *S. pistillata* explants were dark acclimated for a minimum of 9 hours and PAM measurements were taken on the highest irradiated surface (tip). After a significant decrease in F_v/F_m (<0.5) or visible coral tissue loss at high temperature, zooxanthellae were isolated and the experiment was terminated.

3.2.4 Detection of intracellular ROS and membrane permeability- Stylophora pistillata zooxanthellae were collected and isolated from the host tissue using a positive air pressure technique (modified from Berkelmans and van Oppen 2006). The host slurry was filtered across a 25 μm Nytex filter and centrifuged at 750 *g* for 10 minutes at 4 °C. Freshly isolated zooxanthellae were further cleaned by two washes in 0.2 μm filtered seawater and centrifugation (*as above*). The freshly isolated zooxanthellae pellet was suspended in the respective experimental treatment medium (+/-DFB) and treatment temperature (27/31 °C) and was exposed to both a light and dark (200 and 0 μmol photons$\cdot m^{-2}\cdot s^{-1}$, respectively) incubation for one hour prior to flow cytometric measurements. The intracellular ROS and reactive nitrogen species (RNS) nitric oxide (NO), $OH\bullet^{-}$, (peroxynitrite) $ONOO^{-}$ and H_2O_2 were detected using 5-(and 6) chloromethyl-2',7'-dichlorodihydrofluorescein diacetate, acetyl ester (CMH_2DCFDA) (Murrant and Reid 2001) at a final concentration of 5 μM. Superoxide, $ONOO\bullet^{-}$ and $OH\bullet^{-}$ were detected using the fluorescent probe dihydroethidium (DHE) (Murrant and Reid 2001), at a final concentration of 23 μM. Freshly isolated zooxanthellae were incubated with each probe for 30 minutes in the dark prior to analysis on a FACsCalibur flow cytometer (BD, San Jose, California, U.S.A.). Increases in fluorescence (Fl1 and Fl2 channel values of the flow cytometer) were proportional to probe oxidation and indicative of intracellular ROS and RNS, as determined by the probe optimization component completed prior to experimentation (*see below*). All fluorescence measurements were standardized to control signals given by un-probed freshly isolated zooxanthellae of the same treatment, accounting for differences in ambient fluorescence signals.

Table 3.1 Excitation [nm], emission [nm] and final concentration [M] of the flow cytometric probes used to detect ROS, RNS and membrane permeability in *S. pistillata* freshly isolated zooxanthellae (Invitrogen 2009).

Probe	Excitation [nm]	Emission [nm]	Final concentration in sample [mol/Liter]
CMH2DCFDA	492-495	517-527	$5x10^{-6}$
DHE	528	617	$23.1x10^{-6}$
SYTOX® Green	488	504-523	$1x10^{-6}$

In addition to intracellular ROS and RNS measurements, cell membrane permeability was determined by measuring the proportion of SYTOX green uptake of each cell. In the assay, freshly isolated zooxanthellae were subjected to the same incubations as above and probed with SYTOX green, an indicator of cell death (Vardi *et al*. 2006), at a concentration of 1 μM for 10 minutes in the dark prior to flow cytometric analysis. Increases in the green fluorescence of SYTOX green probed cells was gauged as an indication of membrane permeability, as the impermeable dye had traversed the cell membrane and was able to bind cellular DNA, producing a fluorescent signal.

CMH_2DCFDA, DHE and SYTOX green were purchased from Invitrogen-Molecular Probes and working stock solutions were prepared in 0.45 μm dimethyl-sulphoxide (DMSO).

3.2.5 Probe optimization and standard curves- The optimal concentration and incubation time of both ROS probes, CMH_2DCFDA and DHE, were verified by incubating freshly isolated zooxanthellae with (i) different probe concentrations and (ii) with a single probe concentration (CMH_2DCFDA at 5 μM and DHE at 23 μM) monitored over a range of dark incubation times. Furthermore, a standard curve of the probe CMH_2DCFDA, at a concentration of 5 μM, was run against a range of H_2O_2 concentrations (0.05-4.32 M) and a positive control for the probe DHE was conducted at an H_2O_2 concentration of 88 mM to assess each probes ability to detect intracellular H_2O_2 and validate their ROS detection ability.

3.2.6 Statistical Analysis- To determine significant differences between PSII photochemical efficiency (F_v/F_m) with temperature and iron availability over the course of the experiment, a linear mixed model was constructed ($p<0.05$). The linear mixed model and the generalized least squares model (*see below*) were produced using R statistical software (version 2.7.2, 2008). For details on the linear mixed and generalized least squares model synthesis, see Appendix 1.

Two-factorial ANOVA tests were conducted to determine the significance of temperature and DFB addition on the intracellular ROS load and cell membrane permeability of

freshly isolated zooxanthellae ($p<0.05$). Prior to the two-factorial ANOVA analysis, homogeneity of variance was tested using a Levene's test ($p\geq0.05$). Normality was assumed due to the small sample size of 4 and the inability to use a larger sample size because of chamber and experimental room restrictions. ANOVA tests were conducted using SPSS (version 16.0). Where sample variance was not homogeneous, a generalized least squares model was run to determine the significant effects of temperature and DFB addition on the intracellular ROS load of freshly isolated zooxanthellae ($p<0.05$).

3.3 Results

3.3.1 Linear mixed model and PSII photochemical efficiency- A linear mixed model incorporating the random effects of sample day and replicate was tested against a model lacking the random effects. An ANOVA comparing both tests showed that the random effects of sample day and replicate were significant, therefore, the linear mixed model incorporating random effects was selected (*L. ratio*=7.410944, p=0.0065). The effect of fixed factors was determined by running an ANOVA on the complete model and the three-way interaction of temperature, DFB, and sample day was not included in the model because of insignificant effects on F_v/F_m (df=497, F=3.37, p=0.0669). In the final linear mixed model, a significant interaction was detected between temperature and DFB addition on PSII photochemical efficiency (F_v/F_m) in zooxanthellae *in hospite* over sample day (df= 498, t=-1.98344, $p<0.05$, Table 2, Figure 3.1). The negative effect of iron limitation and high temperature on zooxanthellae F_v/F_m across sample days (Figure 3.1) illustrates the negative effect of both factors on zooxanthellae PSII photochemical efficiency.

3.3.2 Cell membrane permeability assay- Cell membrane permeability, as indicated by the uptake of the fluorescent probe SYTOX green, was not significantly affected by high temperature or iron limitation (DFB addition) under the dark incubation (F= 1.747, p=0.209, df=3 and F=0.865,p=0.369 and df=3, respectively, Figure 3.2) or the light incubation (F= 1.729, p=0.211, df=3 and, F=2.258, p=0.157, df=3 respectively).

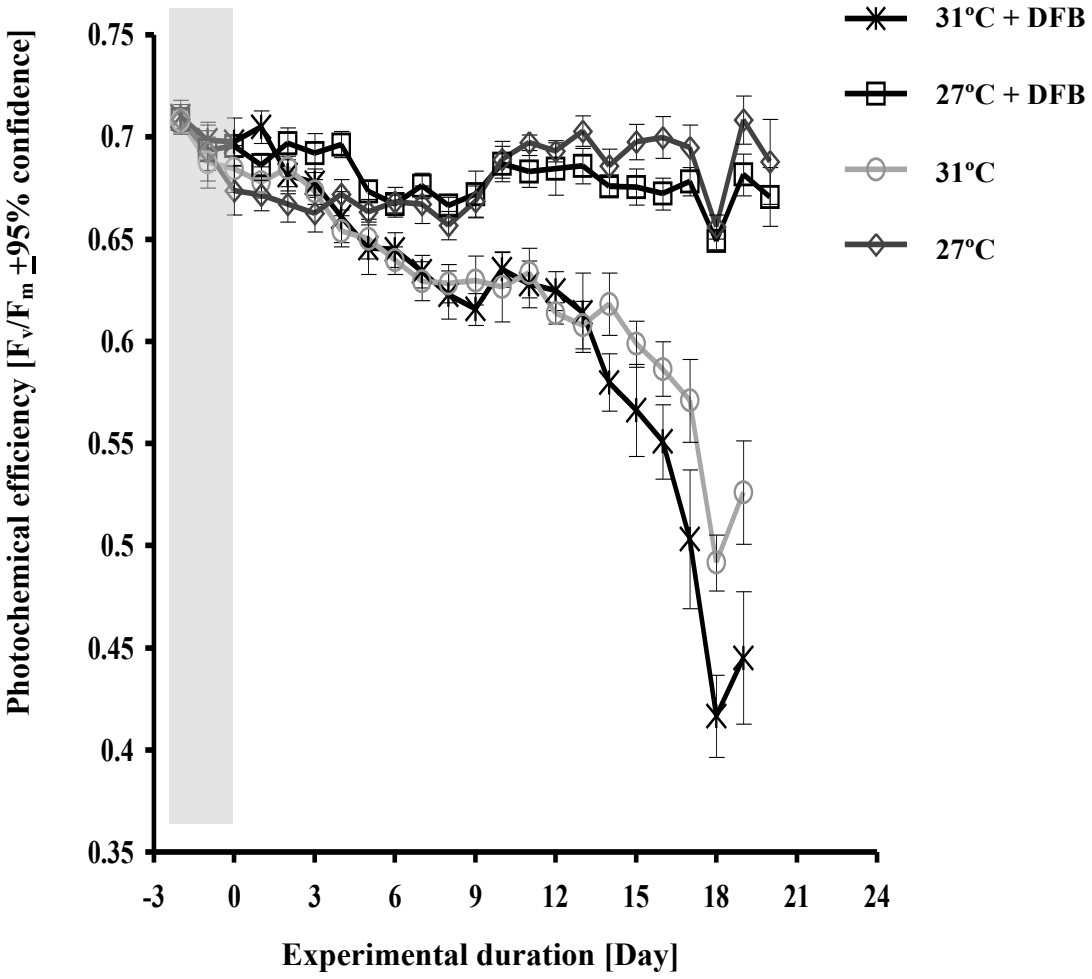
31°C + DFB
27°C + DFB
31°C
27°C
Photochemical efficiency [F_v/F_m ±95% confidence]
0.75
0.7
0.65
0.6
0.55
0.5
0.45
0.4
0.35
-3
0
3
6
9
12
15
18
21
24
Experimental duration [Day]

Figure 3.1 Dark-adapted (12 hours) PSII photochemical efficiency [mean $F_v/F_m \pm$ 95% confidence interval] of *S. pistillata* zooxanthellae exposed to high and low temperatures (31 and 27 °C, respectively) and iron limited or non-limited conditions (+/- 300 nM DFB, respectively). Corals were acclimated to control conditions for three days prior to increases in temperature and DFB addition (indicated by grey shading). Zooxanthellae measured were located on explant tips. Error bars reflect the $\pm$ 95% confidence intervals (n=8). A longitudinal linear mixed model ($p<0.05$) detected a significant interaction between temperature: DFB, DFB:experimental day, and temperature:experimental day.

Table 3.2 Results of a longitudinal linear mixed model comparing dark-adapted photochemical efficiency (F_v/F_m) of *S. pistillata* zooxanthellae exposed to high and low temperatures (31 and 27 °C) and iron-limited or non-limited conditions (addition of 300 nM DFB). Zooxanthellae measured were located on explants tips.

Fixed Factor	Coefficient Value	Standard Error	Degrees of freedom	T-value	p-value
(Intercept)	0.7338851	0.008304668	498	88.37019	0.0000
Date	-0.0127918	0.000688779	498	-18.57173	0.0000
Temperature	-0.0430825	0.010003454	498	-4.30676	0.0000
DFB	-0.0269310	0.010003454	498	-2.69217	0.0073
Date * Temperature	0.0115549	0.000756731	498	15.26949	0.0000
Date * DFB	0.0040648	0.000756731	498	5.37155	0.0000
Temperature * DFB	-0.0138379	0.006976713	498	-1.98344	0.0479

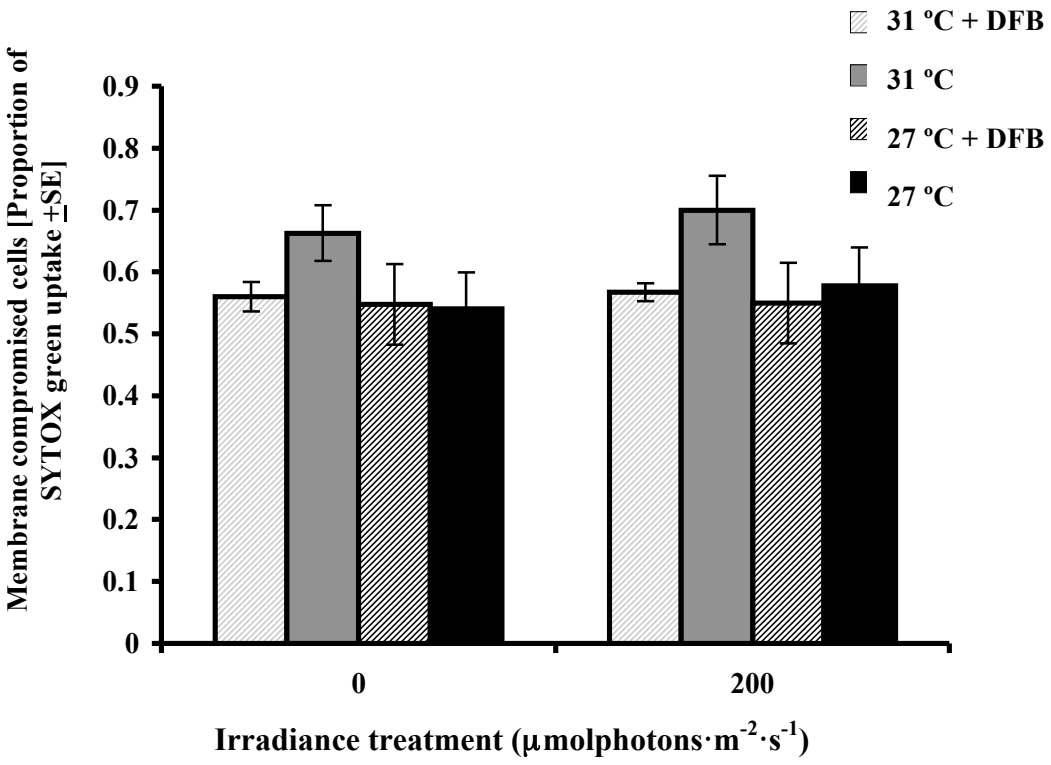
31 ºC + DFB
31 ºC
27 ºC + DFB
27 ºC
Membrane compromised cells [Proportion of SYTOX green uptake ±SE]
0.9
0.8
0.7
0.6
0.5
0.4
0.3
0.2
0.1
0
0
200
Irradiance treatment (µmolphotons·m-2·s-1)

Figure 3.2 Cell viability measured by SYTOX Green uptake of *S. pistillata* zooxanthellae exposed to high and low temperatures (31 and 27 °C, respectively) and iron limited or non-limited conditions (+/- 300 nM DFB, respectively). Freshly isolated zooxanthellae were incubated at 0 and 200 μmol photons·m^{-2}·s^{-1} for 1 hour and probed with SYTOX green (1 μM) for 10 minutes in the dark. Error bars represent the standard error of the four replicate coral explants and no significant difference was detected between treatments.

3.3.3 Probe optimization and standard curve- The concentrations of DHE and CMH_2DCFDA, 23 and 5 μM respectively, were appropriate for use within this study because increases in fluorescence were detected within cells probed with concentrations greater than those values (Figure 3.3-I. and Figure 3.4-I., respectively). These results indicate an appropriate probe concentration as the concentration utilized was not great enough to induce self-quenching by probe. Furthermore, the incubation time of 30 minutes for DHE and CMH_2DCFDA was appropriate for intracellular ROS analysis due to the lack of change in fluorescence value in freshly isolated zooxanthellae after this amount of time (Figure 3.3-II and Figure 3.4-II, respectively).

The sensitivity of the probe CMH_2DCFDA, as indicated by increases in fluorescence, to increases in H_2O_2 concentration (Figure 3.5) and the increase in DHE fluorescence when exposed to a high concentration of H_2O_2 (Figure 3.6) indicate each probe's appropriateness in the assessment of intracellular ROS load. CMH_2DCFDA was particularly sensitive to increases in H_2O_2, while DHE was less sensitive to H_2O_2, requiring a greater H_2O_2 concentration to show increases in fluorescence. Although differing in response to H_2O_2, each probe's fluorescence signal increased in the presence of H_2O_2 (Figures 3.5 and 3.6), indicating that differences in probe fluorescence can be utilized as a proxy for intracellular ROS load in freshly isolated zooxanthellae subjected to variable experimental treatments.

3.3.4 Intracellular reactive oxygen species detection

3.3.4a Dark incubated freshly isolated zooxanthellae- Nitric oxide, $OH\bullet^-$, $ONOO^-$ and H_2O_2, detected by CMH_2DCFDA and manifested as increases in green fluorescence, in freshly isolated zooxanthellae, was reduced under iron-limited conditions (DFB addition) (T=2.500435, p= 0.0266, Figure 3.7-I) and not affected by high or low temperature (27 and 31 °C) treatments (T=-1.197032, p= 0.2527, Figure 3.7-I). An insignificant interaction between temperature (27 and 31 °C) and iron limitation (+/- DFB) in the CMH_2DCFDA fluorescence of freshly isolated zooxanthellae (T=-0.445703, p= 0.6637, Figure 3.7-I) was detected therefore this interaction was not included in the generalized least squares fit model.

I.

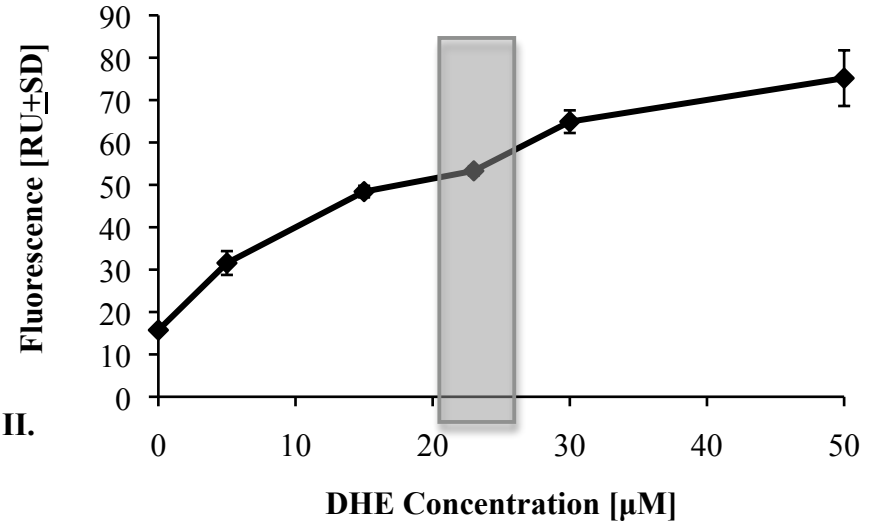
Fluorescence [RU±SD]
90
80
70
60
50
40
30
20
10
0
0
10
20
30
40
50
DHE Concentration [µM]

II.

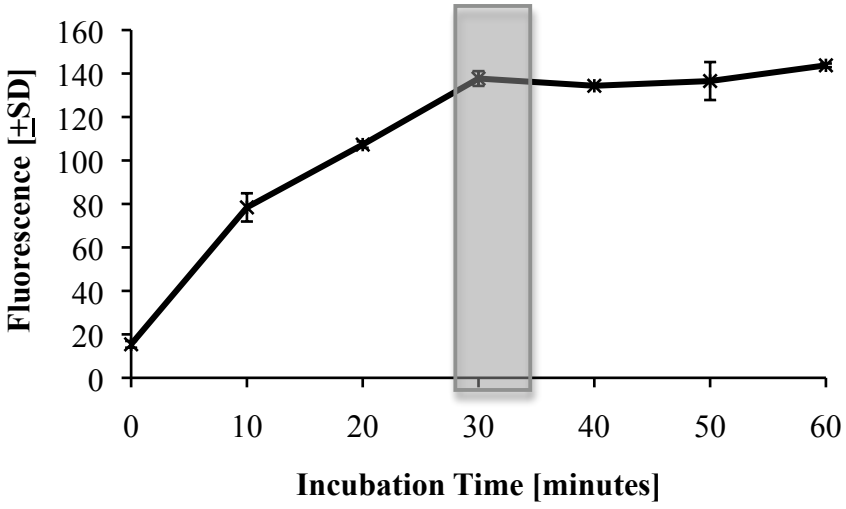
Fluorescence [±SD]
160
140
120
100
80
60
40
20
0
0
10
20
30
40
50
60
Incubation Time [minutes]

Figure 3.3 Mean fluorescence of the ROS probe, DHE, [RU±SD] within freshly isolated zooxanthellae of *S. pistillata* when exposed to (I.) variable probe concentrations for a constant dark incubation time of 30 minutes and (II.) variable dark incubation times with the DHE concentration set to 23.1 μM (n=3). Indicated by the grey box are the probe concentration (I.) and the incubation time (II.) utilized within this study.

I.

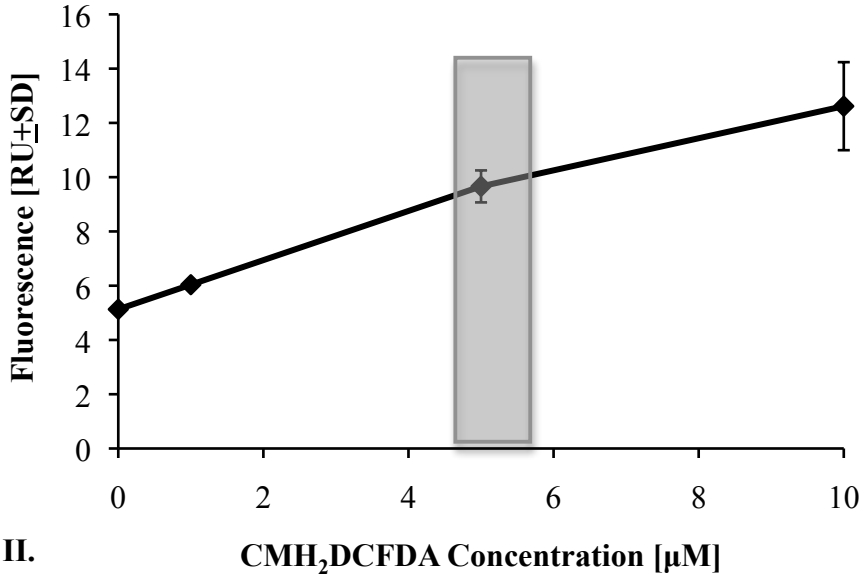
16
14
12
10
8
6
4
2
0
Fluorescence [RU±SD]
0
2
4
6
8
10
CMH2DCFDA Concentration [µM]

II.

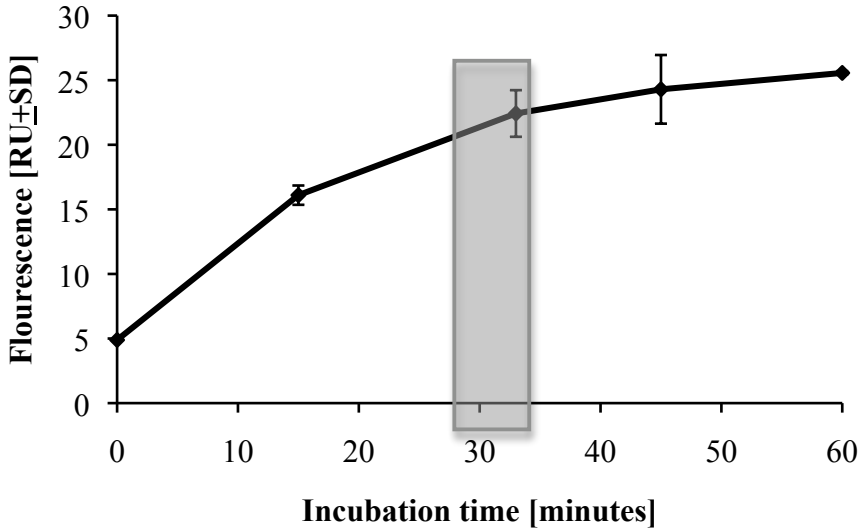
30
25
20
15
10
5
0
Flourescence [RU±SD]
0
10
20
30
40
50
60
Incubation time [minutes]

Figure 3.4 Mean fluorescence of the ROS probe, CMH_2DCFDA, [RU±SD] within freshly isolated zooxanthellae of *S. pistillata* when exposed to (I.) variable probe concentrations for a constant dark incubation time of 30 minutes and (II.) variable dark incubation times with the CMH_2DCFDA concentration set to 5 μM (n=3). Indicated by the grey box are the probe concentration (I.) and the incubation time (II.) utilized within this study.

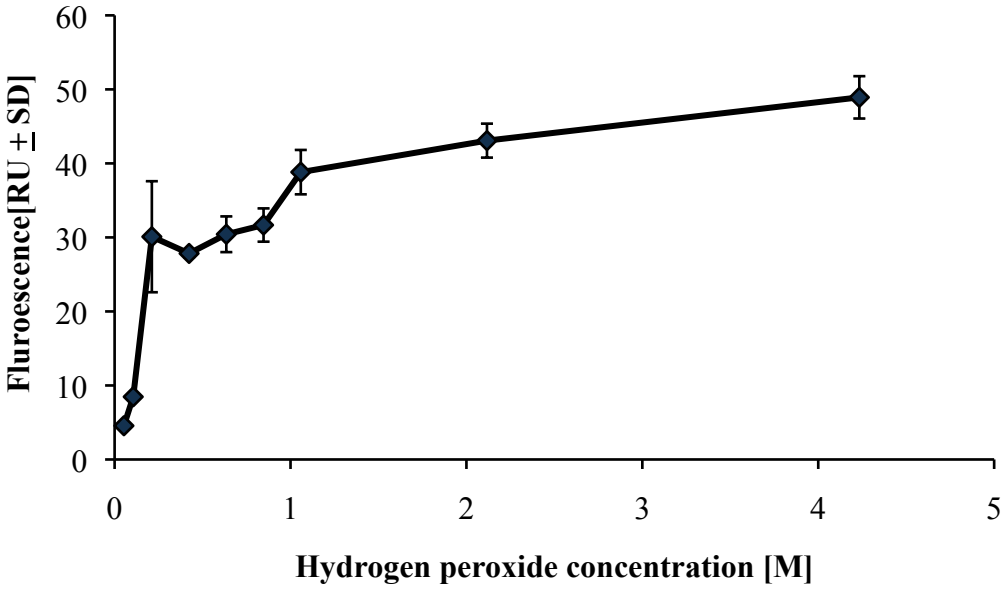
60
50
40
30
20
10
0
Fluroescence[RU ± SD]
0
1
2
3
4
5
Hydrogen peroxide concentration [M]

Figure 3.5 Mean fluorescence of the ROS probe CMH_2DCFDA [RU$\pm$SD] within freshly isolated zooxanthellae of *S. pistillata* when exposed to a range of hydrogen peroxide concentrations (0.05-4.32 M) for an incubation time of 30 minutes in the dark (n=3). The concentration of CMH_2DCFDA was maintained constant at 5 μM.

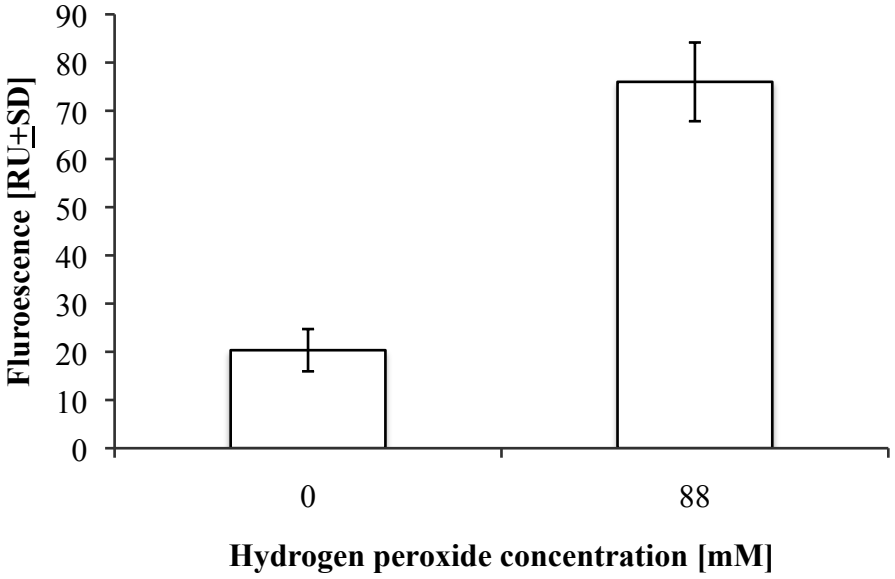
90
80
70
60
50
40
30
20
10
0
Fluroescence [RU±SD]
0
88
Hydrogen peroxide concentration [mM]

Figure 3.6 Mean fluorescence of the ROS probe DHE [RU±SD] within cultured *Symbiodinium* when exposed to hydrogen peroxide (0 and 88 mM) for an incubation time of 30 minutes in the dark (n=4). The concentration of DHE was maintained constant at a 23 μM.

Superoxide, $ONOO^{\bullet-}$ and $OH^{\bullet-}$ in freshly isolated zooxanthellae, as detected by an increase in the orange fluorescence of the probe DHE, were independently affected by both temperature and iron limitation (F=0.602, p=0.453, df=1). Iron limitation (DFB addition) significantly decreased the detected $O_2^{\bullet-}$, $ONOO^{\bullet-}$ and $OH^{\bullet-}$, (F=5.451, p=0.036, df=1, Figure 3.7-II). Furthermore, temperature stress (31 °C) significantly decreased $O_2^{\bullet-}$, $ONOO^{\bullet-}$ and $OH^{\bullet-}$ measurements (F=41.316, p=0.000, df=1, Figure 3.7-II) in dark incubated freshly isolated zooxanthellae.

3.3.4b Light incubated freshly isolated zooxanthellae- Nitric oxide, $OH^{\bullet-}$, $ONOO^-$ and H_2O_2, detected by CMH_2DCFDA, in *S. pistillata* freshly isolated zooxanthellae under temperature stress did not significantly change (31 °C), (F=2.382, p=.147, df=1, Figure 3.8-I). Iron limitation (DFB addition) caused a significant decrease in the ROS and RNS detected by CMH_2DCFDA (F=6.065, p=0.029, df=1, Figure 3.8-I.). No significant interaction was detected between temperature (27 and 31 °C) and iron treatments (+/- DFB) on the ROS and RNS detected by CMH_2DCFDA in freshly isolated zooxanthellae (F=0.399, p= 0.539, df=1, Figure 3.8-I).

Superoxide, $ONOO^{\bullet-}$ and $OH^{\bullet-}$ in freshly isolated zooxanthellae were independently affected by temperature and iron limitation (F=0.431 p=0.524, df=1). Iron limitation (DFB addition) did not significantly affect $O_2^{\bullet-}$, $ONOO^{\bullet-}$ and $OH^{\bullet-}$, (F=4.015, p=0.066, df=1, Figure 3.8-II) but temperature stress (31 °C) caused significant declines in $O_2^{\bullet-}$, $ONOO^{\bullet-}$ and $OH^{\bullet-}$ measurements (F=23.061, p=000, df=1, Figure 3.8-II).

I.

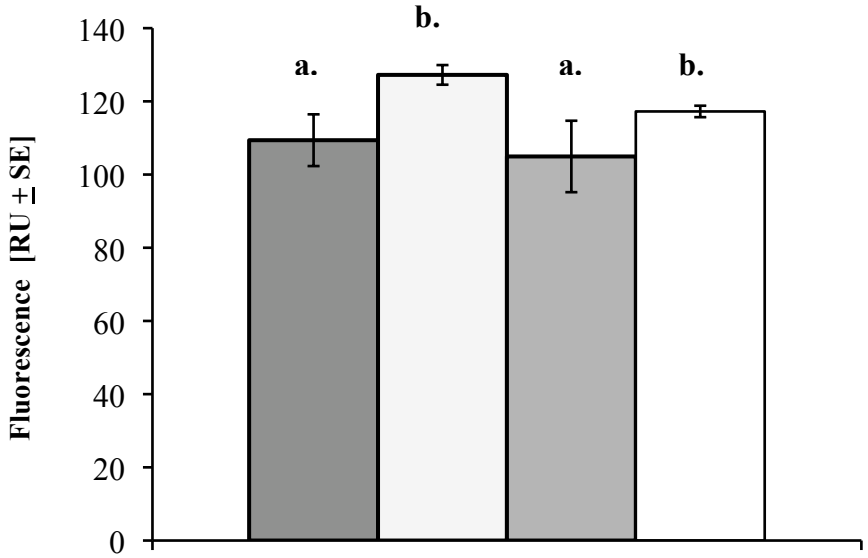
b.
a.
a.
b.
140
120
100
80
60
40
20
0
Fluorescence [RU ± SE]

II.

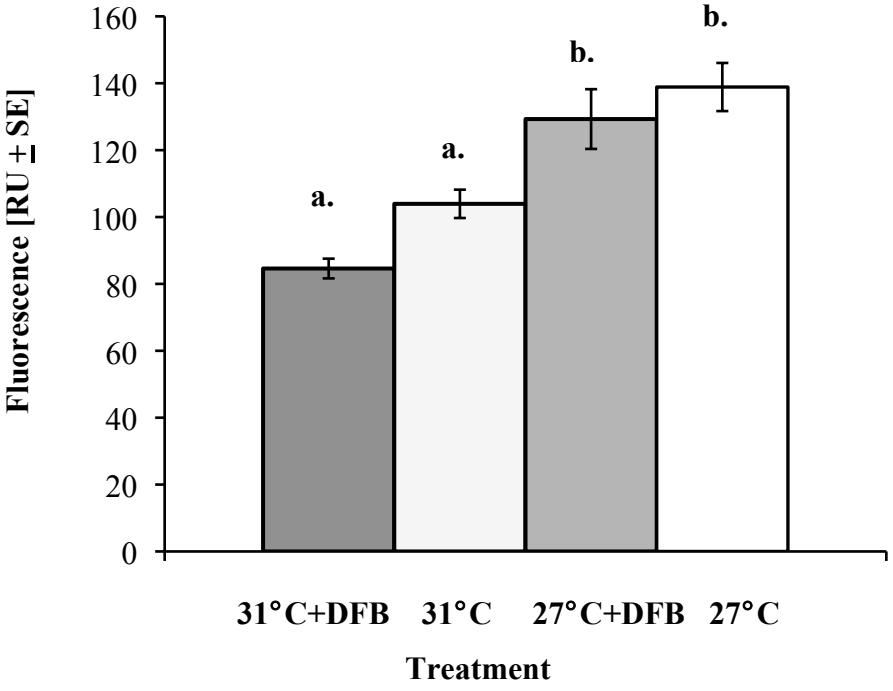
b.
b.
a.
a.
160
140
120
100
80
60
40
20
0
Fluorescence [RU ± SE]
31°C+DFB
31°C
27°C+DFB
27°C
Treatment

Figure 3.7 Mean intracellular (I.) CMH_2DCFDA fluorescence [RU±SE], indicative of the reactive oxygen and nitrogen species (NO, $OH^{\bullet -}$, $ONOO^-$ and H_2O_2) and (II.) mean dihydroethidium fluorescence [RU±SE], indicative of superoxide, $ONOO\bullet^-$ and $OH\bullet^-$ in freshly isolated zooxanthellae of *S. pistillata* exposed to high and low temperatures (31 and 27 °C, respectively) and iron limited or non-limited conditions (+/- 300nm DFB, respectively). Prior to measurements, freshly isolated zooxanthellae were incubated in the dark for one hour. Error bars represent the standard error of the four replicates of each treatment and significant differences are indicated by the presence of a different letter ($p<0.05$).

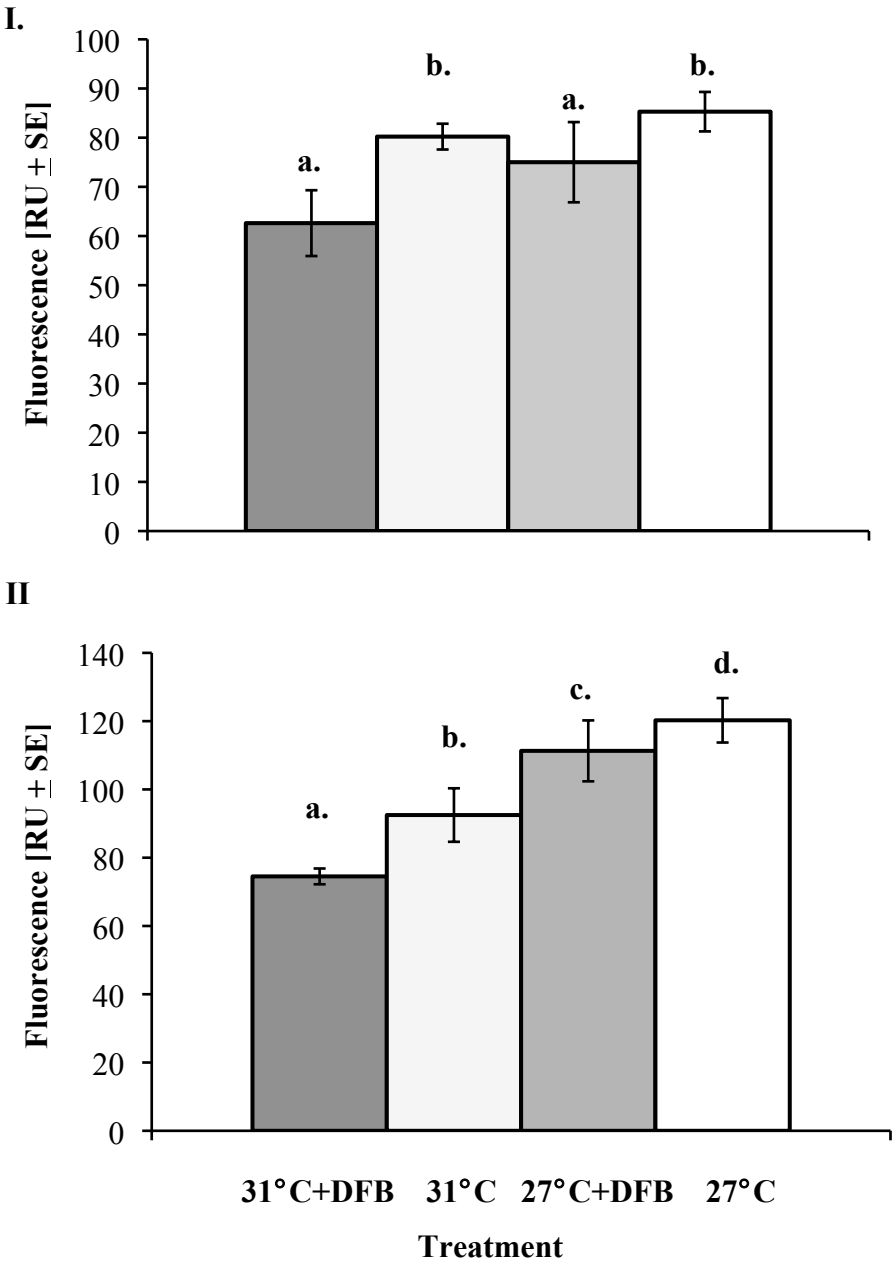
I.
Fluorescence [RU ± SE]
100
90
80
70
60
50
40
30
20
10
0
a.
b.
a.
b.
II
Fluorescence [RU ± SE]
140
120
100
80
60
40
20
0
a.
b.
c.
d.
31°C+DFB
31°C
27°C+DFB
27°C
Treatment

Figure 3.8 Mean intracellular (I.) CMH_2DCFDA fluorescence [RU±SE], indicative of the reactive oxygen and nitrogen species (NO, $OH^{\bullet -}$, $ONOO^-$ and H_2O_2) and (II.) mean dihydroethidium fluorescence [RU±SE], indicative of superoxide, $ONOO^{\bullet -}$ and $OH^{\bullet -}$ in freshly isolated zooxanthellae of *S. pistillata* exposed to high and low temperatures (31 and 27 °C, respectively) and iron limited or non-limited conditions (+/- 300nm DFB, respectively). Prior to measurements, freshly isolated zooxanthellae were incubated under 200 μmol photons$\cdot m^{-2} \cdot s^{-1}$ for 1 hour. Error bars represent the standard error of the treatment replicates and significant differences are indicated by different letters (p<0.05).

3.4 Discussion

The decline in PSII photochemical efficiency (F_v/F_m) of *S. pistillata* zooxanthellae subjected to elevated temperature is a characteristic response of temperature stressed corals (Warner *et al.* 1999, 2002, Berkelmans and vanOppen 2006). Decreases in the photosynthetic efficiency of bleaching corals can occur due to the down-regulation of photosynthesis or photoinhibition (Warner *et al.* 2002). More specifically, the quantum yield of electron transport may decline because of decreases in reduced ETC components. This decline can occur because of decreases in the oxidation of plastoquinone by the cytochrome b_6f complex (usually at sub-saturating light intensities) or because of decreases in the metabolic capacity to consume ATP and NADPH (at saturating light intensities) (Smith *et al.* 2005). In this study, iron limitation enhanced the decrease of PSII photochemical efficiency in temperature stressed zooxanthellae *in hospite*. The negative effect of iron limitation on zooxanthellae F_v/F_m may occur due to the iron rich nature of the photosynthetic apparatus. In cyanobacteria and other algae, iron limitation induces changes in the structure and function of the photosynthetic unit including decreases in chlorophyll content and photosynthetic efficiency. Furthermore, decreases in protein content may occur, resulting from reduced synthesis of the electron transport proteins of PSI, PSII, and the cytochrome b_6f complex (Varsano *et al.* 2003), which all include iron in their structure (*see* Chapter 1). The results of this study are consistent with findings in other algae, where iron limitation decreases photochemical efficiency under stressful environmental conditions, such as elevated temperatures.

The decline in detected intracellular ROS and RNS under iron limitation and elevated temperature in freshly isolated zooxanthellae of this study may represent a physiological stress response to adverse environmental conditions, manifested by increased xanthophyll pigment cycling. The zooxanthellae in this experiment may have quenched excess excitation energy and prevented the generation of dangerous reactive oxygen species by increasing diadinoxanthin to diatoxanthin cycling. This xanthophyll cycling prevents ETC quinone acceptors from becoming over reduced, releasing energy as heat rather than delivering it to the PSII reaction center (Smith *et al.* 2005), which would result in elevated ROS generation. If diadinoxanthin and diatoxanthin cycling were increased

under iron limitation as a stress response to declines in antioxidant enzyme activity and photochemistry, decreases in ROS would be detected because excess energy would not be available to reduce molecular oxygen. Research has shown that iron starved algae increase their ratios of photoprotective xanthophyll cycle pigments relative to chlorophyll *a* (Geider and La Roche 1994). Furthermore, increases in the ratio of diatoxanthin to total diatoxanthin and diadinoxanthin were detected in the freshly isolated zooxanthellae of this study under conditions of temperature stress and iron limitation (*see* Chapter 2). In *S. pistillata* zooxanthellae, iron limitation and high temperature (+DFB and 31 °C) may stimulate a protective response, manifested by an up-regulation of xanthophyll cycling pigments, which results in a quenching of excess excitation energy and a decrease in the detectable levels of intracellular ROS and RNS.

The reduction in ROS and RNS load in zooxanthellae with iron limitation may result from decreases in the iron containing compounds of the photosynthetic ETC. These compounds include the FeS-X complex centers associated with psaA and psaB core polypeptides of PSI, ferredoxin, the FAD enzyme MDAR of PSI (Badger *et al.* 2000) and the cytochrome b_6f complex (Blakenship 2002). If iron is limited to zooxanthellae *in hospite* then the synthesis of these critical ETC components may also decline. Previous research on algae has shown that iron limitation has been associated with decreases in cytochrome quantity and cytochrome *f:*chlorophyll *a* ratios, and an overall decrease in all photosynthetic electron transport chain components (Geider and La Roche, 1994). The decline in iron rich ETC compounds in zooxanthellae would prevent the ability of these compounds to participate in Fenton chemistry and generate detrimental ROS (Murrant and Reid 2001). This decrease in iron rich ETC compounds may account for the decrease in zooxanthellae intracellular ROS under the conditions of iron limitation shown in this study but further research on the expression and function of these ETC components is required to confirm this.

Under the assumptions of the oxidative theory of coral bleaching, zooxanthellae with unnecessary compromised cellular membranes may promote bleaching through increased transfer of ROS to the host. *S. pistillata* zooxanthellae did not show significant

differences in their membrane permeability under iron limitation or temperature stress within this study.

The experimental design within this chapter follows that of Shick *et al.* (2011, Chapter 2), where in which multiple replicate nubbins from a single coral colony were subjected to each experimental treatment. Although this does not permit the extrapolation of the results to the entire coral population, it does provide a representation of the physiological responses of a single *S. pisillata* colony.

The combined effect of temperature stress and iron limitation on *S. pistillata* zooxanthellae is multifaceted. Temperature stress alone caused a decrease in freshly isolated zooxanthellae PSII photochemical efficiency and intracellular ROS. The enhanced negative effect of iron limitation on decreases in F_v/F_m at high temperature may be attributable to decreases in iron-rich photosynthetic electron transport chain components or increased xanthophyll cycling; both of which are supported by the decrease in intracellular ROS and RNS measurements in freshly isolated zooxanthellae exposed to the iron-limiting and high temperature experimental conditions within this study. This study suggests that iron limitation and temperature stress generate protective responses in *S. pistillata* zooxanthellae, manifested by decreases in ROS and RNS and increases in xanthophyll pigment cycling.

3.5 References

Badger, M.R., S.V. Caemmerer, S. Ruuska and H. Nakano. 2000. Electron flow to oxygen in higher plants and algae: rates and control of direct photoreduction (Mehler reaction) and rubisco oxygenase. *Phil. Trans. R. Soc. Land B* 355:1433-1446.

Berkelmans, R. and M.J.H. van Oppen. 2006. The role of zooxanthellae in the thermal tolerance of corals: a 'nugget of hope' for coral reefs in an era of climate change. *Proc. R. Soc. B*. 273: 2305-2312.

Blakenship, R.E. 2002. Molecular mechanisms of photosynthesis. Blackwell Science Ltd. Oxford, UK.

Douglas, A. E. 2003. Coral bleaching- how and why? *Mar. Pollut. Bull*. 46:385-392.

Geider, R.J. and J. La Roche. 1994. The role of iron in phytoplankton photosynthesis, and the potential for iron-limitation of primary productivity in the sea. *Photosyn. Res.* 39: 275-301.

Glynn, P.W. 1993. Coral reef bleaching: ecological perspectives. *Coral Reefs* 12: 1-17.

Jones, R. J., O. Hoegh-Guldberg, A. W. D. Larkum, and U. Schreiber. 1998. Temperature-induced bleaching of corals begins with impairment of the CO_2 fixation mechanism in zooxanthellae. *Plant Cell Envir*. 21: 1219–1230.

Kolber, Z.S., R.T. Barber, K.H. Coale, S.E. Fitzwater, R.M. Greene, K.S. Johnson, S. Lindley and P.G. Falkowski. 1994. Iron limitation of phytoplankton photosynthesis in the equatorial Pacific Ocean. *Nature* 371:145-149.

Lesser, M.P. 1996. Elevated temperatures and ultraviolet radiation cause oxidative stress and inhibit photosynthesis in symbiotic dinoflagellates. *Limnol. Oceanogr*. 41: 271-283.

Lesser, M.P. 1997. Oxidative stress causes coral bleaching during exposure to elevated temperatures. *Coral Reefs* 16: 187-192.

Lesser, M.P. 2006. Oxidative stress in marine environments: biochemistry and physiological ecology. *Annu. Rev. Physiol*. 68:253-78.

Lesser M.P., W.R. Stochaj, D.W Tapley, and J.M. Shick. 1990. Bleaching in coral reef anthozoans: effects of irradiance, ultraviolet radiation and temperature on the activities of protective enzymes against active oxygen. *Coral Reefs* 8:225-232.

Murrant, C.L and M.B. Reid. 2001. Detection of reactive oxygen and reactive nitrogen species in skeletal muscle. *Microsc. Res. Tech*. 55:236-248.

Obata, H., K. Shitashima, K. Issiki, and E. Nakayama. 2008. Iron, manganese and aluminum in upper waters of the western South Pacific Ocean and its adjacent seas. *J. Oceanog.* 64:233-245.

Smith, D.J., D.J. Suggett. and N.R. Baker. 2005. Is photoinhibition of zooxanthellae photosynthesis the primary cause of thermal bleaching in corals? *Global Change Biol.* 11:1-11.

Vardi,A., F. Fomiggini, R. Casottis, A. De Martino, F. Ribalet, A. Miralto and C. Bowler. 2006. A stress surveillance system based on calcium and nitric acid in marine diatoms. *PlosBio*. 4:0411-0419

Varsano, T., D. Kaftan and U. Pick. 2003. Effects of iron deficiency on thylakoid membrane structure and composition in the alga, *Dunaliella salina. J. Plant nutrit*. 26: 2197-2210.

Warner, M.E., K.F.William, and G.W. Schmidt. 1999. Damage to photosystem II in symbiotic dinoflagellates: A determinant of coral bleaching. *Proc. Natl. Acad. Sci.* 96: 8007-8012.

Warner, M.E., G.C. Chilcoat, F.K. McFarland and W.K Fitt. 2002. Seasonal fluctuations in the photosynthetic capacity of photosystem II in symbiotic dinoflagellates in the Caribbean reef-building coral *Montastraea*. *Mar. Biol*. 141:31-38.

Wells M.L. and C.G Trick. 2004. Controlling iron availability to phytoplankton in iron-replete coastal waters. *Mar. Chem*. 86:1-13.

Weis, V.M. 2008. Cellular mechanisms of Cnidarian bleaching: stress causes the collapse of symbiosis J. *Experiment. Boil.* 211: 3059-3066.

Chapter 4

Photochemical and oxidative responses of the symbiotic dinoflagellates of *Stylophora pistillata* colonies isolated from Pith Reef and a Whitsundays Island, Long Island, of the Great Barrier Reef when limited to trace metals and subjected to temperature and irradiance stress.

4.1 Introduction

Coral bleaching, which entails the loss of colouration from coral colonies due to the expulsion of their photosynthetic algal symbionts or the break down of their symbionts photosynthetic pigments (Glynn 1993, Lesser 1997, Douglas 2003) is threatening global reef environments. Coral mortality can result from bleaching events if the algal symbionts are not reestablished within the host (Douglas 2003), making reef flat bleaching events a threat to the persistence of these biodiverse ecosystems.

Increased sea surface temperature, in combination with the high solar radiation present in tropical environments, have been established as the main drivers of coral bleaching because of their effects on photosynthesis and oxidative stress (Lesser *et al.* 1990, Lesser and Farrell 2004, Lesser 2006). Thermal damage in conjunction with the exposure of algal symbionts residing within corals, dinoflagellates of the genus *Symbiodinium*, to elevated temperature results in photoinhibition of photosynthesis (Csaszar *et al.* 2010). In coral algal symbionts of reef building corals subjected to temperature and irradiance stress, photoinhibition has been attributed to damage of the carboxylation processes involved in the Calvin Cycle (sink limitation, Jones *et al.* 1998) and damage of the D1 protective protein of photosystem II due to increased excitation pressure (Warner *et al.* 1999), which represents the proportion of reduced Q_A (an electron acceptor in PSII) (Maxwell *et al.* 1995). Although differing in mechanism, both cause damage to either photosystem II (PSII) or the carbon assimilation processes of photosynthesis, resulting in photoinhibition of photosynthesis, which can increase the reactive oxygen species

generation within the symbiont (Csaszar *et al.* 2010). Excess incoming energy to the photosystem can be quenched through photosynthetic or non-photosynthetic processes. Non-photochemical quenching in *Symbiodinium* involves the cycling of the xanthophyll pigments diadinoxanthin (DD) and diatoxanthin (DT), which release heat and energy from PSII and prevent photosynthetic electron transport chain over-reduction (Jones *et al.* 1998), protecting photosystems from oxidative damage (Csaszar *et al.* 2010). If incoming photon energy is not dissipated or utilized within the photosystem, the excess excitation pressure to PSII can generate increases in various reactive oxygen species (ROS) including superoxide ($O_2^{\bullet-}$), hydrogen peroxide (H_2O_2) and singlet oxygen ($^1O_2$) (Suggett *et al.* 2008). Although energy quenching mechanisms in the algal symbiont are robust in capacity, if they are overwhelmed, ROS may leak from the symbiont to the host and cause bleaching (Csaszar *et al.* 2010). Therefore, understanding oxidative stress within the algal symbionts of reef building corals is essential to understanding the physiology behind bleaching events.

The various intracellular antioxidant enzymes serve as a mechanism to control the generation of detrimental ROS. Imbalances between ROS generation and antioxidant quenching may occur under stress conditions and can result in oxidative stress, which causes damage to lipids, proteins and DNA (Halliwell 2006), and has been implied as a driver of coral bleaching (Lesser *et al.* 1990, Lesser and Farrell 2004, Lesser 2006). Within *Symbiodinium*, various antioxidant enzymes mitigate intracellular ROS generation including: various isoforms of superoxide dismutases (MnSOD, FeSOD, Furla *et al.* 2005), catalase and ascorbate peroxidase (Lesser *et al.* 1990). Each antioxidant converts detrimental ROS into a less noxious form, helping alleviate oxidative load and mitigate bleaching events. Interestingly, the structure and function of antioxidant enzymes involve trace metals, from the iron and manganese present within the superoxide dismutases (Furla *et al.* 2005), to the heme groups present in ascorbate peroxidase and catalase (Lesser 2006). The integral role of trace metals in the structure and function of antioxidant enzymes suggests that any decrease in the availability of these required trace metals to the algal symbiont may result in decreases in antioxidant enzyme quantity and activity, resulting in increased ROS load under stressful environmental conditions.

The oligotrophic nature of coral reef environments may limit Cnidarian-symbiotic algae of the trace metals necessary for proper antioxidant enzyme (Lesser 2006) and photosynthetic electron transport chain function (Shcolnick and Keren 2006), elevating the potential for oxidative stress in the symbiosis. Low total concentrations of the trace metal iron, 0.2-0.3 nM, have been detected in the Coral Sea (Obata *et al.* 2008), adjacent to Australia's Great Barrier Reef (GBR). Low concentrations of available iron have also been detected within the GBR. At the mid-shelf reef, Davies reef, concentrations of Fe ranged from 2 x 10^{-8} M Fe in the surface waters, 66 $\pm$ 26 (1SD) ppm total Fe in the surface sediments and 5 x 10^{-7} M Fe within the interstitial waters near the reef surface (Entsch *et al*.1983). The apparent low concentration of total iron within reef environments indicates that it and other trace metals could be limited to resident corals and their algal symbionts, generating changes in physiology that may affect their temperature and irradiance tolerance.

The goal of this study was to assess the effects of trace metal limitation on two geographically separated reef-building corals of the same species, *Stylophora pistillata,* Esper 1797, and their algal symbionts under elevated temperature and irradiance stress. The hypothesis tested within this study was that reductions in the ambient concentrations of the trace metals iron, manganese, and copper would affect the photochemistry and oxidative load of *S. pistillata* algal symbionts when exposed to elevated temperature and irradiance. The main predictions at the onset of experimentation were that when the symbiotic dinoflagellates were limited to trace metals, their photosynthetic capacity would be compromised and their oxidative load increased due to a limited capacity to quench excess energy and ROS under conditions of high temperature and irradiance.

4.2 Methods

4.2.1 Pith reef colonies-Six large colonies of *S. pistillata* were collected in early January 2010 from Pith reef (Figure 1), an outer reef on Australia's Great Barrier Reef (GBR). Colonies were maintained in an aerated outdoor aquarium circulating 5 μm filtered and chilled seawater (26 °C) at 150-200 μmol photon·m^2·s^{-1} (measured using a PAM PAR sensor, Diving-PAM, S/N: UWFA0257A, Walz Mess-und Regeltechnik, Germany) until

experimentation. Prior to experimentation, nubbins approximately 4-5 cm in length were cut from the upright-growing coral branches and suspended vertically using 0.22 mm monofilament line. To prevent the proliferation of endolithic algae (algae that inhabit the calcium carbonate skeleton of living corals, (Shashar *et al.* 1997)) and bacteria within the coral skeleton, the cut surfaces of the nubbins were sealed with waterproof epoxy (Mr. Sticky's 001327 Underwater Glue, AAI, Fair Oaks, California, USA). Nubbins were allowed to recover indoors for three days in 1 μm-filtered seawater at an irradiance of 200 μmol photons·m^{-2}·s^{-1} and a seawater temperature of 28 °C.

4.2.2 Whitsunday colonies- Fragments of separate *S. pistillata* colonies were collected in mid January 2010 from Long Island in the islands of the Whitsunday (Figure 1) Islands, off Australia's GBR, from a depth of 5-6 meters and an irradiance of 200 μmol photon·m^{2}·s^{-1}. In transit, the fragments were disrupted and broken, so 10 independent bases were selected and marked as separate colonies and nubbins were cut from each to be included within the experiment. The colonies were maintained and the cut surfaces sealed in the same fashion as the Pith reef colonies (*see above*).

4.2.3 Experimental apparatus-S. pistillata nubbins were explanted to trace metal-clean, translucent, 3000 mL plastic KlipIt™ chambers (Sistema Plastics, New Zealand) containing 2 L of medium (Figure 2). Seawater inside each chamber was stirred by a stream of 0.1 μm-filtered air that exited the sealed chamber via a port fitted with another 0.45 μm membrane filter, to avoid contamination by particulate trace metals. Two experimental chambers were placed into four tanks of seawater used as water baths in a flow-through arrangement where temperature was controlled by computer. Chambers were rotated daily between the water baths to compensate for minimal irregularities in temperature (0.1-0.3 °C).

Illumination was provided by a 400 W metal halide lamp (BLV, Germany) above each tank. Each lamp was fitted with a 0.5 cm Schott Robax glass ceramic filter to remove ultraviolet (UV) wavelengths. All nubbins were exposed to an irradiance (PAR) of 200 μmol photons·m^{-2}·s^{-1} for 6 days, which then increased to 400 μmol photons·m^{-2}·s^{-1} for the remainder of the experiment inside the chambers. There was no detectable UVB, and the

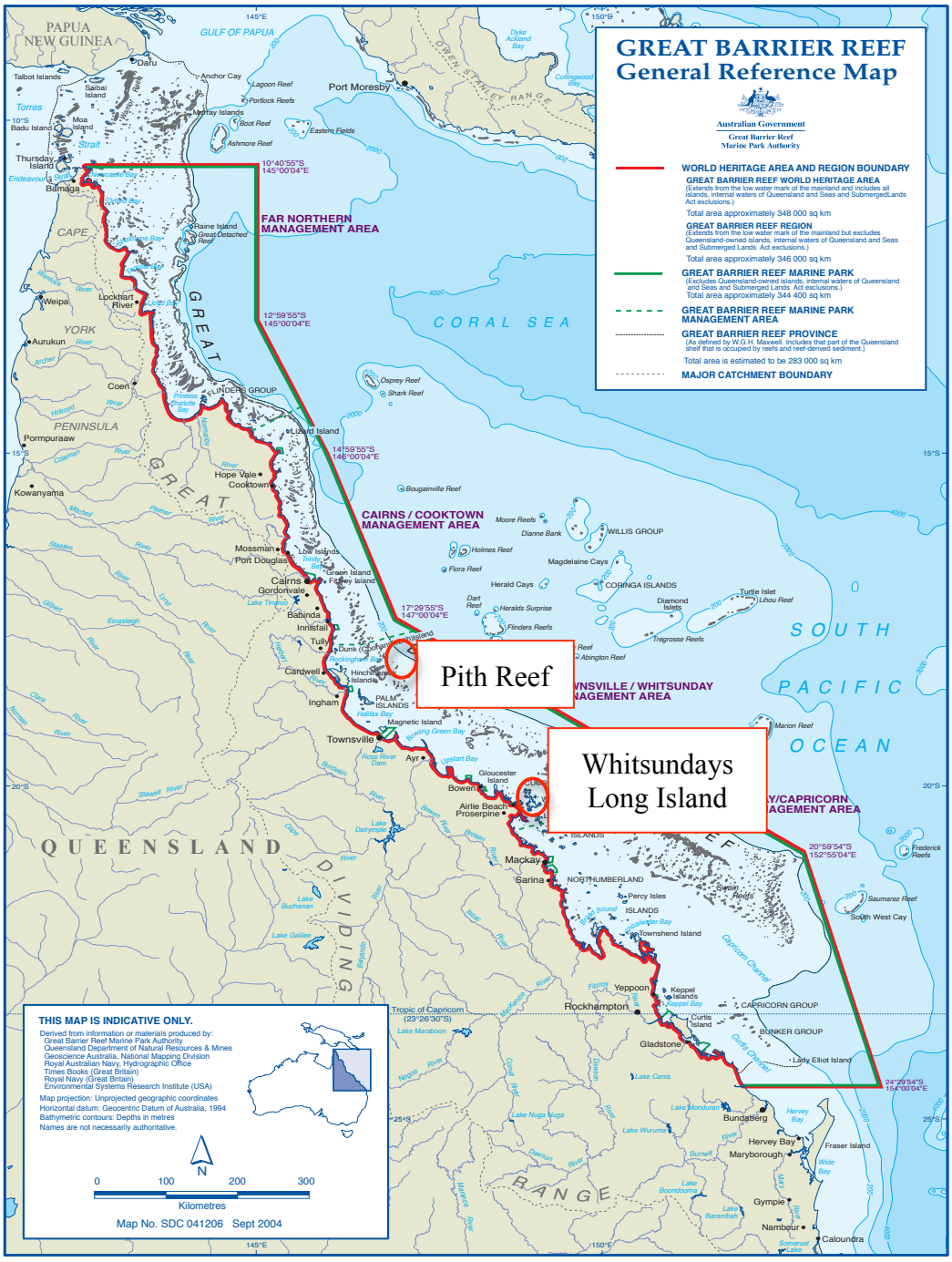
GREAT BARRIER REEF
General Reference Map
Australian Government
Great Barrier Reef Marine Park Authority
WORLD HERITAGE AREA AND REGION BOUNDARY
GREAT BARRIER REEF WORLD HERITAGE AREA
(Extends from the low water mark of the mainland and includes all islands, internal waters of Queensland and Seas and SubmergedLands Act exclusions.)
Total area approximately 348 000 sq km
GREAT BARRIER REEF REGION
(Extends from the low water mark of the mainland but excludes Queensland-owned islands, internal waters of Queensland and Seas and Submerged Lands Act exclusions.)
Total area approximately 346 000 sq km
GREAT BARRIER REEF MARINE PARK
(Excludes Queensland-owned islands, internal waters of Queensland and Seas and Submerged Lands Act exclusions.)
Total area approximately 344 400 sq km
GREAT BARRIER REEF MARINE PARK MANAGEMENT AREA
GREAT BARRIER REEF PROVINCE
(As defined by W.G.H. Maxwell. Includes that part of the Queensland shelf that is occupied by reefs and reef-derived sediment.)
Total area is estimated to be 283 000 sq km
MAJOR CATCHMENT BOUNDARY
FAR NORTHERN MANAGEMENT AREA
CAIRNS / COOKTOWN MANAGEMENT AREA
WNSVILLE / WHITSUNDAY NAGEMENT AREA
Y/CAPRICORN AGEMENT AREA
Pith Reef
Whitsundays
Long Island
PAPUA NEW GUINEA
GULF OF PAPUA
CORAL SEA
SOUTH PACIFIC OCEAN
QUEENSLAND
GREAT DIVIDING RANGE
CAPE YORK PENINSULA
THIS MAP IS INDICATIVE ONLY.
Derived from information or materials produced by:
Great Barrier Reef Marine Park Authority
Queensland Department of Natural Resources & Mines
Geoscience Australia, National Mapping Division
Royal Australian Navy, Hydrographic Office
Times Books (Great Britain)
Royal Navy (Great Britain)
Environmental Systems Research Institute (USA)
Map projection: Unprojected geographic coordinates
Horizontal datum: Geocentric Datum of Australia, 1994
Bathymetric contours: Depths in metres
Names are not necessarily authoritative.
N
0 100 200 300
Kilometres
Map No. SDC 041206 Sept 2004

Figure 4.1 Geographic location of Pith Reef and Long Island (Whitsundays) within the Great Barrier Reef along Australia's coast. Map acquired and modified from the Great Barrier Reef Marine Park Authority, Australian Government.

UVA detected inside of the chambers was <25 μW cm^{-2}, as measured with an IL1400A radiometer and UVA and UVB sensors (Shick *et al.* 1999). The position of each chamber inside its tank of seawater was alternated every four hours to compensate for small irregularities in the light field.

Trace metal-free seawater was prepared by UV treating 0.5 μm filtered seawater at a flow rate of 160 mL•$minute^{-1}$. UV treated seawater was then passed along an ion exchange chelex resin (CHELEX 100) at a flow rate of 8 mL•$minute^{-1}$. Trace metals and vitamins were added back to the trace metal-clean seawater at concentrations based on the Aquil medium recipe (Price *et al.* 1988/99, Table 1). Trace metal and vitamin amendments were added to 45 mL of 0.5 μm filtered, UV treated and chelexed seawater prior to daily PSII photochemical stress measurements. Amendments sat for a maximum of three hours prior to addition to experimental chambers, where they were brought up to 2 L with 0.5 μm filtered, UV treated and chelexed seawater. All measurements and experimental set up was conducted under trace metal-clean conditions (*see* Chapter 2).

4.2.4 Experimental regime: Pith reef colonies- Pith reef colonies were exposed to four trace metal regimes including: trace metal-clean seawater plus (i) full metal treatment (Table 1) (ii) minus Fe treatment (Table 1 modified by adding 0 M Fe) (iii) minus Cu treatment (Table 1 modified by adding 0 M Cu) and (IV) minus Mn treatment (Table 1 modified by adding 0 M Mn). All nubbins were maintained at 28 $\pm$ 1 °C and an irradiance of 200 μmol photons·m^{-2}·s^{-1} for 6 days in their appropriate medium treatments. On day 6, the irradiance was increased to 400 μmol photons·m^{-2}·s^{-1} and the temperature maintained at 28 $\pm$ 1 °C. On day 10, the temperature was ramped up to 31 $\pm$ 1 °C at a rate of 0.07 °C•$hour^{-1}$ for one half of the duplicated metal regimes. The eight final treatments were (i) low temperature (28 °C) +full trace metals (ii) low temperature -Fe (iii) low temperature -Cu (iv) low temperature -Mn (v) high temperature (31 °C) +full trace metals (vi) high temperature-Fe (vii) high temperature-Cu and (viii) high temperature-Mn. Each chamber contained 18 nubbins, isolated from 6 different *S. pistillata* colonies (n=6), and with 8 treatments, there was a total of 144 nubbins in 8 chambers. Seawater in experimental chambers was replaced daily after PAMing to ensure minimal contamination by metals.

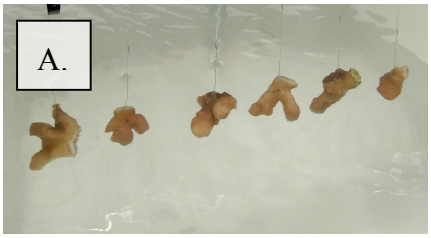
A.


B.


C.

Figure 4.2 Experimental chamber set up. *S. pistillata* nubbins were cut from colony fragments and suspended on monofilament line (A.). Eighteen nubbins were placed into 4L trace metal-clean containers (B.) and placed into a flowing seawater bath (C.).

Table 4.1 Final concentrations [M, gL^{-1}] of the trace metal and vitamin amendments to 0.5 μm filtered, UV treated and chelexed seawater. Values were based on the Aquil recipe of Price *et al.* (1988/89) with modifications made to the Na_2EDTA, $FeCl_3 \cdot 6H_2O$, $MnCl_2 \cdot 4H_2O$, $CuSO_4 \cdot 5H_2O$ components.

Trace metal/Vitamin	**Concentration Used** [M] *unless otherwise specified*
Na_2EDTA	5.0×10^{-6}
$FeCl_3 \cdot 6H_2O$	2.0×10^{-9}
$ZnSO_4 \cdot 7H_2O$	4.0×10^{-9}
$MnCl_2 \cdot 4H_2O$	10.0×10^{-9}
$CoCl_2 \cdot 6H_2O$	2.5×10^{-9}
$CuSO_4 \cdot 5H_2O$	5.0×10^{-9}
$NaMoO_4 \cdot 2H_2O$	0.1×10^{-6}
Na_2SeO_3	10.0×10^{-9}
Vitamin B_{12}	5.5×10^{-7} gL^{-1}
Biotin	0.5×10^{-7} gL^{-1}
Thiamin	1.0×10^{-4} gL^{-1}

4.2.5 Experimental regime: Long Island of the Whitsunday Islands colonies- Each chamber contained a total of 18 nubbins, isolated from 10 different *S. pistillata* fragment bases (n=10), and with 8 treatments, there was a total of 144 nubbins in 8 chambers. The trace metal treatments of the Whitsunday corals mimicked those of the Pith Reef corals, but the Cu treatment was not included within the experiment.

4.2.6 Analysis of PSII photochemical efficiency in zooxanthellae- Dark-adapted PSII photochemical efficiency (F_v/F_m) was measured daily using Pulse Amplitude Modulation (PAM) fluorometry (Diving-PAM, S/N: UWFA0257A, Walz Mess-und Regeltechnik, Germany). All measurements were made under trace metal-clean conditions in a metal-free clean room following the same technique of Shick *et al.* (2011, *see* Chapter 2). *S. pistillata* nubbins were removed for PAM measurements prior to the end of the 12-h dark phase, and the measurements of dark-adapted nubbins were taken on the tip, the middle and bottom region of each nubbin. PAM measurements of the tip, middle and bottom of the nubbin were averaged to obtain a final value for each nubbin. The dark-adapted F_v/F_m measurements from nubbins originating from the same colony (Pith Reef) or fragment (Whitsunday) within each treatment were averaged and a colony dark-adapted F_v/F_m value was obtained. Each colony value represented an independent observation in the sample (n=6 for Pith reef corals, n=10 for Whitsunday corals) and subjected to statistical analysis.

4.2.7 Assessment of intracellular ROS, RNS and membrane permeability- Zooxanthellae were collected by agitating the water surrounding the experimental nubbin with positively pressured air (modified from Berkelmans and van Oppen 2006) in filtered seawater (0.2 μm) after the corals had been exposed to 400 μmol photons$\cdot m^{-2} \cdot s^{-1}$ and treatment temperature for 1.5 hours on the day of experimental termination. The resultant slurry was gently homogenized (PRO250 homogenizer, PRO Scientific, USA) for 10 seconds and the homogenate was filtered across a 53 μm Nytex mesh filter. The filtered homogenate was divided into three equal portions for flow cytometric, pigment and cell density analyses. Once the flow cytometric portion of the sample was removed, the filtered homogenate was centrifuged at 750 × *g* for 10 minutes at 4 °C in a Beckman Coulter Allegra X-15R centrifuge. Freshly isolated zooxanthellae were further cleaned by

two washes in 0.2 μm filtered seawater and centrifugation (*as above*). The resultant pellet was resuspended in 2 mL of 0.2 μm filtered seawater and equally divided for cell density and pigment analysis. The pigment samples were centrifuged at 10000 *g* for 10 minutes at 4 °C on a Beckman Coulter Microfuge 22R centrifuge. The supernatant was removed and the pellets stored at -80 °C until analysis. Cell density samples were stored at 4°C in the dark, and analyzed within 4/5 days of experimental termination.

4.2.8 Intracellular oxidative load analysis- The intracellular ROS and reactive nitrogen species (RNS) nitric oxide (NO), OH•, peroxynitrite ($ONOO^-$), and H_2O_2 were detected using 5-(and 6) chloromethyl-2',7'-dichlorodihydrofluorescein diacetate, acetyl ester (CMH_2DCFDA) (Murrant and Reid 2001) at a final concentration of 5 μM in seawater. Superoxide, $ONOO•^-$ and $OH•^-$ were detected using the fluorescent probe dihydroethidium (DHE) (Murrant and Reid 2001), at a final concentration of 23 μM. Nitric oxide was detected using the probe 4-amino-5-methylamino-2',7'-difluorofluorescein diacetate (DAF-FM) at a final concentration of 2 μM. Mitochondrial ROS was detected using the probe dihydrorhodamine 123 (DHR 123) at a final concentration of 4 μM. Each of the probes was exited at a wavelength of 488 nm and their emissions read at wavelengths of 600-630 nm for DHE and of 515-555 nm for CMH_2DCFDA, DHR (Lesser 1997) and DAF-FM.

Freshly isolated zooxanthellae were incubated immediately with each probe for 30 min in the dark before analysis on a FACsCalibur flow cytometer (BD, San Jose, California, U.S.A.). A minimum of 750 freshly isolated zooxanthellae event counts were collected per cytometry run and samples were diluted with 0.5 μm filtered seawater to maintain an events per second rate of less than 1000. Increases in green and orange fluorescence were proportional to probe oxidation and indicative of intracellular ROS and RNS. All probe fluorescence measurements were standardized to a negative control by subtracting the negative control signal of the sample from the respective probed signal of that same sample. The negative control was generated by adding an equivalent concentration of DMSO (without the probe of choice) to the sample, accounting for differences in freshly isolated zooxanthellae ambient fluorescence signals.

Freshly isolated zooxanthellae were probed with the cell death indicator, SYTOX green (Vardi *et al.* 2006), at a final concentration of 1 μM for 15 min in the dark to assess cell membrane damage. Cell membrane damage was gauged by the number of cells taking up the fluorescent SYTOX Green stain relative to the negative control, measured using flow cytometry.

4.2.9 Probe optimization and standard curves- The concentration and sensitivity of both ROS probes DHR 123 and DAF were verified by incubating cultures of *Symbiodinium* with (i) a range of probe concentrations and (ii) a range of H_2O_2 concentrations at a constant and optimized probe concentration (DHR 123 at 4μM and DAF-FM at 2 μM). The concentration and sensitivity of the probes CMH_2DCFDA and DHE was not tested prior to analysis because each probe's optimization was completed in Chapter 3.

Working stock solutions of CMH_2DCFDA, DHE and DAF and DHR123 were prepared in dimethyl-sulphoxide (DMSO), divided into small aliquots and maintained at -20 °C in the dark until use. The SYTOX green working stock was prepared in 0.2 μm filtered seawater, divided into small aliquots and maintained at -20 °C in the dark until use. All flow cytometric fluorescence dyes were purchased from Invitrogen (Carlsbad, California, U.S.A).

4.2.10 Statistical analysis- A repeated measures two-way ANOVA was conducted to determine significant differences between metal regime and dark-adapted PSII photochemical efficiency over the duration of the experiment. Furthermore, a two-way ANOVA was run on the individual sample days to examine temperature and metal regime effects on the PSII photochemical efficiency, independent of sample day. Detected intracellular ROS and RNS were also analyzed using a two-way ANOVA. If an insignificant interaction term between metal regime and temperature was detected, the main effects of each factor were examined. If a significant effect of metal regime was determined, a Student-Newman-Keuls (SNK) post hock test was run to detect where differences lay. Prior to each ANOVA, a Levene's test of equality of error variance (p<0.05) was run and normality was assumed. All statistical analysis was conducted on PASW (Version 18.00) statistical software.

4.3 Results

The concentrations of DHR 123 and DAF-FM, 4 and 2 μM respectively, were appropriate for use within this study because increases in fluorescence were detected within cells probed with concentrations greater than those values (Figures 4.3-I. and 4.4-I.). These results indicated that the concentration of probe utilized was not high enough to induce self-quenching by the probe, and therefore changes in intracellular ROS load would be detectable by the probes utilized at these concentrations.

The sensitivity of the probes DHR 123 and DAF-FM to increases in H_2O_2 concentration (Figures 4.3-II and 4.4-II, respectively) indicate probe appropriateness in the assessment of intracellular ROS load in freshly isolated symbiotic dinoflagellates. Increases in the fluorescence signal emitted by each probe occurred with increases in H_2O_2 concentration. These results indicate that fluorescence probe differences can be used to determine intracellular ROS load in freshly isolated zooxanthellae subjected to variable experimental treatments.

4.3.1 Pith Reef colonies- From the onset of the temperature increase (day 10), a significant decrease in F_v/F_m was detected, using repeated measures, when the symbiotic dinoflagellates of *S. pistillata* were exposed to high temperature *in hospite* (df=1, F=6.420, p=0.015, Figure 4.5). Metal regime did not significantly affect the F_v/F_m when examined over the course of the entire experiment (df=3, F=0.689, p=0.564, Figure 4.5) but when the F_v/F_m datum was analyzed on the final day of experimentation, t14, it was determined that both temperature (df=1 F=41.488, p=0.000) and metal regime (df=3, F=3.702, p=0.019) had significant effects. Corals bathed in medium devoid of iron contained symbionts with a significantly lower F_v/F_m relative to those bathed in Mn and all metals (Figure 4.6, II.) Algal symbionts bathed in medium devoid of Cu showed a slight decrease in dark-adapted F_v/F_m, but it was not significantly different from the corals bathed in medium devoid of Mn and the control. The influence of trace metal regime was not detected on any other experimental day over the course of the experiment.

I.

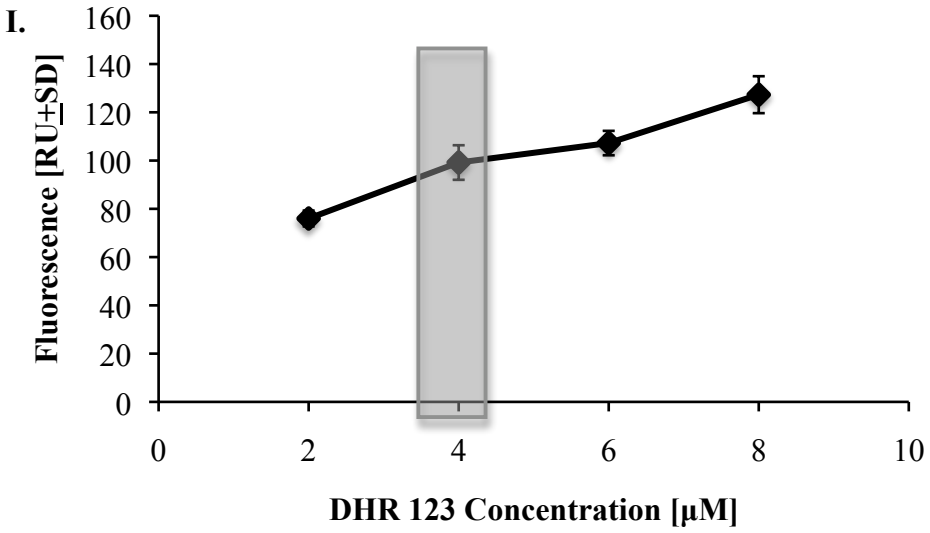
160
140
120
100
80
60
40
20
0
Fluorescence [RU±SD]
0
2
4
6
8
10
DHR 123 Concentration [µM]

II.

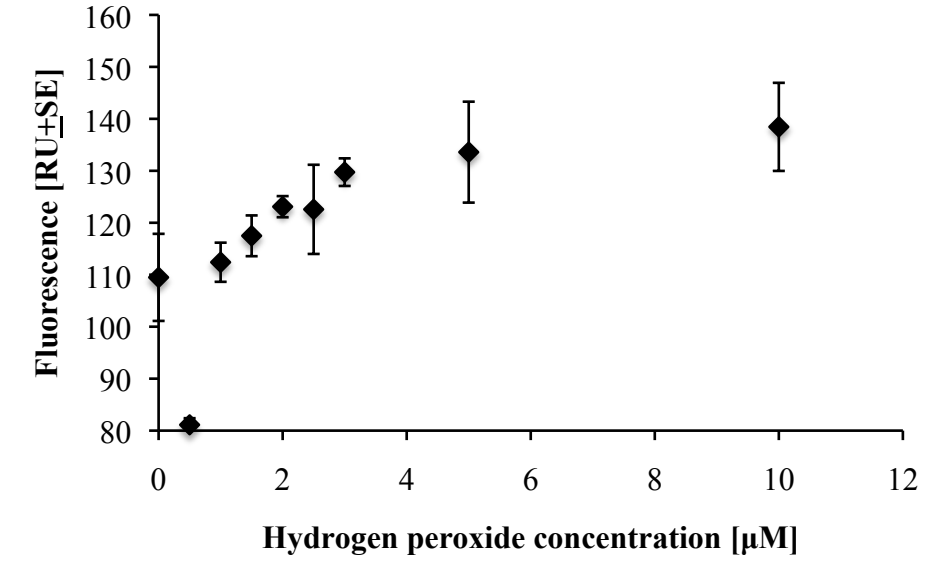
160
150
140
130
120
110
100
90
80
Fluorescence [RU±SE]
0
2
4
6
8
10
12
Hydrogen peroxide concentration [µM]

Figure 4.3 Mean fluorescence of the ROS probe DHR 123 [RU±SD] within cultured *Symbiodinium* sp. when exposed to (I.) a range of DHR 123 concentrations [2-8 μM] and (II.) a DHR 123 concentration of 4 μM and a range of hydrogen peroxide concentrations (0-10 μ M) for an incubation time of 30 minutes in the dark (n=4, n=3 respectively). Indicated by the grey box is the concentration of DHR 123 utilized within this study, a concentration of 4 μM.

I.

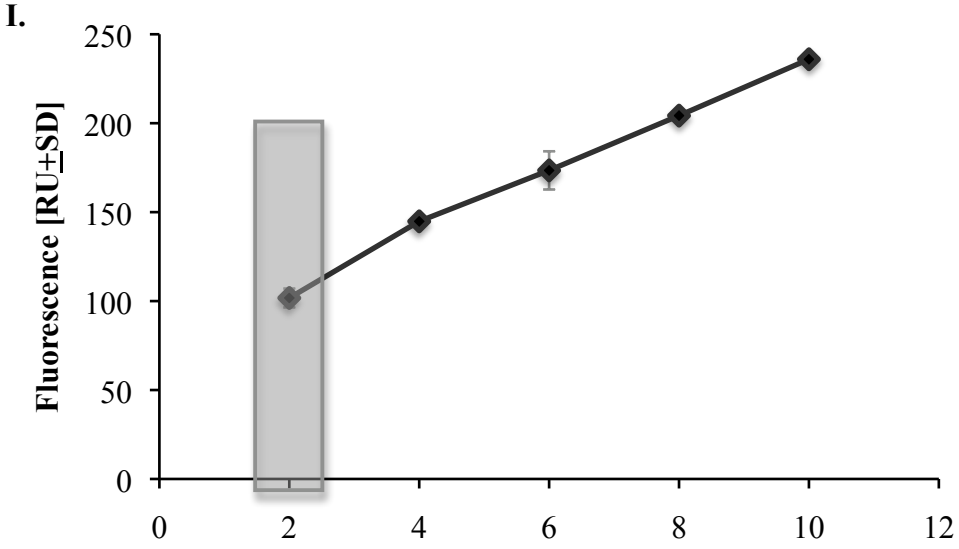
250
200
150
100
50
0
Fluorescence [RU±SD]
0
2
4
6
8
10
12
DAF-FM concentration [uM]

II.

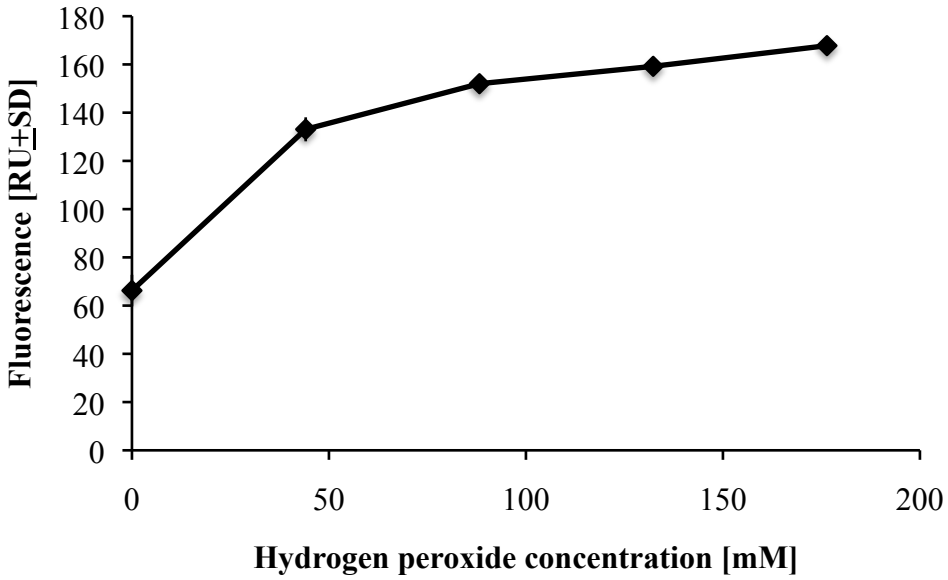
180
160
140
120
100
80
60
40
20
0
Fluorescence [RU±SD]
0
50
100
150
200
Hydrogen peroxide concentration [mM]

Figure 4.4 Mean fluorescence of the ROS probe DAF-FM [RU±SD] within cultured *Symbiodinium* sp. when exposed to (I.) a range of DAF-FM concentrations [2-10 μM] for a 15 minute dark incubation and (II.) a DAF-FM concentration of 2 μM and a range of hydrogen peroxide concentrations for a dark incubation of 60 minutes (0-176 mM) (n=3, n=4 respectively). Indicated by the grey box is the concentration of DAF-FM utilized within this study, a concentration of 2 μM.

Intracellular ROS and RNS were affected by the increase in temperature from 28 to 31±1°C (Figure 4.7, I-IV). Levels of NO and mitochondrial ROS were significantly elevated at the higher temperature treatment with respect to the lower temperature treatment (df=1,F=4.745, p=0.038, and df=1, F=13.397, p=0.001, respectively). An increasing trend in nitric oxide (NO), OH•, peroxynitrite ($ONOO^-$) and H_2O_2, at high temperature was also detected by the intracellular probe CMH_2DCFDA (df=1, F=2.797, p=0.106) while intracellular $O_2^{\bullet -}$, $ONOO^{\bullet -}$ and $OH^{\bullet -}$ detected by DHE was not affected by the temperature change.

Trace metal removal in conjunction with increases in temperature affected cellular membrane permeability, where a significant interaction existed between trace metal treatment and temperature (df=3, F=5.469, p=0.005, Figure 4.9). At elevated temperatures, an increase in cell permeability occurred and it was slightly elevated in the control treatment supplemented with all trace metals.

Trace metal absence did not affect the measured intracellular ROS and RNS detected by the probes CMH_2DCFDA, DHE, and DHR. Trace metal removal did effect intracellular NO, detected by the probe DAF-FM, where reduced levels of NO were detected in the algal symbionts of corals devoid of iron in comparison to those devoid of Mn (df= 3, F=3.482, p=0.029, Figure 4.8).

4.3.2 Whitsunday colonies- Decreases in F_v/F_m were detected in the symbiotic dinoflagellates of *S. pistillata* under the high temperature treatment (df=1, F=4.663, p=0.036, Figure 4.10) relative to the lower temperature treatment when examined under the repeated measures analysis from the onset of temperature increase (day10) until the end of the experiment. Metal addition did not influence the F_v/F_m of Whitsunday corals over the course of the experiment (df=2, F=0.699, p=0.502, Figure 4.10) or when the values were examined on the final day of experimentation (day 14), but, temperature did have a significant negative effect (df=1, F=21.039, p<0.000). A trend was noted on the final day of the experiment where in which corals devoid of iron and fully supplemented with all trace metals (the control) showed a dramatic decrease in F_v/F_m at high temperature relative to those devoid of Mn (Figure 4.10).

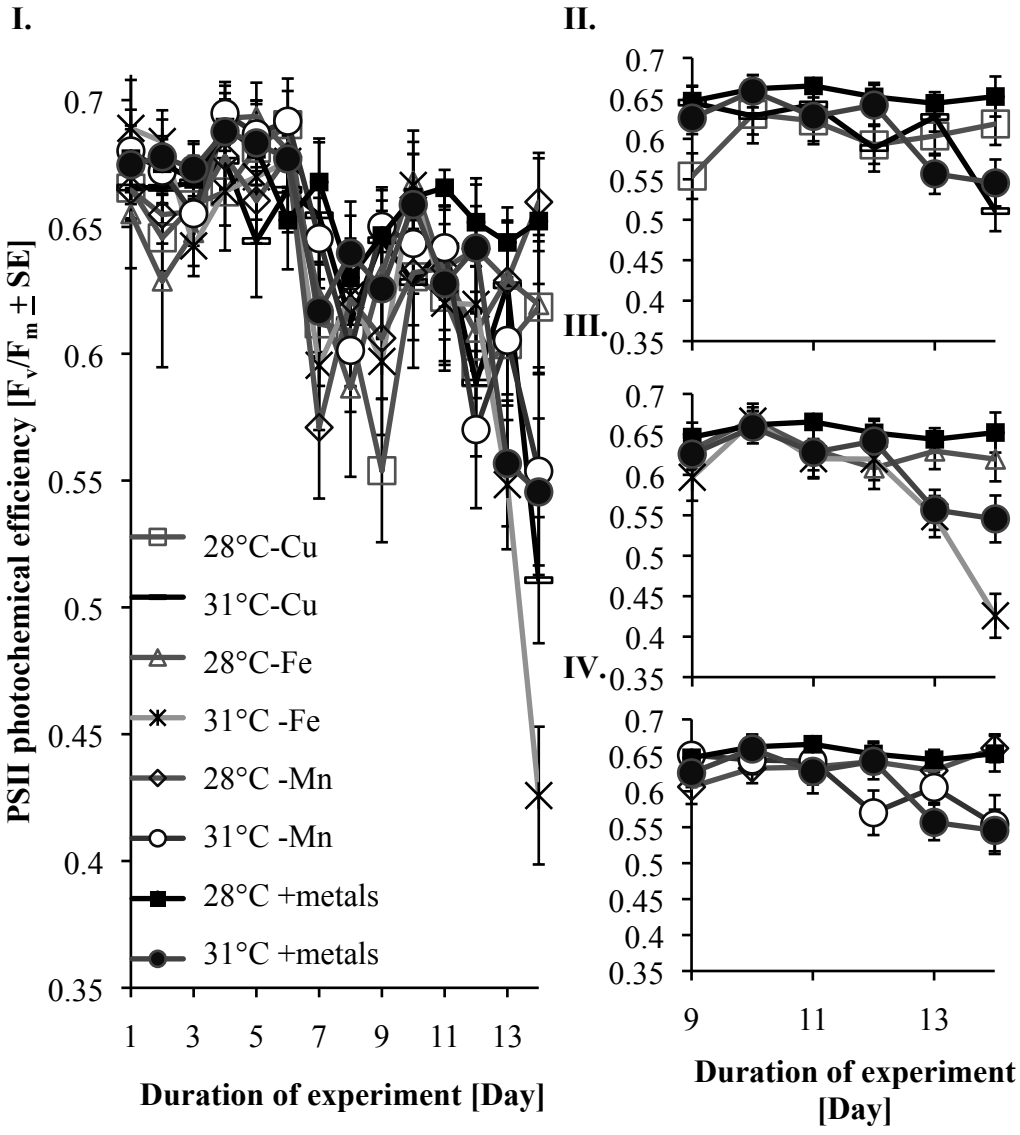
I.
II.
III.
IV.
PSII photochemical efficiency [$F_v/F_m \pm$ SE]
0.7
0.65
0.6
0.55
0.5
0.45
0.4
0.35
28°C-Cu
31°C-Cu
28°C-Fe
31°C -Fe
28°C -Mn
31°C -Mn
28°C +metals
31°C +metals
1
3
5
7
9
11
13
Duration of experiment [Day]
Duration of experiment [Day]

Figure 4.5 Dark adapted PSII photochemical efficiency [mean F_v/F_m] of Pith reef *Stylophora pistillata* symbiotic dinoflagellates exposed to high and low temperatures (31 and 28 °C) and (I) Cu, Fe, and Mn deplete conditions, denoted by: - Cu, Fe or Mn, and a full trace metal treatment, denoted by: + metals. Corals were acclimated to control conditions for six days at low temperature (28 °C) and an irradiance of 200 μmol photons·m^{-2}·s^{-1}. On the sixth day, irradiance was increased to 400 μmol photons·m^{-2}·s^{-1}. Temperature increases occurred on the tenth day of the experiment at a rate of 0.08 °C·$hour^{-1}$ until the high temperature treatment (31°C) was established. PSII photochemical efficiency was measured on the coral nubbin's tip, center and bottom and averaged per nubbin. Panels II-IV highlight the dark adapted PSII photochemical efficiency (mean F_v/F_m) of *S. pistillata* symbiotic dinoflagellates exposed to high and low temperatures (31 and 28 °C) and (II) Cu, (III) Fe, and (IV) Mn-deplete or replete conditions on the days in which temperature stress was established. Error bars reflect the ± Standard Error (n=6). A significant effect of temperature was noted across experimental days 10-14 ($p<0.05$).

I.

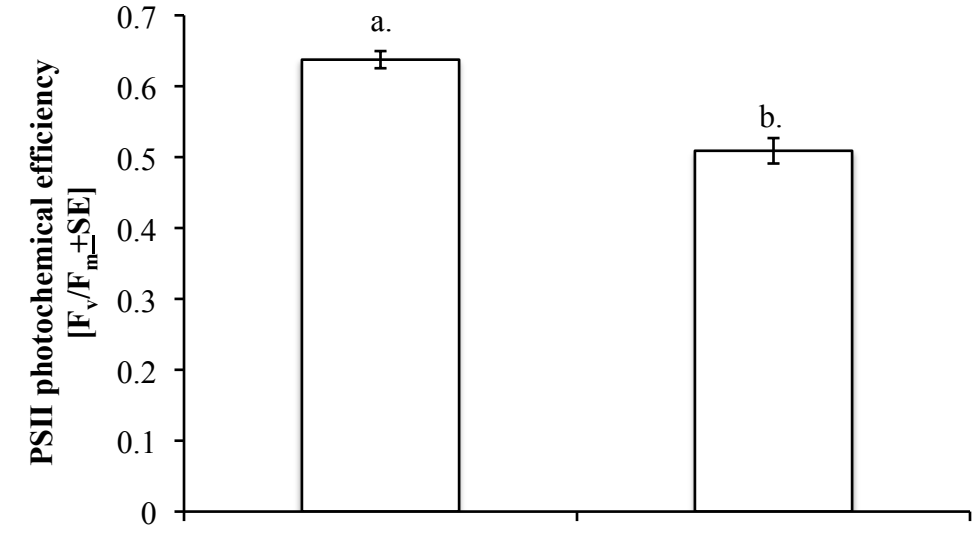
PSII photochemical efficiency
[F_v/F_m ± SE]
0.7
0.6
0.5
0.4
0.3
0.2
0.1
0
a.
b.
27
31
Temperature treatment [°C]

II.

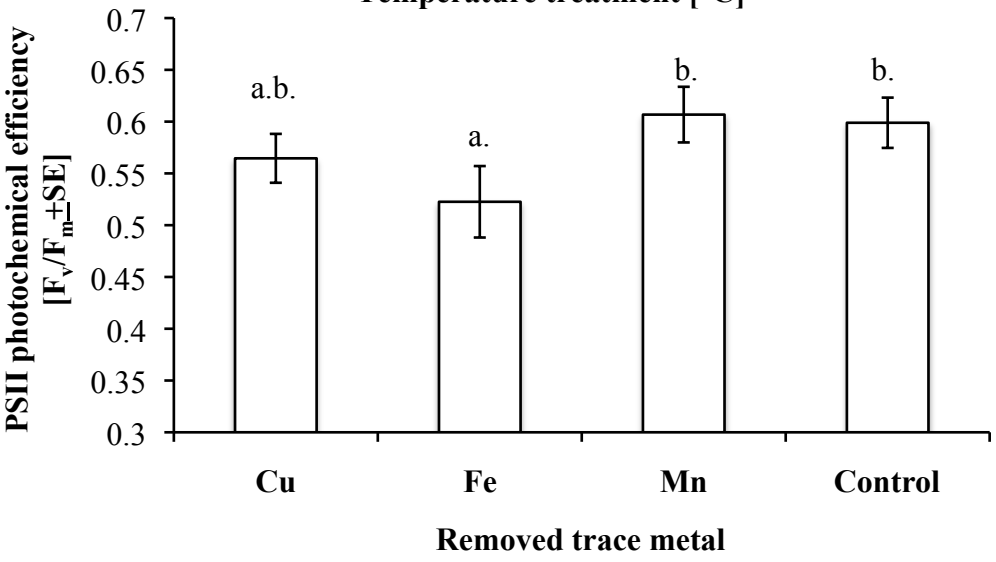
PSII photochemical efficiency
[F_v/F_m ± SE]
0.7
0.65
0.6
0.55
0.5
0.45
0.4
0.35
0.3
a.b.
a.
b.
b.
Cu
Fe
Mn
Control
Removed trace metal

Figure 4.6 Day 14 dark-adapted photochemical efficiency [mean F_v/F_m] of Pith reef *S. pistillata* symbiotic dinoflagellates exposed to high and low temperatures (31 and 28 °C) and Cu, Fe, and Mn-deplete conditions or a full trace metal control (control). The main effects of temperature and metal regime are illustrated (I and II, respectively). Photochemical efficiencies were measured on the coral nubbin's tip, center and bottom and averaged per nubbin. Error bars reflect the $\pm$ Standard Error (n=6). Independent significant effects of temperature and metal regime were detected. Different letters represent significant differences within temperature and trace metal regimes ($p<0.05$).

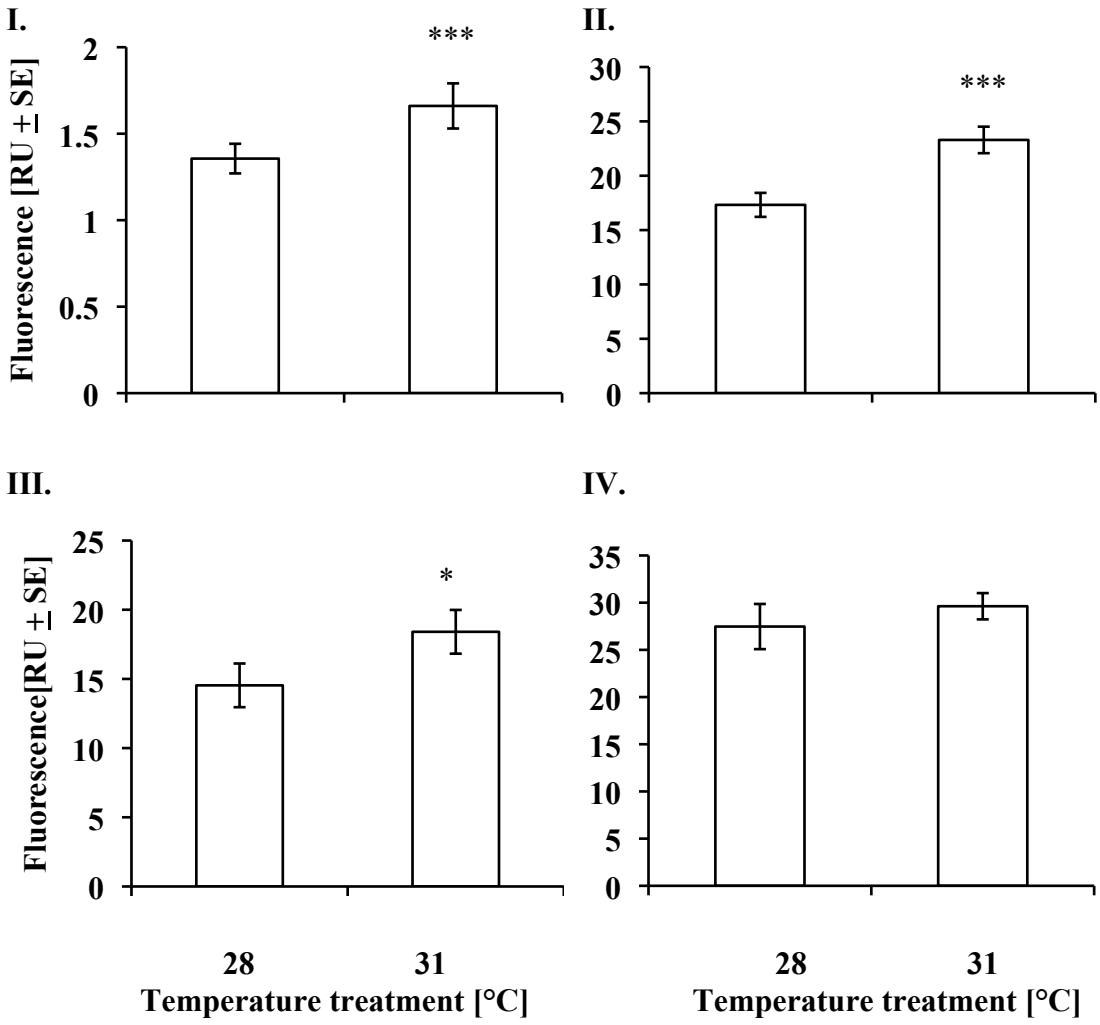
I.
II.
III.
IV.
Fluorescence [RU ± SE]
Fluorescence[RU ± SE]
***
***
*
0
0.5
1
1.5
2
5
10
15
20
25
30
35
28
31
Temperature treatment [°C]
Temperature treatment [°C]

Figure 4.7 Mean fluorescence [RU±SE] of the probes indicative of (I.) nitric oxide, (II.) mitochondrial ROS, (III.) NO, OH•, peroxynitrite ($ONOO^-$) and H_2O_2 and (IV.) superoxide, $ONOO•^-$ and $OH•^-$ (IV.) in symbiotic dinoflagellates of Pith reef *S. pistillata* exposed to high (31 °C) and low (28 °C) temperatures (n=16). Asterisks indicate levels of significance determined in a two-way ANOVA (***$p<0.05$, *$p<0.11$).

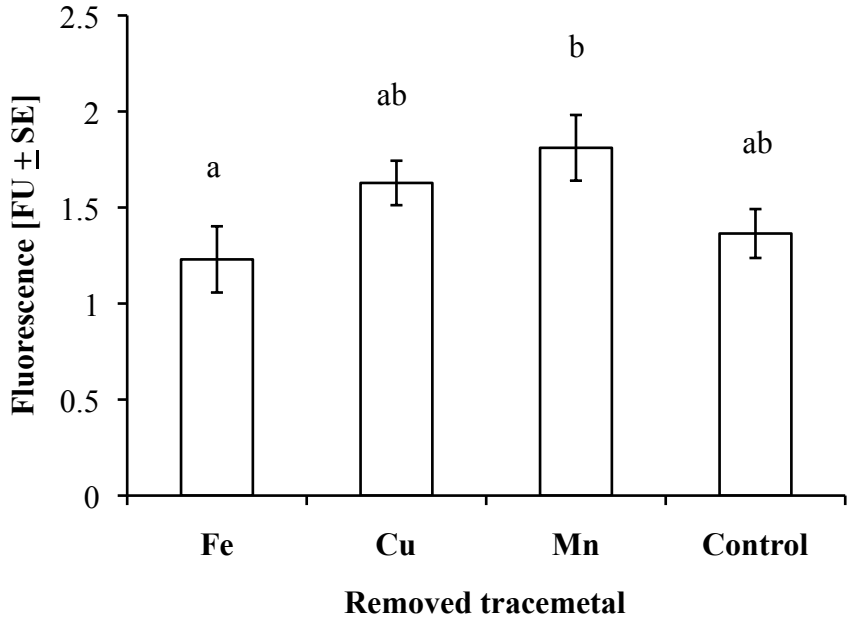
2.5
2
1.5
1
0.5
0
Fluorescence [FU ± SE]
a
ab
b
ab
Fe
Cu
Mn
Control
Removed tracemetal

Figure 4.8 Mean fluorescence of the nitric oxide probe, DAF-FM (RU $\pm$ SE) in symbiotic dinoflagellates of Pith reef *S. pistillata* exposed the variable trace-metal removal (denoted as Fe, Cu and Mn on the x-axis) and a full trace metal treatment (control) (n=8). Shown are the main effects of trace metal regime, and different letters indicate significant differences ($p<0.05$) detected by a two-way ANOVA.

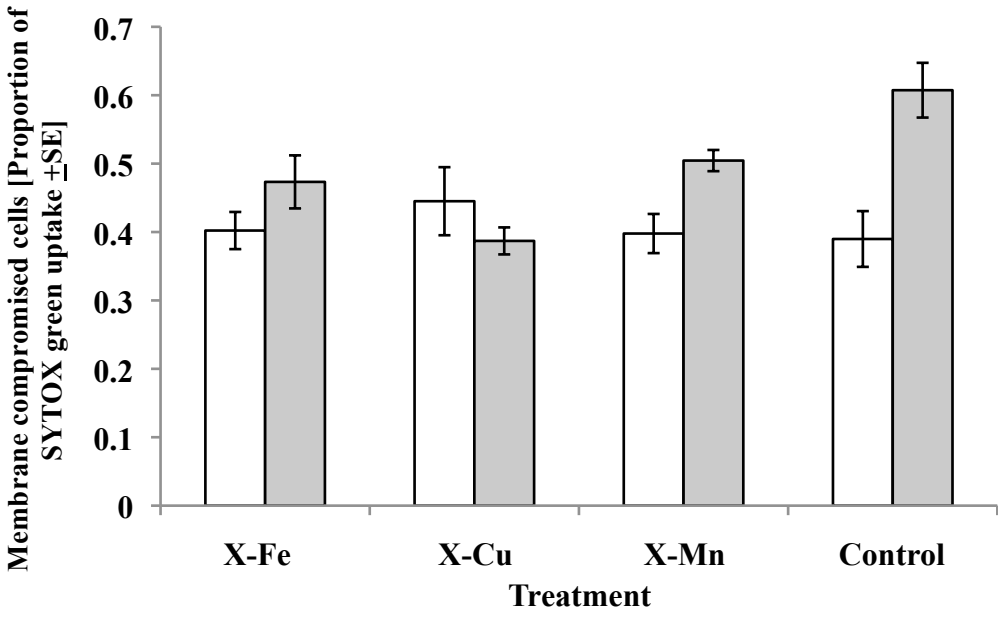
Membrane compromised cells [Proportion of SYTOX green uptake ±SE]
0.7
0.6
0.5
0.4
0.3
0.2
0.1
0
X-Fe
X-Cu
X-Mn
Control
Treatment

Figure 4.9 Cell membrane permeability (proportion of SYTOX stained cells ± SE) of Pith reef *S. pistillata* symbiotic dinoflagellates exposed to low temperature (28°C, white bars) and high temperature (31 °C, grey bars) and variable trace metal removal (X-Fe, X-Cu, X-Mn) or a full trace metal treatment (Control). A two-way ANOVA indicated a significant interaction between temperature and trace metal-limitation ($p<0.05$).

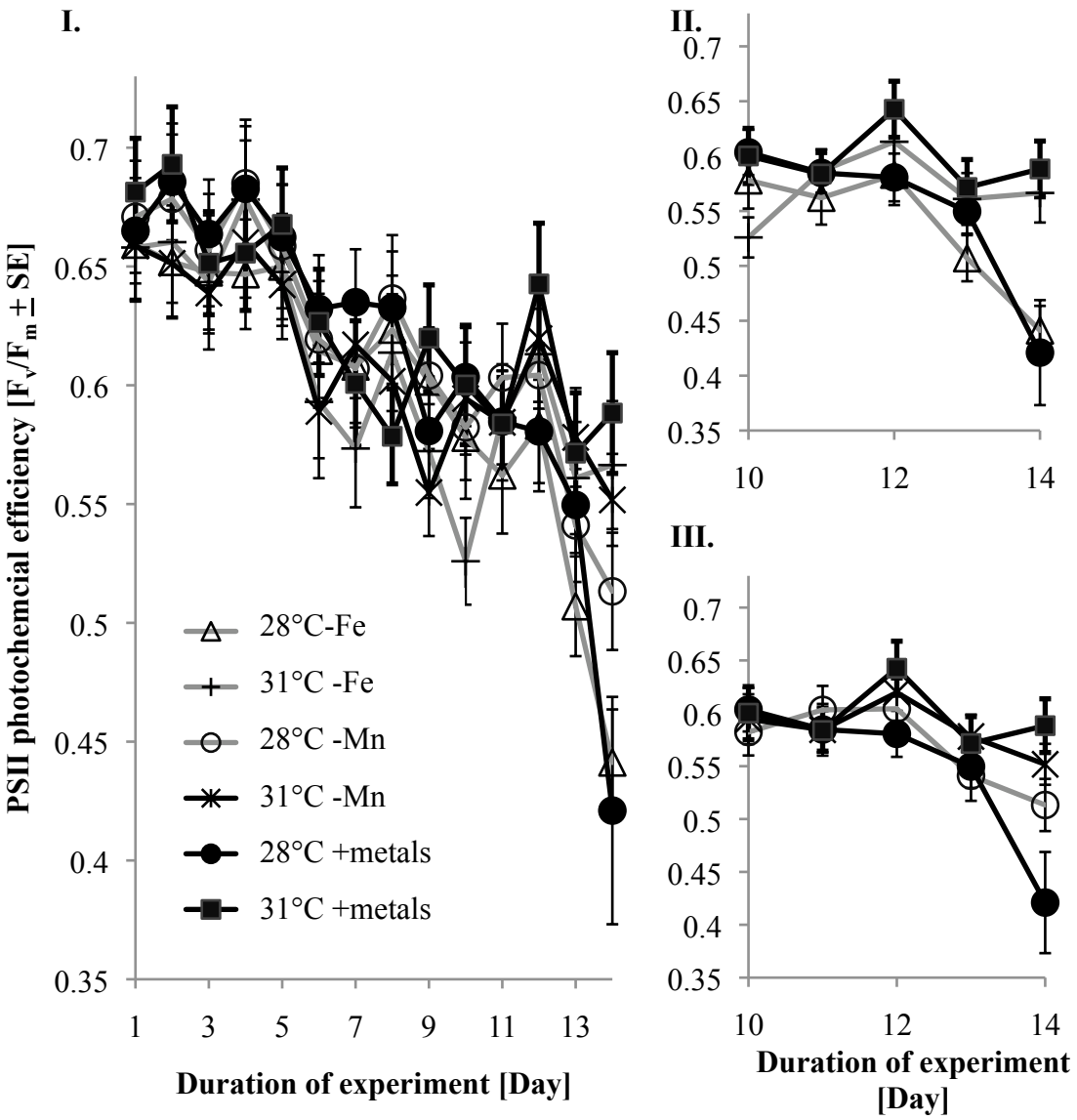
I.
II.
III.
PSII photochemcial efficiency [$F_v/F_m \pm SE$]
0.7
0.65
0.6
0.55
0.5
0.45
0.4
0.35
1
3
5
7
9
11
13
10
12
14
28°C-Fe
31°C -Fe
28°C -Mn
31°C -Mn
28°C +metals
31°C +metals
Duration of experiment [Day]
Duration of experiment [Day]

Figure 4.10 (I) Dark adapted PSII photochemical efficiency [mean F_v/F_m $\pm$SE] of Whitsunday *S. pistillata* symbiotic dinoflagellates exposed to high and low temperatures (31 and 28 °C) and Fe or Mn deplete conditions, denoted by: - Fe or -Mn, and a full trace metal treatment, denoted by: + metals. Corals were acclimated to control conditions for six days at low temperature (28 °C) and an irradiance of 200 μmol photons·m^{-2}·s^{-1}. On the sixth day, irradiance was increased to 400 μmol photons·m^{-2}·s^{-1}. Temperature increases occurred on the tenth day of the experiment at a rate of 0.08 °C·$hour^{-1}$ until the high temperature treatment (31°C) was established. PSII photochemical efficiency was measured on the coral nubbin's tip, center and bottom and averaged per nubbin. Panels II and III highlight the dark-adapted PSII photochemical efficiency [mean F_v/F_m] of *S. pistillata* symbiotic dinoflagellates exposed to high and low temperatures (31 and 28 °C) and (II) Fe and (III) Mn-deplete or replete conditions shown on the days in which temperature stress was established. Error bars reflect the $\pm$ Standard Error (n=10). A significant effect of temperature was noted across experimental days 10-14 ($p<0.05$).

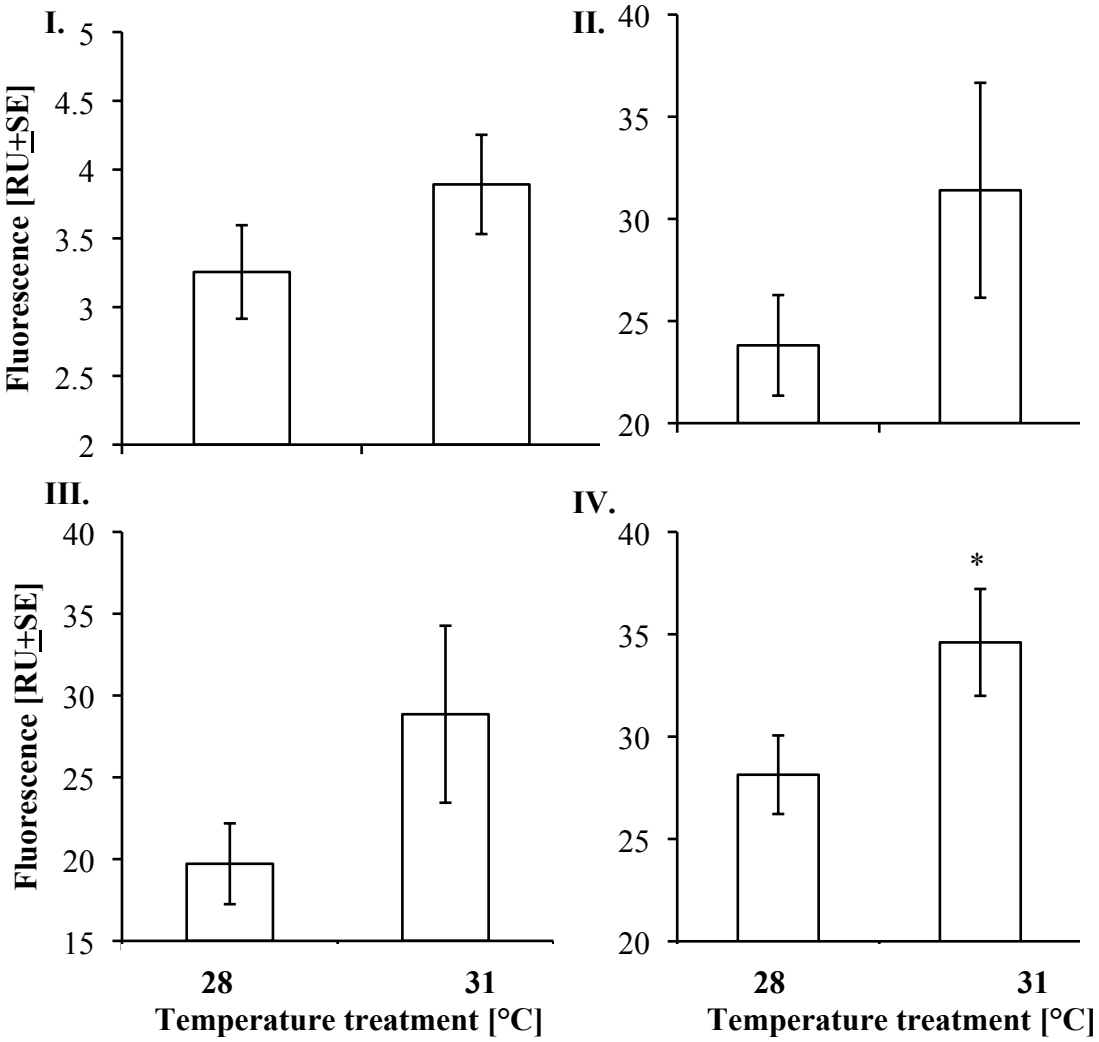
I.
II.
III.
IV.
Fluorescence [RU±SE]
Fluorescence [RU±SE]
5
4.5
4
3.5
3
2.5
2
40
35
30
25
20
15
*
28
31
28
31
Temperature treatment [°C]
Temperature treatment [°C]

Figure 4.11 Mean fluorescence [RU±SE] of the probes indicative of (I) nitric oxide, (II) mitochondrial ROS, (III) NO, OH•, peroxynitrite ($ONOO^-$) and H_2O_2 and (IV) superoxide, $ONOO•^-$ and $OH•^-$ in symbiotic dinoflagellates of Whitsunday *S. pistillata* exposed to high (31 °C) and low (28 °C) temperatures (n=12). Asterisks indicate levels of significance determined in a two-way ANOVA (*$p<0.075$) when analyzing the main effects of temperature.

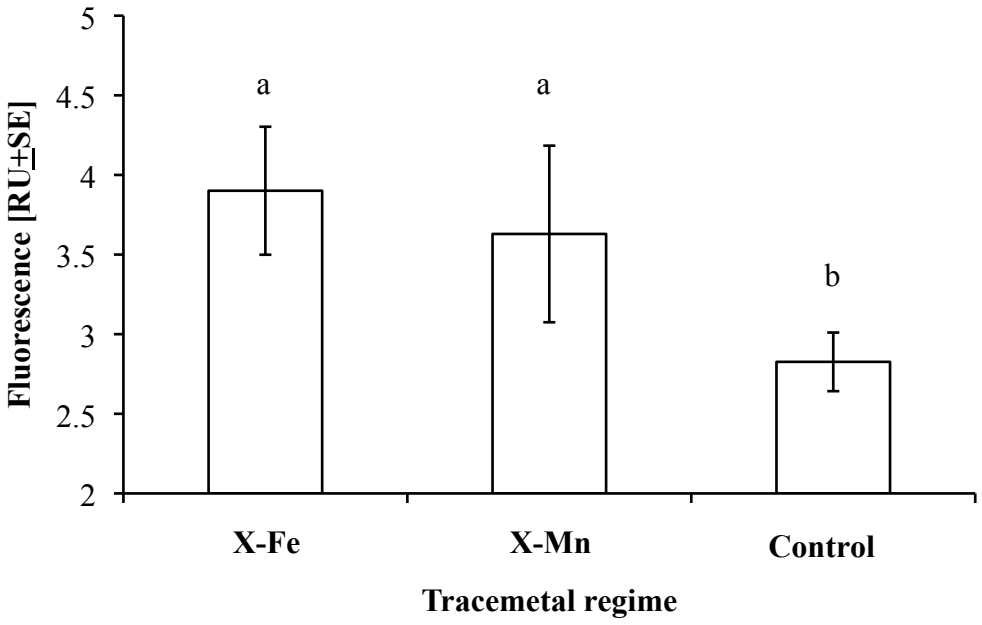
5
4.5
4
3.5
3
2.5
2
Fluorescence [RU±SE]
a
a
b
X-Fe
X-Mn
Control
Tracemetal regime

Figure 4.12 Mean fluorescence of the nitric oxide probe, DAF-FM [RU $\pm$ SE] in symbiotic dinoflagellates of Whitsunday *S. pistillata* exposed the variable trace-metal removal (X-Fe and X-Mn) and a full trace metal control (Control) (n=6). Shown are the main effects of trace metal regime, and different letters indicate significant differences ($p<0.05$) detected by a two-way ANOVA.

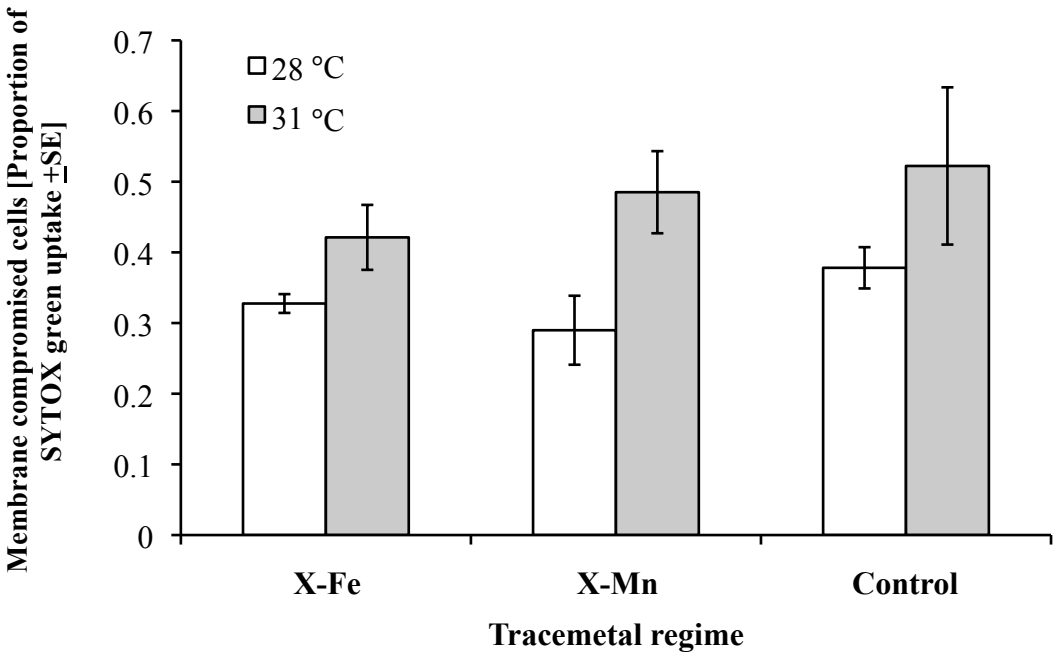
Membrane compromised cells [Proportion of SYTOX green uptake ±SE]
0.7
0.6
0.5
0.4
0.3
0.2
0.1
0
28 °C
31 °C
X-Fe
X-Mn
Control
Tracemetal regime

Figure 4.13 Cell membrane permeability [proportion of SYTOX stained cells ± SE] of Whitsunday *S. pistillata* symbiotic dinoflagellates exposed to low temperature (28 °C, white bars) and high temperature (31 °C, grey bars) and variable trace metal removal (X-Fe, X-Mn) or a full trace metal supplementation (Control). A two-way ANOVA indicated a significant of temperature on cell membrane permeability ($p<0.05$).

Intracellular concentrations of reactive oxygen and nitrogen species were not significantly affected by increases in temperature or trace metal regimes (Figure 4.11). Some interesting trends did occur with increased levels of superoxide, $ONOO\bullet^-$ and $OH\bullet^-$ detected in *S. pistillata's* symbiotic dinoflagellates exposed to high (31°C) temperature relative to those exposed to low temperature (28 °C) ($df=1$, $F=3.625$, $p=0.071$, Figure 4.11). Furthermore, intracellular NO concentrations did show a trend under different trace metal and temperature regimes ($df=2$, $F=2.621$, $p=0.098$ and $df=1$, $F=1.891$, $p=0.184$ respectively), where the full metal regime (control) showed lower levels of NO relative to the treatments devoid of manganese and iron ($p<0.15$, Figure 4.12).

Cell membrane permeability was influenced by the high temperature treatment, with increased permeability detected in symbiotic cells exposed to elevated temperature ($df=1$, $F=6.722$, $p=0.017$), but, the trace metal regime did not show a significant effect ($df=2$, $F=0.918$, $p=0.416$, Figure 4.13).

4.4 Discussion

The decline in F_v/F_m detected in the symbiotic dinoflagellates of *S. pistillata* isolated from Pith Reef and the Whitsundays under conditions of elevated temperature and high irradiance is consistent with the impairment of photosynthesis detected in coral algal symbionts exposed to temperature stress (Iglesias-Prieto *et al.* 1992, Warner *et al.* 1996, Jones *et al.* 1998, Warner *et al.* 1999, Jones *et al.* 2000). Jones *et al.* (1998) detected similar decreases in the optimal quantum yield (F_v/F_m) of *S. pistillata* zooxanthellae of the GBR when exposed to elevated temperatures of 33-34 °C for a duration of 4 hours. Similar declines in F_v/F_m have also been exhibited in the Caribbean coral, *Montastrea annularis*, under outdoor laboratory conditions, when the coral was exposed to an elevated temperature of 31.5 °C for 48 hours (Warner *et al.* 1999). Warner *et al.* (1999) concluded that the impairment of photosynthesis in *M. annularis'* symbiotic dinoflagellates resulted from photodamage, due to the absence of F_v/F_m recovery after sunset and 24 hours of temperature stress, and attributed the response to PSII damage due to the declines in detectable D1 proteins. In contrast to Warner et al.'s (1999) PSII damage notion, Jones *et al.* (1998) proposed that the impairment of photosynthesis in

temperature stressed coral's symbiotic dinoflagellates results from damage to the carboxylation reactions in the Calvin cycle, and that the declines in F_v/F_m were a secondary effect of dark reaction damage. Within the current study, the decline in F_v/F_m of the high temperature symbiotic dinoflagellates of *S. pistillata* may have resulted from PSII damage, damage of the carboxylation dark reactions of the Calvin cycle or increases in the xanthophyll non-photochemical cycling.

The enhanced decline in dark adapted F_v/F_m of the symbiotic dinoflagellates of *S. pistillata* isolated from Pith Reef under conditions of temperature stress and iron limitation is consistent with the study of Shick *et al.* (2011, Chapter 2) and with multiple studies on free living phytoplankton (Green *et al.* 1992, Shi *et al.* 2007). The decline in dark adapted F_v/F_m detected by Shick *et al.* (2011, Chapter 2) in iron-limited *S. pistillata* exposed to temperature stress was attributed to increases in non-photochemical quenching capacity and photodamage to PSII. Similar declines have been detected in the photochemical efficiency of iron limited algal cultures and has been associated and attributed to modifications within the chloroplast under iron-limited conditions. In the diatom, *Phaeodactylum tricornutum*, limitation by iron resulted in decreases in the relative abundance of D1, CP43 and CP47 proteins of PSII (Green *et al.* 1991). From these results, Green *et al.* (1991) suggested that iron limitation generated an increase in the fraction of nonfunctional reaction centers. In *Trichodesmium erythraeum* IMS101, an 80% reduction in PSII quantum yield coincided with reductions in the functional absorption cross-sections of PSIIs and reductions in the Qa-reoxidation rate under iron-limited conditions (Shi *et al.* 2007). From these results, Shi *et al.* (2007) concluded that iron limitation reduced the electron transfer components on the acceptor side of PSII within the photosynthetic electron transport chain. The enhanced decline in dark-adapted F_v/F_m of symbiotic dinoflagellates under iron limitation within this study may have resulted from modifications or photodamage to PSII reaction centers and elevation of the non-photochemical quenching processes, both of which have been shown to occur in *S. pistillata's* symbiotic dinoflagellates under iron limitation and temperature stress.

Iron limitation did negatively affect the dark-adapted F_v/F_m of *S. pistillata* symbiotic dinoflagellates from Pith reef and the Whitsundays but a difference in response to the

control treatment (full trace metal supplementation) was detected. Pith reef isolates showed a significant decline in F_v/F_m of temperature stressed symbionts devoid of iron, but, the Whitsunday isolates showed a decrease in dark-adapted F_v/F_m under conditions of iron limitation and full trace metal supplementation at high temperature. The location of each sampling group may have influenced the response of the coral algal symbionts to their experimental trace metal regime. Pith reef is far removed from Australia's continental shoreline, by approximately 80 kms, while Long Island of the Whitsunday Islands is located closer to the continental edge, approximately 0.07 km from the shoreline (Great Barrier Reef Marine Park Authority 2003). The input of terrestrial trace metals may have been greater to the Whitsunday corals, influencing the initial trace metal quotient of the symbiotic dinoflagellates, causing a negative response in photochemical efficiency in the two treatments that were both supplemented with manganese, the iron-limited treatment and full metal control. Differences in intracellular manganese concentration of symbiotic dinoflagellates have been detected in reef building corals and attributed to the proximity of their coral hosts to the continental shoreline. *Acropora tenuis'* symbiotic dinoflagellates isolated from Magnetic Island, an inshore site, showed higher manganese concentrations relative to the symbiotic dinoflagellates isolated from *A. tenuis* of One Tree Island, an offshore site within the Great Barrier Reef (Reichelt-Brushett and McOrist 2003). Manganese toxicity has been shown to decrease net photosynthetic rates in Tobacco leaves by ~20 to 60% when subjected to1 mM concentrations of Mn^{2+} (Nable *et al.* 1988). The negative response of the Whitsunday *S. pistillata's* symbiotic dinoflagellates to manganese supplementation may have resulted from high intracellular concentrations of manganese at the onset of the experiment but measurements of cellular trace metal concentrations are required to confirm this.

The strong and weak increases in intracellular ROS and RNS detected within algal symbionts of Pith Reef and the Whitsunday isolates, respectively, under temperature stress support the oxidative theory of coral bleaching. The decline in dark-adapted photochemical efficiency (F_v/F_m) at high temperature was coincident with increases in detected intracellular ROS and RNS and decreased membrane integrity, suggesting that the decrease in the efficiency of charge separation within PSII (F_v/F_m) was one of the main sources of oxidative stress in the algal symbionts. Excess photon energy to

photosystems functioning at capacity, unable to dissipate incoming energy as heat or assimilation, can lead to the generation of various ROS including superoxide ($O_2^{\bullet-}$), hydrogen peroxide (H_2O_2) and singlet oxygen ($^1O_2$) (Suggett *et al.* 2008). This study successfully illustrated increases in intracellular oxidative load of the algal symbionts under thermal stress using flow cytometry and fluorescent probes. Furthermore, this study provides direct evidence of increases in the oxidative load, as illustrated by increases in ROS and RNS probe fluorescence, within the algal symbionts coincident with declines in PSII photochemical efficiency, which can lead to bleaching under conditions of elevated irradiance and temperature.

Interestingly, the negative effect of iron limitation on the dark-adapted F_v/F_m of thermally stressed symbionts did not manifest itself as an increase in oxidative load in the same iron-limited cells. These results were unexpected in the light of the important role of iron in the function and structure of many antioxidant enzymes (Furla *et al.* 2005, Lesser 2006). The results presented in this study suggest the use of an alternate quenching mechanism of photon energy within the photosystems of the iron-limited algal symbionts. Shick *et al.* (2011, Chapter 2) detected a higher ratio of DT/(DD+DT) xanthophyll pigments in temperature stressed and iron-limited algal symbionts of *S. pistillata*, which would have increased the cells non-photochemical quenching capacity and reduced their oxidative load. Similarly, the marine phytoplankton *D. tertiolecta* and *P. tricornutum* limited to iron showed declines in F_v/F_m coinciding with increases in non photochemical quenching (Greene *et al.* 1992). The absence of an increase in oxidative load within the algal symbionts of *S. pistillata* devoid of iron at high temperature within this study may be explained by increases in the xanthophyll pigment cycling, which dissipates excess photon energy from PSII, preventing its over reduction (Jones *et al.* 1998) and reduces oxidative load (Csaszar *et al.* 2010).

Overall, this study illustrates an enhanced negative effect of iron limitation on the thermally depressed PSII photochemical efficiency of symbiotic dinoflagellates of *S. pistillata* isolated from two distinct geographical areas. Furthermore, this negative effect of temperature on photochemistry was manifested as an increase in intracellular oxidative load; however, iron limitation did not have the same effect on colonies of *S. pistillata*

isolated from different locations, potentially resulting from an adaptive response to trace metal limitation.

4.5 References

Csaszar, N.B.M., Ralph, P.J., Frankham, R., Berkelmans, R., and van Oppen, M.J.H. 2010. Estimating the potential for adaptation of corals to climate warming. *PlosOne*. 5:1-8.

Douglas, A. E. 2003. Coral bleaching- how and why? *Mar. Pollut. Bull.* 46:385-392.

Entsch, B., Sim, R.G. and Hatcher, B.G. 1983. Indications from photosynthetic components that iron is a limiting nutrient in primary producers on coral reefs. *Mar. Biol.* 73: 17-30.

Furla, P., Allemand, D., Shick, J.M., Ferrier-Pages, C., Richier, S., Plantivaux, A., Merle, P. and Tambutte, S. 2005. The symbiotic anthozoan: a physiological chimera between alga and animal. *Integ. Comp. Biol*. 45: 595-604.

Glynn, P.W. 1993. Coral reef bleaching: ecological perspectives. *Coral Reefs* 12: 1-17

Greene, R.M., R.J.Geider and P.G. Falkowski. 1991. Effect of iron limitation on photosynthesis in a marine diatom. *Limnol. and Oceanogr*. 36:1772-1782.

Green, R.M., Geider, R.J., Kolber, Z. and Falkowski, P.G. 1992. Iron-induced changes in light harvesting and photochemical energy conversion processes in eukaryotic marine algae. *Plant. Physiol*. 100: 565-575.

Great Barrier Reef Marine Park Authority. 2003. Great Barrier Reef marine park zoning plan 2003. MPZ31-Townsville/Whitsunday management area. http://www.gbrmpa.gov.au/corp_site/management/zoning/zoning_maps.html

Halliwell, B. 2006. Reactive species and antioxidants. Redox biology is a fundamental theme of aerobic life. *Plant Physiol*. 141:312-322.

Iglesias-Prieto, R., Matta, J.L., Robins, W.A. and Trench, R.K. 1992. Photosynthetic response to elevated temperature in the symbiotic dinoflagellate *Symbiodinium microadriaticum* in culture. *Proc.Natl.Acad.Sci.* 89:10302-10305.

Jones, R.J., Hoegh-Guldberg, O., Larkum,A.W.D. and Schreiber, U. 1998. Temperature-induced bleaching of corals begins with impairment of the CO_2 fixation mechanism in zooxanthellae. *Plant, Cell and Environ*. 21: 1219-1230.

Lesser, M. 1997. Oxidative stress causes coral bleaching during exposure to elevated temperatures. *Coral Reefs*. 16:187-192.

Lesser, M. 2006. Oxidative stress in marine environments. *Annu. Rev. Physiol*. 68:253-278.

Lesser, M.P. and Farrell, J.H. 2004. Exposure to solar radiation increases damage to both host tissues and algal symbionts of corals during thermal stress. *Coral Reefs*. 23:367-377.

Lesser, M., Stochaj, W.R., Tapley, D.W. and Shick, J.M. 1990. Bleaching in coral reef anthozoans effects of irradiance, ultraviolet radiation, and temperature on the activities of protective enzymes against active oxygen. *Coral Reefs*. 8:225-232.

Maxwell, D.P., Falk,S., and Huner, N.P. 1995. Photosystem II excitation pressure and development of resistance to photoinhibition. Plant Physiol. 107:687-694.

Murrant, C.L. and Reid, M.B. 2001. Detection of reactive oxygen and reactive nitrogen species in skeletal muscle. *Microsc. Res. Techni.*. 55: 236-248.

Nable, R.O., R.L. Houtz and G.M. Cheniae. 1988. Early inhibition of photosynthesis during development of Mn toxicity in tobacco. *Plant Physiol.* 86: 1136-1142.

Obata, H., Shitashima, K., Issiki, K., and Nakayama, E. 2008. Iron, manganese and aluminum in upper waters of the western South Pacific Ocean and its adjacent seas. *J. Oceanogr.* 64:233-245.

Price, N.M., G.I. Harrison, J.G. Hering, R.J. Hudson, P.M.V. Nirel, B. Palenik and F.M.M. Morel. 1988/1989. Preparation and chemistry of artificial algal culture medium Aquil. *Biol. Oceanogr*. 6: 443-461.

Reichelt-Brushett, A.J. and McOrist, G. 2003. Trace metals in the living and nonliving components of scleractinian corals. *Mar. Pollut. Bull*. 46:1573-1582.

Shashar, N., Banaszak, A.T., Lesser, M.P. and D. Amrami. 1997. Coral endolithic algae: Life in a protected environment. *Pac. Sci*. 51: 167-173.

Shi, T., Sun, Y. and Falkowski, P.G. 2007. Effects of iron limitation on the expression of metabolic genes in the marine cyanbobacterium *Trichodesmium erythraeum* IMS101. *Environ. Microbiol*. 9: 2945- 2956.

Shick, M.J., Iglic, K., Wells, M.L., Trick, C.G., Doyle, J. and Dunlap, W.C. 2011. Responses to iron limitation in two colonies of *Stylophora pistillata* exposed to high temperature: Implications for coral bleaching. *Limnol. Oceanogr.* 56: 813-828.

Shick, M.J., Romaine-Lioud, S., Ferrier-Pages, C. and Gattuso, J.-P. 1999. Ultraviolet-B radiation stimulates shikimate pathway-dependent accumulation of mycosporine-like amino acids in coral *Stylophora pistillata* despite decreases in its population of symbiotic dinoflagellates. *Limnol. Oceanogr*. 44: 1677-1682.

Shcolnick, S. and Keren, N. 2006. Metal homeostasis in cyanobacteria and chloroplasts. Balancing benefits and risks to the photosynthetic apparatus. *Plant Physiol*. 141: 805-810.

Suggett, D.J., Warner, M.E., Smith, D.J., Davey, P., Hennige, S., and Baker, N.R. 2008. Photosynthesis and production of hydrogen peroxide by *Symbiodinium* (Pyrrhophyta) phylotpyes with different thermal tolerances. *J. Phycol*. 44: 948-956.

Vardi, A., Fomiggini, F., Casottis, R., De Martino, A., Ribalet, F., Miralto, A. and Bowler,C. 2006. A stress surveillance system based on calcium and nitric acid in marine diatoms. *PlosBiology* 4:0411-0419.

Warner, M.E., Fitt, W.K. and Schmidt, G.W. 1996. The effects of elevated temperature on the photosynthetic efficiency of zooxanthellae in hospite from four different species of reef coral: a novel approach. *Plant, Cell and Environ*. 19:291-299.

Warner, M.E., Fitt, W.K. and Schmidt, G.W. 1999. Damage to photosystem II in symbiotic dinoflagellates: A determinant of coral bleaching. *Proc. Natl. Acad. Sci*. 96:8007-8012.

Chapter 5

The stimulation of oxidative stress in temperature stressed, iron-depleted cultures of *Symbiodinium* (Frudenthal) maintained under continuous growth.

5.1 Introduction

Photosynthetic marine communities are limited in growth and function by the availability of macro- and micronutrients. Within marine environments, the availability of the trace metal iron (Fe) often limits phytoplankton productivity through reduced phytoplankton photophysiology (Kolber *et al.* 1994, Green *et al.* 1991) and growth (Sunda and Huntsman 1995). Although iron is one of the most abundant transition elements in the Earth's crust, iron is severely limited in marine environments. This limitation results from the low solubility (10^{-8} M) of iron's most dominant form, the ferric iron (Fe^{3+}), under aerobic conditions, and is enhanced by minimal atmospheric dust deposition to open ocean environments (Shi *et al.* 2007). Although different in structure from open ocean systems, coral reef environments far removed from coastal shorelines may experience similar limitations in iron. Entsch *et al.* (1983) found low total iron concentrations (2 x 10^{-8} M) in the surrounding seawater of Davies Reef, a mid-shelf reef of the Great Barrier Reef (GBR), off the Eastern coast of Australia. Furthermore, a recent study of the Coral Sea adjacent to the GBR detected low concentrations of total iron, ranging from 0.2- 0.3 nM (Obata *et al.* 2008). The low concentration of iron detected within the mid-shelf reef of the GBR indicate that species living within this reef environment may be limited by the essential trace metal and experience physiological modifications as a result.

Iron limitation in coral reef environments can influence the relationship between the coral animal host and their symbiotic dinoflagellates (Genus *Symbiodinium)*, commonly termed zooxanthellae, by altering the alga's physiology. In an analysis of Davies reef species, zooxanthellae of the soft coral, *Sinularia sp*. showed a three fold decrease in total iron and ferredoxin relative to zooxanthellae isolated from the giant clam, *Tridacna maxima* (Entsch *et al.* 1983). These results suggest that iron limitation does influence

zooxanthellae *in hospite* and to different degrees between different host species. Furthermore, iron-stress in primary producers on a coral reef may influence growth rates, biomass, and distribution of species (Entsch *et al*. 1983) and their ability to handle environmental stressors.

Elevations in temperature and irradiance in coral reef waters are known to stimulate coral bleaching events (Lesser and Farrell 2004) and iron limitation under these conditions could enhance the negative effect of each stressor. Coral bleaching occurs when the animal host expels its symbiotic dinoflagellates or the photosynthetic pigments within the symbionts break down, giving the corals a pale and bleached appearance (Glynn 1993, Lesser 1997, Douglas 2003), resulting in coral mortality if the algal symbionts are not restored within the coral host (Douglas 2003). The direct link between coral bleaching and iron limitation within reef environments lies in the fact that oxidative stress has been established as the main driver of coral bleaching under temperature and irradiance stress (Lesser *et al.* 1990, Lesser 2006, 2011). The oxidative stress aspect of bleaching is critical because increases in reactive oxygen species have been detected in *Symbiodinium* strains with decreased photosynthetic capacity at high temperature and irradiance (Suggett *et al.* 2008) and iron limitation to the symbiont may enhance this effect.

Modifications to the photosynthetic apparatus have been detected in phytoplankton species exposed to iron limitation and these modifications have also been linked to increased oxidative load. Iron limitation to the diatom *Phaeodactylum tricornutum* resulted in decreased levels of the D1, CP43 and CP47 proteins of photosystem two (PSII), suggesting an increase in the fraction of nonfunctional reaction centers under iron-limited conditions because the levels of light-harvesting chlorophyll proteins did not change (Green *et al.* 1991). Such conditions could have the potential to generate ROS within the chloroplast due to the high levels of oxygen and reducing equivalents along the electron transport chain (Lesser 1997). Peers and Price (2004) detected such results in the diatom *Thalassiosira weissflogii*, where iron-limiting conditions generated an increase in oxidative load, detected using the fluorescent probe H_2DCF-DA and fluorometry. Any change to the assimilation of photon energy along the photosynthetic electron transport chain under conditions of excess solar radiation and elevated temperature, common to the

reef environments, has the potential to increase oxidative stress and iron limitation may pose as one such means of modification. Furthermore, the presence of iron within critical antioxidant enzymes such as catalase and superoxide dismutase (Lesser 2006) indicates that under iron-limited conditions, the activity of such antioxidants, which transform detrimental reactive oxygen species to less harmful molecules (Scandalios 1993), may be limited and further enhance oxidative stress under stressful environmental conditions.

The effects of iron on *Symbiodinium* photophysiology *in hospite* has been demonstrated within this thesis (Chapters 2-4) with decreases in PSII photochemical efficiency detected in symbiotic dinoflagellates under iron-limited conditions. The role of iron in the intracellular ROS and RNS load of *Symbiodiniun in hospite* is yet to be clarified. Results thus far have shown either minor decreases in detected intracellular ROS of symbiotic dinoflagellates under iron-limited conditions (Chapter 3) or no effect of iron limitation on the symbiotic dinoflagellate ROS and RNS load (Chapter 4). Differences in the response of freshly isolated symbiotic dinoflagellates to iron limitation may have occurred due to alterations in protocol (freshly isolated symbiotic dinoflagellates incubated for one hour in light or dark conditions prior to probe incubation, Chapter 2, versus freshly isolated zooxanthellae probed right after being isolated from the host, Chapter 4) or due to genetic differences between the symbionts, *Symbiodinium*, which have been shown to vary in coral hosts of the same species (Goulet and Coffroth 1997, Santos *et al.* 2001). In order to assess the affect of iron limitation on intracellular ROS and RNS load, an approach that involves controlled conditions and cultures of single *Symbiodinium* species is essential.

The goal of this study is to assess the relationship between iron limitation and oxidative load within symbiotic dinoflagellates maintained in culture when exposed to elevated temperature and irradiance. To mimic the slow growth rate of symbiotic dinoflagellates *in hospite*, ranging between 0.013 and 0.0094 day^{-1} (Falkowski *et al.* 1984), cultures of *Symbiodinium* were grown under a continuous culture regime (Figure 1). Within continuous culture systems, steady state algal growth can be reached and maintained by establishing a fixed rate of fresh medium delivery to the system in conjunction with culture out-flow from the system (Buttons 1985). This occurs by setting the culture growth rate to a value that is high enough to prevent total culture loss by dilution and low

enough to allow nutrient replenishment (Buttons 1985). Continuous culture growth systems are an appealing way to study iron limitation because they are effective at maintaining growth under nutrient limited conditions by diluting the cultures with fresh medium at a rate that determines algal growth rate (Buttons 1985, Weger 1999). In this way, the cultures can be manipulated and one can address questions of their physiology, such as the implications of iron limitation on oxidative load. The hypothesis of this study was that iron limitation to *Symbiodinium* cultures maintained at a low growth rate will affect the oxidative load of the cells under conditions of temperature and irradiance stress. Predictions at the onset of experimentation were that decreases in iron available for growth would result in elevated intracellular reactive oxygen species, and that this response would be enhanced under temperature and irradiance stress. This study is unique because it is the first to address the oxidative effects of iron limitation on *Symbiodinium* cultures maintained under steady growth, thus providing insight to the role of the trace metal in coral bleaching events.

5.2 Methods

5.2.1 Culture maintenance- Cultures of *Symbiodinium* (Frudenthal 1962) strains 2432 and 831 were acquired from the Provasoli-Guillard National Center for Culture of Marine Phytoplankton (CCMP, Table 1) located at the Bigelow Laboratory for Ocean Sciences in Maine, USA. Batch cultures of each strain were established in twice chelexed Aquil artificial seawater containing Aquil trace metal enrichments (Price *et al.* 1989/99) amended with Guillard's F/2 nitrate, phosphate, iron, EDTA and vitamin additions (Guillard 1973) in 500 mL Erlenmeyer flasks. These cultures were maintained at 22-24°C and 65-85 μmol photon•m^{-2}•s^{-1} and used as the inoculum cultures for the chemostat experiments.

Table 5.1 *Symbiodinium* isolate information.

Strain Number	Culture Collection	Host Species
2432	Provasoli-Guillard National Center for Culture of Marine Phytoplankton	*Leptastrea purpurea*
831	Provasoli-Guillard National Center for Culture of Marine Phytoplankton	Clam host

5.2.2 Sterilization and trace-metal free protocol- Experimental glass- and plastic-ware were rinsed with 10% hydrochloric acid (HCL) followed by three consecutive rinses with ultra pure water (NANOpure Infinity UV/UF, Barstead International) to establish surfaces devoid of trace metals. All chemostat tubing was soaked in 10% HCL for a minimum of 24 hours, rinsed twice with NANOpure water and once with 95% ethanol for sterilization. Microwave medium sterilization was achieved by bringing the medium to a boil twice with a minimum 10 minute cooling interval between each boiling period (Keller *et al.* 1988). All hard goods were microwave sterilized in the presence of a water bath for 10 minutes in ventilated plastic containers prior to use. Synthetic ocean water (SOW) was passed twice over a Chelex 100 column to remove trace metals (Price *et al.* 1989/99). Column regeneration between 40 L batches of SOW was achieved by rinsing the beads with 1 M HCL, two-three washes with NANOpure water, followed by a rinse with 1 M sodium hydroxide (NaOH) and two final rinses with NANOpure water. Once the column was repacked, washes with SOW and NANOpure water were conducted until the pH was approximately 8. Prior to trace metal-clean SOW collection, a minimum of 200 mL of SOW was passed through the column as a rinse to ensure the collection of trace metal-free SOW.

5.2.3 Chemostat set up- Cells were cultured at an inoculum of 10% (v/v) in batch culture within 250 mL glass tubes and grown at 75-100 μmol photon•m^{-2}•s^{-1} and 25 °C within a circulating water bath. Four media regimes were established by varying the amount of amended $FeCl_3$•$6H_2O$. The four treatments consisted of a range of iron availabilities from replete to deplete (11.7, 1.17, 0.117 and 0.0117 μM, respectively). The primary iron stock was acidified to a pH of 3 to prevent precipitation of iron in the solution and the prepared media sat for a minimum of 24 hours to allow chemical speciation to occur. Homogenous cultures were established by bubbling the culture tubes with 0.2 μm filtered air and through the mixing of magnetic stir bars placed within each tube (Figure 5.1). On the seventh day of growth, the cells were diluted with fresh medium delivered from a MinipulsTM 3 peristaltic pump fitted with an eight-channel pump head and 0.38 mm PVC tubing. The established flow rate ranged between 2.5 $\pm$ 0.47 mL/hour, accomplishing a specific growth (μ_N) and dilution (D) rate ranging between 0.01025 and

0.014925 (MacIntyre and Cullen, 2005) within the cultures. Each experiment consisted of one iron treatment tube per *Symbiodinium* strain (strains 831 and 2432), resulting in a total of 8 tubes per experiment. Each experiment was repeated four times (n=4). The chemostat was run for a minimum of 5 days to establish steady state growth, which was determined by taking cell density measurements (see below).

5.2.4.Cell density determination- Cellular density was determined during the running of the chemostat to establish a plateau in cell density within each culture tube, indicative of steady growth (Figure 5.2). Samples (0.5-2 mL) were collected in triplicate from each culture tube and cell density was determined using a FACsCalibur flow cytometer (BD, San Jose, California, U.S.A.), using side scatter (SSC) and cell auto fluorescence (FL3) to define the cells.

5.2.5 Temperature stress experiments- After 6-8 days of steady growth, 10-20 mL of sample was collected and probed to establish the oxidative load in cells grown at 75-100 μmol photon•m^{-2}•s^{-1} and 25 °C. Post probing, the temperature of the circulating water bath was increased to 30.5 $\pm$ 0.5 °C over the course 6-7 hours. The cultures were maintained at the elevated temperature for a minimum of 12 hours, after which samples were collected for oxidative load determination using flow cytometry.

5.2.6.Temperature and irradiance shift stress experiments- The two iron concentrations that showed the greatest impact on physiology in the full regime experiments, 1.17 and 0.0117 μM Fe, were chosen for irradiance and temperature shift experiments. Cultures were grown, treated and sampled in the same protocol as above, and each experiment was run three independent times (n=3). Once cells were sampled for oxidative load at 30.5 $\pm$ 0.5°C, they were shifted to an elevated irradiance. Each strain was diluted in trace metal free-SOW to ensure approximately equal cell density between iron-deplete and replete cultures, establishing an equal irradiance exposure. Once diluted, the sample was divided and ~50 mL of culture was poured into a 150 mL glass tube and placed in front of a halogen lamp at 790-820 μmol photon•m^{-2}•s^{-1}, while the other ~50mL was placed into a separate 150mL glass tube and placed in the dark (dark control). Both light and dark treatments remained under their conditions for 50 minutes in a heated circulating water bath (30.5 $\pm$ 0.5°C).

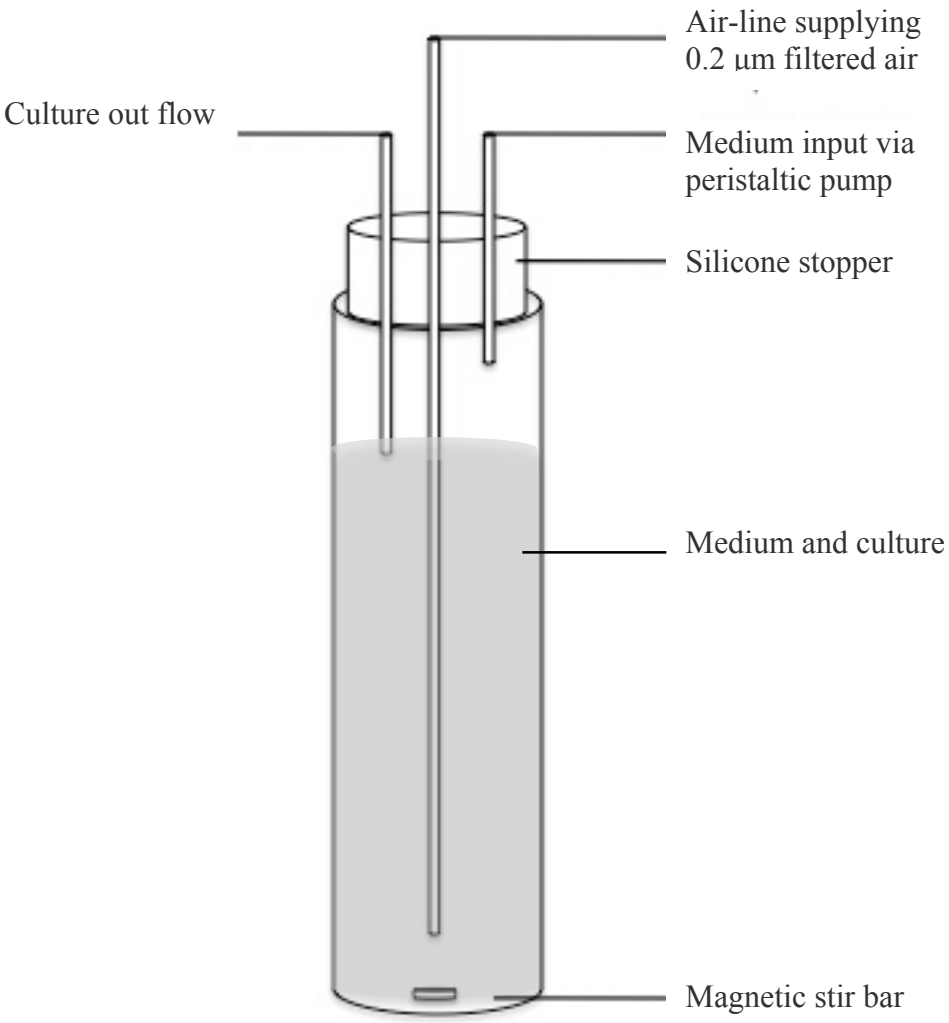
Air-line supplying
0.2 µm filtered air
Culture out flow
Medium input via
peristaltic pump
Silicone stopper
Medium and culture
Magnetic stir bar

Figure 5.1 Chemostat experimental set up.

Tubes were covered with parafilm (Parafilm M*) to ensure minimal dust contamination. Post irradiance treatment, light and dark exposed cells were probed for oxidative load. At this point, light exposed cultures were then placed in the dark for 40 minutes after which they were probed for oxidative load to assess ROS and RNS recovery.

5.2.7 Intracellular ROS/RNS measurements- The intracellular ROS and reactive nitrogen species (RNS) nitric oxide (NO), OH•, peroxynitrite ($ONOO^-$) and H_2O_2, were detected using 5-(and 6) chloromethyl-2',7'-dichlorodihydrofluorescein diacetate, acetyl ester (CMH_2DCFDA) (Murrant and Reid 2001) at a final concentration of 5 μM in seawater. Superoxide, $ONOO•^-$ and $OH•^-$ were detected using the fluorescent probe dihydroethidium (DHE) (Murrant and Reid 2001), at a final concentration of 23.1 μM. NO was detected using the probe 4-amino-5-methylamino-2',7'-difluorofluorescein diacetate (DAF-FM) at a final concentration of 2 μM. Mitochondrial ROS was detected using the probe dihydrorhodamine 123 (DHR 123) at a final concentration of 4 μM (Lesser 1996). Samples were incubated with each probe for 30 min in the dark before analysis on a FACsCalibur flow cytometer. All ROS and RNS cell fluorescence measurements were taken on the appropriate flow rate to ensure an events·$second^{-1}$ rate of less than 1050. Increases in green and orange fluorescence were proportional to probe oxidation (*see optimization in* Chapters 3 and 4) and indicative of intracellular ROS and RNS. All probe fluorescence measurements were standardized to a negative control by subtracting the negative control fluorescence signal from the probe fluorescence signal. A negative control for each sample was prepared by adding an equivalent concentration of DMSO to the sample, accounting for differences in ambient cellular fluorescence signals.

Working stock solutions of CMH_2DCFDA, DHE and DAF and DHR123 were prepared in dimethyl-sulphoxide (DMSO), divided into small aliquots and maintained in the dark at -20 °C until use. All flow cytometric fluorescence dyes were purchased from Invitrogen (Carlsbad, California, U.S.A) and each probed sample was run in duplicate or triplicate.

I.

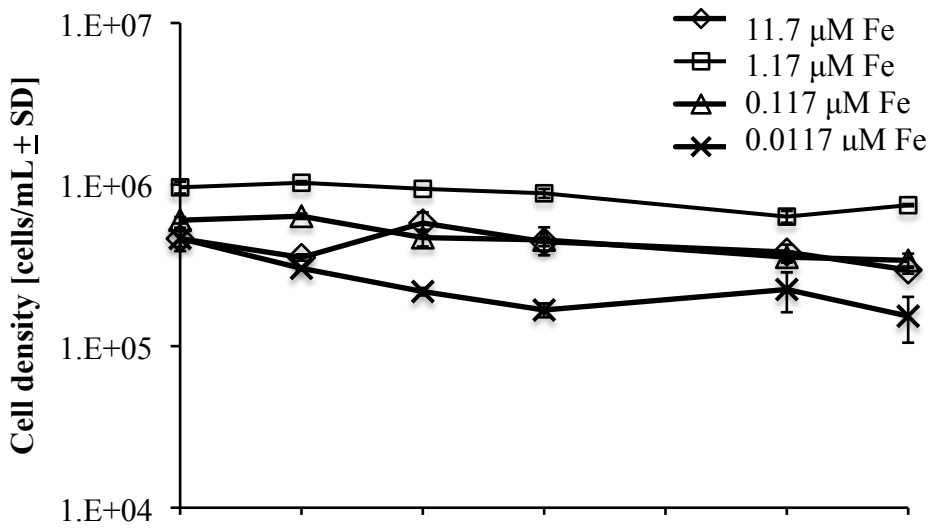
11.7 µM Fe
1.17 µM Fe
0.117 µM Fe
0.0117 µM Fe
1.E+07
1.E+06
1.E+05
1.E+04
Cell density [cells/mL ± SD]

II.

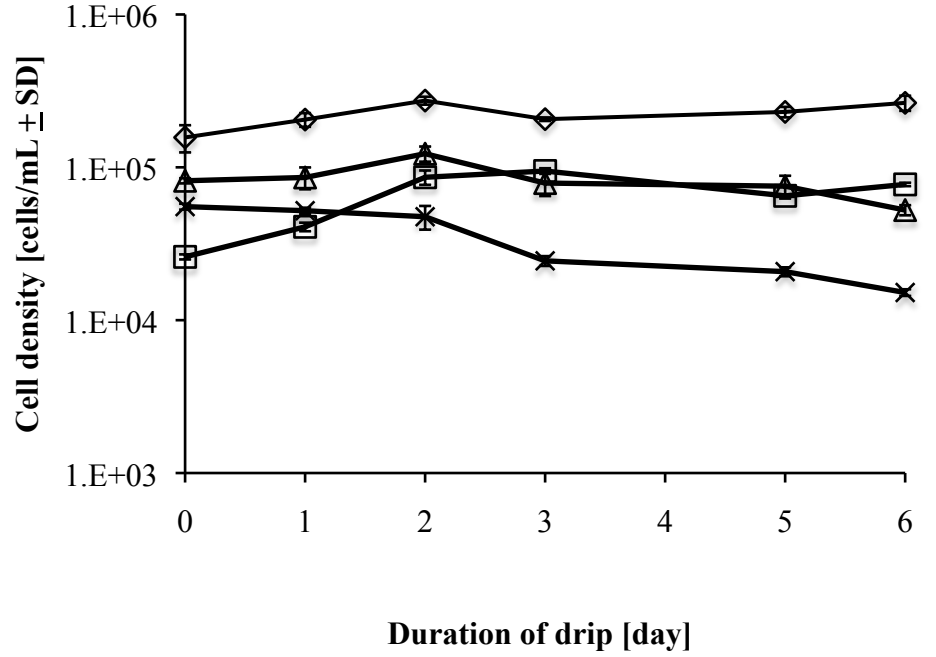
1.E+06
1.E+05
1.E+04
1.E+03
Cell density [cells/mL ± SD]
0
1
2
3
4
5
6
Duration of drip [day]

Figure 5.2 Mean cell density [cells•mL^{-1} $\pm$ SD] of *Symbiodinium* strains 2432 [I.] and 831 [II.] grown under variable iron amendments [μM] at 75-100 μmol photon•m^{-2}•s^{-1} and 25 °C. Data illustrate cell densities from the onset of chemostat dilution until experimental termination. Standard deviation taken from three sub samples collected from one tube (n=1) and illustrate the variability in sampling technique.

5.2.8 Statistical analysis-One-way ANOVA tests were run to determine significant differences in cell density, intracellular ROS and intracellular RNS under variable iron amendments and stress treatments within each strain. If a significant effect of iron amendment was found, a Student Newman Keuls (SNK) post hoc test was run to determine significant differences between each iron regime. Prior to each ANOVA, a Levene's test of equality of error variances ($p<0.05$) was run and normality was assumed. If equal variances were not determined, data were log transformed to achieve equal variance. Log transformations are an effective means of correcting data with unequal variance when the variance is proportional to the mean (Zar 1999). If log transformations were insufficient to establish equal variance, Kruskal Wallis non-parametric tests were run to determine significant differences between the means of the non-equal variance data groups.

Within the iron, temperature and irradiance shift experiments, T-tests were run to determine significant differences between cell density, intracellular ROS and intracellular RNS between the iron treatments (1.17 and 0.0117 μM) per strain and probe type at high temperature before, during and after the light incubations. All statistical analyses were run on PASW statistical software (Version 18.00).

5.3 Results

5.3.1 Full range iron treatments subjected to temperature stress- Increasing concentrations of iron within the medium positively affected cell density in both *Symbiodinium* strains. Strain 2432 showed the greatest cell density at steady growth when treated with 1.17 μM Fe relative to the two lowest Fe treatments of 0.117 and 0.0117 μM (data log transformed for ANOVA analysis, df=3, F=5.031, p=0.017, Figure 5.3). The highest iron treatment of 11.7 μM Fe positively affected the cell density for strain 831 relative to the 0.117 μM Fe amendment (df=3, F=2.901, p=0.079, Figure 5.3). Furthermore, the overall cell density of strain 2432 was higher across all treatments when grown under continuous culture relative to strain 831.

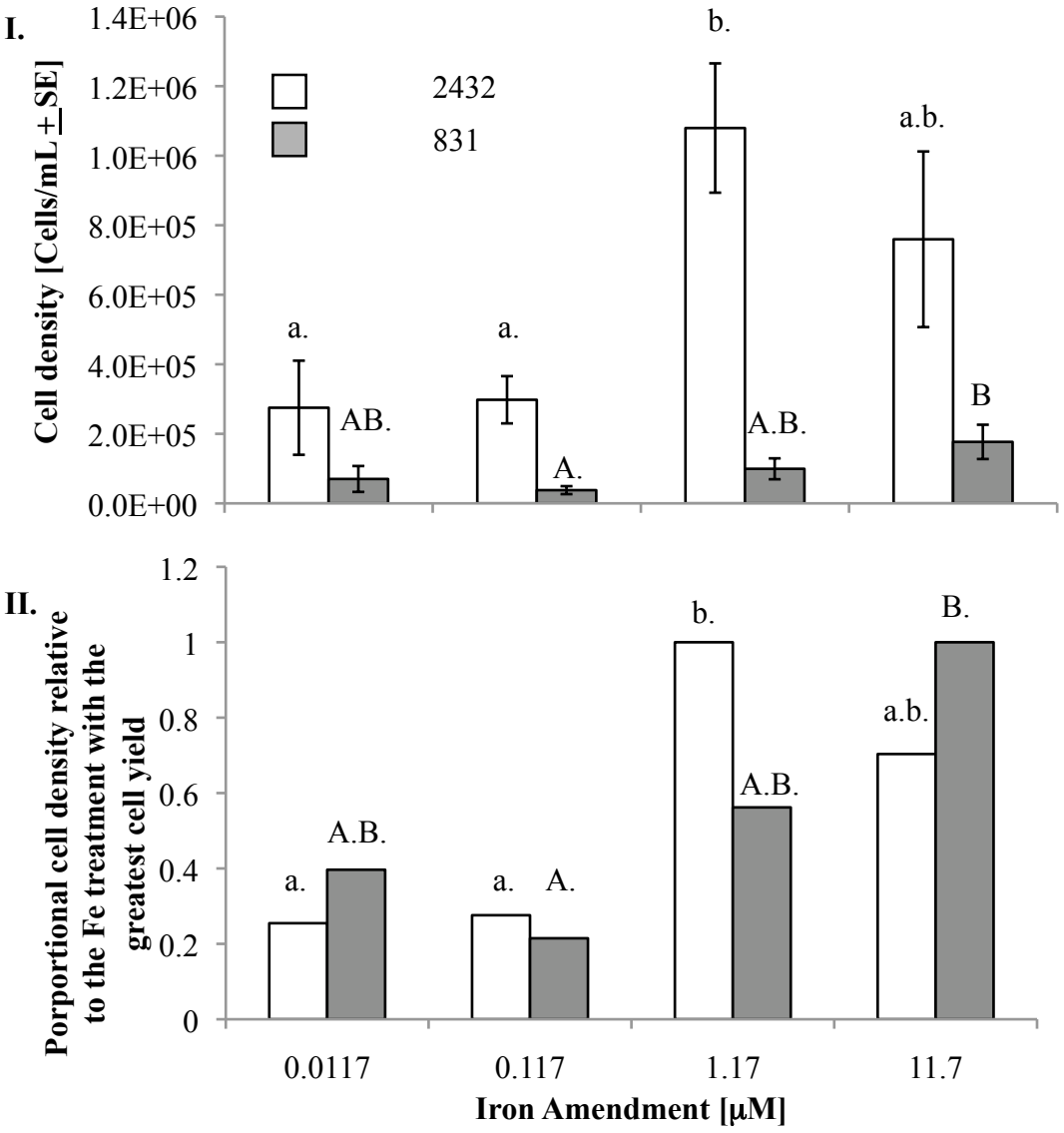
I.
Cell density [Cells/mL ± SE]
1.4E+06
1.2E+06
1.0E+06
8.0E+05
6.0E+05
4.0E+05
2.0E+05
0.0E+00
2432
831
a.
AB.
a.
A.
b.
A.B.
a.b.
B
II.
Porportional cell density relative to the Fe treatment with the greatest cell yield
1.2
1
0.8
0.6
0.4
0.2
0
a.
A.B.
a.
A.
b.
A.B.
a.b.
B.
0.0117
0.117
1.17
11.7
Iron Amendment [μM]

Figure 5.3 Mean (I.) steady state cell density [cells•mL^{-1} ± SE] of *Symbiodinium* sp. strains 2432 and 831 (white and grey bars, respectively) and (II.) the proportional cell density (data taken from I.) of each strain relative the highest cell density obtained from the iron amendments [μM] when grown at 75-100 μmol photon•m^{-2}•s^{-1} and 25 °C. Different letters represent significant differences within each strain under the variable iron amendments (n=4), where lowercase letters represent significance differences between strain 2432 cell density ($p<0.05$) and uppercase letters represent significance differences between strain 831 cell density ($p<0.08$), when subject to the different iron regimes.

5.3.2 Intracellular ROS and RNS results- Variable iron regimes did not affect the intracellular fluorescence of the mitochondrial ROS probe, DHR 123, detected within strains 2432 and 831 when grown under continuous culture at 25 °C and 75-100 μmol photon•m^{-2}•s^{-1}. A marked difference was detected within strain 2432 when the cultures were shifted to an increased temperature of 30.5 °C ($df=3$, $F=4.971$, $p=0.018$), with lower mitochondrial ROS probe fluorescence detected in cells grown under 11.7 and 1.17 μM Fe relative to cells grown at 0.117 and 0.0117 μM Fe ($p<0.05$, Figure 5.4). A similar trend was noted within strain 831, with the lowest detected mitochondrial ROS probe fluorescence occurring within the cells treated with 1.17 μM Fe relative to all other iron treatments when the cells were grown 30.5 °C.

The fluorescence of the intracellular superoxide, $ONOO^{\bullet -}$ and $OH^{\bullet -}$ probe, DHE, within strains 2432, and 831 was not affected by variable iron regime under continuous growth at 25°C and 75-100 μmol photon•m^{-2}•s^{-1}. A marked decrease in intracellular probe fluorescence, indicating levels of superoxide, $ONOO^{\bullet -}$ and $OH^{\bullet -}$, was detected in strain 831 grown at 1.17 μM Fe relative to cells grown at 0.117 and 0.0117 μM Fe when the cultures were shifted to 30.5 °C ($df=3$, $F=6.285$, $p=0.008$, Figure 5.5). The shift in growth temperature to 30.5 °C did not affect the intracellular fluorescent probe signal within strain 2432.

Variable iron regime did not affect the fluorescence signal of the intracellular NO probe, DAF-FM, within strains 2432 and 831 when grown under continuous culture at 25 °C and 75-100 μmol photon•m^{-2}•s^{-1}. Differences in NO probe fluorescence did occur within strains 2432 and 831 when the cultures were grown at an increased temperature of 30.5 °C ($df=3$, $F=3.484$, $p=0.5$, $df=3$, $F=3.527$, $p=0.49$, respectively, Figure 5.6). Strain 2432 grown under the iron treatment of 11.7 μM Fe exhibited a lower fluorescence signal, indicative of a decreased NO load, relative to all other iron treatments ($p<0.05$) while strain 831 cells exhibited the lowest fluorescence, and therefore NO load, under the iron treatment of 1.17 μM Fe relative to all other iron treatments ($p<0.06$ Figure 5.6).

I.

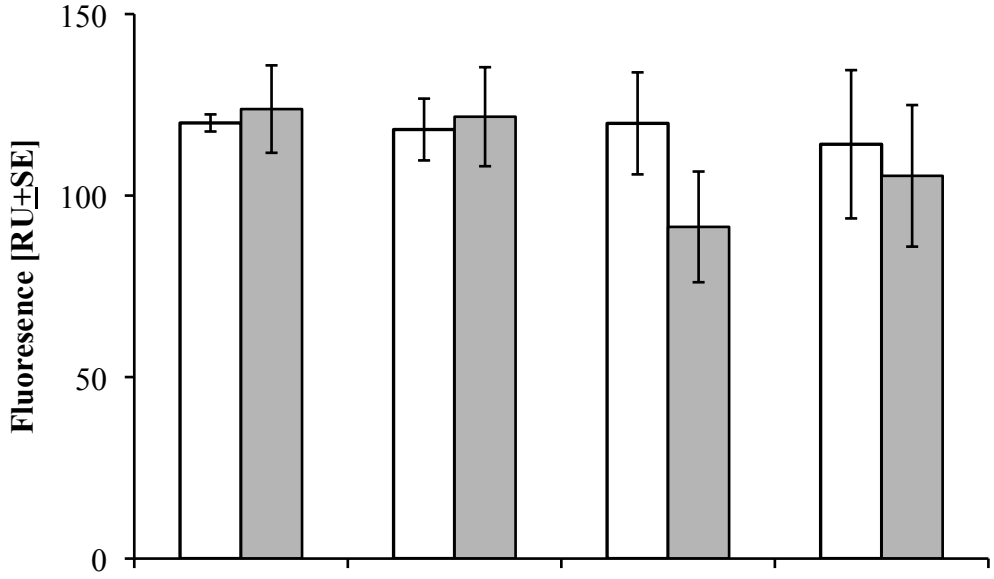
150
100
50
0
Fluoresence [RU±SE]

II.

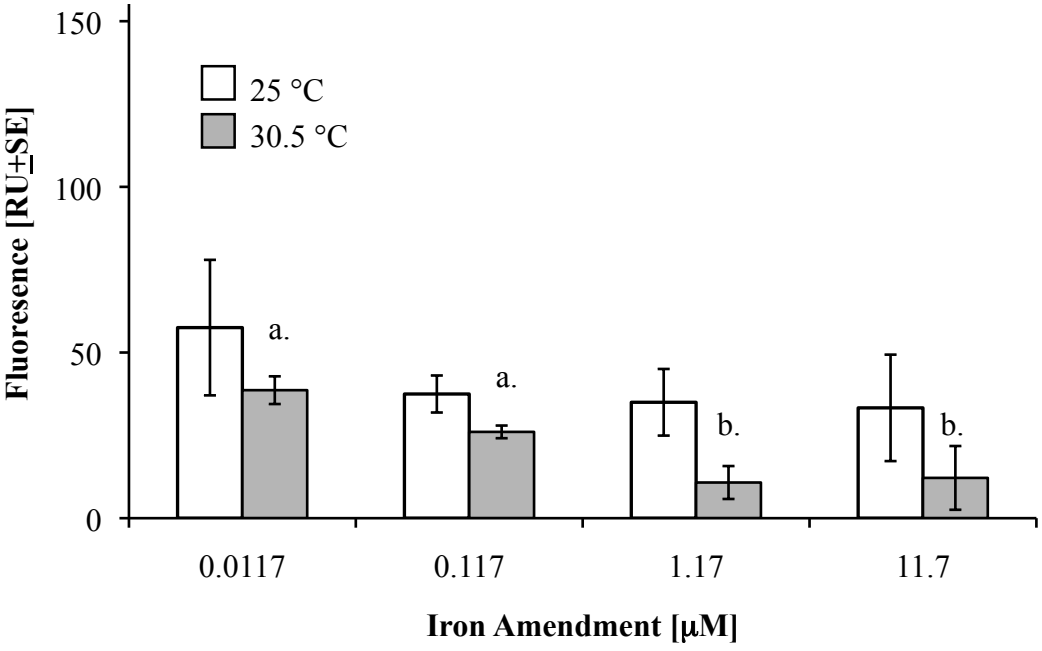
150
100
50
0
Fluoresence [RU±SE]
25 °C
30.5 °C
a.
a.
b.
b.
0.0117
0.117
1.17
11.7
Iron Amendment [µM]

Figure 5.4 Mean fluorescence [RU $\pm$ SE] of the mitochondrial general ROS probe, DHR 123, in *Symbiodinium* strains 831 (I.) and 2432 (II.) grown under continuous culture and maintained at 25 $\pm$ 0.5 °C (white bars) and 30.5 $\pm$ 0.5 °C (grey bars) and variable iron amendments [μM]. Different letters represent significant differences between iron amendments within each temperature regime and strain ($n=4$, $p<0.05$).

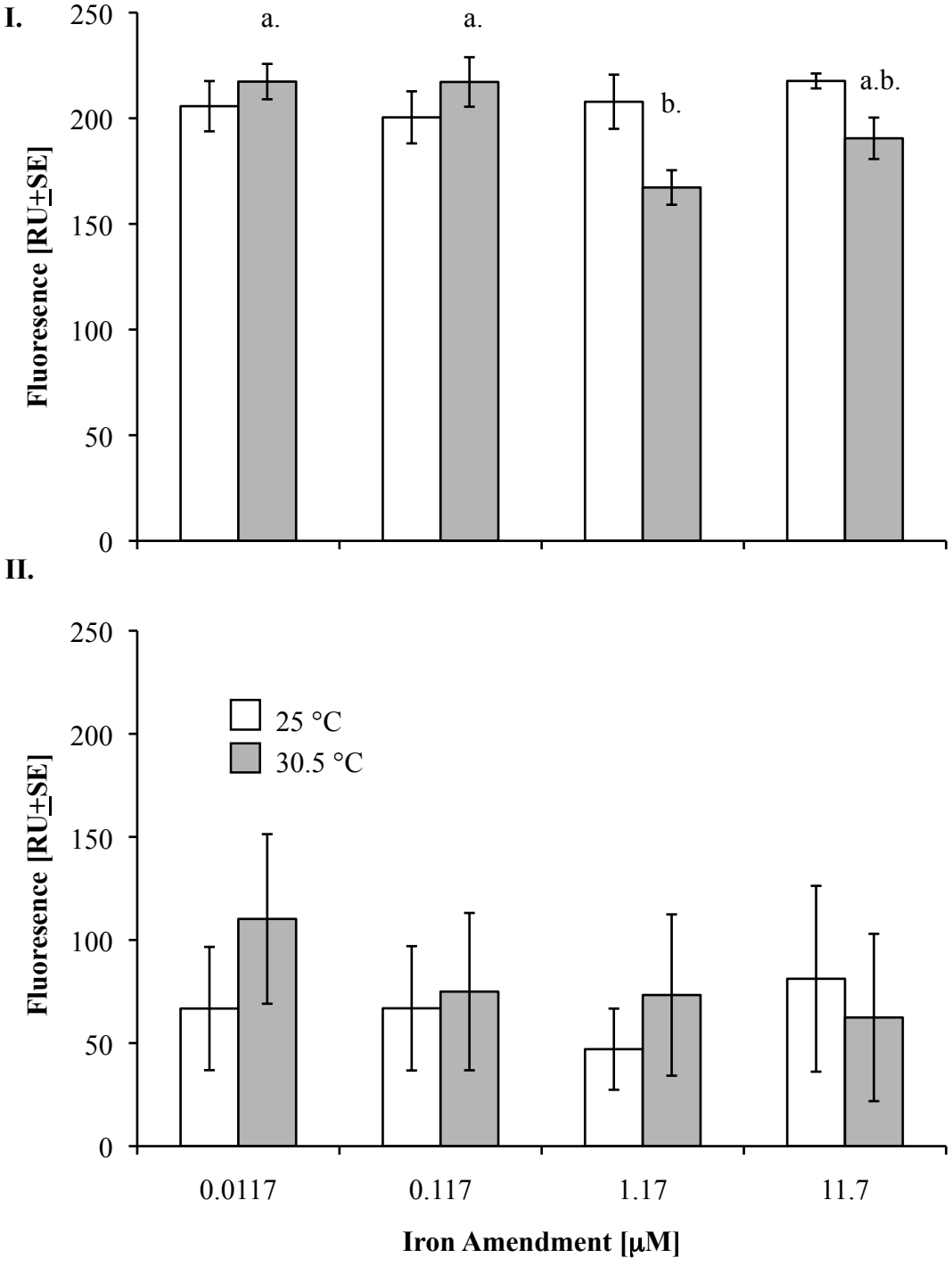
I.
250
200
150
100
50
0
a.
a.
b.
a.b.
Fluoresence [RU±SE]
II.
250
200
150
100
50
0
25 °C
30.5 °C
Fluoresence [RU±SE]
0.0117
0.117
1.17
11.7
Iron Amendment [μM]

Figure 5.5 Mean fluorescence [RU $\pm$ SE] of the superoxide, $ONOO^{\bullet -}$ and $OH^{\bullet -}$ probe, DHE, in *Symbiodinium* strains 831 (I.) and 2432 (II.) grown under continuous culture and maintained at 25 $\pm$ 0.5 °C (white bars) and 30.5 $\pm$ 0.5 °C (grey bars) and variable iron amendments [μM]. Different letters represent significant differences between iron amendments within each temperature regime and strain ($n=4$, $p<0.05$).

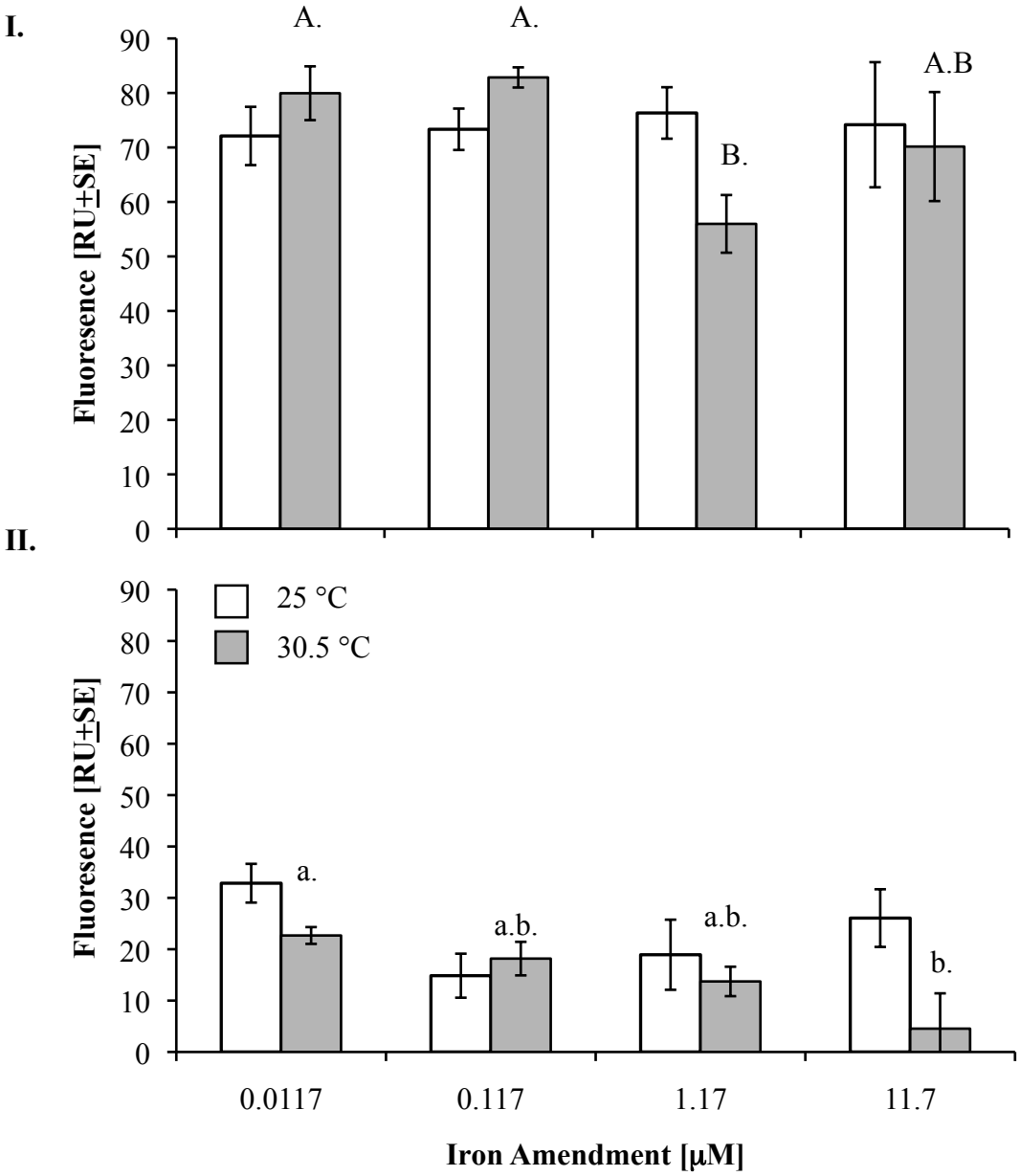
I.
A.
A.
A.B
B.
Fluoresence [RU±SE]
90
80
70
60
50
40
30
20
10
0
II.
25 °C
30.5 °C
a.
a.b.
a.b.
b.
0.0117
0.117
1.17
11.7
Iron Amendment [μM]

Figure 5.6 Mean fluorescence [RU $\pm$ SE] of the intracellular nitric oxide probe, DAF-FM in *Symbiodinium* strains 831 (I.) and 2432 (II.) grown under continuous culture and maintained at 25 $\pm$ 0.5 °C (white bars) and 30.5 $\pm$ 0.5 °C (grey bars) and variable iron amendments [μM]. Different lower case letters (a,b) represent significant differences below the significance level of $p<0.05$ and different uppercase letters (A,B) represent significant differences at a significance level below $p<0.055$, between iron amendments within each temperature regime and strain (n=4).

5.3.3. Cell density at 1.17 and 0.0117 μM Fe at elevated temperatures- Similar increases in cell density at steady growth were detected within each *Symbiodinium* strain under high iron amendments when maintained under optimal growth conditions when the chemostat experiments were re-run for the stress shift experiments. Strain 2432 showed the greatest cell density at 1.17 μM Fe relative to the reduced Fe treatment of 0.0117 μM (data log transformed, t_4=2.902, p=0.044, Figure 5.7). Strain 831 showed a similar effect of iron addition on cell density, where in which cells maintained at 1.17 μM relative to those maintained at 0.0117 μM Fe showed an elevated cell density; t_4=6.184, p=0.003, Figure 5.7. Clearly, when *Symbiodinium* strains are continuously grown under iron deplete conditions, at optimal irradiance and temperature, cell density is reduced.

5.3.4 Intracellular ROS and RNS results, high temperature effects under variable iron regimes- Intracellular ROS and RNS probe fluorescence within each strain of *Symbiodinium* was elevated under iron-deplete conditions (Figure 5.8). Strain 2432 showed marked decreases in the fluorescence of the intracellular superoxide, $ONOO•^-$ and $OH•^-$ probe DHE (t_4=2.592,p=0.061), the fluorescence of the mitochondrial ROS probe DHR 123 (t_4=3.185, p=0.033) and the fluorescence of the NO probe, DAF-FM (equal variances not assumed, $t_{2.206}$=9.224, p=0.008) when cells were maintained in iron-replete medium at high temperature. Increases in the fluorescence of the intracellular superoxide, $ONOO•^-$ and $OH•^-$ probe DHE were also detected in strain 831 (t_4=20.527, p=0.000)but no difference lay in the fluorescence of the NO probe DAF-FM (t_4=-0.026,p=0.981) detected within iron-replete or deplete cells. Furthermore, a trend of increased fluorescence in the mitochondrial ROS probe DHR 123 ($t_{2.306}$=-2.867, p=0.088) was detected in strain 831 cells maintained in iron-replete conditions.

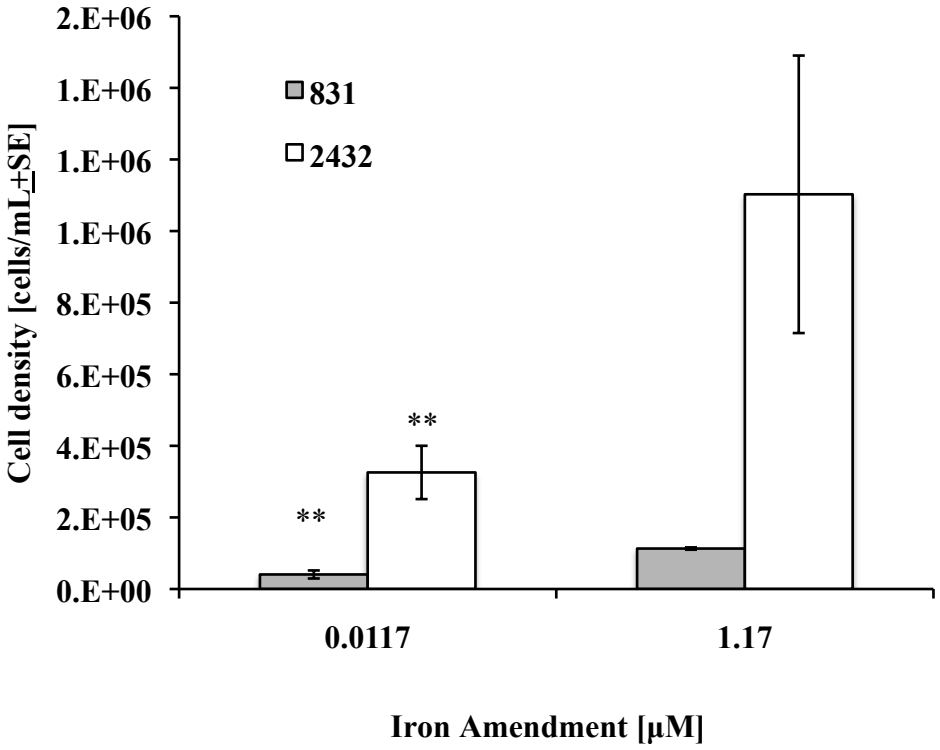
2.E+06
1.E+06
1.E+06
1.E+06
8.E+05
6.E+05
4.E+05
2.E+05
0.E+00
Cell density [cells/mL±SE]
831
2432
**
**
0.0117
1.17
Iron Amendment [µM]

Figure 5.7 Mean cell density [cells•mL^{-1} $\pm$ SE] of *Symbiodinium* strains 2432 and 831 (white and grey bars, respectively) grown under variable iron amendments [μM] at 25 °C and 75-100 μmol photon•m^{-2}•s^{-1} for the temperature and irradiance shift stress experiments. ** Represent significant differences detected between iron amendments within each *Symbiodinium* strain (n=3, $p<0.05$).

5.3.5 Increased irradiance effects at high temperature and variable iron regimes- Shifts in irradiance for a period of 50 minutes at high temperature (30.5 °C) caused marked iron effects on the intracellular ROS and RNS loads in both *Symbiodinium* strains. Strain 2432 showed elevated fluorescence with the intracellular superoxide, $ONOO^{\bullet-}$ and $OH^{\bullet-}$ probe, DHE, in iron-deplete cells exposed to both light and dark incubations (t_4=2.955,p=0.042, Figure 5.9). Although increases were detected by the probe DHE, no differences in the fluorescence of the mitochondrial ROS probe, DHR 123, or the NO probe, DAF-FM, were detected within strain 2432 under the different iron and irradiance regimes (Figure 5.9).

An enhancement of ROS and RNS load under iron limitation was evident in strain 831 under the conditions of the irradiance incubation (Figure 5.10). Intracellular superoxide, $ONOO^{\bullet-}$ and $OH^{\bullet-}$ detected by the probe DHE (equal variance not assumed, $t_{2.116}$=8.315,p=0.012), and NO detected by the probe DAF-FM (t_4=3.183, p=0.033) were elevated in iron-deplete cells exposed to elevated irradiance but mitochondrial ROS did not increase.

Following the irradiance incubation, each strain was placed in the dark to assess recovery, and the levels of ROS and RNS detected within the *Symbiodinium* species varied. Strain 2432 did not show a recovery from the elevated level of ROS and RNS that were generated by the irradiance exposure, and iron regime did not influence detectable oxidative load (Figure 5.8). Strain 831 was influenced by iron regime, with cells exposed to iron-replete conditions showing elevated intracellular superoxide, $ONOO^{\bullet-}$ and $OH^{\bullet-}$ (equal variance not assumed, $t_{2.137}$=11.155,p=0.006, Figure 5.10i), mitochondrial ROS (equal variance not assumed, t_2=4.998,p=0.038) and NO (equal variance not assumed, $t_{2.014}$=21.563,p=0.002) after the dark incubation.

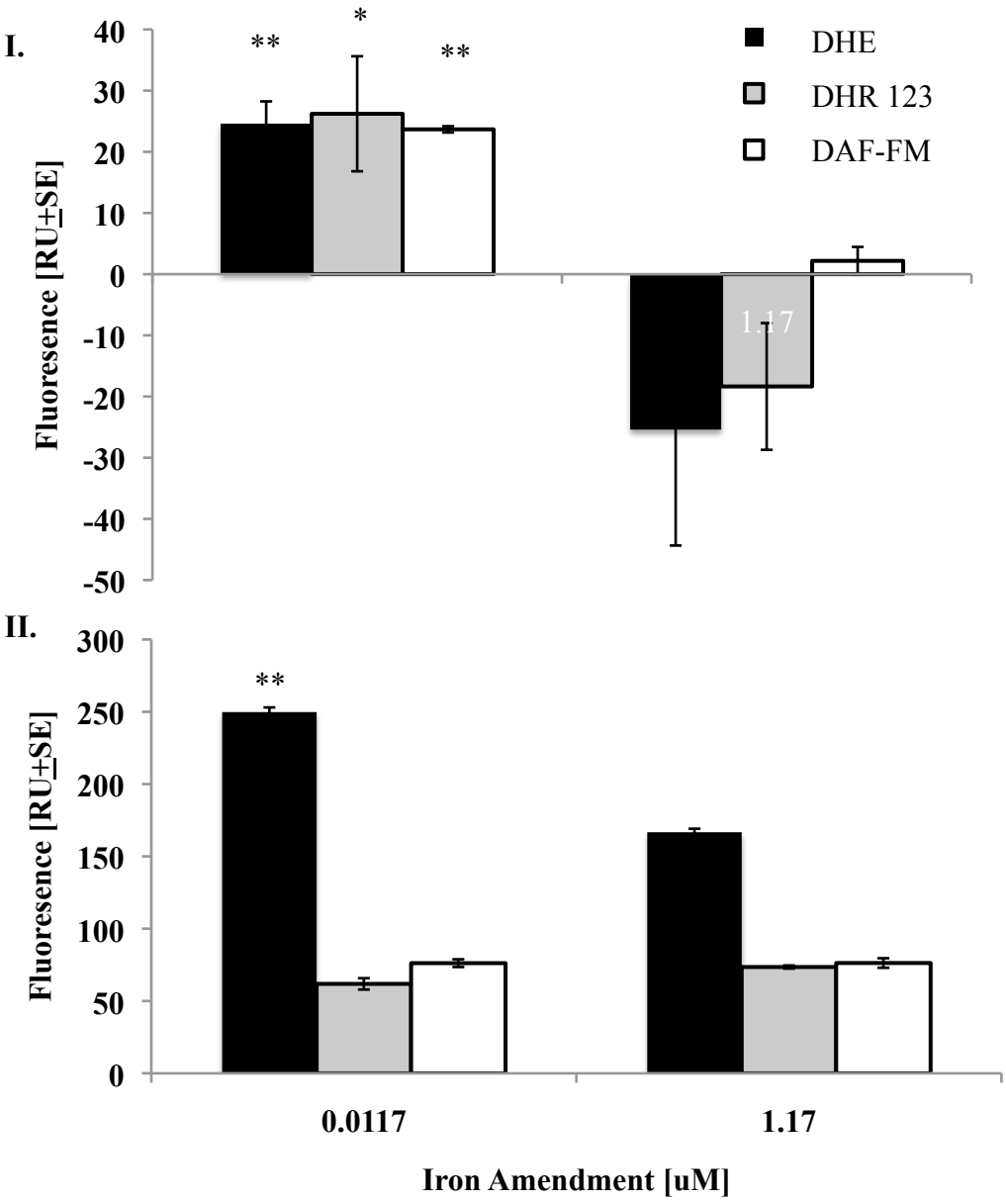
I.
II.
DHE
DHR 123
DAF-FM
Fluoresence [RU±SE]
40
30
20
10
0
-10
-20
-30
-40
-50
300
250
200
150
100
50
0
**
*
**
1.17
0.0117
1.17
Iron Amendment [uM]

Figure 5.8 Mean fluorescence of intracellular ROS and RNS probes that indicate superoxide, $ONOO\bullet^-$ and $OH\bullet^-$ [RU $\pm$ SE, DHE], mean mitochondrial ROS [RU$\pm$SE, DHR 123] and mean nitric oxide [RU$\pm$SE, DAF] of *Symbiodinium* strains (I.) 2432 and (II.) 831 grown under continuous culture and maintained at a temperature of 30.5 $\pm$ 0.5 °C, and irradiance of 75-100 μmol photon$\bullet m^{-2}\bullet s^{-1}$ and variable iron amendments [μM]. The shaded bars represent the different ROS and RNS probes: Black=DHE, grey=DHR 123 and white=DAF-FM. * Represent significant differences between iron amendments within each ROS and RNS probe type within each strain (n=3, **<0.05, *<0.1).

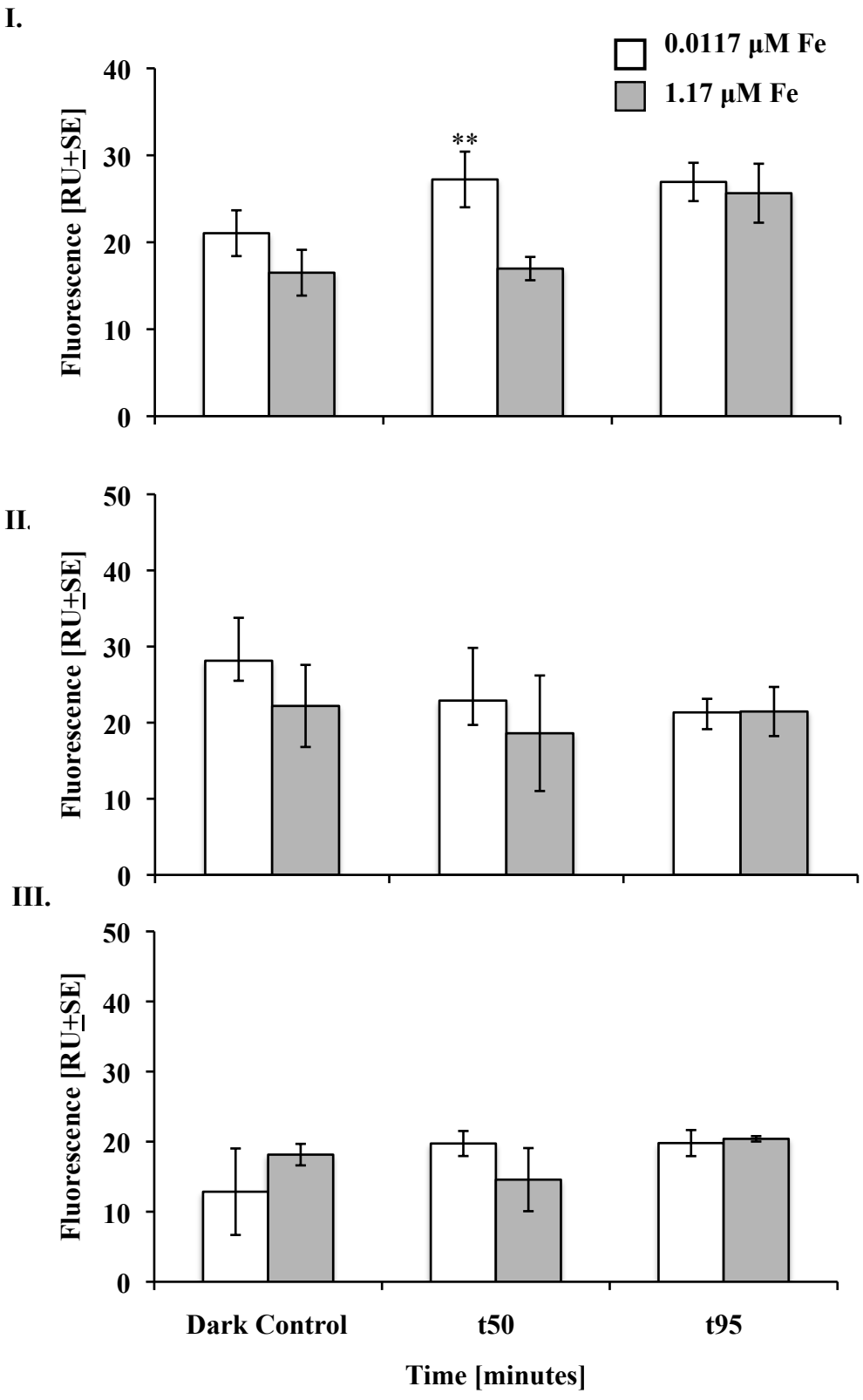
I.
0.0117 µM Fe
1.17 µM Fe
Fluorescence [RU±SE]
40
30
20
10
0
**
II.
Fluorescence [RU±SE]
50
40
30
20
10
0
III.
Fluorescence [RU±SE]
50
40
30
20
10
0
Dark Control
t50
t95
Time [minutes]

Figure 5.9 Mean intracellular fluorescence of the probe (I.) dihydroethidium which indicates superoxide, $ONOO\bullet^-$ and $OH\bullet^-$ load [RU $\pm$ SE], (II.) the mitochondrial ROS probe dihydrorhodamine 123, [RU $\pm$ SE] and (III.) the nitric oxide probe, DAF-FM, [RU $\pm$ SE], within *Symbiodinium* strain 2432 maintained at 30.5 $\pm$ 0.5 °C under variable iron amendments (White bars=0.0117 μM Fe, grey bars=1.17 Fe μM) after a 50 minute irradiance shift (denoted as t50, 800 μmol photon$\bullet m^{-2}\bullet s^{-1}$) and a 46 minute dark recovery period (denoted as t95, n=3, **<0.05). The dark control bars represent the probed intracellular fluorescence signal given off by *Symbiodinium* strain 2432 of each iron treatment maintained in the dark for 50 minutes, effectively a dark control in comparison to the light incubated (t50) cells.

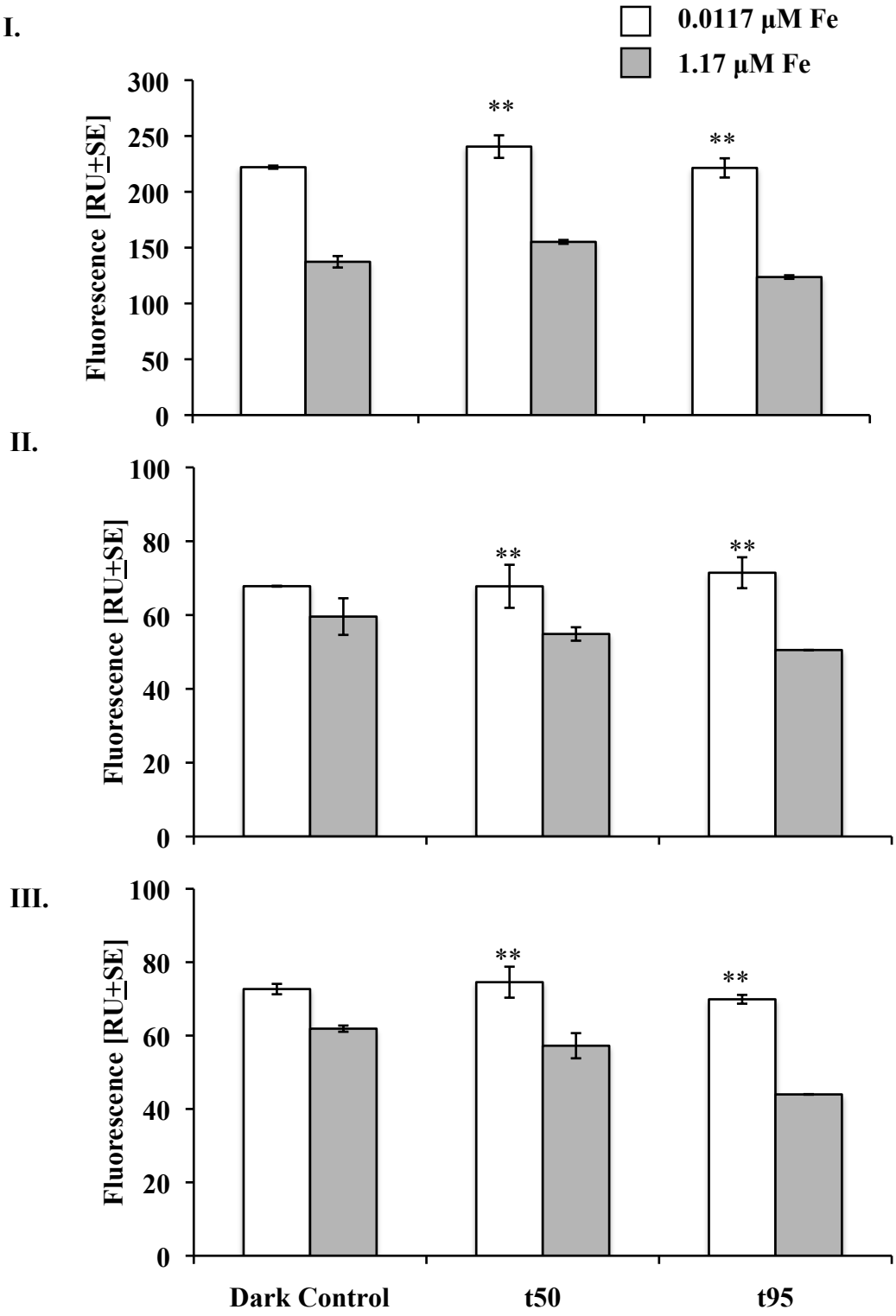
I.
II.
III.
0.0117 µM Fe
1.17 µM Fe
Fluorescence [RU±SE]
300
250
200
150
100
50
0
100
80
60
40
20
0
**
Dark Control
t50
t95

Figure 5.10 Mean intracellular fluorescence of the probe (I.) dihydroethidium which indicates superoxide, $ONOO^{\bullet -}$ and $OH^{\bullet -}$ load [RU $\pm$ SE], (II.) the mitochondrial ROS probe dihydrorhodamine 123, [RU $\pm$ SE] and (III.) the nitric oxide probe, DAF-FM, [RU $\pm$ SE], within *Symbiodinium* strain 831 maintained at 30.5 $\pm$ 0.5 °C under variable iron amendments (White bars=0.0117 μM Fe, grey bars=1.17 Fe μM) after a 50 minute irradiance shift (denoted as t50, 800 μmol photon$\cdot m^{-2} \cdot s^{-1}$) and a 46 minute dark recovery period (denoted as t95, n=3, **<0.05). The dark control bars represent the probed intracellular fluorescence signal given off by *Symbiodinium* strain 831 of each iron treatment maintained in the dark for 50 minutes, effectively a dark control in comparison to the light incubated (t50) cells.

In strain 831, elevated fluorescence, and by association ROS and RNS loads, were detected in all probes relative to strain 2432, indicating marked differences in response to temperature and iron limitation. Furthermore, strain 2432 showed increases in oxidative load under iron-deplete conditions when exposed to elevated temperature, but strain 831 only showed significant elevation in superoxide, $ONOO^{\bullet-}$ and $OH^{\bullet-}$ at high temperature and iron-deplete conditions (Figure 5.8). Only when exposed to elevated temperature and irradiance did strain 831 show an elevation in the fluorescence of the intracellular ROS and RNS probes under conditions of iron limitation (Figure 5.10).

5.4 Discussion

The decrease in cell yield in both *Symbiodinium* strains subjected to iron-deplete conditions at a constant growth rate is a characteristic response of algae to iron limitation. Limitation to iron has shown to decrease specific growth rates in the diatoms *Thalassiosira oceanic, T. pseudonana, T. weissflogii, Prorocentrum minimum* and *Emaliana huxleyi* (Sunda and Huntsman 1995) and within iron-limited chemostats, the cell density of *Chlamydomonas reinhardtii* was reduced with decreasing iron amendments to medium (Weger 1999). The significant role that iron plays in phytoplankton physiology indicates that under iron-limited conditions, deviations from optimal physiology may arise, including increases in ROS and RNS load.

The enhancement of oxidative load, shown by elevated fluorescence of intracellular ROS and RNS probes, within both *Symbiodinium* strains under iron limitation and elevated temperature (predominantly strain 2432) and irradiance (predominantly strain 831) indicates a causal link between iron limitation and oxidative stress. This link exists due to the intricate role that iron plays in phytoplankton physiology, especially in the chloroplast of photosynthetic eukaryotes, with 26 molecules of iron required per photosynthetic unit (Sunda and Huntsman 1995). Iron is a critical component to the photosynthetic electron transport chain (ETC), where it is involved in the structure and function of PSII, the cytochrome b_6F complex, PSI, ferredoxin, and cyc c553 (Shi *et al* 2007) making it an essential trace metal for proper electron transport. Should iron be limiting to cells, decreases in the efficiency of PSII photochemistry can occur, as illustrated in the algal

strain *Trichodesmium erythraeum,* which showed an 80% reduction in PSII quantum yield under iron-limited conditions (Shi *et al.* 2007). Conditions of reduced photochemical efficiency enhance ROS production within the chloroplast due to the organelle's high oxygen environment (Lesser 1997), and many reducing agents (Asada 1996), which may have attributed to the increased ROS and RNS evidenced in both *Symbiodinium* strains under iron-deplete conditions at high temperature and irradiance. In addition to the role that iron plays within the ETC, it is a critical component of the antioxidant enzymes catalase and Fe-SOD (Lesser 2006), which convert detrimental ROS to less toxic molecules (Halliwell 2006). Decreases in the availability of iron to these enzymes may enhance intracellular ROS and RNS levels due to the cells inability to quench the detrimental molecules. In the diatom *T. weissflogii,* iron limitation resulted in increases in oxidative load, which was apparent by increases in detected intracellular ROS with the fluorescent probe H_2DCF-DA (Peers and Price 2004). Both *Symbiodinium* strains may have encountered elevated ROS and RNS under iron-limited conditions at high temperature and irradiance within this study due to the impairment of the photosynthetic ETC or antioxidant enzyme activity resulting from iron's critical role in their structure and function.

Interestingly, differences between ROS and RNS load of each *Symbiodinium* strain were detected and each strain differed in their susceptibility to trace metal limitation, thermal and irradiance stress. Within every analysis of oxidative load, strain 831 showed a higher oxidative load than strain 2342. Furthermore, strain 2432 showed a significant enhancement of intracellular ROS and RNS under iron-deplete conditions when exposed to elevated temperature but strain 831 required both elevated irradiance and temperature to show significant iron-limited enhancement of ROS and RNS by all three probes. The difference in oxidative response between the strains under the same experimental conditions may result from their genetic composition. Genetic differences between *Symbiodinium* strains have been shown to equip certain *Symbiodinium* clades (clade D) with a higher tolerance to elevated temperature than other clades within the same species, such as clade C (Berkelmans and van Oppen 2006). Genotypic analysis has shown that strain 831 belongs to clade A (Saragosti *et al.* 2010) but the phylogenetic position of strain 2432 is yet to be determined. If *Symbiodinium* strain 2432 is of a different

phylogenetic position than strain 831, perhaps a clade that is more resistant to elevated temperatures (ex. clade D), then strain 2432 may response differently under stress conditions. The elevated levels of ROS in strain 831 within every ROS and RNS analysis of this study may be due to strain 831's phylogenetic position and a greater susceptibility to elevated temperature.

Although strain 831 did exhibit elevated ROS and RNS under all conditions when compared to strain 2343, strain 2432 was more sensitive to iron-limited conditions, with elevated levels of intracellular ROS and RNS detected under conditions of iron limitation and elevated temperature. The increase in detected levels of ROS and RNS within strain 2432 under iron-limited conditions and temperature stress may attribute to its cellular demand for iron and its ability to uptake iron from the environment. Differences in open-ocean and coastal diatom species Fe-requirements were shown in a study by Sunda *et al.* (1991), where oceanic species were able to outgrow coastal species at low iron concentrations due to their low cellular iron requirement. Phytoplankton can shift their cellular demands for iron by making adjustments to iron-containing molecules. Such changes include the use of flavodoxin instead of ferrodoxin (an enzyme containing two iron molecules), the use of plastocyanin (which contains copper) instead of the iron-containing cytochrome c-553, and the use of Mn-SOD or Cu/Zn-SOD antioxidant enzymes instead of the iron containing Fe-SOD and catalase (Sunda and Huntsman 1995). Perhaps strain 2432 had lower cellular requirements for iron, evidenced by its greater biomass across all iron treatments at steady growth relative to strain 831. A low cellular iron requirement would explain the heightened sensitivity of strain 2432 to iron limitation at high temperature because each cell would contain a lower concentration of iron at the onset of temperature stress, inducing a greater ROS and RNS response in iron-limited cells. The ability of strain 831 to tolerate decreased iron conditions under elevated temperature may have resulted from a greater cellular demand for and concentration of iron within the cells prior temperature stress. If strain 831 contained a higher intracellular quotient of iron per cell prior to the temperature stress treatment then the levels of ROS and RNS would not be elevated under iron limited conditions. These results were detected within iron limited and temperature stressed strain 831 cells. Strain 831's iron reserves must have become exhausted by the additional irradiance stress because an increased

oxidative load was detected in iron deplete cells under these conditions. In addition to their cellular iron requirements, the strains of *Symbiodinium* were isolated from different original host species, which may have influenced their physiological response to the experimental conditions. Although both strains were collected from the Great Barrier Reef in Australia, strain 2432 was isolated from the hard coral *Leptastrea purpurea* and strain 831 was isolated from a clam host (CCMP). In the field, it has been shown that different host species affect symbiont iron concentrations (Entsch *et al.* 1983). Host specific modifications may have been made on strains 831 and 2432, resulting in physiological differences between the strains. Clearly, physiological differences exist between the two isolates of *Symbiodinium* utilized within this study and have direct implications for the alga's ability to tolerate iron-deplete conditions under elevated temperature and irradiance.

The results of this study indicate that iron limitation has pronounced effects on the oxidative load of *Symbiodinium* species when maintained under continuous growth, high temperature and irradiance. The increase in intracellular ROS detected within each strain under iron-deplete conditions at high temperature (strain 2432) and irradiance (strain 831) highlight the potential for iron-limited enhancement of oxidative bleaching events. If *Symbiodinium in hospite* is iron-limited, elevated levels of ROS and RNS may result under temperature and irradiance stress, stimulating coral bleaching events, according to the oxidative theory of coral bleaching (Lesser 2006). Understanding the effect of iron limitation on coral algal symbionts is therefore critical to understanding the response of these organisms to the environmental changes that may influence future bleaching events and global coral reef sustainability.

5.5 References

Asada, K. 1996. Radical production and scavenging in the chloroplasts. Pp. 123-150. *In.* Baker, N. R. [ed.] Photosynthesis and the Environment. Kluwer Academic Publishers. The Netherlands.

Berkelmans, R. and J.H. van Oppen, M. 2006. The role of zooxanthellae in the thermal tolerance of corals: a 'nugget of hope' for coral reefs in an era of climate change. *Proc. R. Soc. B*. 273: 2305-2312.

Buttons, D.K. 1985. Kinetics of nutrient-limited transport and microbial growth. *Microbiological Reviews* 49. 270-297.

Entsch, B., R.G. Sim and B.G. Hatcher. 1983. Indications from photosynthetic components that iron is a limiting nutrient in primary producers on coral reefs. *Mar. Biol*. 73: 17-30.

Falkowski, P.G., Z. Dubinsky, L. Muscatine and J.W. Porter.1984. Light and bioenergetics of a symbiotic coral. *Biosci*. 34: 705-709.

Freudenthal, H.D. 1962. *Symbiodinium* gen. nov. and *Symbiodinium microadriaticum* sp. nov., a Zooxanthella: taxonomy, life cycles and morphology. *J. Protozoology* 9: 45-52.

Douglas, A. E. 2003. Coral bleaching- how and why? *Mar. Pollut. Bull.* 46:385-392.

Glynn, P.W. 1993. Coral reef bleaching: ecological perspectives. *Coral Reefs* 12: 1-17.

Goulet, T.L. and M.A. Coffroth. 1997. A within colony comparison of zooxanthellae genotypes in the Caribbean gorgonian *Plexaura Kuna*. *Proc. 8th. Int. Coral Reef Sym.* 1331-1334.

Greene, R.M., R.J.Geider and P.G. Falkowski. 1991. Effect of iron limitation on photosynthesis in a marine diatom. *Limnol. and Oceanogr*. 36:1772-1782.

Guillard, R.R.L. 1973. Division rates. p. 289-312. *In*: Stein, J.R. [ed.] Handbook of Phycological Methods: Culture Methods and Growth Measurements**.** Cambridge University Press, Cambridge.

Halliwell, B. 2006. Reactive species and antioxidants. Redox biology is a fundamental theme of aerobic life. *Plant Physiol*. 141:312-322.

Keller, M.D., W.K. Bellows and R.R.L. Guillard. 1988. Microwave treatment for sterilization of phytoplankton culture media. *J. Exp. Mar. Biol. Ecol.* 117:279-283.

Kolber, Z.S., R.T. Barber, K.H. Coale, S.E. Fitzwater, R.M. Greene, R.M., K.S. Johnson, S.Lindley and P.G. Falkowski. 1994. Iron limitation of phytoplankton photosynthesis in the equatorial Pacific Ocean. *Nature* 371:145-148.

Lesser, M.P. 1996. Elevated temperatures and ultraviolet radiation cause oxidative stress and inhibit photosynthesis in symbiotic dinoflagellates. *Limnol. Oceanogr*. 41: 271-283.

Lesser, M. 1997. Oxidative stress causes coral bleaching during exposure to elevated temperatures. *Coral Reefs* 16:187-192.

Lesser, M. 2006. Oxidative stress in marine environments. *Annu. Rev. Physiol*. 68:253-278.

Lesser, M.P. 2011. Coral bleaching: causes and mechanisms, pp. 405-419. *In* Z. Dubinsky and N. Stamber [eds.], Coral reefs, an ecosystem in transition. Springer science USA.

Lesser, M.P. and J.H. Farrell. 2004. Exposure to solar radiation increases damage to both host tissues and algal symbionts of corals during thermal stress. *Coral Reefs* 23:367-377.

Lesser M.P., W.R. Stochaj, D.W Tapley, and J.M. Shick. 1990. Bleaching in coral reef anthozoans: effects of irradiance, ultraviolet radiation and temperature on the activities of protective enzymes against active oxygen. *Coral Reefs* 8:225-232.

Macintyre, H.L. and J.J. Cullen. 2005. Using cultures to investigate the physiological ecology of microalgae, pp. 287-326. *In* R.A. Andersen [ed.], Algal culturing techniques. Elsevier Academic Press. MA, USA.

Murrant, C.L. and M.B. Reid. 2001. Detection of reactive oxygen and reactive nitrogen species in skeletal muscle. *Microsc. Res. Techniq*. 55:236-248.

Obata, H., Shitashima, K., Issiki, K., and Nakayama, E. 2008. Iron, manganese and aluminum in upper waters of the western South Pacific Ocean and its adjacent seas. *J. Oceanogr.* 64:233-245.

Price, N.M., G.I. Harrison, J.G. Hering, R.J. Hudson, P.M.V. Nirel, B. Palenik and F.M.M. Morel. 1988/1989. Preparation and chemistry of artificial algal culture medium Aquil. *Biol. Oceanogr*. 6: 443-461.

Peers, G. and N.M. Price. 2004. A role for manganese in superoxide dismutase's and growth of iron-deficient diatoms. *Limnol. Oceanogr*. 49: 1774-1783.

Santos, S.R., D.J. Taylor and M.A. Coffroth. 2001. Genetic comparisons of freshly isolated versus cultured symbiotic dinoflagellates: implications for extrapolating to the intact symbiosis. J. Phycol. 900-912.

Sargosti, E., D. Tchernov, A. Katsir, and Y. Shaked. 2010. Extracellular production and degradation of superoxide in the coral *Stylophora pistillata* and cultured *Symbiodinium. PLOSOne*. 5:1-10.

Scandalios, J.G. 1993. Oxygen stress and superoxide dismutase's. *Plant Physiol*. 101: 7-12.

Shi, T., Y. Sun and P.G. Falkowski. 2007. Effects of iron limitation on the expression of metabolic genes in the marine cyanbobacterium *Trichodesmium erythraeum* IMS101. *Enviornen. Microbiol.* 9: 2945- 2956.

Suggett, D.J., M.E. Warner, D.J. Smith, P. Davey, S. Hennige and N.R. Baker. 2008. Photosynthesis and production of hydrogen peroxide by *Symbiodinium* (Pyrrhophyta) phylotypes with different thermal tolerances. *J. Phycol.* 44: 948-956.

Sunda, W.G. and S.A Huntsman. 1995. Iron uptake and growth limitation in oceanic and coastal phytoplankton. *Mar. Chem.* 50: 189-206.

Sunda, W.G., D.G. Swift and S.A. Huntsman. 1991. Low iron requirement for growth in oceanic phytoplankton. *Nature* 351: 55-57.

Weger, H.G. 1999. Ferric and cupric reductase activities in the green alga *Chlamydomonas reinhardtii*: experiments using iron-limited chemostats. *Planta* 207: 377-384.

Zar, J. H. 1999. Comparing simple linear regression equations, p. 360–376. *In* J. H. Zar, Biostatistical analysis 4th ed. Prentice Hall, Englewood Cliffs, NJ.

Chapter 6
Conclusions

6.1 Trace metal limitation and photochemistry of coral algal symbionts

Trace metal limitation in coral reef environments is likely to occur due to their oligotrophic nature (Entsch *et al.* 1983) but the effect of this limitation on the physiology of corals and their symbiotic algae has received little research to date. This thesis examined the effect of trace metal limitation on the growth, photosystem II (PSII) photochemistry and intracellular reactive oxygen and nitrogen species (ROS and RNS, respectively) status of coral algal symbionts in culture and *in hospite,* enhancing our understanding of the role of decreased levels of trace metals in these environments.

Of all trace metals studied within this thesis (Cu, Fe, Mn and Zn), iron had the greatest discernable impact on the PSII photochemistry of algal symbionts *in hospite* when the corals were subjected to elevated temperature and irradiance. Reductions in PSII photochemistry were observed in the symbiotic dinoflagellates of *S. pistillata* isolated from a mid-shelf reef (Davies reef, Chapter 1), a near shore reef (Orpheus Island, Chapters 1&2) and an outer reef (Pith Reef, Chapter 3) when subjected to iron-deplete conditions under elevated temperatures (Chapters 1-3) and irradiance (Chapter 3).

The uniform PSII photochemical response of symbiotic dinoflagellates of *S. pistillata* isolated from various locations within the GBR evidences the susceptibility of these corals to conditions of low iron availability, a condition common to reef environments (Obata *et al*. 2008, Entsch *et al.* 1983). The concern regarding a decrease in PSII photochemical efficiency in symbiotic dinoflagellates when subjected to iron-deplete conditions at high temperature and irradiance is that these conditions result in oxidative stress when photosynthetic electron transport chain (ETC) capacity is exhausted. When the ETC receives an excess photon flux, ROS can be generated within the ETC of the chloroplast if carbon assimilation (photochemical quenching, Asada 2006) and/or

xanthophyll cycling (non photochemical quenching) do not adequately quench incoming energy (Lesser 2006). Decreases in PSII photochemical efficiency in coral algal symbionts under conditions of temperature stress have been detected and can be attributed to the damage of the protective D1 protein of PSII (Warner *et al.* 1999) or damage to the carboxylation processes involved in the Calvin Cycle (Jones *et al.* 1998), both of which can decrease the transport of electrons down the photosynthetic electron transport chain and result in increases in intracellular ROS (Suggett *et al.* 2008). If iron-deplete conditions enhance this decrease in PSII photochemical efficiency, potentially due to the integral role that iron plays in the structure of the photosynthetic electron transport chain (Shi *et al.* 2007), there is a potential for increased ROS to be generated. An elevation in symbiont ROS can result in an elevated transfer of ROS to the host, triggering bleaching events (Smith *et al.* 2005, Lesser 2006, Weis 2008). If iron-limited conditions have the potential to increase ROS generation through the impairment of PSII photochemistry, as illustrated in this thesis, then iron-limited conditions in the environment may promote thermally induced bleaching events.

6.2. Trace metal limitation and its effect on intracellular ROS

The role of trace metal limitation on the intracellular ROS and RNS quotient of freshly isolated symbiotic dinoflagellates from *S. pistillata* from the GBR and of *Symbiodinium* cultures was also addressed within this thesis. In contrast to the original model where iron-deplete conditions would result in elevated ROS, when freshly isolated symbiotic dinoflagellates were collected from corals subjected to iron-deplete and replete conditions and elevated temperature (Chapters 2 and 3), decreased intracellular ROS levels were detected under the iron-deplete conditions. This decrease in intracellular ROS was coincident with an increase in xanthophyll pigments (Chapter 2), involved in PSII excitation energy dissipation (Jones *et al.* 1998), in the freshly isolated symbiotic dinoflagellates under the iron-limited conditions. Freshly isolated symbiotic dinoflagellates from other *S. pistillata* colonies exposed to iron-deplete conditions in synthetic ocean water amended with no iron did not show the same decrease in intracellular ROS as illustrated by freshly isolated symbiotic dinoflagellates in Chapters 2 and 3. In contrast, iron limitation did not stimulate or reduce detectable intracellular ROS.

In fact, increases in intracellular ROS were only detected in freshly isolated symbiotic dinoflagellates isolated from temperature stressed colonies, regardless of the trace metal treatment (Chapter 4). The absence of change in intracellular ROS or RNS within the freshly isolated symbiotic dinoflagellates of iron-deplete conditions, obtained by not amending the medium with iron (Chapter 4), may have resulted due to genetic differences between the symbionts of the *S. pistillata* colonies utilized in Chapters 2, 3 and 4. Alternately, differences in response may have occurred due to iron contamination of the system from the coral host skeleton, which has been shown to contain variable levels of iron in natural systems (Entsch *et al.* 1983).

Interestingly, when coral-algal symbionts were maintained in culture, Chapter 5, they were far more susceptible to iron limitation, and ROS and RNS were stimulated under iron-deplete conditions at high temperature and irradiance (30.5 $\pm$ 0.5 °C and 800 μmol photon•m^{-2}•s^{-1}, respectively). The results of this chapter indicate that potential differences between *Symbiodinium in hospite* and in culture may result due to the role of the host in nutrient availability. *In hospite*, the algal symbionts encounter different microenvironments due to the controlled transfer of nutrients from the host (Falkowski *et al.* 1984) while in culture they have the ability to actively uptake iron from their surrounding environment (Hudson and Morel 1990). Furthermore, the presence of a coral host skeleton within the system may act as a potential contamination source for trace metals (Entsch *et al.* 1983), preventing a clear response of ROS and RNS to trace metal limited conditions. Overall, differences between the ROS and RNS response of *Symbiodinium* to iron-deplete conditions in culture were evident relative to those *in hospite*.

6.3 The oxidative theory of coral bleaching

Increases in oxidative loads, under conditions of temperature and irradiance stress, have been stipulated as one of the main drivers of coral bleaching (Lesser 2006, Weiss 2008, Lesser 2011). Interestingly, the coral algal symbionts probed for oxidative stress within this thesis only showed increases in intracellular ROS and RNS at elevated temperature and irradiance in two sets of experiments (Chapter 4 and Appendix II). Under conditions

of thermal stress, no significant increase in intracellular ROS and RNS was detected within freshly isolated symbiotic dinoflagellates of *S. pistillata* (Chapter 3) and within cultures of *Symbiodinium* (Chapter 5). In Chapters 2 and 3, the absence of intracellular ROS increase at high temperature may have resulted from the up-regulation of xanthophyll pigments. These pigments actively shunt energy away from PSII, dissipating it as heat (Csaszar *et al.* 2010), and were shown to increase in algal symbionts under the high temperature treatments (Chapter 2). Furthermore, a lack of increase in intracellular ROS and RNS at high temperature in Chapters 2, 3 and 5 may have resulted because of insufficient stress. In Chapter 4, the corals were subjected to acute elevations in temperature and irradiance (31°C at a rate of 1.68 °C d^{-1} and 400 μmol photons·m^{-2}·s^{-1}) over the course of the experiment but in Chapters 2 and 3, the irradiance was maintained at 150 μmol photons·m^{-2}·s^{-1} and the temperature was increased very gradually to 31°C at a rate of 0.5-0.7 °C d^{-1}. It is possible that the conditions employed within Chapters 2 and 3 were sufficient to generate decreases in PSII photochemical efficiency but insufficient to generate dramatic increases in intracellular ROS required for detection through fluorescent probes and flow cytometry.

The technique of positive pressure air extraction of symbiotic dinoflagellates presents a challenge when examining intracellular ROS due to the high concentration of oxygen utilized in the process. Although the technique may have increased the "standing stock" of intracellular oxygen, the lack of increase in intracellular ROS within *Symbiodinium* cultures at high temperature (30.5 °C) relative to low temperature (25 °C, Chapter 5) suggest that that technique did not greatly interfere with intracellular ROS measurements of freshly isolated symbiotic dinoflagellates (Chapters 3 and 4). Future work should include the exposure of *Symbiodinium* cultures to greater temperatures (>34°C) to determine the effect of elevated temperature on ROS generation within *Symbiodinium* when maintained in a host-free environment. The lack of detectable increases in oxidative load within *Symbiodinium* in culture and *in hospite*, other than under extreme temperature and irradiance conditions, suggests that under conditions of moderate thermal stress, coral algal symbionts have the ability to mitigate intracellular ROS and RNS, perhaps by increasing their non-photochemical quenching and antioxidant mechanisms.

The work presented in this thesis illustrates the intricate role of iron in the oxidative load of coral-algal symbionts. Although a significant stimulation of intracellular ROS and RNS was detected within freshly isolated symbiotic dinoflagellates exposed to elevated temperature and irradiance (Chapter 4) and conditions of temperature and irradiance extremes (34 °C and 900 μmol photon·$m^{-2}s^{-1}$, Appendix II), the response was not consistent. Future work is required to determine the influence of temperature and irradiance stress on the coral-algal symbiosis using flow cytometry and fluorescent probes.

6.4 Future studies

The significant role that iron plays in coral physiology has been illustrated within this thesis but continued research is required to clarify the effects of iron and trace metal limitation on the coral-algal symbiosis and its role in the oxidative stress response in coral-algal symbionts. The experimental field component presented in this thesis focused on the Indo Pacific reef building coral, *S. pistillata* but understanding the response of other hard corals to trace metal limitation under temperature and irradiance stress will be important in order to elucidate the effects of ambient trace metal limitation on coral bleaching events. Species that could be studied in the future include the Indo Pacific corals of the genera *Acropora, Montastrea, Porites* and *Pocillopora*, all of which have been detected within the GBR (Done 1982). By testing the effect of trace metal limitation on a wide range of coral species an understanding will be established pertaining to the effects of trace metal limitation on coral bleaching events.

The differences in oxidative load detected between the symbiotic dinoflagellates freshly isolated from *S. pistillata* and free living *Symbiodinium* species maintained in culture under iron-deplete conditions serve as a basis for future research. Research on the sea anemone *Anthropleura elegantissima* would reveal the role of the host skeleton in trace metal provision. If algal symbionts receive trace metals from the host coral's skeleton, which have been shown to contain variable levels of iron (Entsch *et al.* 1983), ambient iron concentrations may not become limited. The absence of a skeleton in the sea

anemones removes a potential source of trace metal contamination, providing an effective system to study trace metal limitation and the coral-algal symbiosis.

Furthermore, alternate methods of ROS and RNS analysis should be explored to ascertain the effects of trace metal limitation on oxidative load. The method of oxidative load detection utilized within this thesis was dependent upon fluorescent probes and flow cytometry. Although the technique has many positive attributes, alternate measures of oxidative load could be explored, in conjunction with flow cytometry, to truly establish the role of reactive oxygen species in thermally induced coral bleaching events. The air-gun stripping method utilized to isolate the symbiotic dinoflagellates from the coral host (Chapters 2-4) may have influenced the intracellular ROS load of the freshly isolated zooxanthellae. As such, more stable by-products of oxidative stress could be explored in future work. One such method involves detecting intracellular αβ-unsaturated reactive aldehydes, such as malondialdehyde (MDA) and isopostanes, which are stable end products of lipid peroxidation. Isopostane analysis is attractive because the measurement of a particular isopostane, F2-IsoPs, is one of the most reliable approaches for the assessment of oxidative stress *in vivo* (Dalle-Donne *et al.* 2006), can be measured by mass spectrometry (Halliwell and Whiteman 2004) and may be applicable to oxidative events in coral algal symbionts. By utilizing various approaches for determining oxidative load within coral algal symbionts and the animal host, a clear understanding of the role of ROS and RNS in bleaching events may be evidenced.

6.5 Implications for coral reef ecosystems

The dynamic effect of trace metal limitation on PSII photochemistry and its potential role in the oxidative load of coral-algal symbionts is evident from the research presented within this thesis. Although differences were detected between coral algal symbionts in culture relative to those *in hospite*, the significant physiological response of each to trace metal limitation indicates the important role of trace metals, especially iron, in the tolerance of corals to elevated heat and irradiance. If low ambient trace metal concentrations limit a coral and its algal symbiont's ability to handle elevated temperature and irradiance, increases in coral bleaching events may arise, threatening global coral

reefs. Under projected models of climate change and emission scenarios, sea surface temperatures are projected to rise by 1.8 - 4 °C (Hoegh-Guldberg *et al.* 2007), threatening reefs due to the bleaching effect of elevated temperature and irradiance (Brown *et al.* 2000, Lesser and Farrell 2004). Should low ambient trace metal concentrations, common to the oligotrophic nature of reef environments (Entsch *et al.* 1983), occur in conjunction with the projected elevated temperatures under conditions of high irradiance, the severity of bleaching events will be increased, threatening the existence of global coral reefs. Coral reef ecosystems are of great importance due to their roles as biodiversity hotspots and as major sources of economically significant ecosystem services (Hoegh-Guldberg *et al.* 2007). Understanding the effects of trace metal limitation on algal symbiont physiology and coral bleaching events is essential if these ecosystems are to be maintained and preserved.

6.6 References

Asada. 2006. Production and scavenging of reactive oxygen species in chloroplasts and their functions. *Plant Physiol*. 141: 391-396.

Brown, B.E., R.P. Dunne, M.E. Warner, I. Ambarsari, W.K. Fitt, S.W. Gibb and D.G. Cummings. 2000. Damage and recovery of photosystem II during a manipulative field experiment on solar bleaching in the coral *Goniastrea aspera*. *Mar. Ecol. Prog. Ser*. 195:117-124.

Csaszar, N.B.M., P.J. Ralph, R. Frankham, R. Berkelmans, and M.J.H and van Oppen. 2010. Estimating the potential for adaptation of corals to climate warming. *PlosOne*. 5:1-8.

Dalle-Donne, I., R. Rossi, R. Colombo, D. Giustarini and A. Milzani. 2006. Biomarkers of oxidative damage in human disease. *Clin. chem*. 52: 601-623.

Done, T.J. 1982 Patterns in the distribution of coral communities across the central Great Barrier Reef. *Coral Reefs* 1:95-107.

Dykens, J.A., J.M. Shick, C. Benoit, G.R Buettner and G.W. Winston. 1992. Oxygen radical production in the sea anemone *Anthropleura elegantissima* and its endosymbiotic algae. *J. Exp. Biol.* 168. 219-241.

Entsch, B., R.G. Sim and B.G. Hatcher. 1983. Indications from photosynthetic components that iron is a limiting nutrient in primary producers on coral reefs. *Mar. Biol.* 73: 17-30.

Falkowski, P.G., Z. Dubinsky, L. Muscatine and J.W. Porter.1984. Light and bioenergetics of a symbiotic coral. *Biosci*. 34: 705-709.

Halliwell, B. and M. Whiteman. 2004. Measuring reactive species and oxidative damage *in vivo* and in cell culture: how should you do it and what do the results mean? *Brit. J. Pharmacol*. 142: 231-255.

Hoegh-Guldberg, O., P.J. Mumby, A.J. Hooten, R.S. Steneck, P. Greenfield, E. Gomez, C.D. Hervell, P.F. Sale, A.J. Edwards, K. Caldeira, N. Knowlton, C.M Eakin, R. Iglesias-Prieto, N. Muthiga, R.H. Bradbury, A. Dubi and M.E. Hatziolos. 2007. Coral reefs under rapid climate change and ocean acidification. *Science.* 318:1737-1742.

Hudson, R.J.M. and F.M. Morel. 1990. Iron transport in marine phytoplankton: Kinetics of cellular and medium coordination reactions. *Limnol. Oceanogr.* 35: 1002-1020.

Jones, R.J., O. Hoegh-Guldberg, A.W.D. Larkum and U. Schreiber. 1998. Temperature-induced bleaching of corals begins with impairment of the CO_2 fixation mechanism in zooxanthellae. *Plant, Cell Environ*. 21: 1219-1230.

Lesser, M.P. 2006. Oxidative stress in marine environments: biochemistry and physiological ecology. *Annu. Rev. Physiol.* 68:253–78.

Lesser, M.P. 2011. Coral bleaching: causes and mechanisms, pp. 405-419. *In* Z. Dubinsky and N. Stamber [eds.], Coral reefs, an ecosystem in transition. Springer science USA.

Lesser, M.P. and J.H. Farrell. 2004. Exposure to solar radiation increases damage to both host tissues and algal symbionts of corals during thermal stress. *Coral Reefs* 23:367-377.

Obata, H., K. Shitashima, K. Issiki, and E. Nakayama. 2008. Iron, manganese and aluminum in upper waters of the western South Pacific Ocean and its adjacent seas. *J. Oceanogr.* 64:233-245.

Shi, T., Y. Sun and P.G. Falkowski. 2007. Effects of iron limitation on the expression of metabolic genes in the marine cyanbobacterium *Trichodesmium erythraeum* IMS101. *Environ. Microbiol*. 9: 2945- 2956

Smith, D.J., D.J.Suggett and N.R. Baker. 2005. Is photoinhibition of zooxanthellae photosynthesis the primary cause of thermal bleaching in corals? *Global Change Biol.* 11:1-11.

Suggett, D.J., M.E. Warner, D.J. Smith, P. Davey, S. Hennige and N.R. Baker. 2008. Photosynthesis and production of hydrogen peroxide by *Symbiodinium* (Pyrrhophyta) phylotypes with different thermal tolerances. *J. Phycol.* 44: 948-956.

Warner, M.E., W.K. Fitt and G.W. Schmidt, G.W. 1999. Damage to photosystem II in symbiotic dinoflagellates: a determinant of coral bleaching. *Proc. Natl. Acad. Sci*. 96: 8007-8012.

Weis, V.M. 2008. Cellular mechanisms of Cnidarian bleaching: stress causes the collapse of symbiosis. *J. Exp.Biol.* 211: 3059-3066.

Appendices

Appendix 1: Chapter 2 statistical model building

A1.1 Methods: building the linear mixed model

The primary step involved in building the model was to determine whether the random effects of sample day and replicate were to be included. This was accomplished by building and running both a generalized least square model and a liner mixed effect model that incorporated random effects, all treatment factors and their interactions (West 2007). Once complete, both models were tested against each other using an ANOVA. If a 95% significant difference was detected between the models, the random effects were included and the linear mixed effect model chosen. Secondly, the inclusion of treatment-factor interactions was tested by running a linear mixed-effect model followed by an ANOVA of that same model. If the interaction terms were found to be significant, the analysis was stopped; however if the interactions were insignificant they were removed from the model (West *et al.* 2006). This testing of the interacting factors in the model occurred until a significant interaction was encountered or all interaction terms were removed. The results of the model were interpreted by analyzing whether the deviance of the coefficients for each fixed factor from zero was significant.

A1.2 Results: The linear mixed model to assess photophysiology

A linear mixed model incorporating the random effects of sample day and sample replicate was tested against a generalized least squares model lacking the random effects. An ANOVA comparing both tests showed that the random effects of sample day and replicate were significant, therefore, the linear mixed model incorporating both random effects was selected (*L. ratio*=7.410944, p=0.0065). The effect of fixed factors was determined by running an ANOVA on the complete model and the three-way interaction of temperature, DFB, and sample date was not included in the model because of its insignificant effects on F_v/F_m (df=497, F=3.37, p=0.0669). In the final model, the fixed factors tested were: date, temperature, DFB addition, date by temperature, date by DFB

addition, and temperature by DFB addition. A significant interaction was detected between temperature and DFB addition on the deviation of its coefficient from zero (df= 498, T=-1.98344, p<0.05, Table 1, Figure 1). Additionally, significant interactions were detected between DFB addition and sample date, and between temperature and sample date (df=498,T=5.37155,p<0.05, df=,T= 15.26949,p<0.05 respectively). The negative coefficient displayed for the interaction between iron limitation and high temperature (-0.0138379) illustrated that over the course of the experiment both factors had a negative effect on the predicted F_v/F_m of zooxanthellae *in hospite* by the model (Figure 1). Furthermore, the positive coefficients displayed by the interaction between both DFB removal and sample date, and low temperature and sample date, indicate that the absence of the stress factors of DFB addition and high temperature increased F_v/F_m by a factor significantly greater than 0 (0.0040648 and 0.0115549, respectively).

A1.3 References

West, B.T., Welch, K.B. and Galecki, A.T. 2006. Linear mixed models: a practical guide using statistical software. Chapman and Hall.

Appendix 2

The efficacy of fluorescent intracellular probes and flow cytometry in the measurement of intracellular reactive oxygen species generated within irradiance and temperature stressed coral algal symbionts.

A2.1 Introduction

Coral reef ecosystems are some of the most productive and biodiverse systems on the planet. The success of these biodiverse ecosystems lies in a symbiotic relationship between a Cnidarian animal host and photosynthetic dinoflagellate of the genus *Symbiodinium*, most commonly referred to as zooxanthellae (Weis 2008). Within this relationship, the alga can transfer up to 90% of their photosynthate to the host (Falkowski *et al.* 1984) in return for inorganic nutrients, allowing each symbiotic participant to survive nutrient poor (oligotrophic) waters. Although successful for millions of years, coral reefs are currently threatened by a phenomenon called coral bleaching. This process involves the paling of a coral due to the expulsion of their algal symbiont or the breakdown of the algal symbionts' pigments (Glynn 1993). Coral bleaching can result in coral death if the symbiotic dinoflagellates are not reestablished within the host after a short period of time (Douglas 2003), negatively effecting the surrounding reef and its prosperity.

The relationship between the coral animal host and their photosynthetic dinoflagellates can be disrupted by several environmental factors that upset the physiological balance required in symbiosis. The two main factors known to trigger coral bleaching include increased sea surface temperature and solar radiation (Fitt and Warner 1995, Hoegh-Guldberg and Jones 1999, Warner *et al.* 1999). Both factors disturb the physiological balance between coral host and algal symbiont because they can result in the over generation of reactive oxygen species (ROS) under conditions outside of the physiological optimum (Lesser *et al.* 1990, Lesser 1996, 1997). Although ROS are

products of daily physiology, they are damaging when their generation exceeds their removal. Oxidative stress results under these conditions because the antioxidant defenses within cells are inadequate in detoxifying the generated ROS (Halliwell and Whiteman 2004). Excess ROS production can result in damage to lipids, DNA and proteins due to their high reactivity (Lesser 2006). Each member in the coral-dinoflagellate symbiosis generates a variety of ROS, including such species as hydrogen peroxide (H_2O_2), superoxide ($O_2\cdot^-$) and the hydroxyl radical ($OH\cdot^-$) (Lesser 2006).

The photosynthetic nature of the algal symbiont increases its susceptibility to ROS production. Under conditions of excess photon flux, ROS are formed in the photosynthetic electron chain (ETC) of the chloroplast if carbon assimilation (photochemical quenching) (Asada 2006) and/or xanthophyll cycling (non photochemical quenching) are inadequate in removing excess energy (Lesser 2006). Natural defenses do exist to quench photosynthetically derived ROS, including the turnover of the protective D1 protein of PSII and the activity of antioxidant enzymes (catalase and superoxide dismutase) (Lesser 2006). Inclusively, these quenching mechanisms are effective at mitigating oxidative load but under stressful conditions ROS production can exceed quenching. The transfer of ROS from the algal symbiont to the coral host may preclude bleaching events, as the host would expel the symbiont as a means of protection. The over generation of ROS, therefore, can be viewed as a primary step in the physiology of coral bleaching (Lesser 2006, Weis 2008) and must be quantified and studied to understand bleaching events.

The intricate role of ROS in bleaching make measuring the oxidative load of freshly isolated symbiotic dinoflagellates from bleaching corals critical in understanding the physiology behind coral bleaching. Natural levels of ROS in symbiotic dinoflagellates *in hospite* are difficult to measure for many reasons including: the short persistent time of reactive species *in vitro*, the difficulty inherent in their direct measurement (Halliwell and Whiteman 2004), the high affinity of ROS for scavenging systems and the requirement of a detection system close to the site of ROS production (Driever *et al.* 2009). Flow cytometry and the use of fluorescent molecular probes are advantageous because they overcome many of the limitations inherent in ROS measurements. The use of fluorescent

probes in ROS detection is attractive due to their high sensitivity, simplicity in use and reproducibility (Chen *et al.* 2010). In combination with flow cytometry, fluorescent ROS probes permit the measurement of intracellular ROS (Halliwell and Whiteman 2004) at the cellular sites of ROS production. The application of both techniques, therefore, is appropriate to understand the oxidative load in symbiotic dinoflagellates prior to coral bleaching events.

The purpose of this study is to understand the effect of irradiance stress on the oxidative load in symbiotic dinoflagellates freshly isolated from *Stylophora pistillata,* Esper 1797, maintained at high temperature. Furthermore, the application of fluorescent probes and flow cytometry to measure these changes in oxidative load will be revealed. It is hypothesized that at increased irradiance, a higher oxidative load will be detected, flow cytometrically with fluorescent ROS probes, in the freshly isolated symbiotic dinoflagellates of *S. pistillata* when maintained at high temperature.

A2.2 Methods

A2.2.1 Coral collection and maintenance- One large colony of *S. pistillata*, was collected in late June 2009 from Pith reef, an outer reef on Australia's Great Barrier Reef (GBR), from a depth of 8.9 m. The colony was maintained in an aerated outdoor aquarium circulating 5 μm filtered seawater at a temperature of 26-28 °C and an irradiance range of 75-200 μmol photons·m^{-2}·s^{-1} (measured using PAM PAR sensor, Walz Mess-und Regeltechnik, Germany) until experimentation. Nubbins approximately 4-5 cm in length were then cut from the colony and suspended vertically using 0.22 mm monofilament fishing line. Nubbins recovered for 24 hours in 1 μm filtered and aerated seawater (28 °C) at an irradiance of 50-200 μmol photons·m^{-2}·s^{-1} in a controlled temperature and irradiance aquarium room.

A2.2.2 Experimental stress regime- S. pistillata nubbins (n=3) were placed under different irradiance regimes, (i) low light (10-40 μmol photons·m^{-2}·s^{-1}) (ii) Medium light (500-530 μmol photons·m^{-2}·s^{-1}) and (iii) high light (900-950 μmol photons·m^{-2}·s^{-1}) for 4 hours, at a temperature of 32.5 $\pm$ 1 °C. Illumination was provided by a 400 W metal halide lamp

(BLV, Germany) fitted with a 0.5 cm Schott Robax glass ceramic filter to remove ultraviolet (UV) wavelengths. The temperature of the water bath was increased from 28 to 32.5 $\pm$ 1°C prior to the initiation of the photoperiod at a rate of 2 °C/hour.

A2.2.3 Analysis of photosystem two (PSII) photochemical efficiency in zooxanthellae- Light-adapted (effective) PSII photochemical efficiency (F_v/F_m) and ambient chlorophyll fluorescence (F_o) was measured after a 4-hour irradiance incubation at 32.5 $\pm$ 1 °C using Pulse Amplitude Modulation (PAM) fluorometry (Diving-PAM, S/N: UWFA0257A, Walz Mess-und Regeltechnik, Germany). PAM measurements were taken on the tip, middle and bottom region of each nubbin and these measurements were then averaged to obtain a final mean F_v/F_m or F_o value per nubbin.

A2.2.4 Assessment of intracellular ROS and membrane permeability- Zooxanthellae were collected by air blasting the coral nubbin (modified from Berkelmans and van Oppen 2006) in 0.2 μm filtered seawater after the 4-hour irradiance exposure at 32.5 $\pm$ 1°C. The resultant slurry was gently homogenized for 10 seconds and the homogenate was filtered across a 53 μm Nytex mesh filter. Once filtered, the resultant sample of freshly isolated symbiotic dinoflagellates was diluted with 0.5 μm filtered seawater and instantly probed for intracellular ROS and RNS.

The intracellular ROS and reactive nitrogen species (RNS) nitric oxide (NO), OH•, peroxynitrite ($ONOO^-$) and H_2O_2, were detected using 5-(and 6) chloromethyl-2',7'-dichlorodihydrofluorescein diacetate, acetyl ester (CMH_2DCFDA) (Murrant and Reid 2001) at a final concentration of 5 μM in seawater. Superoxide, $ONOO•^-$ and $OH•^-$ were detected using the fluorescent probe dihydroethidium (DHE) (Murrant and Reid 2001), at a final concentration of 23.1 μM. NO was detected using the probe 4-amino-5-methylamino-2',7'-difluorofluorescein diacetate (DAF-FM) at a final concentration of 2$\mu mol \cdot L^{-1}$. Mitochondrial ROS was detected using the probe dihydrorhodamine 123 (DHR 123) at a final concentration of 4 μM (Lesser 1996). Freshly isolated symbiotic dinoflagellates were incubated with each probe for 30 min in the dark before analysis on a FACsCalibur flow cytometer (BD, San Jose, California, U.S.A.). Freshly isolated symbiotic dinoflagellate samples were diluted with 0.5 μm-filtered seawater to maintain

an events·second^{-1} rate of less than 1000. Increases in green and orange fluorescence (Fl1 and Fl2 channels of the flow cytometer) were proportional to probe oxidation and indicative of intracellular ROS and RNS (see optimization of probes in Chapters 3 and 4). All probe fluorescence measurements were standardized to a negative control by subtracting the negative control fluorescence signal from the probe fluorescence signal. The negative control for each freshly isolated symbiotic dinoflagellates sample was prepared by adding an equivalent concentration of DMSO to the sample, accounting for differences in freshly isolated symbiotic dinoflagellates ambient fluorescence signals.

Freshly isolated symbiotic dinoflagellates were probed with the cell death indicator, SYTOX green (Vardi *et al.* 2006) at a final concentration of 1μM for 10-15 min in the dark. Cell membrane damage was determined by counting the number of cells taking up the fluorescent SYTOX Green stain relative to the negative control.

Working stock solutions of CMH_2DCFDA, DHE and DAF and DHR123 were prepared in dimethyl-sulphoxide (DMSO), divided into small aliquots and maintained in the dark at -20 °C until use. The SYTOX green working stock was prepared in 0.2 μm filtered seawater divided into small aliquots and maintained at -20 °C in the dark until use. All flow cytometric fluorescence dyes were purchased from Invitrogen (Carlsbad, California, U.S.A).

A2.2.6 Statistical analysis- One-way ANOVA tests were run to determine significant differences in measurements of PSII photochemical efficiency, intracellular ROS, intracellular RNS and cell viability under temperature stress and variable irradiance treatments. If a significant effect of irradiance was detected, a Tukey's HSD test was run to determine where significant differences lay. Prior to each ANOVA, a Levene's test of equality of error variances (p<0.05) was run and normality was assumed. All statistical analyses were run on SPSS (Version 17.00) statistical software.

A2.3 Results

A2.3.1 Light adapted PSII photochemical efficiency- Each increase in irradiance exposure to the symbiotic dinoflagellate's of *S. pistillata* caused a significant decrease in the

effective photochemical efficiency of PSII under conditions of temperature stress (Figure 1, *df*=2, *F*=92.752,*p*=0.00). At the lowest irradiance level, 10-40 μmol photons·m^{-2}·s^{-1}, the highest F_v/F_m was detected and was significantly greater than those of the other two irradiance treatments ($p<0.05$). The highest irradiance level treated symbiotic dinoflagellates, 900-950 μmol photons·m^{-2}·s^{-1}, showed a significantly lower F_v/F_m relative to both the 10-40 and 500-550 μmol photons·m^{-2}·s^{-1} treated symbiotic dinoflagellates ($p<0.05$).

Ambient chlorophyll fluorescence (F_o) did not significantly differ among the irradiance treatments after the temperature stress incubation period (Figure 1). A slight decrease in F_o did occur at the 500 μmol photons·m^{-2}·s^{-1}but it was not as pronounced as the decrease in F_v/F_m.

A2.3.2.Intracellular ROS and RNS- High irradiance levels positively affected the intracellular ROS load within freshly isolated symbiotic dinoflagellates (Figure 2). The fluorescence of the mitochondrial ROS probe, DHR 123, was the highest in freshly isolated symbiotic dinoflagellates exposed irradiance treatments of 900-950 μmol photons·m^{-2}·s^{-1} relative to those exposed to an irradiance treatment of 10-40 μmol photons·m^{-2}·s^{-1} under temperature stress (Figure 2, df=2,F=7.160, *p*=0.026). Furthermore, the fluorescence of the intracellular superoxide, $ONOO•^-$ and $OH•^-$ probe was elevated by increased irradiance (df=2,F=16.15,p=0.004), showing significantly higher levels of the oxidative products in both the 500 and 900 μmol photons·m^{-2}·s^{-1} irradiance treatments relative to the 20 μmol photons·m^{-2}·s^{-1} treatment (Figure 2, $p<0.05$). The fluorescence of the nitric oxide probe, DAF-FM, showed a trend to be elevated under high irradiance levels (Figure 3) but the fluorescence of the probe detecting NO, OH•, $ONOO^-$ and H_2O_2, CMH_2DCFDA, did not show the same relationship (Figure 3). These results show that increasing irradiance levels positively influence the intracellular ROS load of freshly isolated symbiotic dinoflagellates of *S. pistillata* and may also play a role in NO generation.

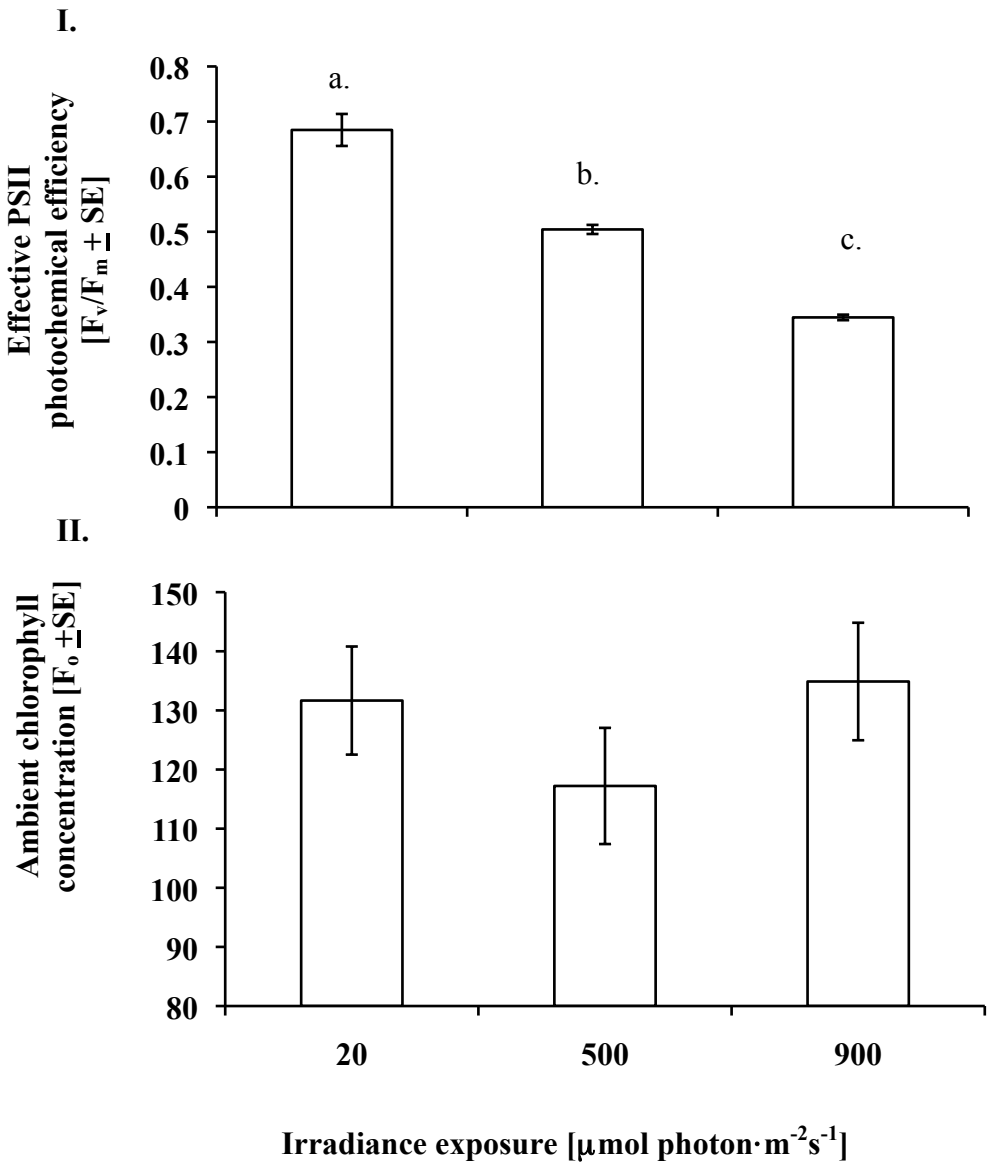
I.
Effective PSII photochemical efficiency [$F_v/F_m \pm SE$]
0.8
0.7
0.6
0.5
0.4
0.3
0.2
0.1
0
a.
b.
c.
II.
Ambient chlorophyll concentration [$F_o \pm SE$]
150
140
130
120
110
100
90
80
20
500
900
Irradiance exposure [μmol photon·$m^{-2}s^{-1}$]

Figure A2.1 Mean effective PSII photochemical efficiency (I.) [$F_v/F_m \pm$ SE] and mean chlorophyll fluorescence (II.) [$F_o \pm$ SE] of symbiotic dinoflagellates of *S. pistillata* exposed to high temperature [32 °C] and variable irradiance incubations [20, 500 and 900 μmol photon·$m^{-2}s^{-1}$] for a duration of 4 hours. Different letters represent significant differences ($p<0.05$).

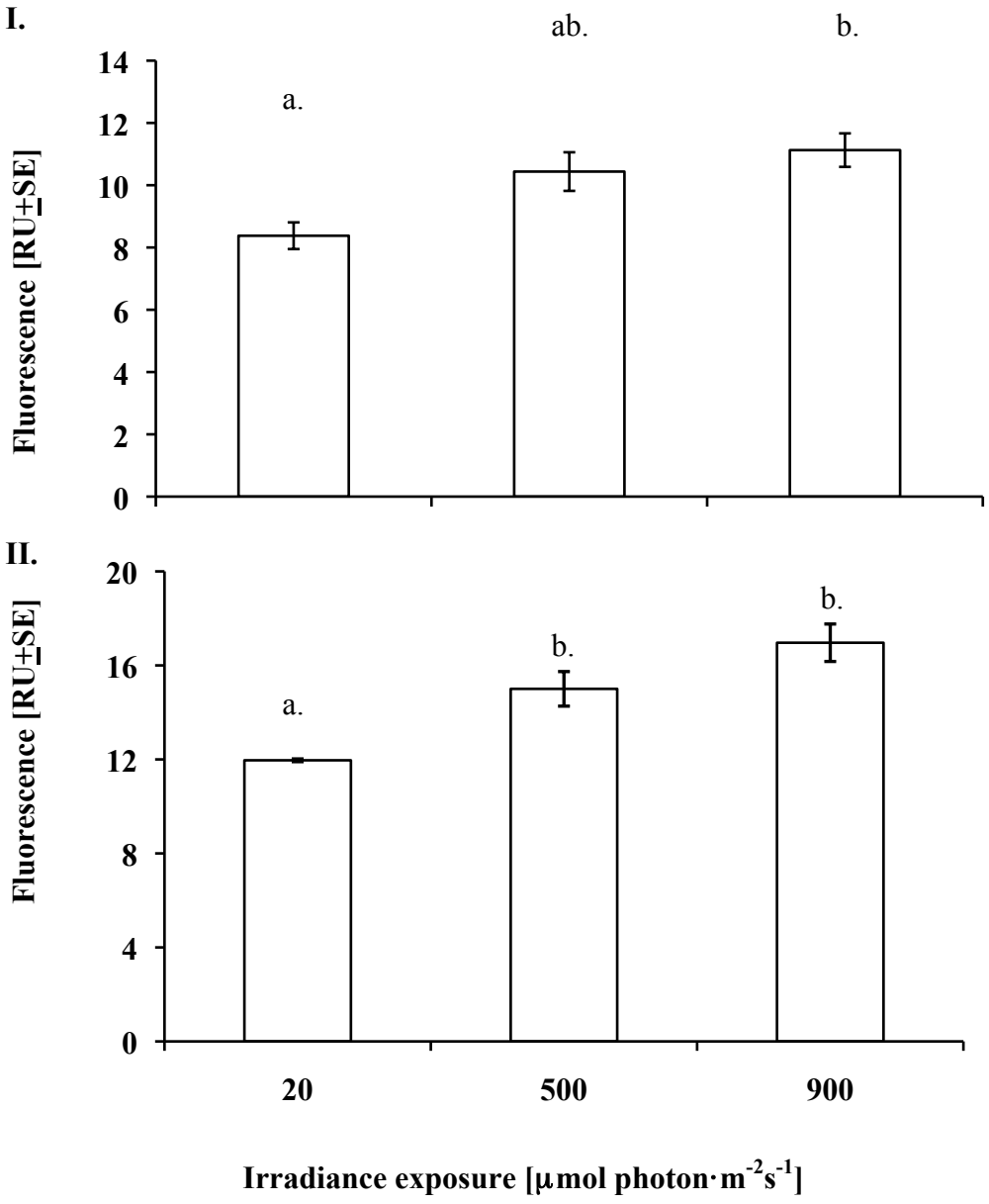
I.
ab.
b.
a.
14
12
10
8
6
4
2
0
Fluorescence [RU±SE]
II.
20
16
12
8
4
0
b.
b.
a.
Fluorescence [RU±SE]
20
500
900
Irradiance exposure [µmol photon·m-2s-1]

Figure A2.2 Mean intracellular (I.) mitochondrial ROS probe fluorescence [FU $\pm$ SE] and (II.) superoxide, $ONOO\bullet^-$ and $OH\bullet^-$ probe fluorescence [FU $\pm$ SE] of symbiotic dinoflagellates of *S. pistillata* exposed to high temperature (32 °C) and variable irradiance regimes [20, 500 and 900 μmol photon$\cdot m^{-2}s^{-1}$]. Different letters represent significant differences ($p<0.05$).

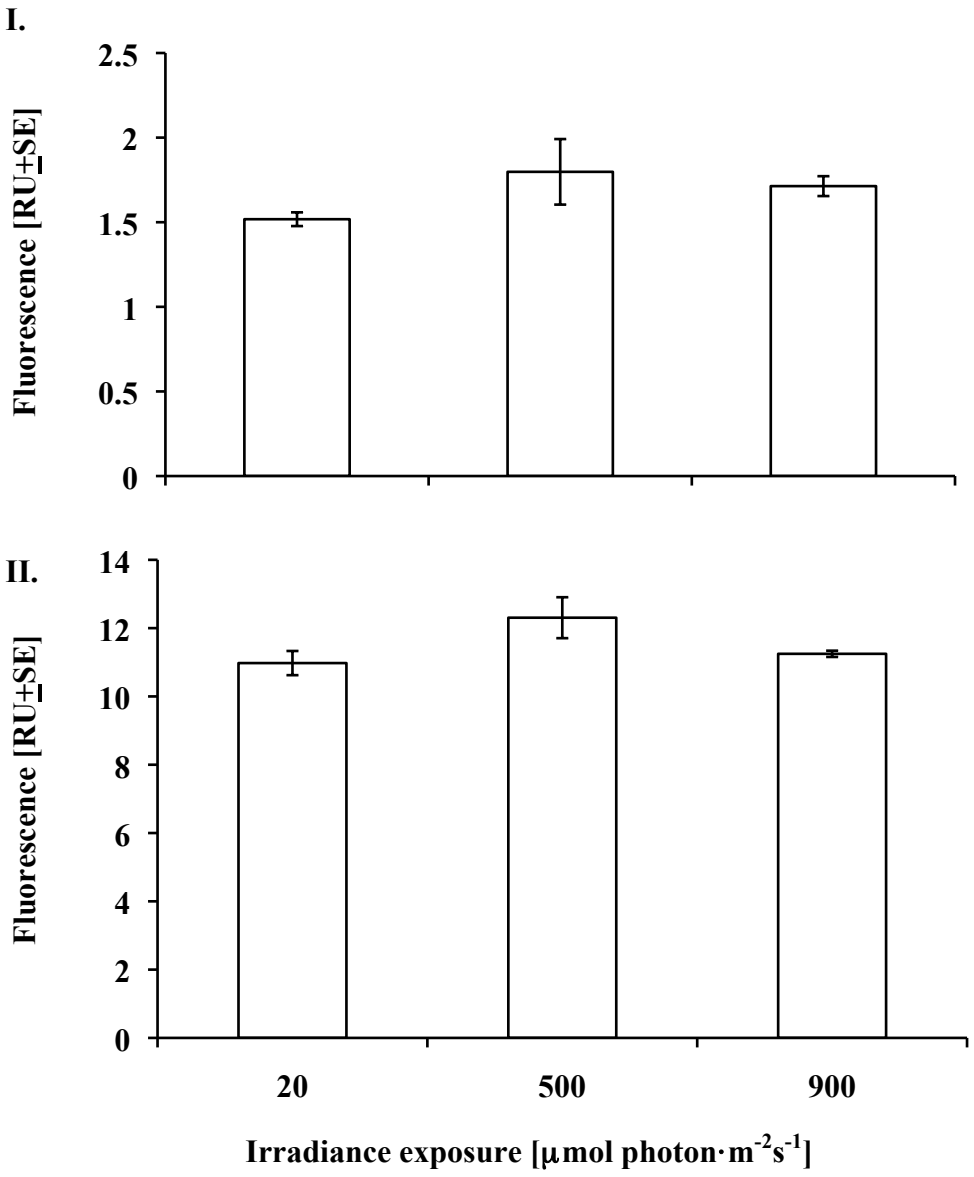
I.
Fluorescence [RU±SE]
2.5
2
1.5
1
0.5
0
II.
Fluorescence [RU±SE]
14
12
10
8
6
4
2
0
20
500
900
Irradiance exposure [µmol photon·m-2s-1]

Figure A2.3 Mean intracellular (I.) nitric oxide probe fluorescence [FU ± SE] and (II.) general ROS probe fluorescence [FU ± SE] of symbiotic dinoflagellates from *S. pistillata* exposed to high temperature (32 °C) and variable irradiance regimes [20, 500 and 900 μmol photon·$m^{-2}s^{-1}$].

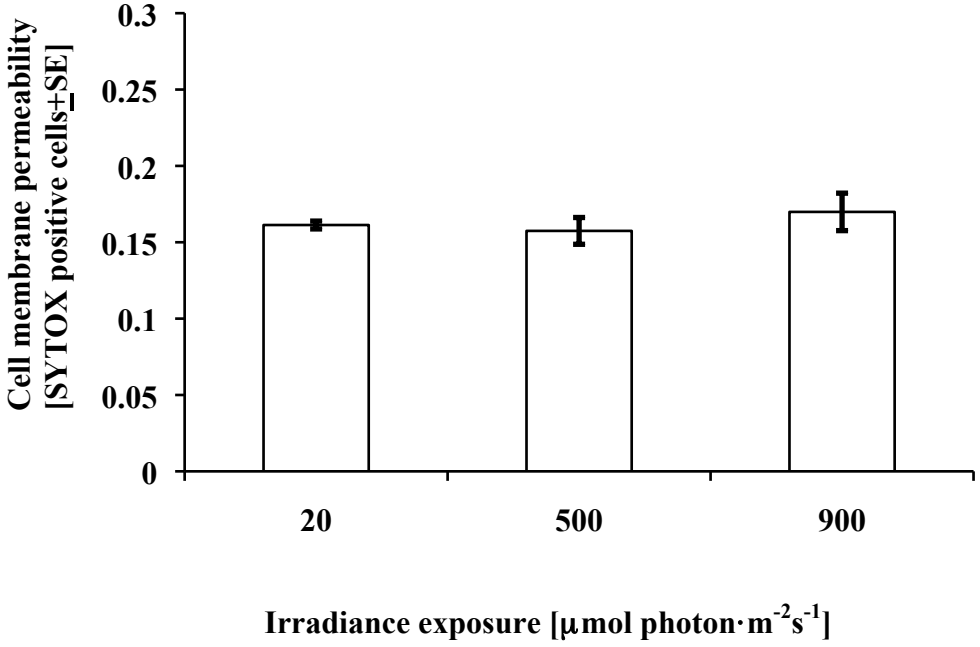
Cell membrane permeability
[SYTOX positive cells±SE]
0.3
0.25
0.2
0.15
0.1
0.05
0
20
500
900
Irradiance exposure [µmol photon·m-2s-1]

Figure A2.4 Mean proportion of permeabilized cells [SYTOX positive cells ± SE] of symbiotic dinoflagellates from *S. pistillata* exposed to high temperature (32 °C) and variable irradiance regimes [20, 500 and 900 μmol photon·$m^{-2}s^{-1}$].

A2.3.3 Cell Viability- The viability of freshly isolated symbiotic dinoflagellates exposed to different irradiance treatments under temperature stress did not differ among the treatments (Figure 4). All values were within the range of 14-18 % cell death, although the high irradiance treatment (900-950 μmol photons·m^{-2}·s^{-1}) did show a slight elevation relative to the lower irradiance treatments (10-40 and 500-550 μmol photons·m^{-2}·s^{-1}).

A2.4 Discussion

The proportional decline in the effective PSII photochemical efficiency of *S. pistillata's* symbiotic dinoflagellates with increasing irradiance treatment is a common response of this coral species (Bhagooli and Hidaka 2004) and other hermatypic coral species' symbiotic dinoflagellates to temperature and irradiance stress (Warner *et al.* 2002). Decreases in dark-adapted photochemical efficiency have been shown by symbiotic dinoflagellates of *S. pistillata* under temperature stress (Winters *et al.* 2009) and in reef building corals *in situ* under high irradiance and temperature stress (Hoegh-Guldberg and Jones 1999; Warner *et al.* 1999). Declines in effective photochemical efficiency with increasing irradiance treatment at high temperature can result from the up regulation of non-photochemical quenching mechanisms (Fitt *et al.* 2001) or changes in the proton gradient across the thylakoid membrane associated with excess photon energy relative to carbon assimilation (Asada 2006). Furthermore, declines in photochemical efficiency may be indicative of photoinhibition or photodamage, which can result from limited PSII repair (Nishiyama *et al.* 2006) and limited CO_2 assimilation under excess levels of energy provision (Apel and Hirt 2004). Limited PSII repair (manifested by the degradation of the D1 protein) and saturation of the dark reactions of photosynthesis under conditions of high temperature and light have also been attributed to decreases in the photochemical efficiency of symbiotic dinoflagellates in corals (Jones *et al.* 1998, Warner *et al.* 1999). This study confirms the negative effect of irradiance stress on the photochemical efficiency of *S. pistillata* symbiotic dinoflagellates maintained at high temperature.

The increase in intracellular ROS of *S. pistillata's* symbiotic dinoflagellates with elevated irradiance and temperature indicates a causal link between ROS load and stress responses

in reef building corals' symbiotic dinoflagellates. The elevation in intracellular ROS at high irradiance and temperature can result from the oversaturation of the photosynthetic electron transport chain with energy. The formation of ROS in the chloroplast occurs when molecular oxygen is reduced to superoxide by reduced electron transport components (Apel and Hirt 2004) and by the formation of singlet oxygen by triplet chlorophyll at PSII (Asada 2006). Although mechanisms exist to quench formed ROS, under conditions of stress, these mechanisms become exhausted, increasing the ROS load. Increased levels of superoxide and hydrogen peroxide were detected in cultured *Symbiodinium* exposed to increased temperature and UV treatment concomitantly with increases in antioxidant enzyme activity (Lesser 1996). The symbiotic dinoflagellates of *S. pistillata* in this study also exhibited an increase in intracellular ROS with elevated irradiance and temperature in coordination with a decline in effective photochemical efficiency. These results support the oxidative theory of coral bleaching (Lesser 1996, Lesser 2006) and illustrate the intimate link between ROS, temperature and irradiance stress in corals and their algal symbionts.

This study is the first to use flow cytometry to detect increases in intracellular ROS at elevated irradiance and temperature in freshly isolated symbiotic dinoflagellates of *S. pistillata.* The application of such a technique is invaluable because it provides a snapshot of the physiological stress response in the symbiotic dinoflagellates of reef building corals freshly isolated from their coral host. Flow cytometry, therefore, is an effective tool for understanding the physiology and causes pertaining to coral bleaching.

A2.5 References

Apel, K., and H. Hirt 2004. Reactive oxygen species: metabolism, oxidative stress and signal transduction. *Annu. Rev. Plant Biol*. 2004. 55:373–9.

Asada. 2006. Production and scavenging of reactive oxygen species in chloroplasts and their functions. *Plant Physiol.* 141: 391-396.

Berkelmans, R. and M.J.H. van OppeN. 2006. The role of zooxanthellae in the thermal tolerance of corals: a 'nugget of hope' for coral reefs in an era of climate change. *Proc. R. Soc. B*. 273: 2305-2312.

Bhagooli, R. and M. Hidaka. 2004. Photoinhibition, bleaching susceptibility and mortality in two scleractinian corals, *Platygyra ryukyuensis* and *Stylophora pistillata*, in response to thermal and light stresses. *Comp. Biochem. Physiol. Part A*. 137: 547-555.

Chen, X., Z. Zhong, Z. Xu, L. Chen, Y. Wang. 2010. 2`,7`-Dichlorodihydrofluorescein as a fluorescent probe for reactive oxygen species measurement: forty years of application and controversy. *Free Radical Res*. 44**:**587-604.

Douglas, A. E. 2003. Coral bleaching- how and why? *Mar. Pollut. Bull.* 46:385-392.

Driever, S.M, M.J. Fryer, P.M. Mullineaux and N.R. Baker. 2009. Imagining of reactive oxygen species *in vivo*. *Methods Mol Biol.* 479:109-16.

Falkowski, P.G., Z. Dubinsky, L. Musacatine and J.W. Porter. 1984. Light and the bioenergetics of a symbiotic coral. *Biosci.* 34: 704-709.

Fitt, W.K., B.E. Brown, M.E. Warner and R.P. Dunne. 2001. Coral bleaching: interpretation of thermal tolerance limits and thermal thresholds in tropical corals. *Coral Reefs* 20: 51-65.

Fitt, W.K and M.E. Warner. 1995. Bleaching patterns of four species of Caribbean reef corals. *Biol. Bull.* 189: 298-307.

Glynn, P.W. 1993. Coral reef bleaching: ecological perspectives. *Coral Reefs* 12: 1-17.

Halliwell, B. and M.Whiteman (2004) Measuring reactive species and oxidative damage *in vivo* and in cell culture: how should you do it and what do the results mean? *Brit. J. pharmacol.* 142: 231-255.

Hoegh-Guldberg, O. and R.J. Jones. 1999. Photoinhibition and photoprotection in symbiotic dinoflagellates from reef-building corals. *Mar. Ecol. Prog. Ser.* 183:73-86.

Jones, R.J., O. Hoegh-Guldberg, A.W.D. Larkum and U. Schreiber. 1998. Temperature-induced bleaching of corals begins with impairment of the CO_2 fixation mechanism in zooxanthellae. *Plant, Cell Environ*. 21: 1219-1230.

Lesser, M.P. 1996. Elevated temperatures and ultraviolet radiation cause oxidative stress and inhibit photosynthesis in symbiotic dinoflagellates. *Limnol. Oceanogr*. 41:271-283.

Lesser, M.P. 1997. Oxidative stress causes coral bleaching during exposure to elevated temperatures. *Coral Reefs*. 16:187-192.

Lesser, M.P. 2006. Oxidative stress in marine environments: biochemistry and physiological ecology. *Annu. Rev. Physiol.* 68:253–78.

Lesser, M.P., W.R. Stochaj, D.W. Tapley and J.M. Shick. 1990. Bleaching in coral reef anthozoans: effects of irradiance, ultraviolet radiation, and temperature on the activities of protective enzymes against active oxygen. *Coral Reefs* 8:225-232.

Murrant, C.L. and M.B. Reid. 2001. Detection of reactive oxygen and reactive nitrogen species in skeletal muscle. *Microsc. Res. Techniq*. 55: 236-248.

Nishiyama, Y., S.I. Allakhverdieve and N. Murata. 2006. A new paradigm for the action of reactive oxygen species in the photoinhibitition of photosystem II. *Biochimica et Biophysica Acta.* 1757: 742-749.

Vardi, A., F. Fomiggini, R. Casottis, A. De Martino, F. Ribalet, A. Miralto and C. Bowler. 2006. A stress surveillance system based on calcium and nitric acid in marine diatoms. *PlosBiology* 4:0411-0419

Warner, M.E., G.C. Chilcoat, F.K. McFarland and W.K. Fitt. 2002. Seasonal fluctuations in the photosynthetic capacity of photosystem II in symbiotic dinoflagellates in the Caribbean reef-building coral *Montastraea*. *Mar. Biol*. 141:31-38.

Warner, M.E., W.K. Fitt and G.W. Schmidt. 1999. Damage to photosystem II in symbiotic dinoflagellates: a determinant of coral bleaching. *Proc. Natl. Acad. Sci.* 96: 8007-8012.

Weis, V.M. 2008. Cellular mechanisms of Cnidarian bleaching: stress causes the collapse of symbiosis. *J. Exp. Biol.* 211: 3059-3066.

Winters, G., S. Beer, B.B. Zvi, I. Brickner and Y. Loya. 2009. Spatial and temporal photoacclimation of *Stylophora pistillata*: zooxanthellae size, pigmentation, location and clade. *Mar Ecol Prog Ser*. 384. 107-119.

Curriculum Vitae

Katrina Iglic

Education

2006-Present **Ph.D. Biology** University of Western Ontario
Trace metal limitation and its role in oxidative stress of coral algal symbionts: implications for thermally induced coral bleaching events.
Supervisor: Dr. Charles Trick
Completion date: September 2011

2006 **Summer Course** Bermuda Institute Of Ocean Sciences
Microbial oceanography: The biogeochemistry, ecology and genomics of oceanic microbial ecosystems.

2006 **Honours Bachelor of Science (HBSc) Biology** University of Western Ontario
Specialization Ecology and Evolution

Professional Teaching Experience

2006-Present Teaching assistant University of Western Ontario
Laboratory demonstrator for first year biology (2006-2007)
First year biology tutorial leader (2007-2010)
Ecosystem ecology teaching assistant (2008)
Masters in Environment and Sustainability: Ecosystem health teaching assistant (2009)

2007-Present Guest lecturer University of Western Ontario
Marine Environments 2010 "Coral reef environments"
Ecosystem Health 2009 "Coral reefs ecosystems: More than aesthetically pleasing"
Marine Environments 2009 "Linking trace metal limitation to coral bleaching"
Conservation Biology 2007 "Coral reefs: ecosystems in peril"

Teaching development workshops and conferences at the University of Western, Ontario

2010
Facilitating online learning
Strategies for engaging students in science
Teaching assistant mentoring program
Fall perspectives on teaching conference: mental health on campus
Teaching assistant training program, weekend workshop
Effectively integrating technology into instruction
Designing learning activities for students with all learning styles

2006 Teaching assistant day

Awards

2009-Present **Natural Sciences and Engineering Research Council of Canada (NSERC) PGS-2D**

2009 **American Society for Limnology and Oceanography Student Poster Award;** ASLO Aquatic Sciences Meeting, Nice

2006-2008 **NSERC PGS-2M**

2006 **CABBS Scholarship;** Bermuda Institute of Ocean Sciences

2006 **NSERC Undergraduate Student Research Award**

2006 **Gold Medal in Ecology and Evolution;** University of Western Ontario

2005 **The David M. Scott Scholarship;** University of Western Ontario

2005 **The Robert and Ruth Lumsden Scholarship;** University of Western Ontario

2004 **NSERC Undergraduate Research Student Award**

Contributions: oral and poster presentations

2010 Iglic, K.L. The effect of trace-metal limitation on the photophysiology and reactive oxygen speciation of *in hospite* symbiotic dinoflagellates of the Indo Pacific coral, *Stylophora pistillata*. (Oral presentation) *Biology graduate research forum, University of Western Ontario*

Iglic, K.L. Anemic coral's: The role of trace metals in coral bleaching. (Oral presentation) *Earth Day Colloquium, University of Western Ontario*

2009 Iglic, K.L. Iron and Temperature Effects on Photosynthetic and Photoprotective Pigments in *Stylophora pistillata* Zooxanthellae. (Poster presentation) *Canadian society for Plant Physiologist*

2008 Iglic, K.L. To bleach or not to bleach: A question of trace metal limitation? (Oral presentation) *Earth Day Colloquium, University of Western Ontario*

Iglic, K., Hewlett, V. B, Shick, J. M., Wells, M. L., Trick, C. G., Dunlap, W. C. Flow cytometric measurements of oxidative stress in freshly isolated algal symbionts as a function of temperature and iron availability to coral colonies. (Poster presentation) *American Society of Limnology and Oceanography,*

2007 Iglic, K.L. and Trick, C.G. Methyl Viologen: An appropriate tool to measure oxidative stress in *Symbiodinum* sp. (Freudenthal) with fluorescent probes? (Poster presentation) *Canadian society for Plant Physiologists.*

Publications

J. Malcolm Shick, Katrina Iglic, Mark L. Wells, Jason Doyle, Charles G. Trick, and Walter C. Dunlap. 2010. Responses to iron limitation in two colonies of *Stylophora pistillata* exposed to high temperature: implications for coral bleaching. *Limnol. and Oceanogr.* 56(3), 2011, 813-828

Professional memberships

American Society of Limnology and Oceanography, Phycological Society of America, The Society for Teaching and Learning in Higher Education (STLHE), Educational Developers Caucus (STLHE)

Committees

UWO Society of Graduate Students Sustainability Committee